

Die approbierte Originalversion dieser Dissertation ist in der Hauptbibliothek der Technischen Universität Wien aufgestellt und zugänglich.

<http://www.ub.tuwien.ac.at>

The approved original version of this dissertation is available at the main library of the Vienna University of Technology.

<http://www.ub.tuwien.ac.at/eng>



Diese Dissertation haben begutachtet:

.....

Dissertation

Humic-like Substances in Austrian PM10: Occurrence and possible Origin

ausgeführt zum Zwecke der Erlangung des akademischen Grades einer Doktorin der
technischen Wissenschaften unter der Leitung von

Ao. Univ.Prof. Dipl.-Ing. Dr.techn. Hans Puxbaum

E 164 Institut für Chemische Technologien und Analytik

eingereicht an der Technischen Universität Wien

Fakultät für Technische Chemie

von

DI Barbara Klatzer

Matrikelnummer: 9525873

Schönbrunner Schlosstraße 43/DG3

1120 Wien

Wien, am 29.8.2013

.....

Abstract

Aerosols impact a variety of atmospheric processes and influence the human health. They are involved in the formation of clouds and precipitation, the distribution and availability of gaseous aerosol compounds and affect the terrestrial radiation budget (reviewed by Pöschl et al., 2005). The better understanding of these properties poses the central driving force for aerosol related research.

Humic-Like Substances (HULIS), water and alkaline extractable organic compounds with molecular weights of several hundred Dalton and chemical characteristics very similar to naturally occurring terrestrial and aquatic humic acids, therefore termed **HUmic-Like Substances (HULIS)**, are major contributors to organic aerosol. Although these substances got in the scope of interest decades ago (e.g. Havers et al., 1998; Zappoli et al., 1999) there are still open questions regarding their sources and composition.

The present work aims at elucidating the atmospheric abundance, seasonality and sources of HULIS_T - with HULIS_T denoting the sum of alkaline and water-extractable fractions of HULIS – in different environments.

A three city study, comprising 10 sites with (sub-) urban and rural characteristics in Vienna, Graz and Salzburg revealed annual averaged HULIS_T levels in a range of 0.46 to 1.24 µg C/m³ and contributions to organic carbon (OC) up to 28.9%. All ten sites showed winter enrichment factors between 2.0 and 2.8. The establishment of soot stemming from diesel engined vehicles (EC_D) as dilution tracer at two urban traffic impacted sites revealed, that additional sources and/ or higher formation rates are almost exclusively responsible for the observed winter enrichment. HULIS_T carbon in source emission samples from wood, lignite and anthracite combustion, diesel engined cars and cooking activities revealed contributions to PM₁₀ in the range of 1-7%, 4-5%, 0.9-1.3% and up to 0.7%, respectively. These results indicate that beside wood smoke, combustion of fossil fuels can not be ignored in considerations on the potential sources of HULIS_T. Processing ratios of HULIS_T carbon and unique or main tracers in source emissions on ambient tracer levels revealed that, on annual average, up to 25% of HULIS_T could be of primary origin, emitted by diesel vehicles and wood stoves. Seasonal resolved correlation analysis indicated a strong connection of wintry HULIS_T levels with secondary species, the wood smoke tracer levoglucosan and with tracers connected to fossil fuel combustion. Correlation patterns in summer indicate as well secondary formation and the combustion of fossil fuels and partly biomass combustion to contribute to atmospheric HULIS_T.

Abundance and seasonality of HULIS_T was investigated and compared at 23 Austrian sites and no trend for HULIS_T was observed to occur preferred at sites with urban or rural characteristics. The majority of the 23 sampling sites showed maximum HULIS_T

concentrations in fall or winter with a winter enrichment factor in the range of 2-4. The impact of wood smoke and its relation to HULIS_T was assessed by comparison of HULIS_T and levoglucosan levels. The winter average of HULIS_T carbon and levoglucosan ratios occurred in a rather narrow range of 1.1- 5.9 at the 23 sites. The average ratio in samples from wood stove emissions was much lower (0.33). Seasonal averaged HULIS carbon and levoglucosan ratios in Vienna, Graz and Salzburg maximise in summer with values 4-7 times higher than in winter. Significant correlation of HULIS and levoglucosan was observed for most, but not all, sites in winter. We observed significant and good correlation for the sites in Vienna ($r \sim 0.74-0.93$) and Salzburg ($r \sim 0.70-0.88$). Lacking correlation of HULIS_T and levoglucosan levels at the background and urban fringe sites in Upper Austria and Carinthia indicate other sources than wood combustion being important for the atmospheric abundance of HULIS_T. HULIS_T levels at the 23 sites furthermore did not show a uniform trend to maximise in regions with highest wood smoke impact.

The investigations of water and alkaline extracted atmospheric HULIS fractions with a thermal method shed light on seasonal and spatial variations of HULIS at two sampling sites in Upper Austria. All thermograms showed peak maxima from slightly below 300°C up to 350°C and very refractory behaviour. The differences regarding thermal characteristics between HULIS_{AS} and HULIS_{WS} are rather small. Wintry urban HULIS showed a considerable shift to higher refractive material with peak maxima shifted from ~300 to 350°C, evidencing a change of composition compared to summerly and rural wintry isolates. These regional differences have not been observed for summerly HULIS isolates. Both HULIS - fractions showed almost congruent thermogram curves, which also suggests that they are structurally similar. The similar thermal stability of both HULIS fractions at the rural and urban sampling site could indicate that the type of sources which contribute to the atmospheric abundance of HULIS_T in summer plays a minor role with regard to their composition.



Colours of HULIS, isolated from atmospheric PM10, wood chips and potting soil (for details see section 9.2.1)

Kurzfassung

Aerosole beeinflussen die Erdatmosphäre, das Klima und nicht zuletzt die menschliche Gesundheit. Sie spielen eine Rolle in der Bildung von Wolken und Niederschlag, der Verteilung und Verfügbarkeit von atmosphärischen Spurengasen und beeinflussen den Strahlungshaushalt der Erde (rezensiert von Pöschl, 2005). Das bessere Verständnis dieser komplexen Wechselspiele ist die entscheidende Triebfeder in der aktuellen Atmosphärenforschung.

Huminstoffartige Substanzen, wässrig und alkalisch extrahierbare organische Verbindungen mit einem Molekulargewicht von mehreren hundert Dalton, sind eine der Hauptkomponenten von organischem Aerosol. Diese Substanzen zeigen chemische Eigenschaften sehr ähnlich zu natürlich vorkommenden terrestrischen und aquatischen Huminsäuren und werden daher huminstoffartige Substanzen, **HUmic-LIke Substances (HULIS)**, genannt. Obwohl diese Verbindungen schon seit mehreren Jahrzehnten Gegenstand der Forschung sind (z.B. Havers et al., 1998; Zappoli et al., 1999), gibt es immer noch offene Fragen bezüglich ihrer Quellen und Zusammensetzung.

Die gegenständliche Arbeit hat zum Ziel das atmosphärische Auftreten und die Saisonalität von HULIS_T zu untersuchen und mögliche Quellen zu identifizieren. HULIS_T in der gegenständlichen Arbeit verstehen sich als die Summe der wässrigen und alkalischen Fraktionen von HULIS.

In einer Drei-Städte-Studie, mit Messstationen in und um Wien, Graz und Salzburg, zeigten sich Jahresmittelwerte von HULIS_T im Bereich zwischen 0.46 und 1.24 $\mu\text{g C/m}^3$ und Beiträge zu organischem Kohlenstoff (OC) von bis zu 28.9 %. Alle zehn Messstellen zeigten höhere HULIS-Konzentrationen in der kalten Jahreszeit mit Winteranreicherungsfaktoren zwischen 2 und 2.8. Die Entwicklung eines atmosphärischen Verdünnungstracers unter Zuhilfenahme von Ruß, emittiert von Dieselfahrzeugen, zeigte, dass ungünstige Wetterlagen in der kalten Jahreszeit, wie Inversionen in Bodennähe, von eher untergeordneter Bedeutung für die beobachtete Winteranreicherung von HULIS_T sind. In Emissionen von Holz- und Kohleverbrennung, Dieselfahrzeugen und Kochvorgängen zeigten sich Beiträge von HULIS_T zu PM10 in Bereichen von 1-7%, 4-5%, 0.9-1.3% und bis zu 0.7%. Diese Ergebnisse zeigen, dass die Verbrennung von fossilen Brennstoffen, und hier besonders der Verkehrssektor und die industrielle Kohleverbrennung, nicht außer Acht gelassen werden können bei Überlegungen zu potentiellen Emissionsquellen von HULIS. Um abzuschätzen zu welchen Teilen HULIS_T primär in die Atmosphäre emittiert werden können, wurden Faktoren von HULIS und Tracerkomponenten in verschiedenen Quellenemissionen (Holzöfen, Dieselfahrzeuge und Kochvorgänge) berechnet und auf atmosphärische Tracerkonzentrationen angewendet. Daraus ergab sich, dass im Jahresmittel bis zu 25 % der atmosphärischen HULIS_T direkt, ohne sekundäre

Umwandlungsprozesse, von Holzöfen und Dieselfahrzeugen, emittiert werden können. Saisonal aufgelöste Korrelationsanalyse mit anderen Aerosolbestandteilen, zeigte einen starken Zusammenhang zwischen HULIS_T und sekundären Spezies, Holzrauch und mit Aerosolkomponenten welche hauptsächlich durch die Verbrennung von fossilen Brennstoffen in die Atmosphäre gelangen. Korrelationsmuster in den Sommermonaten deuten ebenfalls auf die sekundäre Bildung von HULIS_T und einen Beitrag von Verbrennung von biogenen und fossilen Brennstoffen zu atmosphärischen HULIS_T hin.

Das Vorkommen und die Saisonalität von HULIS_T wurden an 23 österreichischen Messstellen untersucht und miteinander verglichen. Es konnte kein Trend beobachtet werden, dass HULIS_T bevorzugt an städtischen oder ländlichen Messstellen auftritt. An der Mehrheit der 23 Messstellen konnten maximale HULIS_T Konzentrationen im Herbst oder Winter beobachtet werden. Die Winteranreicherungsfaktoren zeigten Werte zwischen 2 und 4. Der Einfluss von Holzrauch auf das Auftreten von HULIS_T wurde an den 23 Messstellen anhand des Vergleiches der Konzentrationen von HULIS_T und Levoglucosan untersucht. Der Winterdurchschnitt der Verhältnisse von HULIS_T und Levoglucosan fand sich in einem relativ engen Bereich zwischen 1.1 und 5.9 an den 23 Messstellen. Dieses Verhältnis war mit 0.33 deutlich niedriger in Proben von Holzofenemissionen. Die saisonalen Mittelwerte des Verhältnisses von HULIS-Kohlenstoff und Levoglucosan in Wien, Graz und Salzburg sind im Sommer um vier- bis siebenmal höher als im Winter. Signifikante Korrelationen von HULIS_T und Levoglucosan wurde an den meisten aber nicht allen Messstellen beobachtet. Signifikante und starke Korrelationen zeigten sich in Wien ($r \sim 0.74-0.93$) und Salzburg ($r \sim 0.70-0.88$). Fehlende Korrelation von HULIS_T und Levoglucosan an den Hintergrundmessstellen in Kärnten und Oberösterreich impliziert, dass Holzrauch dort keinen bedeutende Rolle für das atmosphärische Auftreten von HULIS_T spielt. Es zeigte sich österreichweit kein eindeutiger Trend, dass HULIS_T in den am stärksten von Holzrauch beeinflussten Regionen in den höchsten Konzentrationen auftrat. Die Untersuchung von wässrigen und alkalischen Extrakten von HULIS mit einer thermischen Methode wurde dazu herangezogen um qualitative Unterschiede zwischen HULIS-Isolaten von städtischen und ländlichen Messstellen, jahreszeitlichen Unterschieden und Unterschieden zwischen den alkalisch und wässrig extrahierten Fraktionen von HULIS qualitativ zu untersuchen. Alle Thermogramme zeigten Peakmaxima von knapp unter 300°C bis zu 350°C und sehr hitzebeständiges Verhalten. Die qualitativen Unterschiede zwischen den alkalischen und wässrigen HULIS-Isolaten sind eher gering. HULIS extrahiert aus winterlichem, städtischem PM₁₀ zeigte eine deutliche Verschiebung des Peakmaximums von 300 zu 350°C, was auf Unterschiede der Zusammensetzung von HULIS im Winter im Vergleich zu sommerlichem HULIS und HULIS aus ländlichen Gebieten hinweist. Bei den Vergleichen von HULIS, isoliert aus Proben von den Sommermonaten, konnten keine Unterschiede zwischen städtischen und ländlichen Proben festgestellt werden. Beide HULIS - Fraktionen zeigten nahezu

deckungsgleiche Thermogrammverläufe, was auch darauf hindeutet, dass sie strukturell ähnlich sind. Die ähnliche thermische Stabilität beider Fraktionen an der ländlichen und städtischen Messstelle, könnte bedeuten, dass die Art der Quellen die zum atmosphärischen Erscheinen von HULIS im Sommer beitragen eine untergeordnete Rolle bezüglich der Zusammensetzung von HULIS spielen.



Die Farben von HULIS, isoliert aus Feinstaub, Blumenerde und Holzspänen (Für Details siehe Kapitel 9.2.1)

Personal Acknowledgements

I want to thank Dr. Hans Puxbaum for giving me the opportunity to conduct my doctoral thesis in his team, for sharing his knowledge and experience, his generosity and trust, giving advices and the possibility to work, grow, and collect a lot of experience during my time in his group. Further I want to thank Dr. Heidi Bauer (she left us much too early) and Dr. Anneliese Kasper-Giebel for their appreciable help and encouragement. Dr. Andreas Limbeck, Markus Handler und Bernhard Neuberger I want to thank for passing their knowledge about the "HULISATOR" to me. Thanks to Dr. Regina Hitzenberger for valuable input and cooperation.

My colleagues and co-members of the AQUELLA Team during my time at the institute I want to thank for good collaboration, sharing coffee breaks and celebrations, knowledge about where things might hide, helpful hands, discussions about science and off-science topics and caring for many other things that made it so nice to be a member of this team. Thank you: Parissa Pouresmaeil, Dr. Niki Jankowski, Dr. Christof Schmidl, Klaus Leder, Christoph Puls, Astrid Dattler, Lylian Sampaio-Cordeiro Wagner, Rémi Sevikian, Dr. Petra Kotianova, Dr. Alexandre Caseiro, Dr. Iain Marr, Dr. Magda Kistler, Matthias Gartler, Lorena Andrade-Sanchez, Carlos Ramirez-Santa Cruz, Martin Koller, Christian Effenberger und Johannes Frank.

Thanks to those from other Universities I shared interesting cooperations with: Dr. Urs Baltensperger, Dr. Josef Dommen, Dr. Maria Cristina Facchini, Dr. Stefano Decesari, Emanuela Finessi, Dr. Thorsten Hoffmann, Dr. Marianne Geiser and Dr. Markus Kalberer from the Paul Scherrer Institut, the Italian National Research Council, the University of Bern and the University of Mainz. It was a pleasure to meet you and work with you.

Thanks as well to Christian Nagl (Environment Agency Austria) for unbureaucraticly providing ozone and sulphur dioxide data.

My deepest thanks to my parents and my brother Thomas for love, understanding and their endless belief in me and to Hannes for encouragement, patience, new ideas, graphical advice, formatting, sharing breaks, love and laughter and walking next to me on the way.

For accompanying me on my winding road to the goal, being around and helping me recover my balance, I express my thanks to old friends, new colleagues and my wonderful big family.

And last but not least: Thank you, all you coffee farmers and roasters in the world, Studio One, Sseed, Jorge Cham, Beach Boys, Metallica, Soulfly, Eva Ulmer-Jahnes, Bachblüten Notfallstropfen, Stromberg, Kurt Krömer, Ginkolecithin, Matt Ruff, Charles Bukowsky, Susanne Clarke, Ralf König, Paul Watzlawick, Eskimo, DJ Koze, Tom Waits, Nightmares on Wax, James Brown...

General Acknowledgements

HULIS analysis in ambient samples was part of the projects AQUELLA Vienna (MA22-3869/03), AQUELLA Salzburg , AQUELLA Graz (GZ: FA17C 72.002-2/03-59) (Bauer et al., 2006, Bauer et al., 2007a and 2007b), AQUELLA Lower Austria (RU4-A-152/077-04; Bauer et al., 2008b), AQUELLA Carinthia and AQUELLA Upper Austria (Bauer et al., 2008a; Jankowski et al., 2009b), funded by the Provincial Governments of Vienna, Styria, Graz, Carinthia, Lower Austria and Upper Austria.

HULIS determination in source samples was part of the Aquellis IGL – project (Emissions of industry, craft and agriculture, GZ 54 4449/2-V/4/03) funded by the Austrian Federal Ministry of Agriculture, Forestry, Environment and Water Management (Puxbaum et al., 2006), the project D16421050500 - “Aquellis M” – PM10 Aerosol Emissions of Mobile Sources, Source Profiles of Vehicle Emissions: Exhaust, Brake and Tire Abrasion Products for application in the CMB Model (Jankowski et al., 2009a) and „AQUELLIS – FB“ AEROSOLQUELLEN – Combustion of solid fuels (Schmidl et al., 2008c).

Appreciation to Lylian Sampaio-Cordeiro Wagner and Remi Sevikian for doing parts of the HULIS analysis and thanks as well to all members of the AQUELLA-Team at the Institute of Chemical Technology and Analytics, Vienna University of Technology, for doing metal, sugar, ion, polar and apolar compound and carbon analysis and experimental set-up of source emission experiments and filter sampling.

Thanks as well to the Environmental Agency Austria (Umweltbundesamt) for providing ozone and sulphur dioxide data.

Glossary

| | |
|----------------------------|---|
| AAS | Atomic absorption spectroscopy |
| a. s. l. | Above sea level |
| ATOF | Aerosol time-of-flight mass spectrometer |
| BVOC | Biogenic volatile organic compound |
| C18 | Octadecyl functionalized silica |
| CC | Carbonate carbon |
| CCN | Cloud condensation nuclei |
| CE-ESI-MS | Capillary electrophoresis-electrospray ionization-mass spectrometry |
| CMB | Chemical mass balance |
| Da | Dalton, one twelfth of the mass of an unbound neutral atom of carbon-12 |
| DEAE | Diethylaminoethyl |
| DMA | Differential mobility analyser |
| DPF | Diesel particle filter |
| EC | Elemental carbon |
| EC _D | Elemental carbon stemming from diesel vehicles (calculated) |
| EC _w | Elemental carbon stemming from wood smoke (calculated) |
| ELSD | Evaporative light scattering |
| ESI-FTICR-MS | ESI-Fourier-transform ion cyclotron resonance MS |
| ESI-MS | Electrospray ionisation mass spectrometry |
| FA | Fulvic acid |
| FID | Flame ionization detector |
| FTIR | Fourier transform infrared spectroscopy |
| GC-MS | Gas chromatography-mass spectrometry |
| GF-AAS | Graphite furnace- atomic absorption spectroscopy |
| HA | Humic acid |
| HLB | Hydrophilic-lipophilic-balanced |
| HNMR | Proton nuclear magnetic resonance |
| HPLC | High performance liquid chromatography |
| HTSR | HULIS/tracer-source ratio |
| HULIS C | Carbon bound to HULIS |
| HULIS | Humic-like substances |
| HULIS _{AS} | Alkaline soluble fraction of HULIS |
| HULIS _{Prim, DVE} | HULIS emitted primarily by Diesel vehicles (calculated) |
| HULIS _{Prim, WSE} | HULIS emitted primarily by wood stoves (calculated) |
| HULIS _T | Total fraction of HULIS (in the present work sum of HULIS _{AS} and HULIS _{WS}) |

| | |
|---------------------------|---|
| HULIS_{ws} | Water soluble fraction of HULIS |
| ICP-OES | Inductively coupled plasma optical emission spectrometry |
| IR | Infrared |
| ITMS | Ion trap mass spectrometry |
| LDI-MS | Laser desorption/ionization mass spectrometry |
| LOD | Limit of detection |
| LOQ | Limit of quantitation |
| LVOC | Low-volatile organic compound |
| LV-OOA | Low-volatility oxygenated organic aerosol |
| m/z | Mass-to-charge-ratio |
| MALDI-MS | (Matrix assisted) Laser desorption ionisation mass spectrometry |
| MMC | Macromolecular compounds |
| MW | Molecular weight |
| NDIR | Non-dispersive infrared |
| NEXAFS | near-edge X-ray absorption fine structure spectroscopy |
| NVOC | Non-volatile organic compound |
| OC | Organic carbon |
| OM | Organic matter |
| ON | Organonitrate |
| ORVOC | Other reactive volatile organic compound |
| OS | Organosulfate |
| PAH | Polycyclic aromatic hydrocarbons |
| PEG | Polyethylene glycol |
| PM1 | Particulate matter with an aerodynamic diameter < 1 μm |
| PM10 | Particulate matter with an aerodynamic diameter < 10μm |
| PM10_w | PM10 stemming from wood smoke |
| PM2.5 | Particulate matter with an aerodynamic diameter < 2.5 μm |
| PMA | Polymethacrylic acids |
| r | Correlation coefficient |
| R² | Coefficient of determination |
| ROS | Reactive oxygen species |
| RP-HPLC-FLD | Reversed phase high pressure liquid chromatography with fluorimetric detection |
| SAX | Strong anion exchange |
| SEC-UV | Size exclusion chromatography |
| SOA | Secondary organic aerosol |
| SOC | Secondary organic carbon |
| SPE | Solid phase extraction |
| SRFA | Suwannee River fulvic acid |

| | |
|-----------------------|--|
| SVOC | Semi-volatile organic compound |
| SV-OOA | Semi-volatility oxygenated organic aerosol |
| TOC | Total organic carbon analyser |
| UF | Ultra filtration |
| UV-VIS | Ultraviolet and visible portion of the electromagnetic spectrum |
| VDTMA | Volatility tandem differential mobility analyser |
| VOC | Volatile organic compound |
| VPO | Vapour pressure osmometry |
| WSOC | Water soluble organic carbon |
| WSOM | Water soluble organic matter |
| XAD-2 | Hydrophobic cross linked polystyrene copolymer resin |
| ¹³C | Isotopic ratio of ¹³C/¹²C between a sample and reference standard |

Index

| | |
|---|-------------|
| Abstract | i |
| Kurzfassung | iii |
| Personal Acknowledgements | vi |
| General Acknowledgements | vii |
| Glossary | viii |
| Index | xi |
| 1 Introduction | 1 |
| 2 Aim and Outline | 3 |
| 3 Literature Review | 4 |
| 3.1 Appearance of HULIS on the Stage of Aerosol Science | 4 |
| 3.2 The Eponyms-Terrestrial and Aquatic Humic Acids..... | 5 |
| 3.3 Nomenclature of Fractions of Organic Aerosol related to HULIS..... | 7 |
| 3.4 Studies on Characterisation and Quantification of atmospheric HULIS | 9 |
| 3.5 Laboratory Studies | 21 |
| 3.6 Atmospheric Relevance and physical Properties of HULIS-Recent Findings Bit by Bit | 24 |
| 3.7 Overview and open Questions..... | 28 |
| 4 Sampling Sites | 35 |
| 5 Sampling | 53 |
| 5.1 Atmospheric PM10..... | 53 |
| 5.2 Source samples | 53 |
| 6 Analytical Methods | 55 |
| 6.1 Extraction, Separation and Quantification of HULIS | 55 |
| 6.2 Analytical Methods for other Species and Parameters..... | 58 |
| 6.2.1 Weighing and sample preparation..... | 58 |
| 6.2.2 Ions..... | 59 |
| 6.2.3 Cellulose | 59 |
| 6.2.4 Carbon Analysis | 59 |
| 6.2.5 Anhydrosugars, Sugars and Sugar Alcohols | 60 |
| 6.2.6 Metals..... | 60 |

| | | |
|----------|--|------------|
| 6.2.7 | Organic Trace Components | 61 |
| 6.2.8 | Gaseous compounds | 61 |
| 7 | A three City Study: Seasonal Behaviour and possible Origin of atmospheric HULIS..... | 62 |
| 7.1 | Introduction | 62 |
| 7.2 | Experimental | 62 |
| 7.2.1 | Ambient Aerosol Samples | 62 |
| 7.2.2 | Source Samples | 64 |
| 7.2.3 | Extraction, Isolation and Quantification of HULIS..... | 65 |
| 7.2.4 | Determination of other Species and Parameters | 66 |
| 7.3 | Results | 66 |
| 7.3.1 | Analytical Performance..... | 66 |
| 7.3.2 | HULIS Carbon Quantification and Humic Acid Standard | 67 |
| 7.3.3 | Comments on recent Comparisons of Methods for Isolation, Separation and Quantification of HULIS | 70 |
| 7.3.4 | Atmospheric Abundance, spatial Variation and seasonal Patterns of HULIS _T in Austrian PM10..... | 79 |
| 7.3.5 | Contributions of HULIS _T to PM10 and Organic Carbon..... | 84 |
| 7.3.6 | Water and alkaline soluble Fractions of HULIS..... | 88 |
| 7.3.7 | Meteorological Influence on the Seasonality of HULIS _T | 95 |
| 7.3.8 | Estimations on the primary Emissions of HULIS _T | 101 |
| 7.3.9 | Seasonal resolved Correlation Analysis..... | 117 |
| 7.4 | Discussion..... | 126 |
| 8 | HULIS over Austria- Spatial and temporal Variations of HULIS_T and Wood Smoke | 129 |
| 8.1 | Experimental | 129 |
| 8.2 | Results | 130 |
| 8.2.1 | Atmospheric Abundance | 130 |
| 8.2.2 | Seasonal Variations | 130 |
| 8.2.3 | Contributions of HULIS _T Carbon to OC and HULIS _T to PM10..... | 133 |
| 8.2.4 | Wood Smoke and HULIS _T - Comparison of atmospheric Abundance of HULIS _T and Levoglucosan | 136 |
| 8.3 | Discussion..... | 143 |
| 9 | Thermal Characterisation of HULIS_{AS} and HULIS_{WS} isolated from Upper Austrian PM10..... | 146 |

| | | |
|-----------|--|------------|
| 9.1 | Sampling Sites and chemical Analysis | 146 |
| 9.2 | Results | 148 |
| 9.2.1 | The Colour of HULIS and thermal Characteristics of Humic Acid Standards.. | 148 |
| 9.2.2 | General Characteristics of Thermograms of HULIS | 149 |
| 9.2.3 | Comparison of thermal Characteristics of HULIS _{WS} and HULIS _{AS} | 152 |
| 9.2.4 | Spatial and seasonal Variations of thermal Characteristics of HULIS Isolates | 154 |
| 9.3 | Discussion..... | 160 |
| 10 | Summary and Conclusions | 162 |
| | References | 167 |
| | List of Tables | 192 |
| | List of Figures..... | 194 |
| | List of Equations | 200 |
| | Appendix | 201 |

1 Introduction

The impact of aerosols on the atmosphere, the climate and on public health is the central driving force in current environmental research. Aerosol particles absorb and scatter solar and terrestrial radiation, are involved in the formation of clouds and precipitation as cloud condensation nuclei (Hitzenberger et al., 1999) and affect the abundance and distribution of atmospheric trace gases by heterogeneous chemical reactions and other multiphase processes (reviewed by Pöschl, 2005; based on Houghton et al., 2001; Lohmann et al., 2005; Finlayson-Pitts et al., 2000; Seinfeld et al., 1998). Furthermore, airborne particles play an important role in the spreading of biological organisms, reproductive materials and pathogens such as pollens and bacteria (Bauer et al., 2002 a and b; Bauer et al., 2003) and can negatively influence human health by causing or enhancing respiratory, cardiovascular, infectious and allergic diseases (Bernstein et al., 2004; Finlayson-Pitts et al., 1997; Figure 1).

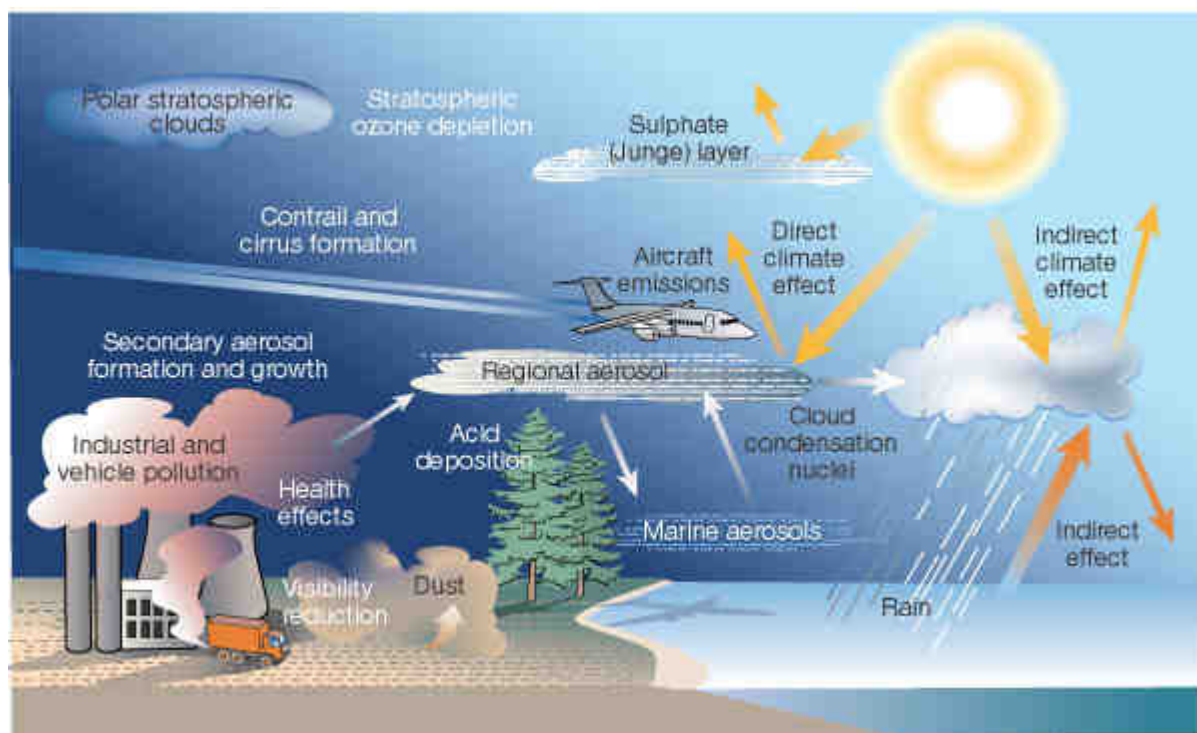


Figure 1: Aerosols — the big picture (from Kolb, 2002)

In his review Pöschl (2005) stated, that aerosol research is confronted with challenging properties of atmospheric aerosol such as their wide range of particle diameters, the contribution of hundreds of compounds to aerosol composition and the high spatial and temporal variability of amount, size and composition of airborne aerosol. Organic compounds are, together with sulphate, nitrate, ammonium, sea salt, mineral dust and black or elemental carbon, a predominant fraction of airborne particulate matter. Each of these major contributors typically accounts for about to 10 – 30 % of the mass load. At

different locations, times, meteorological conditions and particle size fractions, the relative abundance of different chemical components can vary by an order of magnitude or more (Pöschl, 2005). The ubiquitous carbonaceous aerosol components, including black or elemental carbon and organic compounds, exhibit a wide range of molecular structures. To determine the overall mass, molecular composition, physicochemical properties and potential toxicity of organic air particulate matter, the identification of all relevant chemical components on a molecular level is necessary. Although a myriad of individual organic compounds have been identified so far, together they constitute only a minor fraction of organic carbon (OC) of urban and rural aerosol (Saxena et al., 1996; Puxbaum et al., 2000; Rogge et al., 1993a).

Major contributors to continental organic aerosol were found to be water and alkaline soluble high molecular weight compounds (Havers et al., 1998; Zappoli et al., 1999) with chemical characteristics very similar to naturally occurring terrestrial and aquatic humic acids, therefore termed **HUmic-Like Substances (HULIS)**. HULIS are able to affect aerosol properties, due to their ability to form cloud condensation nuclei and light absorbing characteristics (e.g. Zelenay, 2011) and may even influence the ozone budget on a regional scale (Baduel et. al, 2011). Very recently even strong evidence was found that HULIS may have adverse health effects, by catalyzing reactive oxygen species generation, thus causing oxidative stress in affected cells (Lin et al., 2011). A growing body of studies broaches the issue of their occurrence in aerosol, cloud and rain water, analytical methods for chemical characterization and quantification, laboratory studies concerning possible formation pathways, potential precursor substances, physical properties and their role in atmospheric processes.

2 Aim and Outline

The present work aims at elucidating the seasonal and spatial variation of HULIS_T (as sum of water and alkaline soluble HULIS) in airborne PM₁₀, potential sources, possible primary shares contributing to atmospheric HULIS, meteorological influences on HULIS winter enrichment and differences and similarities between the alkaline and water soluble fraction of HULIS.

Chapter 3 gives an extensive overview on HULIS research from the very beginning on up to now (based on the work of Graber and Rudich, 2006 and Gelencsér, 2004) and highlights questions that are still unanswered. Chapter 4 provides information on the characteristics of the 23 Austrian sampling sites. Details on sampling methods and sample pooling can be found in Chapter 5. Extraction of HULIS and analytical analysis of HULIS and other analytes are described in detail in Chapter 6.

Chapter 7 presents spatial and seasonal variations of HULIS_T in three Austrian cities at sites with urban as well as rural characteristics. Furthermore meteorological influences on HULIS winter enrichment is investigated by establishing an atmospheric dilution tracer. Observations of correlations between HULIS_T and other aerosol constituents shed light on potential sources of HULIS_T and last but not least the potential primary emission of HULIS_T is estimated by quantifying HULIS_T in source emission samples and establishment of an HULIS/ tracer – source ratio.

Chapter 8 compares abundance and seasonality of HULIS_T at the 23 Austrian sites and investigates the relationship of biomass burning and HULIS_T in the different regions and seasons.

Chapter 9 presents thermal characterisation of HULIS_{WS} and HULIS_{AS} isolated from a rural background site and an urban traffic impacted site in Upper Austria in airborne PM₁₀ collected in the January and July.

3 Literature Review

HULIS have been puzzling atmospheric scientists now for more than three decades, leaving them busy with answering questions, regarding their chemical structure, physical properties and their involvement in atmospheric processes, their primary or secondary origin, thus sources and precursors and seasonal and spatial variations of HULIS characteristics and abundance, to name a few. Figure 2 gives an impression on the number of publications on this topic since the term HULIS was coined in (Havers et al., 1998). The present chapter gives an insight in conducted scientific research on HULIS in aerosol science from the very beginning down to the present day, based on the reviews of Graber and Rudich (2006) and Gelencsér (2004), and highlights open questions and crucial issues.

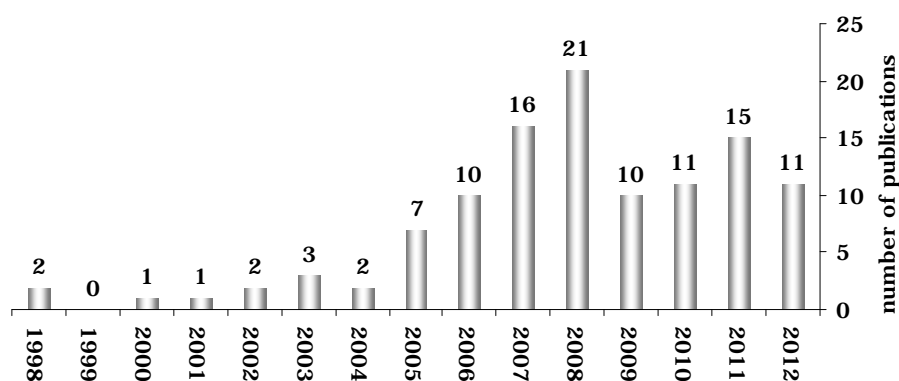


Figure 2: Scientific publications containing the keyword “HULIS” (from SciFinder®)

3.1 Appearance of HULIS on the Stage of Aerosol Science

Graber and Rudich (2006) and Gelencsér (2004) reviewed the first steps of HULIS on the stage of aerosol science. Highlights of their reviews are presented in this subchapter. First evidence for such humic-like substances in airborne particulate matter was reported as early as 1980 by Simoneit. In this work a terrestrial soil origin, due to H/C ratios and ^{13}C values, was suggested, corresponding to the actual origin of dust particles. In a later Japanese study of rural aerosol, humic substances were reported to contribute in a range of 1-6 % to the total organic carbon fraction (Mukai and Ambe, 1986). Infrared and UV-VIS spectroscopic investigations and elemental fingerprinting observations revealed that humic acids extracts were most similar to extracts from biomass burning smoke particles. The authors also suggested a polycyclic ring structure with hydrocarbon side chains, and hydroxyl, carboxyl and carbonyl groups. This general chemical structure

for atmospheric HULIS suggested more than 30 years ago is still the current consensus. Remarkably, the examination of particles from biomass burning was an early attempt to link the existence of atmospheric HULIS to this source and nowadays is still assumed to be a major source. A different approach in the early eighties by fractionating dissolved macromolecular organic carbon in rural rain water by ultrafiltration techniques was achieved by Likens and Galloway (1983). The macromolecular portion accounted for 35 – 43 % to the total organic carbon, with carbohydrates, tannins, lignins and organic nitrogens being important constituents. Based on the chemical attributes, degradation and dissolutions of, plant structural material was suggested to be the source of the macromolecular fraction. At about the same time, another line of research was started. These studies were the very first to establish the presence of polymeric matter in fine aerosol and postulated its secondary origin. In the thermograms of rural aerosol samples poorly resolved peaks were distinguished by Puxbaum (1979), and postulated to originate from biogenic polymeric substances. Ellis and Novakov (1982) observed such peaks, in thermograms from aerosol collected at an urban and a receptor site in the region of Los Angeles during periods of intense photochemical smog. They suggested the two poorly resolved peaks occurring between 230 and 450 °C to be a first order measure for secondary organic carbon and suggested them to be of high molecular weight polymeric material, judged solely on the basis of their thermal/optical properties. These assumptions were ground-breaking from a present-day point of view, but at that time, didn't find widespread recognition (Gelencsér, 2004). More than ten years later Havers et al. (1998) observed macromolecular substances similar to humic and fulvic acids in airborne particulate matter and launched the term humic-like substances (HULIS).

3.2 The Eponyms-Terrestrial and Aquatic Humic Acids

Humic substances constitute a complex class of refractory organic macromolecules, mainly produced by microbial degradation of plant residues (Stevenson et al., 1994; Allard et al., 1991). Their physico-chemical properties, the history of structural suggestions and analytical separation techniques were reviewed and summarised by Graber and Rudich, (2006) and Fooker (1999). Humic substances represent a significant sink in the global carbon cycle and play an important role in the fertility of soils and a number of processes in aquatic environments. Humic substances may form various chemical species of high stability with environmentally relevant trace constituents like heavy metals and pesticides, and are therefore supposed to be responsible for the transport and bioavailability of pollutants. In contrast to most substances in chemistry, humic substances are not defined according their molecular structure but to their solubility characteristics due to their high

complexity and diversity (Havers et al., 1998; Graber and Rudich, 2006 and references therein). Humic substances are classified (Stevenson et al., 1994) into:

- fulvic acids: soluble in aqueous acids and alkalis
- humic acids: not soluble in acids, but soluble in alkalis
- humins: insoluble in acids and alkalis

The colours of humic substance fractions range from bright yellow to golden brown (fulvic acid), through dark brown to greyish black (humic acids) to deep black (humins) (Fooker, 1999 and references therein). HULIS isolates from aerosol samples extracted with the technique applied in the present work appear in the same colour tones as fulvic acids of terrestrial and aquatic origin. First suggestions for the structure of aquatic or terrestrial humic acids were proposed by Fuchs et al (1930) based on determinations of carboxylic and phenolic hydroxyl functional groups. This model was dominated by an aromatic structure with phenolic and carboxylic moieties. Aliphatic side chains and hetero atoms such as nitrogen and sulphur, always traceable in humic acids, were not included in the model. Numerous suggestions for possible structures followed (Dragunov et al., 1948; Haworth et al., 1971; Schnitzer et al., 1978) with the latter suggesting a polycyclic aromatic building block connected via hydrogen bridges, Van-der-Waals forces or atomic bonding with phenolic acids, hydrocarbons, metals and peptides. The most complex structure was suggested by Schulten and Leinweber in 1996 (Figure 3). The modelled structure is based on data of numerous studies of aquatic and terrestrial humic acids, where results from pyrolysis, spectroscopic and elemental analysis, electron microscopy, oxidative and reductive degradation and colloidal investigations were applied, resulting in a structure consisting of 738 atoms.

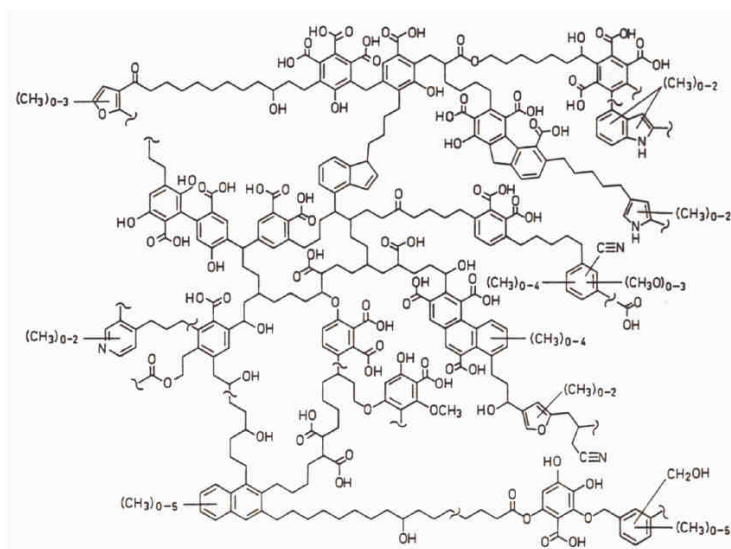


Figure 3: Suggested structure for aquatic humic acid after Schulten and Leinweber, 1996.

Aromatic cores connected by aliphatic chains with $-\text{COOH}$, $-\text{CH}_2\text{OH}$, $-\text{COCH}_3$ or $-\text{CH}_3$ terminal groups are as well a widely accepted structure for atmospheric HULIS, described in more detail in the following. The classic theory on the formation of humic substances suggests the microbial degradation of biopolymers such as lipids, carbohydrates, proteins, lignin and pigments stemming from dead organisms, into smaller units. These building blocks (e.g. sugar, amino acids, fatty acids, aromatic hydrocarbons, phenols or organic acids) condense or polymerize to fulvic acid. After further polymerization and condensation reactions humic acid and at the end humins are formed (Schnitzer et al., 1978; Dereppe et al., 1980). Departing from this approach Vanderbroucke et al. (1985) suggests a primary humic substance stemming from dead plant material that is converted to secondary humic substances via biological and chemical condensation reactions. This approach is supported by the fact that humic substances can be extracted from dead as well as from fresh plant material. Hatcher and Orem (1985) are turning it the other way round and claim humins as precursor substances for fulvic and humic acids via oxidative degradation and incorporation of microbial generated polysaccharides. Terrestrial and aquatic humic substances and their airborne equivalent HULIS do not only feature similarities in their chemical properties but both leave still open questions concerning their formation pathways.

3.3 Nomenclature of Fractions of Organic Aerosol related to HULIS

Before examining the state of knowledge regarding chemical properties, formation pathways and atmospheric occurrence of HULIS, this chapter gives a short overview about terms that occurred in literature, naming fractions of organic aerosol that are suggested to be related or even overlapping with the (operationally defined) fraction of humic-like substances (Figure 4).

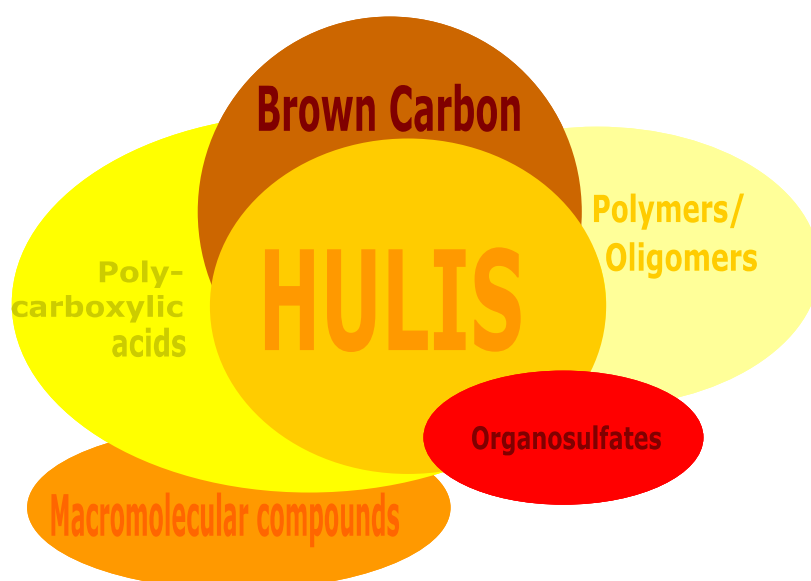


Figure 4: Terms reported in literature, naming fractions of organic aerosol, related to HULIS.

Airborne humic-like substances (HULIS) are regarded as polymeric material with polar, polyacidic and chromophoric properties and high molecular weights of several hundred Dalton. The different terms, displayed in Figure 4, developed according to the observed chemical or physical characteristics and the applied analytical method. To some extent the willingness to link observed properties of “HULIS” of airborne organic aerosol to those of humic acids of terrestrial and marine origin may be reflected as well (Gelencsér et al., 2004). “HULIS”, “polycarboxylic acids” (e.g. Decesari et al. 2000) and “macromolecular compounds” (MMC) (e.g. Zappoli et al., 1999) are notions stemming from investigations on atmospheric aerosol and are assumed to overlap to large extents due to observed characteristics of the respective fractions such as water-solubility, polyacidic appearance (HULIS-Polycarboxylic acids) (Gelencsér et al., 2004) and their atmospheric occurrence being strongly connected to biomass combustion (HULIS-MMC), respectively. The terms oligomers/polymers (used in context with organic aerosol science) originated from smog-chamber observations (e.g. Kalberer et al., 2004; Baltensperger et al., 2005) where molecules with masses up to 1000 Da were observed in aerosol generated via photo-oxidation or ozonolysis of biogenic or anthropogenic gaseous precursors (e.g. Kalberer et al., 2004; Baltensperger et al., 2005) and were linked to HULIS due to their size, albeit it is not clear to which extent these “polymers/oligomers” are in fact water-soluble. Organosulfates were recently suggested to form a subset of HULIS (e.g. Gomez et al., 2008) referring to their water-solubility, acidity, thermal stability and high-molecular weights (Surratt et al., 2007). Both, organosulfates and oligomers, were detected in atmospheric as well as in smog-chamber generated aerosols. Very recently organosulfates finally were determined in water soluble HULIS isolates from airborne PM10 in East Asia by Lin et al. (2012a). “Brown carbon” is defined as light-absorbing organic matter (other than soot) in atmospheric aerosol of various origins (Andreae and Gelencsér, 2006). Water-soluble brown carbon was linked to HULIS due to its light-absorbing properties and similar atmospheric behaviour (Lukács et al., 2007). Brown carbon was determined with the integrated sphere method in atmospheric aerosol (PM10) and compared to biomass smoke particulate organic matter and HULIS levels during biomass smoke episodes caused by Easter bonfires (Wonaschütz et al., 2009). Not enough with different notions for possible overlapping fractions of organic aerosol, the term “HULIS” itself is applied for fractions isolated and quantified with several principally different methods. Thus even if accordance might be given regarding the general properties of observed fractions it is unclear to which extent atmospheric scientists are speaking about the same thing, if they are talking about HULIS as such. It is highly desirable to investigate the various “kinds” of HULIS on chemical structure and molecular size. Additionally it would be very helpful as well to quantify HULIS in atmospheric samples in an inter-laboratory comparison. Details on methods mentioned

above as well as the converging of results from laboratory studies and atmospheric observations are treated in the following subchapters.

3.4 Studies on Characterisation and Quantification of atmospheric HULIS

This subchapter is based on the extensive reviews conducted by Graber and Rudich (2006) and Gelencsér (2004). For a better overview and readability of the scientific history of HULIS, from the beginning until the year 2005, their reviews are compiled in this subchapter.

Havers et al. (1998) found macromolecular substances similar to humic and fulvic acids in airborne particulate matter, contributing up to 10 % or more to aerosol organic carbon, and introduced the term HULIS. The alkaline extracts of these substances were isolated by ion exchange and characterised with various methods. Humic acids were first reported in aeolian dust by Simoneit (1977 and 1980) and therefore the occurrence of HULIS in soil-derived aerosol seemed to be well understood. However, Havers et al. (1998) argued, that dust particles from soil surfaces are most likely a minor source for airborne HULIS, because of the different molecular weight distribution of terrestrial humic substances.

Almost contemporaneously with the findings of Havers et al. in 1998, Zappoli et al. (1999) published results on the bulk properties of water soluble organic matter in aerosol from a rural site in the Great Hungarian Plain and a polluted site in the Po Valley. Their major finding was that water soluble organic carbon (WSOC) made up a significant fraction of fine aerosol carbon, and its detailed analytical characterization revealed as well resemblance to reference humic acid. Zappoli et al. (1999) termed this fraction “macromolecular”, although none of their analytical methods yielded direct evidence that these species were indeed of high molecular weight (Gelencsér, 2004).

Similar chemical characteristics of HULIS than those of humic acid were observed by Gelencsér et al. (2000a and b). Combination of a thermal profiling method, evolved gas analysis, together with water extraction revealed additional features of bulk organic matter. About half of the refractory aerosol component appeared to be soluble in water. The thermal properties of this refractory carbon differed from those of the coarse aerosol, but seemed to resemble those of a reference humic acid on pre-baked quartz filters (Gelencsér et al., 2000a). It was shown that the electrochemical properties and metal-complexing ability of bulk organic matter in polluted fog water were nearly the same as those of a reference humic acid (Gelencsér et al., 2000b). Capillary zone electrophoresis of polluted fog water and aqueous extract of rural fine aerosol suggested a broad distribution of charge-to-size ratios of HULIS (Krivácsy et al., 2000). The observed pH-dependence implied that most acidic groups were found to be weaker acids than acetic acid (Gelencsér et al., 2004).

Decesari et al. (2000) separated the WSOC of the fine aerosol collected at a polluted site and the organic fraction was divided into three classes by preparative ion-exchange chromatography. These were neutral/basic compounds, mono- and dicarboxylic acids, and polycarboxylic acids. They determined the chemical structure of these broad compound classes by ^1H NMR spectrometry. The spectra of the neutral/basic compounds revealed the presence of mainly hydroxylated/alkoxylated aliphatic species, with indications for the presence of polyols. Mono- and dicarboxylic acids were shown to be predominantly aliphatic carboxylic acids and hydroxycarboxylic acids, whereas polycarboxylic acids had a more pronounced unsaturated character, with an aromatic core having aliphatic chains with acid and hydroxyl terminal groups. The SRFA standard showed similar retention time on the weak anion exchanger as the polyacidic fraction (Decesari et al., 2000). Mono- and diacids were the most abundant WSOC fraction in summer, whereas the rest of the year the polycarboxylic acids dominated (Decesari et al., 2001). A large fraction of the WSOC was UV-absorbing, and the specific UV-absorptivity was highest for the class of polycarboxylic acids. Varga et al. developed another preparative-scale separation method for the isolation of HULIS from the aqueous extracts of aerosol (2001). They developed a method to isolate the fraction of WSOC that retained the key spectral properties also characteristic for reference humic and fulvic acids. The elemental composition of HULIS, isolated with the method developed by Varga et al. (2001) from rural fine aerosol, was found to be remarkably constant throughout the year (Kiss et al., 2002). Furthermore Gelencsér (2004) stated, that a step towards the understanding of the origin of HULIS in rural aerosol collected in summer was the determination of their molecular weight distribution by ultrafiltration (UF), liquid chromatography-atmospheric pressure ionization mass spectrometry, and vapour pressure osmometry (Kiss et al., 2003). One finding of this study was that virtually all WSOC passed through an ultrafiltration membrane having a 500 Da nominal molecular weight cut-off. The isolated HULIS was further characterized by determining the ion mass distribution which was found to be continuous between about 100 and 500 Daltons, with maxima in the range of 200-300 Da. These conclusions were confirmed by vapour pressure osmometry which provided direct estimates for the average MW of HULIS. The average molecular weight was found to be markedly lower than those of reference aquatic humic and fulvic acids under the same conditions. These observations are among the very few that pointed to important differences between HULIS and natural humic substances, and therefore imply distinct formation mechanisms. Yu et al. have evaluated the mass size distributions of WSOC in marine and continental aerosol (Yu et al., 2004). Regardless of their origin, WSOC in aerosol exhibited a bimodal size distribution, with a dominant fine mode and a minor coarse mode having mass mean aerodynamic diameters of 0.7 ± 0.1 and 4.0 ± 0.3 μm , respectively. The mass in the fine mode ranged from two-thirds to four-fifths of that of the total WSOC. Both modes were further deconvoluted to low, medium, and high molecular weight polar compounds based

on their thermal evolution features. While the low molecular weight species had a bimodal distribution with a dominant coarse mode, the medium and high molecular weight compounds exhibited a single peak in the droplet mode. This was interpreted as evidence that these latter species—which might also be humic-like substances—likely form during cloud-processing of aerosol. This finding would support the possible formation of HULIS in cloud processes (Gelencsér et al., 2003).

Very few analytical techniques are capable of providing chemical information directly on the carbonaceous component of the bulk aerosol collected on filter substrates or impactor plates. One of these methods, however, is pyrolysis-gas chromatography-mass spectrometry which allows organic structure elucidation directly from aerosol filters. Taking into account the fact that HULIS contains functional groups (e.g. carboxylates) which yield non-specific thermal decomposition products (e.g. carbon dioxide) upon conventional analytical pyrolysis a derivatization technique was introduced (Gelencsér et al., 2000c). The thermally assisted hydrolysis-methylation allowed labile functional groups to be converted into their respective esters, thus preventing decarboxylation upon pyrolysis and yielding more specific pyrolysis products. The analysis of rural fine aerosol by this method revealed overall structural similarities to those of natural humic substances. The predominant pyrolysis degradation products both in aerosol and terrestrial humic acids were n-alkanoic acids, α,ω -dicarboxylic acids (in the carbon number range of C₄–C₉), and benzene dicarboxylic acids. The apparent structural similarity to terrestrial humic substances made the authors suggest the term “atmospheric humic matter” in place of HULIS. The rationale behind this suggestion was that HULIS in aerosol were thought to be chemically indistinguishable from the wide variety of natural humic substances present in other reservoirs (Gelencsér, 2004). Using the same method Subbalakshmi et al. found similar compounds in urban aerosol, except that there higher substituted lignin pyrolysis products were also observed (2000). The pyrograms of biomass burning aerosol from Brazil, however, revealed some differences with respect to those of rural fine aerosol (Blazsó et al., 2003). Most importantly, in biomass burning aerosol there were several higher substituted aromatic compounds which were absent from rural aerosol. These species—which are typical lignin degradation products—were also shown to be present in the pyrogram of soil humic and fulvic acids (Martin et al., 1994; reviewed by Gelencsér, 2004).

Samburova et al. (2005a) investigated water-soluble humic-like substances (defined as substances eluting after SEC with nominal MW > 300 Da calibrated with PMA and PGA in ambient urban aerosol with size exclusion chromatography-UV spectroscopy (SEC-UV) and laser desorption/ionization mass spectrometry (LDI-MS). They found two major peaks in the high-molecular-range between 200 and 600 Da with both, SEC-UV and LDI-MS. In a follow up study (Samburova et al. 2005b) they found that maximum molecular weight of atmospheric HULIS occurred to be significantly higher in winter than in

summer. Since additionally positive correlations with temperature and ozone in summer were found they suggested secondary, photochemically driven formation processes of “summer”-HULIS. Analysing ^{14}C in several carbon containing particle fractions from the same filters revealed that 80 % of the total organic carbon was not from fossil fuel sources and up to 38 % of the total OC was attributed to biomass burning (Szidat et al., 2004) they suggested a substantial fraction of HULIS in winter to stem from primary emissions from wood combustion.

Duarte et al., 2005a developed a method where they isolated a fraction of WSOC which they linked to water soluble polyacidic substances and, albeit not explicitly mentioned, HULIS. The gained isolates were quantified via the colorimetric detection of CO_2 . Application of this method on ambient $\text{PM}_{2.5}$ samples from a rural site near Aveiro (Portugal) and structural investigations of the extract with several spectroscopic methods revealed aliphatic structures, carboxyl groups and aliphatic carbons single bonded to one oxygen or nitrogen atom. The higher aromaticity of WSOC extracts from sampling during the cold season and spectral features similar to lignin breakdown products made them suggest biomass burning as a major contributor to atmospheric HULIS abundance (Duarte et al., 2005b).

Several authors (Table 2, based on Kalberer et al., 2006; updated and extended by extraction/isolation techniques) used spectroscopic methods such as UV absorption and fluorimetric detection for quantifying HULIS with humic substances as surrogate for calibration standards. One drawback of these analytical methods for the determination of HULIS is that they rely strongly on the spectroscopic properties of the calibration standard, although it is not yet clarified how similar humic substances and HULIS are actually regarding their structure. To overcome this problem response factors with reference samples were determined to correlate the UV signal of separated HULIS with dissolved organic carbon of the investigated samples (Decesari et al., 2001). This type of quantification assumes that UV-absorbing compounds are representative for the whole water soluble fraction of the organic aerosol and that the chemical composition of the investigated samples is similar to that of the reference samples. The method applied in the present work (Limbeck et al., 2005) overcomes these drawbacks by direct determination of isolated HULIS carbon. The liquid chromatographic method for the separation of HULIS from other organic aerosol constituents followed by the quantification of the organic carbon content, reported by Limbeck et al., 2005, is based on an off-line C_{18} solid phase extraction (SPE) for pre-separation and pre-concentration and an anion exchange micro-column flow injection system coupled with a detection system for the carbon-specific determination of HULIS. The two pre-separation steps, one by polarity the second by acidity, ensure that only carbon stemming from humic-like substances is detected. The obtained detection limits are among the lowest known values in the literature for humic-like substances with respect to the small sample volumes used for

analysis. This allows the direct determination of HULIS carbon in environmental samples even for samples with restricted sample amounts. The main advantage of this method is the considerable chemical selectivity achieved by combination of two separation steps with different mechanisms, excluding interferences with organic matrix constituents present in airborne particulate matter and the possibility of preparative isolation of HULIS for further analytical investigations.

In 2005 aerosol compounds got into the scope of interest that were suggested to substantially contribute to airborne HULIS due to their high water-solubility and high molecular weights, the organosulfates. Ion trap mass spectra of aqueous aerosol extracts from ambient samples gave first evidence of the existence of sulphate covalently bound to HULIS (Romero et al., 2005). Generally, sulphation occurs either by addition of sulphuric acid to alkenes or by esterification of an alcohol with sulphuric acid. Considering the chemical conditions for a sulphation (water, sulphate/sulphuric acid and HULIS), the possibility of sulphation in aerosol droplets in the atmosphere is real, but concerning this study it was not possible to distinguish between a sulphation process of HULIS in the atmosphere, on the filter after collection or in the extract solution (Romero et al., 2005). These reservations were negated by Liggio et al. in 2006 who observed organosulfates in studies of pinonaldehyde reactions with acidic sulphate aerosols using aerosol mass spectrometry, during which a significant fraction of the pinonaldehyde reaction products was found to consist of organosulfate compounds that account for 6-51% of the initial SO₂ mass. Resultant aerosol mass spectra were consistent with proposed sulphate ester formation mechanisms, which likely form stable products. The existence of organosulfates was also confirmed in studies of the reaction system in bulk solution. Further studies confirmed the formation of organosulfates in chamber experiments with biogenic precursor model compounds via the ozonolysis of β -pinene (Iinuma et al. 2007), the photooxidation mixtures of monoterpenes (e.g. pinene, limonene, terpine, terpinolene) (Surratt et al, 2007 and 2008) and the photooxidation of isoprene and unsaturated fatty acids (Gomez et al., 2008). Each of the last three mentioned studies could confirm the existence of such compounds in ambient aerosol as well. Surratt et al., 2007, explicitly suggested organosulfate compounds to comprise a significant fraction of HULIS in atmospheric aerosol due their high water solubility, acidity, thermally stability and high-molecular weights, all of which are common properties of HULIS.

A method, a further development of the method reported by Fuzzi et al., 2001, relying on a separation of neutral compounds, mono-, di-, and polyacidic acids via HPLC and subsequent carbon quantification was reported by Mancinelli et al. in 2007. The water soluble fractions, separated via HPLC could be directly quantified by the total organic carbon analyser instead of former UV detection. Mono-carboxylic acids could be distinguished from dicarboxylic acids. Although this method seemed to be less time consuming a satisfactory separation of phenols, expected to occur in the neutral fraction,

and tri-carboxylic acids, that were also found in the fraction of dicarboxylic acids, was not reached. Reported atmospheric levels for the polyacidic fraction (~HULIS) were 0.05-1.8 $\mu\text{g C/m}^3$ for a rural site northern Italy in spring. As the method developed by Mancinelli et al. (2007), the method developed by Limbeck et al. (2005) uses carbon quantification as well, which was applied in the present work, where an interference study showed that phenols and tricarboxylic acids could be separated satisfactorily from the HULIS fraction. Another detection method that relies on accurate chromatographic separation of HULIS/oligomers from other particle components was presented by Emmenegger et al. (2007). The separation via SEC-UV and quantification of HULIS in aerosols by evaporative light-scattering is as well largely independent of the chemical properties of the calibration compounds. In their interference study they reported that from the tested substances, only phthalic acid was not separable from the HULIS fraction. Application of this method on aqueous extracted (preconcentrated via solid phase extraction on octadecyl bonded silica gel (C18)) of wintry suburban PM 1 samples yielded in HULIS shares of up to 6 % of PM1 and absolute HULIS levels of 0.46-2.29 $\mu\text{g/m}^3$. Their interference study unfortunately does not include the anhydrosugar levoglucosan, which can occur in similar concentrations as HULIS in biomass affected atmospheric aerosols (Caseiro et al., 2009) and might therefore also be recovered as HULIS. However the authors decided to overcome the potential interference of phthalic acid by defining and quantifying HULIS as the fraction eluting after SEC in a certain time window (retention time 5 -7 min). Investigation of the C18 eluate with ESI-MS showed most intense peaks between m/z 200-500 with maxima up to m/z 800.

Applying the quantification via ELSD on HULIS (isolated after the protocol of Varga et al., 2001) Samburova et al., 2007 presented further insights in atmospheric abundance of HULIS and, by H-NMR analysis, in their structure. Investigated ambient aerosol samples from summer and winter revealed contributions of aliphatic groups and carboxylic groups to HULIS of about 4 % and 5.5 %, respectively, for summer as well as winter samples. Arylic and phenolic groups were enriched in HULIS from samples collected during the cold season and accounted to HULIS occurring in winter aerosol for 1 and 5 %. The reason for the higher arylic and phenolic hydrogen concentration in winter was suggested to be the high ozone concentration and increased photochemical activity in summer, which leads to a faster degradation of aromatic compounds in aerosols. Additionally higher source strength of smoke stemming from wood combustion in winter could lead to higher concentrations of aromatic compounds in the particle phase.

Biomass burning for space heating was also suggested to be a major source for HULIS precursors in winter in a study of water and alkaline extractable atmospheric HULIS in samples from six background sites in Europe by Feczko et al. in 2007 (using the quantification method based on Limbeck et al., 2005) due to significant correlations between the biomass burning tracer levoglucosan and both observed HULIS fractions at

low continental background sites. In this study a distinct seasonal cycle was observed for the low level sites reflecting the regional source strength of HULIS. This work is one of the very few reported in literature that as well considers the alkaline extractable HULIS fraction, which approximately doubles the amount of water-soluble HULIS. The study of Feczko et al. (2007) was conducted in the framework of CARBOSOL a 2-year study of present-day carbonaceous aerosol in air and precipitation in western/central Europe with the trends of climatically relevant species in Alpine ice cores (Legrand et al., 2007b).

Within the same framework Lukács et al. (2007) investigated the atmospheric abundance of brown carbon, a light absorbing fraction of WSOC which is strongly linked to HULIS (e.g. Hoffer et al., 2006b) at the same six continental background sites. Brown carbon within this study was determined via UV/VIS measurements of the bulk WSOC. For quantification the UV/VIS method was calibrated with HULIS isolated (after the protocol reported by Varga et al., 2001) from a subset of aerosol samples. They found largely similar trends for brown carbon and HULIS. Another scope of interest within the CARBOSOL project was long-time changes in European aerosol, which were investigated by investigating alpine ice cores. Strong seasonality of brown carbon (after Lukács et al., 2007) was as well observed in this study. The authors as well observed an overall increasing trend for atmospheric brown carbon levels since the end of World War II, linking it to the increasing anthropogenic emissions thus enhancing the levels of potential precursor and atmospheric oxidants (Legrand et al., 2007 a). The link between biomass burning and the atmospheric occurrence of HULIS was as well confirmed with a totally different approach using near-edge X-ray absorption fine structure (NEXAFS) spectroscopy for investigating black carbon reference materials and individual carbonaceous atmospheric aerosols (Hopkins et al., 2007). The obtained NEXAFS spectra from biomass burning impacted aerosol showed very good agreement with those of humic and fulvic acid in contrast to aerosol stemming from regions heavily impacted by fossil fuel combustion.

The mass ratio between OM and OC (the organic-aerosol-to-organic carbon mass conversion factor) is one of the most important factors of uncertainty in aerosol chemical mass closure calculations involving OM. Investigating fractions of water soluble fractions in urban airborne particulate matter (PM 2.5) not affected by biomass burning at an urban site in Hungary, an OC/OM ratio of 1.81 was found (Salma et al., 2007). The authors found this factor in good agreement with factors for HULIS in rural and urban environments and factors for SOA formed in smog chamber experiments (Salma et al., 2007 and references therein). Furthermore they observed artefacts formed during sampling accounting for 20 % of the HULIS carbon on the front filter. They concluded that the direct adsorption of HULIS being a polymer-type material in considerable amounts on the (back) filters is rather unlikely due to their low volatility (Gelencsér et al., 2000a und 2000c). Therefore, it is thought that HULIS on the back filters were formed during the

sampling process by adsorption of volatile (aromatic) gaseous precursors on the filter surface, and by heterogeneous reactions with oxidants, which was followed by their formation processes (e.g., polymerization) similar to their formation paths in the atmosphere (Salma et al., 2007). However, since they stated in the same study that a disadvantage of their HULIS protocol is that some fatty acids, long-chain monocarboxylic acids, and aromatic alcohols could possibly remain in the isolated chemical fraction. Therefore it is possible they recovered some of those high or semi-volatile substances on the filters. The artefact corrected HULIS levels were in the range of $2 \mu\text{g}/\text{m}^3$ and contributed about 6% to atmospheric PM_{2.5} levels.

HULIS isolated from urban PM_{2.5} aerosol, quantified with a total organic carbon analyzer and characterised with UV/VIS and electrochemical impedance spectroscopy resulted in MW of 400 and 700, respectively, depending on the applied empirical correlation relationship (Salma et al., 2008a and references therein). The molecular weight for SRFA (Suwanee River fulvic acid) estimated in both cases was higher about a factor of ~ 1.5 . The aromaticity, estimated by molar absorptivity at 280 nm, was 16 % what was found to be in good agreement with the findings of Dinar et al., 2006a. In a subsequent work Salma et al., 2008b reported pK values of HULIS dissolved in water, derived for the negligible and significant anionic conductivities of 3.3 and 3.4, respectively. These acidity constants were found to correspond to moderately strong/weak common organic acids as formic acid (pK=3.74). The values obtained are in excellent agreement with that for fulvic and humic acids of pK=3.4 and 3.7, respectively and with that reported for the SRFA standard. The acidity constant is well comparable to the major maximum at pK=4.0 estimated by Samburova et al. (2007) for HULIS samples isolated from PM₁.

Polarity fractionation of atmospheric aerosols and characterization and quantification with FT-IR and carbon analysis, respectively, led to further insights in the chemical nature of suburban particulate matter (Polidori et al., 2008). The authors linked the fraction of organic aerosol that eluted with methanol to HULIS due to occurrence of a lignite humic acid standard in the same solvent fraction and the similarities to reported FT-IR spectra aquatic and terrestrial fulvic acids and airborne HULIS. The seasonality of observed characteristics in FT-IR spectra, with missing signals of polysaccharide substructures missing in summer samples, lead them to the conclusion that photochemical processes are a major pathway for the formation of HULIS and or oligomers. The observed OM/OC ratio ~ 2 is in good agreement with reported ratios in literature.

By applying a very complex extraction protocol on dew water, including extractions with DEAE columns, XAD-2 resins, precipitation via acidification and ultrafiltration, Okochi et al. (2008) differentiated between a humic acid and a fulvic acid fraction, contributing to approximately equal shares to the total dissolved HULIS. Correlation with potassium and the absence of soil derived ions such as calcium let them link the occurrence of HULIS in dew water to biomass combustion as well.

In one of the few studies in marine aerosol Krivácsy et al. (2008) found a more regular mass pattern in isolated marine HULIS compared to those extracted from urban aerosol suggesting this is caused by the presence of homologues of fatty acids. Moreover they observed the same seasonality for absolute marine HULIS levels as reported for continental urban and rural sites, namely lower levels during the warm and maximising levels during the cold season. UV-absorbance ratios (250 vs. 350 nm) as proxies for aromaticity, showed a trend for lower aromaticity during summer and at less polluted sites. Therefore the authors suggested this ratio possibly to be useful to differentiate between sources.

Stone et al., 2009 investigated water-soluble aerosol (PM_{2.5}) at several urban, suburban and rural sites in spring/summer with liquid chromatography tandem mass spectrometry. They found an upper limit of m/z at 600 in all aerosol samples. They compared the abundance of functional groups of the high molecular weight fractions to existing CMB (chemical mass balance) modelled source attributions and found that SOA (secondary organic aerosol) is an important pathway for the formation of high molecular weight compounds and HULIS. The comparison of standard humic/fulvic acid and ambient HULIS showed very similar m/z patterns. Interestingly the mass continuum for humic and fulvic acids tailed off at m/z 500, what is rather low for reported HA and FA. The major difference they found was the presence of organosulfates in ambient HULIS and the absence in reference humic substances.

In 2009, Baduel et al. presented a method based on an extraction step on DEAE cellulose and subsequent carbon determination with a TOC analyser. In their interference study they tested a variety of substances but did not perform tests on di- or triacids, which can be present in considerable amounts in the atmosphere. Especially in summer when HULIS concentrations are rather low and di- and triacids with MW above 130 can occur in considerable amounts ($\sim 0, 2 \mu\text{g C}/\text{m}^3$, Fisseha et al., 2006) these compound can co-elute and mimic about half of the HULIS fraction (e.g. Fisseha et al., 2006). A comparison of separation and extraction methods for HULIS (Fan et al., 2012) confirms the shortcoming of this method. The method by Varga et al., 2001 is as well affected by interferences of some carboxylic acids and oxy substituted aromatic compounds (Salma et al., 2010). These interferences though most likely did not interfere the investigations on the chirality of isolated HULIS due to their achirality. Because of spectral characteristics Salma et al. (2010) assigned aromatics from anthropogenic emissions and photooxidation of biogenic VOC to the investigated urban and rural site, respectively. Biomass burning aerosol furthermore showed spectral characteristics more similar to SRFA than to HULIS extracted from urban or rural atmospheric particulate matter due to the abundance of lignin breakdown products (Salma et al., 2010).

A combination of an extraction protocol of water soluble HULIS, based on solid phase extraction, using a hydrophilic-lipophilic-balanced (HLP) sorbent, reported by Varga et al.,

2001, and detection with evaporative light scattering (ELSD), reported by Emmenegger et al., 2007, was applied for investigating HULIS in ambient PM 2.5 at a rural site in China (Lin et al., 2010a). The atmospheric abundance of HULIS in the biomass burning impacted aerosol was in the range 5.9 – 18.1 mg/m³, accounting up to 60 % of WSOM and 10 % of PM 2.5, respectively. Size fractionated sampling showed that the major part of HULIS occurs in the droplet mode (81%). The authors suggested that HULIS stemming from primary emissions from biomass burning and secondary formation through heterogeneous reactions or aerosol-phase reactions have initially resided in the condensation mode and shifted to the droplet mode when these particles were cloud-activated. They found further evidence for biomass burning, primary emissions as well as secondary formation, to be a major source for HULIS in ambient PM 2.5 at an suburban and urban site in Asia, due to correlations with sulphate, oxalate, K⁺ and oxidants (Lin et al., 2010 b).

Ng et al. (2010) compiled factor analysis of 43 Aerosol Mass Spectrometer datasets. By plotting f44 vs. f43, ratio of m/z 44 and m/z 43, respectively and total signal in the component mass spectrum, they found that ambient HULIS and FA (fulvic acid) fall in the LV-OOA range of the figure, with the exception from one sample from K-Pusztta. This rural sample appears to fall in the SV-OOA region of the plot and it was assumed that it has large contributions from freshly formed biogenic SOA, and also has different optical properties than the biomass burning and pollution HULIS which appear in the LV-OOA (low-volatility oxygenated organic aerosol) region. They furthermore found that laboratory generated SOA is more similar to SV-OOA (semi-volatility oxygenated organic aerosol) what likely arises from higher loadings and limited oxidation time in most laboratory experiments. Ambient HULIS in the study of Ng et al. (2010) was extracted after the protocol developed by Dinar et al. (2006a). This method is based on the scheme used by the International humic substances Society for separating aquatic humic acid and FA. Briefly, filters are subjected to consecutive water and water-base extractions; FA-HULIS, by definition soluble at any pH, were separated from other water soluble and base-soluble aerosol organic and inorganic species by preferential absorption onto a XAD-8 resin (Supelco Inc.), followed by elution in a basic solution. The eluant was cation-exchanged on an H⁺-saturated cation-exchange resin (AG MP-50, Bio-Rad Laboratories) to produce protonated acids.

Baduel et al. (2010) observed, that the seasonal differences between specific UV absorbances of HULIS at several urban site are more significant than intra-seasonal or geographic variability. Low specific absorbances, as an indicator for higher aliphatic content, and co-variation with biomass burning markers in winter and oxalic acid in summer, led them to the conclusion that biomass burning and secondary formation are the main sources for HULIS and might be valid in general for urban environments (Baduel et al., 2010). However, the authors did not report on correlations of biomass burning tracers in summer and oxalic acid in winter. Secondary origin of HULIS, isolated

with the protocol reported by Baduel et al. (2009), in an urban background environment is suggested by El Haddad et al. (2011) due to good correlation of water soluble HULIS to co called CMB SOC (un-apportioned OC via a CMB model), directly implying to be found in the biogenic SOC fraction, together with organosulfates. HULIS levels at this maritime site in summer were $0.65 \mu\text{g}/\text{m}^3$ and 14.4 % of OC, respectively.

The importance of a selective HULIS protocol gets much more accentuated, when looking at samples other than atmospheric particulate matter. Diacids and HULIS in arctic snow were found in levels of 10-100 and 1-16 $\mu\text{g}/\text{l}$, with oxalic acid contributing to the dissolved organic carbon with up to 95% (Voisin et al., 2012). Due to optical properties the origin of HULIS was linked to aged biomass aerosol and oceanic phytoplankton in that study.

Pavlovic et al. (2012) investigated the chemical nature and molecular weight distribution of the water soluble fine and ultrafine particulate matter in rural aerosol during summer and fall in the U.S. They estimated HULIS concentrations by comparing the UV absorbance of bulk WSOC to those of SRFA standard, remarking that it is known, that absolute HULIS levels might be overestimated but since they assume the bias to be systematic, comparison of relative levels of HULIS in different size fractions the authors argued this approach to be valid. They found that HULIS in the ultrafine PM ($\text{PM}_{<0.1}$) fraction contributes the most to the total HULIS concentration, significantly higher than concentrations/contributions in summer. They suggested that the variation indicates that different processes are involved in formation of the nucleation mode during the summer and fall periods leading to more high MW compounds in fall. An increase in absorptivity, aromaticity and average molecular weight (AMW) in all size fractions found in the fall samples indicates different formation processes for the organic carbon between the summer and fall periods. The ultrafine fraction ($\text{PM}_{<0.1}$) collected in fall demonstrated characteristics different from the other two PM size fractions and were more similar to aquatic fulvic acids. It had the highest HULIS/WSOC ratio, molar absorptivity, and AMWs up to about 700 Da when analyzed by the UV/VIS method and about 475 Da by ESI/MS. Higher concentrations of organosulfate (OS) compounds and polycarboxylic acids were detected in the summer samples while organonitrate (ON) compounds and monocarboxylic acids were higher in the fall samples (Pavlovic et al., 2012).

HULIS isolated from atmospheric aerosol from sites with urban, suburban, rural and background characteristics were investigated with ultra-high resolution mass spectroscopy by Lin et al. (2012a). For the first time organosulfates were detected in isolated HULIS fractions. Derived elemental formulas were similar to those of organosulfates from chamber experiments with biogenic VOC such as mono- and sesquiterpenes. It was found that up to 50% of the organosulfates in the HULIS fraction are terpene derived suggesting that they are important precursors for OS in HULIS. In one urban sample the OS from known biogenic VOCs precursor accounted only for 20%

to the total OS, indicating the dominant presence of other precursor in the heavily polluted urban atmosphere. Up to 90% of OS in HULIS were shown to have aliphatic character. No organosulfates were detected in HULIS from a regional background sites although HULIS concentrations were by far highest under the 8 investigated sites. Either isoprene derived OS was not retained on the SPE column during HULIS extraction due to their higher polarity or the formation of OS requires the presence of both acidic sulphate seed particles and oxidation products of VOC (Lin et al., 2010a). The investigation of isolated HULIS from the same region with positive and negative electrospray high-resolution mass spectrometry gave further insight in the elemental composition of HULIS (Lin et al., 2012 b). This work shows that atmospheric HULIS contain numerous compounds that have multiple carboxyl groups and reduced nitrogen groups. These functional groups possess electron lone pairs and can serve as ligands to form complexes with transition metals, thereby influencing the atmospheric chemistry and redox chemistry of metals, which in turn has implications to health effects imposed by aerosols (Lin et al., 2012b).

Further elucidation of formation pathways of HULIS was accomplished by Claeys et al. (2012). They aimed at chemical characterisation of atmospheric HULIS from urban, rural, and biomass impacted environments with high performance liquid chromatography with UV/Vis photodiode array detection and electrospray ionisation mass spectrometry and focused on tracers for biomass burning, biogenic and anthropogenic aerosols, including primary and secondary tracers. They suggested 4-nitrocatechol as a tracer for secondary formation of HULIS from gaseous VOCs emitted by biomass burning but as well noted that it remains to be demonstrated whether hydrocarbons present in traffic exhaust, serve as precursors for nitro-aromatic catecholic compounds. Highest contributions of terpenoic acids and 3-methyl-1,2,3-butanetricarboxylic acid (MBCTA) at the urban and rural site led them to the suggestion that they may be valid as tracers for biogenic SOA. However, the chemical characterised substances are accounting for HULIS less than 1% and their MW are well below 300 which do not assign them as macromolecular compounds (Claeys et al., 2012). The appearance of phthalic acid in the HULIS fraction, known to be recovered in the HULIS fraction almost quantitatively with the isolation protocol used in the work of Claeys et al. (2012)-solid phase extraction with hydrophilic-lipophilic balanced sorbents-raises the question, to which extent these compounds do actually belong to the HULIS fraction.

One of the very few studies concerning the size distribution of HULIS in particulate matter showed 80 % of HULIS appearing in the fine fraction (51 % and 31% in the condensation and droplet mode, respectively) and ~ 20 % in the coarse mode (Salma et al., 2013). The geometric mean aerodynamic diameter for condensation, droplet and coarse mode were 0.31 μm , 1.22 μm and 6.4 μm , respectively. Different sources for coarse and fine aerosol are expected and the authors did not exclude resuspended soil in

a first straight forward suggestion on the origin of coarse HULIS. Summarizing it can be stated that progress has been made in the state of knowledge concerning the characteristics of atmospheric HULIS, recently even on an individual compound level (Claeys et al., 2012). An excerpt of reported quantification and characterisation of atmospheric HULIS is given in Table 1 and Table 2 (based on the work of Kalberer, 2006 and Krivácsy et al., 2008; including characterisation of laboratory generated HULIS aka oligomers aka organosulfates aka polyacidic fraction). Both tables clarify the crucial point if talking about HULIS as such: their operationally defined nature and the application of a variety of extraction, isolation/separation protocols and quantification methods, thus raising the question to which extent we are looking at the same compounds, if talking about “HULIS”.

3.5 Laboratory Studies

A number of laboratory studies have focused on photochemical and oxidative processes that could lead to the formation of HULIS and large macromolecules in atmospheric aerosol particles. These studies range from smog chamber experiments to flow tube studies and bulk laboratory experiments, and involve polymerisation and oligomerisation reactions for formation of secondary organic aerosol in the presence and absence of acid seed particles (reviewed by Graber and Rudich et al., 2006; Gelencsér, 2004 and Kalberer, 2006). In general secondary organic aerosol (SOA) components are formed by chemical reaction and gas-to-particle conversion of volatile organic compounds (VOCs) in the atmosphere which may proceed through different pathways (Pöschl, 2005):

- **New particle formation:** formation of semi-volatile organic compounds (SVOCs) by gas-phase reactions and participation of the SVOCs in the nucleation and growth of new aerosol particles.
- **Gas-particle partitioning:** formation of SVOCs by gas-phase reactions and uptake (adsorption and absorption) by pre-existing aerosol and cloud particles.
- **Heterogeneous or multiphase reactions:** formation of low-volatility or non-volatile organic compounds (LVOCs, NVOCs) by chemical reaction of VOCs or SVOCs at the surface or in the bulk of aerosol cloud particles.

Gelencsér (2004) summarised, that the formation of secondary organic aerosol from volatile organic precursors is an important process in the troposphere, especially in regions where photochemical ozone formation is significant. It represents a major sink for the semi-volatile photo-oxidation products of a suite of anthropogenic hydrocarbons and biogenic volatile organic compounds (VOC). Thousands of volatile organic compounds (VOC) are emitted into the atmosphere from various biogenic and anthropogenic sources. Most of them are involved in tropospheric photochemistry, thereby controlling hydroxyl radical concentrations over most of the troposphere. Thus they indirectly affect the mixing ratio of important greenhouse gases, such as methane and carbon monoxide, therefore

they also have an impact on the climate. However of this vast array of VOC only a small suite of compounds is of relevance for secondary organic aerosol formation. Most important on a global scale for the formation of SOA is the group of monoterpenes, with α -pinene being the dominating species. However, even if global fluxes of anthropogenic VOC are much smaller than those of biogenic VOC, they might be important in regions under strong anthropogenic influence (Gelencsér, 2004 and references therein).

Extensive reviews on laboratory experiments on the formation of HULIS, oligomers and organosulfates were conducted by Graber and Rudich (2006), Gelencsér (2004) and Kalberer (2006).

Carlton et al. suggested in 2007 in which they proposed SOA formation through in-cloud processing of glyoxal and other water-soluble products of alkenes and aromatics of anthropogenic, biogenic and marine origin. In that work, aqueous-phase photochemical reactions of glyoxal and hydrogen peroxide were observed at pH values typical of clouds and fogs. Beside the formation of oxalic acid they also found formic acid and larger multifunctional compounds. These multifunctional compounds, covalently bound oligomers or compounds with relatively high pK_a values and carboxylic acid or alcohol functional groups, are consistent with proposed cloud water HULIS components (Capiello et al., 2003). As Blando et al. (2000) and Gelencsér et al. (2004) suggested, the study of Carlton et al. (2007) provides evidence that larger multi-functional compounds can also form in dilute solutions as cloud or fog droplets. A further experiment reported by Holmes and Petrucci (2007) investigated the reactions of levoglucosan with hydroxyl radicals produced from Fenton chemistry in solution, with reaction times between one and seven days as a proxy for biomass burning aerosols. Due to the high molecular weight and the saccharic structure of observed reaction products they suggested oligomerisation products of levoglucosan to be source and/or precursor for HULIS. In the year 2005 organosulfates were suggested to constitute a fraction of atmospheric HULIS (Romero et al., 2005). Particle phase reactions contribute to the formation of SOA, with enhancement of SOA yields in the presence of acidic seed aerosol. The chemical composition of SOA from the photo-oxidations of α -pinene and isoprene, in the presence and absence of sulfate seed aerosol, was investigated in chamber experiments (Surratt et al., 2007). By applying ESI-MS analysis sulfate esters in SOA, produced in laboratory experiments, were identified for the first time. Many of the isoprene and α -pinene sulfate esters identified in these chamber experiments are also found in ambient aerosol collected in the southeastern United States. These esters could contribute significantly to the HULIS fraction of ambient aerosol due to their high water solubility, acidity, thermal stability and high molecular weights. Iinuma et al. (2007) and Gomez et al. (2008) as well observed the formation of organosulfates in smog chamber experiments by ozonolysis of α -pinene with acidic and neutral seed particles and photo-oxidation of isoprene in the presence of unsaturated fatty acids, respectively. Gomez et al. (2008) could structural characterize unknown polar

compounds in K-Puszta fine aerosol as organosulfates derivatives of compounds that originate from the photo-oxidation of unsaturated fatty acids and of α -pinene. The deprotonated molecules of certain sulphated hydroxyacids show features observed by ESI-MS that are characteristic for HULIS. Based on the work of Surratt et al., (2007), where the authors suggested oligomerisation of sulphated esters during the photo-oxidation of isoprene in the presence of acidified inorganic seed aerosol, Gomez et al. (2008) compared chamber derived aerosol to ambient aerosol from K-Puszta, Hungary, which is known to contain high amounts of isoprene photo-oxidation products and inorganic sulfate contributions to PM_{2.5} of up to 25%. Through this comparison they were able to identify unknown polar compounds in ambient K-Puszta aerosol as organosulfate derivatives of compounds that originate from the photo-oxidation of unsaturated fatty acids and α -pinene. Generally sulphation provides a mechanism by which polar compounds containing hydroxyl groups or carbonyl compounds become associated with the particle phase and can contribute to its cloud condensation nuclei properties. Oligomers were as well detected in aqueous phase photo-oxidation experiments of methylglyoxal, a water-soluble product of both gas phase biogenic and anthropogenic hydrocarbon oxidations and hydroxyl radicals to simulate cloud processing (Altieri et al., 2008). Reaction products were investigated by ESI-MS-MS and occurred in the mass range 245 – 800 Da. The average OM:OC ratio of 2 is consistent with that of aged aerosol and atmospheric HULIS.

One question that arises while comparing smog chamber studies and atmospheric observations on the existence and formation of high molecular weight species in the aerosol phase is to which extent the terms “oligomer/polymer” and “HULIS” can be used interchangeably. In general spectra from high molecular weight species generated in smog-chamber-generated SOA extend to higher masses, and exhibit more regular structures pointing to polymerisation/oligomerisation reactions (e.g. Baltensperger et al., 2005). One reason might be the simplified chemical mixture compared to the much more complex aerosol matrix in atmospheric aerosol. Another crucial point is that direct comparison of the different characterization methods applied in laboratory studies and those used for analysis of collected aerosol particles is not straightforward.

Answering questions about how nitrogen is incorporated into HULIS and its subsequent atmospheric processing is important for developing a better understanding of the aging of fine particulate matter in the troposphere (Zahardis et al., 2007). For this purpose Zahardis et al. (2007) launched flow reactor based experiments to investigate the ozonolysis of primary aliphatic amines in fine particles. They observed secondary and tertiary amides and suggested them to play a role in the formation of nitrogen enriched HULIS fractions.

Another pathway for HULIS in atmospheric waters was suggested (De Laurentis et al., 2013b) to be phenol transformation and dimerisation, photosensitised by the triplet state of 1-nitronaphthalene. Reaction products were linked to HULIS due to their fluorescence

peaks in the region where fulvic acids showed their fluorescence maxima. They as well suggested this pathway for fulvic like substances in surface waters (De Laurentis et al., 2013a) despite the more common “top down” (degradation of larger materials from humins to humic substances and fulvic substances) approach, they suggested a bottom up (formation of fulvic acids via oligomerisation of smaller molecules) pathway, what is the common approach for atmospheric HULIS.

In general it seems that laboratory generated SOA has more semi-volatile characteristics than atmospheric HULIS and fulvic acids who are more similar to low volatility oxygenated organic aerosol (Ng. et al., 2010). Studies on formation of high molecular weight organic aerosol (aka HULIS aka polyacidic fraction aka organosulfates) and its characterisation are summarised in Table 2 (based on Kalberer et al., 2006; updated and extended by extraction/isolation techniques).

It is one thing to identify high molecular weight species in laboratory experiments and another to actually get evidence that they contribute to the atmospheric HULIS fraction. The confirmation of laboratory results was recently successful in the case of organosulfates, which were identified in a HULIS fraction, isolated after the method developed by Varga et al. (2001), in ambient particulate matter (Lin et al., 2012a).

3.6 Atmospheric Relevance and physical Properties of HULIS-Recent Findings Bit by Bit

Trace gases, clouds, and atmospheric aerosols influence Earth’s radiation balance. In contrast to the relatively robust understanding and low uncertainty associated with the effect of trace gases, large uncertainties remain regarding the contribution of aerosols and clouds (Dinar et al., 2007, and references therein). Aerosols affect Earth’s radiation balance both directly and indirectly. The indirect effect is related to aerosol–water interactions when aerosols act as Cloud Condensation Nuclei (CCN), altering cloud microphysical properties and consequently precipitation and Earth’s albedo (IPPC, 2001). The direct climatic effect of aerosols occurs through scattering and absorption of incoming solar radiation and absorption of outgoing longwave radiation. Absorption of radiation by aerosols heats the atmosphere and can cause cloud dissipation (the “semi-direct” climatic effect) and possible changes in atmospheric circulation. Therefore, accurate measurements of aerosol scattering and absorption are crucial for estimating Earth’s energy balance (IPPC, 2001). Moreover aerosols affect the abundance and distribution of atmospheric trace gases by heterogeneous chemical reactions and other multiphase processes. The airborne particles furthermore play an important role in the spreading of biological organisms, reproductive materials, and pathogens (pollen, bacteria, spores, viruses, etc.), and they can cause or enhance respiratory,

cardiovascular, infectious, and allergic diseases (e.g. Pöschl et al., 2005; Dinar et al., 2007 and references therein).

HULIS, as a major and ubiquitous contributor to atmospheric aerosol, and surrogate substances were investigated to elucidate their influence on the earth's atmosphere and on human health, summarised in the following.

Several studies investigated and confirmed the **influence of HULIS on cloud formation**. For example HULIS (isolated by the method proposed by Varga et al., 2001) showed stronger surface tension effects compared to reference humic and fulvic acids and thus have an influence on cloud formation (Kiss et al., 2005). The authors did as well observe a seasonal trend of surface tension characteristics, being most pronounced in summer, decreasing towards spring and minimizing in wintry extracts of HULIS isolates. Another study showed that a humic acid standard influenced the hygroscopic growth of aerosol particles (Badger et al., 2006). HULIS isolated from urban aerosol in Rehovot (Israel) activated at lower diameters than SRFA (Dinar et al., 2006a). Taraniuk et al. (2007) processed the same method (Dinar et al., 2006 a und b) for the isolation of HULIS from ambient urban PM10 and compared their surfactant properties to those of SRFA. Estimated MW for ambient HULIS were found to be similar to those of SRFA with 410 - 610 and 520 - 657 and the diffusion of HULIS to the droplet surface was found more rapid than the hygroscopic growth. Thus cloud and microphysics are influenced by the presence of HULIS. HULIS (isolated after Varga et al., 2001) from urban PM2.5 showed lower CCN activity and hygroscopic growth than in the entire water soluble organic carbon (WSOC) fraction (Ziese et al., 2007).

The **optical properties** of HULIS and their atmospheric relevance was investigated by Hoffer et al. (2006b), who showed that HULIS isolated (after Varga et al., 2001) from biomass burning impacted aerosol were responsible for up to 50 % of light absorption at 300 nm and up to 9 % for the entire solar spectrum (Hoffer et. al, 2006b). Utry et al. (2013) found out that isolated HULIS from rural PM1 have mass specific absorption coefficient (at ~300 nm) comparable to that of BC (Utry et al., 2013). HULIS (isolated after Dinar et al. 2006a and 2006b; Varga et al., 2001) in biomass smoke and pollution aerosols, in addition to black carbon, can contribute significantly to light absorption in the ultraviolet and visible spectral regions and lead in most cases to a significant decrease in the single scattering albedo and to a significant increase in aerosol radiative forcing efficiency, towards more atmospheric absorption and heating (Dinar et al., 2007). Direct scattering effects of HULIS were assessed by Dinar et al. (2006b) who measured and compared the effective densities of humic like substances (HULIS) extracted from smoke and pollution aerosol particles to those of molecular weight-fractionated aquatic and terrestrial humic substances (HS). HULIS were furthermore found to be the major chromophore in Alaskan snow and are responsible for about 30 % of light absorption on

snow surfaces (Beine et al., 2011). Strong contributions of HULIS to light absorbing properties in snow were as well confirmed by France et al. (2012).

The **influence of HULIS on cloud chemistry** was investigated by Mancinelli et al. (2006). They found that HULIS, isolated from fog droplets, influence the (photo-) chemistry due to their capability of increasing the solubility of metals (Mancinelli et al., 2006). Hede et al. (2011) furthermore suggested influence of HULIS (based on experiments with the model substances cis-pinonic acid, pinic acid and pinonaldehyde) on cloud microphysics due to their effects on surface tension (Hede et al., 2011).

Several studies investigated the role of HULIS in **tropospheric chemistry**. For example HULIS cause considerable uncertainty in modelling and predicting transport of organic pollutants in the atmosphere due to their humidity dependent sorption features (Taraniuk et al. 2009). Arakaki et al. (2010) found evidence that fulvic acid could be important to the night-time production of hydroxy-radicals via the Fenton mechanism, and thus HULIS might play a role in the global oxidant budget. By means of a wetted-wall flow tube, Brigante et al. (2008) studied the multiphase chemistry of ozone on aqueous solutions containing fulvic acids (FA), taken as proxies for atmospheric HULIS. In these experiments, the loss of gaseous O₃ was monitored by UV-visible absorption spectroscopy at the reactor outlet (i.e., after contact between the gaseous and liquid phases). The reported uptake coefficients are greatly increased over those measured on pure water, demonstrating that the presence in solution of fulvic acids does greatly enhance the uptake kinetics. Accordingly, the chemical interactions of fulvic acids (or HULIS) may be a driving force for the uptake of ozone on liquid organic aerosols and can also represent an important mechanism for the O₃ deposition to rivers and lakes (Brigante et al., 2008). Baduel et al. (2011) investigated photochemical aging of alkaline extracted HULIS by ozone from atmospheric PM affected by biomass burning. In accordance with other studies they observed a decrease of carbon content and increase of carboxylic acid functional groups. They suggest losses of VOC or CO to be responsible for the major part of the carbon lost by photochemical aging of HULIS. The ozone uptake is prone to reduce the molecular size of the HULIS fraction and increase the number of acidic functional groups, strongly influencing their physical properties (Baduel et al., 2011). Using different laboratory findings and a model for mesoscale chemistry transport Konovalov et al. (2012) evaluated the light induced ozone loss at the surface of biomass burning aerosol during the period of intense wildfires in western Russia. The ozone loss rate in this study has been parameterized as a function of the HULIS fraction in aerosol, ambient ozone mixing ratio, photon flux and relative humidity. Their results indicated that maximum decreases of ozone concentration with up to 40% can occur in biomass burning plumes, HULIS playing a major part in that process (Konovalov et al., 2012). Indication for enhancing the photolysis of nitrate on snow surfaces and thus potentially influence on the global nitrogen flux was reported by France et al. (2011 and 2012).

Years before similar was suggested by Beine et al (2008) who reported strong correlation of nitrous acid (HONO) emissions from snow samples and amounts of added humic acid. Furthermore HULIS was found to be the major redox active constituent of WSOC in PM, thus serving as electron carriers to catalyze the formation of reactive oxygen species (ROS). The reversible redox sites of HULIS might lead to continuous production of reactive oxygen species what, accompanied by cellular respiration, can pose **adverse health effects** (Lin et al., 2011).

3.7 Overview and open Questions

This subchapter integrates a summary of the extensive reviews conducted by Graber and Rudich (2006) and Gelencsér (2004). For a better overview and readability of the scientific history of HULIS, from the beginning until the year 2005, their reviews are summarised in this subchapter.

First evidences for humic-like compounds in atmospheric aerosol were reported more than three decades ago (Simoneit et al., 1977 and 1980). The term HUmic-Like Substances (HULIS) was coined in 1998 by Havers et al. who found HULIS contributing with 10% and more to aerosol organic carbon and characterized the alkaline aqueous extract by molecular size distribution, carbon content, UV-VIS, Fourier transform infrared (FTIR) and nuclear magnetic resonance ($^1\text{H-NMR}$) spectra (Havers et al., 1998). Since then many different approaches for extracting HULIS from atmospheric particulate matter, atmospheric waters such as fog, cloud water, rain, and snow surfaces and ice cores aimed at the elucidation of their atmospheric abundance, chemical characteristics, their relevance to the earth's atmosphere and on human health.

The **atmospheric relevance** of HULIS was investigated in several studies and gave evidence that HULIS have direct and indirect on the earth's radiative balance due to their light absorbing properties (Hoffer et al., 2001; Dinar et al., 2006a, 2006b, 2007; Beine et al., 2011; Utry et al., 2013) and their influence on hygroscopic growth and CCN activity of organic aerosol (Kiss et al., 2005; Dinar et al., 2006a; Taraniuk et al., 2007; Ziese et al., 2007). They as well influence atmospheric (photo-) chemistry due to their influence on the abundance, availability and transport of atmospheric oxidants (Brigante et al., 2008; Arakaki et al., 2009; Beine et al., 2008; Konovalov et al., 2012), metals (Mancinelli et al., 2006) and organic pollutants (Taraniuk et al., 2009). Recent findings indicate that the influence of HULIS on atmospheric substance cycles might be of major importance even on a global scale (France et al., 2011 and 2012). The capability of HULIS to catalyse the production of reactive oxygen species even indicates potential adverse **effects on human health** (Lin et al., 2011; Verma et al., 2012).

The **atmospheric abundance** of HULIS was investigated all over the world processing various combinations of extraction, isolation and quantification protocols (Table 1; based on Krivácsy et al., 2008; updated and extended). The investigations confirmed their ubiquitous abundance and their substantial contribution to the organic fraction of airborne atmospheric aerosol. A crucial issue when talking about HULIS as such is their operationally defined nature. Since separation/ isolation and quantification methods rely on different properties of HULIS such as their polarity, acidity, molecular weight and optical properties at distinct wavelengths these methods may capture isolates and quantities of differing fractions of HULIS, though to large extents referring to the same

group of compounds. While the different methods might lead to, at best, systematically higher or lower atmospheric HULIS levels due to interfering atmospheric components or discriminating extraction protocols, this question gets even more vital when looking at chemical characteristics of atmospheric HULIS, which have been investigated with numerous methods in isolated HULIS fractions as well as in bulk WSOC, ambient particulate matter and SOA generated in laboratory experiments and reaction solutions from laboratory experiments on the formation of HULIS in aqueous phase etc (Table 2, based on Kalberer et al., 2006; updated and extended by extraction/isolation techniques).

However, the **chemical structure** of HULIS was suggested very early to consist of polycyclic ring structures with hydrocarbon side chains, and hydroxyl, carboxyl and carbonyl groups with organic nitrogen, carbohydrates tannins/lignins being important constituents (e.g. Mukai and Ambe, 1986). Overall these findings are still valid today. Aliphatic and aromatic structures with carboxylic, acrylic, phenolic and reduced nitrogen groups have been identified in several studies (Duarte et al., 2005; Samburova et al., 2007; Salma et al., 2008a; Dinar et al., Lin et al., 2012b). Studying ambient and laboratory generated aerosol, organosulfates were suggested to form a subset of HULIS due to their polyacidic nature, their water solubility and molecular weight (Romero et al., 2005; Surratt et al., 2007; Stone et al., 2009). Recently organosulfates were identified in HULIS extracts (Lin et al., 2012a). The **molecular weight** of atmospheric HULIS reported in literature ranged well below 1000 Da, much lower than the molecular weight of their eponyms the aquatic and terrestrial humic and fulvic acids. Using several mass spectrometric techniques, size exclusion chromatography, ultrafiltration, and calculations from UV absorbencies at specific wavelengths, size distributions between 200 and 600 Da (e.g. Likens and Galloway, 1983; Kiss et al., 2003; Samburova et al., 2005 a and 2005 b; Emmenegger et al., 2007; Salma et al., 2008a; Stone et al., 2009; Krivácsy et al., 2008) have been reported for airborne HULIS from urban, rural and biomass burning impacted environments. Interestingly the molecular size of fulvic acids, with in general molecular masses higher than 1000 Da, were reported by two studies to be only 1.5 times higher (fulvic acids investigated with UV/VIS by Salma et al., 2008a) and to show an upper end of m/z signals at 500 (fulvic and humic acids investigated with LC-MS-MS by Stone et al., 2009), respectively.

An urgent question arising, when HULIS was first detected in airborne particulate matter of course was: what are the **sources and formation pathways** of HULIS? Due to their resemblance to terrestrial occurring humic substances the atmospheric origin was suggested to be primarily terrestrial (Simoneit et al., 1980). Only a few years later macromolecular compounds were identified in rural rainwater. Chemical characterisation of the high molecular weight fractions (> 1000 Da nominal weight cut-off) gained by ultrafiltration, revealed lignins carbohydrates and organic nitrogen as important

constituents (Likens and Galloway, 1983). Therefore the authors suggested degradation and dissolution of plant material as source for these macromolecular compounds.

Whereas the proposed primary origin of HULIS from dissolution of plant degradation material turned out to be of minor importance for the atmospheric HULIS abundance, the suggestion of Mukai and Ambe (Mukai and Ambe, 1986) is still valid today. They extracted humic acid- like brown substances from soil, dead leaves, particles stemming from biomass burning and automotive soot, compared it to extracts from rural airborne particulate matter and suggested biomass burning to be the major source for these brown substances due to the resemblance of infrared and ultraviolet spectra characteristics.

Since then results from laboratory studies and observational evidence, respectively, back up a variety of hypothesis for the origin of atmospheric HULIS. Kalberer et al. (2006), Graber and Rudich (2006) and Gelencsér (2004) reviewed the scientific history of laboratory studies connected to the better understanding of HULIS, from the beginning until the year 2006, their reviews are compiled in this subchapter.

Early suggestions for the origin of HULIS were:

- primary terrestrial (Simoneit et al., 1980)
- degradation and dissolution of plant material (Likens and Galloway, 1983)
- primary origin from open biomass combustion (Zappoli et al., 1999; Mayol-Bracero et al., 2002)
- primary marine origin (Cini et al., 1994 and 1996; Calace et al., 2001)

The first two sources seem to be of minor importance since the water soluble carbon, which HULIS is part of, is prevalently found in fine mode aerosol (Cavalli et al., 2004, Yu et al., 2004). Biomass burning is widely accepted to play an important role in the atmospheric occurrence of HULIS via primary emissions as well as secondary formation from gaseous precursor compounds (Duarte et al., 2005; Samburova et al., 2005b; Feczko et al., 2007; Hopkins et al., 2007; Samburova et al. 2007; Schmidl et al., 2008a und 2008b; Lin et al., 2010a und 2010b; Claeys et al., 2012). Secondary formation of biogenic and anthropogenic gaseous precursors are assumed to be of major importance for the HULIS formation in summer in the northern hemisphere (Duarte et al., 2005; Samburova et al., 2005b; Polidori et al., 2008; Salma et al., 2010; Baduel et al., 2010), due to observations such as lower impact of the biomass burning tracer levoglucosan during the warm season, different size, structural characteristics and optical properties of HULIS during summer and winter. Laboratory studies investigated a variety of compounds which are able to form high molecular weight species in heterogeneous and multiphase reactions. Suggested formation pathways playing a role in HULIS formation or its precursors are:

- oxidation of soot (Decesari et al., 2002). Due to the soot surrogates higher resemblance to soot from fossil fuel burning compared to soot from biomass burning Decesari et al. (2002) suggested secondary formation via ozonolysis of soot from fossil fuel burning as a source of atmospheric HULIS.
- heterogeneous reactions of isoprene in the presence of sulphuric acid (Limbeck et al., 2003)
- radical dimerisation/oligomerisation of 3,5-dihydroxybenzoic acid, as a model for aromatic mono/diacids which are abundant lignin pyrolysis products in biomass burning aerosol (Gelencsér et al., 2003).
- Photo-oxidation of 1,3,5-trimethylbenzene (TMB) (Kalberer et al., 2004). TMB is an anthropogenic VOC emitted by fossil fuel combustion.
- oligomerisation of levoglucosan (Holmes and Petrucci, 2007). Levoglucosan is emitted during biomass burning in vast amounts.
- ozonolysis of primary aliphatic amines (Zahardis et al., 2008). Aliphatic amines stem from biogenic and anthropogenic sources such as animal husbandry, agriculture, biomass burning, vehicular emissions, marine bubble bursting (Zahardis et al., 2008 and references therein).
- In-cloud glyoxal reactions (Altieri et al., 2008). Glyoxal is an oxidised reaction product of isoprene and anthropogenic VOCs.
- dimerisation of phenols (De Laurentis et al., 2013b)
- formation of organosulfates, recently identified in aqueous HULIS extracts (Lin et al., 2012), was observed via
 - Photooxidation of α -pinene and isoprene in the presence of acidic aerosol (Surratt et al., 2007)
 - Ozonolysis of α -pinene (Iinuma et al., 2007)
 - Photo-oxidation of isoprene and unsaturated fatty acids (Gomez et al., 2008)

Although there is a growing body of literature focusing on the elucidation of atmospheric abundance, chemical characteristics and sources and formation pathways there are still **open questions**. Some of them, which the present work aims to shed light on, are:

- Which sources contribute to the atmospheric abundance of HULIS?

- To which extent is atmospheric HULIS of primary or secondary origin?
- Do HULIS prevalently occur at background or urban sites?
- Do HULIS_T follow the same seasonal trend as HULIS_{WS}?
- To which extent are the observed higher HULIS levels in winter due to additional sources or to plain accumulation caused by unfavourable meteorological dispersion conditions?
- Are summer and winter sources for HULIS really that different and if yes, how does this change the properties of HULIS?
- What are the differences between the alkaline and water soluble fractions of HULIS?

Table 1: Atmospheric abundance of HULIS (based on Krivácsy et al., 2008; updated and extended)

| Site | Date | Environment | Type of sample | Analytical method E (extraction) I (isolation) S (separation) Q (quantification) | Absolute HULIS concentration | Relative HULIS concentration | Reference |
|---|--|---|----------------------|--|---|--|---------------------------|
| Tsukuba, Japan | September 1983 - September 1984 | Rural | total aerosol | E: solvent and alkaline extraction I: acid precipitation Q: carbon measurement | 0.10-0.26 $\mu\text{g C}/\text{m}^3$ | 0.6-3% of TC | Mukai and Ambe, 1986 |
| Sauerland, Germany Dortmund, Germany | Spring and Summer 1995-1996 | rural urban (industrial) | total aerosol (dust) | E: alkaline extraction; I: anion exchange column Q: TOC | - | 1.8-1.9% of TC | Havers et al., 1998 |
| Po Valley, Italy K-puszta, Hungary | June-September 1996 | rural (polluted) rural (background) | PM1.5 | E: water extraction I/S: SEC Q: UV/VIS | 0.6-2.5 $\mu\text{g}/\text{m}^3$ 0.9-1.8 $\mu\text{g}/\text{m}^3$ | 21-55% of WSOC | Zappoli et al., 1999 |
| Zurich, Switzerland and | Aug 2002/ Feb, Mar 2003 | urban background | PM 10 | E: water extraction S: SEC Q: UV-VIS | 0.28 - 1.59 $\mu\text{g}/\text{m}^3$ | 2.5 % of PM10 6-31% of OC | Samburova et al., 2005b |
| Vienna, Austria | June 1999-May 2000 | urban | PM10 | E: water extraction I: SPE (C18)-anion exchange (SAX) Q: TOC | 0.1 - 1.8 $\mu\text{g C}/\text{m}^3$ | 5-40 % of OM | Limbeck et al., 2005 |
| Dübendorf, Switzerland | December 05-January 2006 | suburban | PM 1 | E: water extraction I: SPE (C18) S: SEC Q: ELSD | 0.46 - 2.29 $\mu\text{g}/\text{m}^3$ | 10-35 % of OM | Emmenegger et al., 2007 |
| Azores, Aveiro (Portugal), Puy de Dome (France), Schauinsland (Germany), Somblick (Austria), K-Puszta (Hungary) | September 2002-May 2004 | continental background | PM2.5 | E: water and alkaline extraction I: SPE (C18)-anion exchange (SAX) Q: TOC | 0.075-1.68 $\mu\text{g C}/\text{m}^3$ (annual averages) | 6-40 % of WSOC | Feczko et al., 2007 |
| Mace Head, Ireland | August - September 2001 | marine background | PM10 | | ~0.08 $\mu\text{g}/\text{m}^3$ * | 19 % of WSOC | |
| Auckland and Christchurch, New Zealand | January - February and June-July 2001 | urban polluted | PM10 | E: water extraction I: SPE (HLB) Q: TOC | -0.5-11 $\mu\text{g}/\text{m}^3$ * | 34-51 % of WSOC | Krivácsy et al., 2008 |
| Budapest, Hungary | April-May 2002 | urban polluted | PM2.5 | | ~1.8 $\mu\text{g}/\text{m}^3$ * | 25 % of WSOC | |
| Marseilles, France | February 2008 | urban (tunnel) | PM2.5 PM10 | E: water extraction I: DEAE Q: TOC | 1.71-2.28 $\mu\text{g}/\text{m}^3$ (PM2.5) 2.69-3.98 $\mu\text{g}/\text{m}^3$ (PM10) | - | El Haddad et al., 2009 |
| Pearl Delta River, South China | Nov. 07 | rural, (biomass impacted) | PM 2.5 | E: water extraction I: SPE (HLB) Q: ELSD | ~12 $\mu\text{g}/\text{m}^3$ (in ambient PM) ~220-1200 $\mu\text{g}/\text{m}^3$ (in biomass burning plume) | ~12% of PM2.5 (ambient) 60% of WSOC (ambient) ~8-12 % of PM 2.5 (biomass burning plume) ~30 % of WSOC | Lin et al., 2010a |
| Paris, Lille, Strasbourg, Grenoble, Chamonix, Marseilles, Toulouse France | Nov-Dec 2007 Jan-Oct 2008 | urban background (biomass impacted) | PM10 | E: water extraction* I: DEAE Q: TOC | 0.51-1.47 $\mu\text{g C}/\text{m}^3$ - 1.02-2.94 $\mu\text{g}/\text{m}^3$ (seasonal averages) | 12.7-22% of OC 23.4-42.7 % of WSOC | Baduel et al., 2010 |
| Hong Kong, Guangzhou, China | July 2007- August 2008 | urban, suburban | PM2.5 | E: water extraction I: SPE (HLB) Q: ELSD | 0.23- 22.3 $\mu\text{g}/\text{m}^3$ (daily min-max) 4.9-7.1 $\mu\text{g}/\text{m}^3$ (annual average) | ~10 % of PM2.5 | Lin et al., 2010b |
| K-Puszta, Budapest, Hungary Rondonia Brazil | May 2008 June 2008 September 2002 | rural, urban, rural (biomass burning) | PM 2.5 | E: water extraction I: SPE (HLB) Q: TOC & gravimetric | 1.65 $\mu\text{g}/\text{m}^3$ (rural) 2.2 $\mu\text{g}/\text{m}^3$ (urban) 43-60 $\mu\text{g}/\text{m}^3$ (rural biomass burning) | 35 % of WSOC (rural) 48 % of WSOC (urban) 43- 60% of WSOC (rural biomass burning) | Salma et al., 2010 |
| Marseille, France | June-July 2008 | urban (background) | PM2.5 | E: water extraction I: DEAE Q: TOC | 0.65 $\mu\text{g}/\text{m}^3$ | 14.4% OC | El Haddad et al., 2011 |
| Pearl River Delta, China Taipei, Yunlin County, Mt. Lulin, Mt. Bei Tungyen Taiwan | Sep 2004, Jan 2009, Nov 2008, Oct 2006, Dec 2006, Mar 2008, Feb & Mar 2007 | urban, suburban, rural, regional background | PM 2.5 | E: water extraction I: SPE (HLB) Q: TOC | 2.2 - 19.2 $\mu\text{g}/\text{m}^3$ | - | Lin et al., 2012b |
| Potsdam, New York USA | July- October 2009 | rural | PM2.5 | E: water extraction Q: UV/VIS | 0.13-1.33 $\mu\text{g}/\text{m}^3$ | 21- 55 % of WSOC | Pavlovic et al., 2012 |
| Guangzhou, China | July 2006 January 2007 | urban, suburban, biomass impacted | TSP | E: water extraction I: SPE (HLB) Q: TOC & gravimetric | 3.3-13.4 $\mu\text{g}/\text{m}^3$ | 1.6-3.6 % of TSP 36-44% of WSOC | Song et al., 2012 |
| Budapest, Hungary | April & May 2002 | urban (traffic impacted) | PM2.4 | E: water extraction I: SPE (HLB) Q: TOC | 1.31 $\mu\text{g}/\text{m}^3$ | ~3% of PM2.4 ~43% of WSOC | Salma et al., 2013 & 2007 |

*a small subset of samples from samples collected during winter in Chamonix were extracted aqueous and alkaline (Baduel et al., 2009).

Table 2: Analytical methods for the characterization of HULIS, polycarboxylic acids, oligomers, organosulfates and macromolecular compounds in organic aerosol (based on Kalberer et al., 2006; updated and extended by extraction/isolation techniques)

| Investigated property | Analytical method | Sample type | Extraction/isolation/separation | Reference | Investigated property | Analytical method | Sample type | Extraction/isolation/separation | Reference | | |
|--------------------------|-------------------|-------------------|---|-------------------------------|------------------------------|-------------------|---|--|-------------------------|--|---------------------|
| Molecular size | ESI-MS | Field, laboratory | water/SPE (HLB) | Kiss et al., 2003 | Concentration | UV | Field | bulk WSOC | Zappoli et al., 1999 | | |
| | | Field, laboratory | water/SPE (C18) | Feng et al., 2004 | | | Field | bulk WSOC | Samburova et al., 2005 | | |
| | | Laboratory | | Tolocka et al., 2004 | | | Field | water/SPE (C18) | Emmenegger et al., 2007 | | |
| | | Laboratory | | Inuma et al., 2004 | | | Field | bulk WSOC | Pavlovic et al., 2012 | | |
| | | Laboratory | | Gao et al., 2004 | | | Field | water/SPE (C18)- IEC/(SAX) | Limbeck et al., 2005 | | |
| | | Field | water/SPE (C18) | Emmenegger et al., 2007 | | | Field | | Facchini et al., 1999 | | |
| | | Field | water/SPE (HLB) | Krivascy et al., 2008 | | | Field | water&alkaline/SPE (C18)-IEC (XAD) | Feczko et al., 2007 | | |
| | | Field | water/SPE (HLB) | Lin et al., 2012b & 2012b | | | Field | water/ polyacidic fraction after HPLC | Mancinelli et al., 2007 | | |
| | | ESI-UHRMS | Field | water/SPE (HLB) | | | Claeys et al., 2012 | Field | water/SPE (HLB) | Krivascy et al., 2008 | |
| | | LC-ESI-MS | Field | bulk WSOC | | | Stone et al., 2009 | Field | water/SPE (HLB) | Salma et al., 2010 & 2013 | |
| | (MA) LDI-MS | Field, laboratory | bulk WSOC | Samburova et al., 2005 | Field | water/DEAE | Baduel et al., 2010 | | | | |
| | | Laboratory | bulk SOA | Kalberer et al., 2004 | Field | water/SPE (HLB) | Song et al., 2012 | | | | |
| | SEC | Laboratory | bulk SOA | Baltensperger et al., 2005 | VTDMA | Laboratory | bulk SOA | Kalberer et al., 2004 | | | |
| | | Field, laboratory | bulk SOA | Kalberer et al., 2006 | DMA | Laboratory | | Jang et al., 2002 | | | |
| | | Field | bulk WSOC | Zappoli et al., 1999 | | Laboratory | | Inuma et al., 2004 | | | |
| | | Field | bulk WSOC | Samburova et al., 2005 | | Laboratory | | Gao et al., 2004 | | | |
| | VPO | Field | bulk WSOC | Romero et al., 2005 | ELSD | Field | water/SPE (C18)/SEC | Emmenegger et al., 2007 | | | |
| | | Field | water/SPE (HLB) | Kiss et al., 2003 | | Field | water/SPE (HLB) | Lin et al., 2010a&2010b | | | |
| | UF | Field | water/SPE (HLB) | Kiss et al., 2003 | RP-HPLC FLD | Field, laboratory | | Góra et al., 2005 | | | |
| | ATOF | Laboratory | bulk SOA | Gross et al., 2006 | Elemental composition | EA | Field | water/SPE (HLB) | Song et al., 2012 | | |
| ESI-FTICR-MS | Laboratory | acetonitril&water | Reinhardt et al., 2007 | Isotopical composition | ¹⁴ C | Field | water/SPE (HLB) | Song et al., 2012 | | | |
| UV/VIS | Field | water/SPE (HLB) | Salma et al., 2008 | Metal content | ICP-MS | Field | water/SPE (HLB) | Lin et al., 2011a | | | |
| Functional groups | NMR | Field | water/PA fraction after IEC | Decesari, 2000 | Formation process | ESI-MS (MS) | Laboratory | | Hoffer et al., 2004 | | |
| | | Field | water/SPE (C18) | Samburova et al., 2007 | | | Laboratory | | Tolocka et al., 2004 | | |
| | | Field | water/SPE (HLB) | Song et al., 2012 | | | Laboratory | | Inuma et al., 2004 | | |
| | FTIR | Laboratory | | Jang et al., 2002 | | | Laboratory | | Gao et al., 2004 | | |
| | APCI-MS-MS | Field | 0.1 M NaOH/IEC (HiTrap FF)/SPE (C18) | Baduel et al., 2011 | | | Field, laboratory | | Hoffer et al., 2006 | | |
| Structure | LDI-MS | Laboratory | bulk SOA | Kalberer et al., 2004 | (MA)LDI-MS | | Field | bulk reaction solution | Altieri et al., 2008 | | |
| | ESI-MS | Laboratory | | Tolocka et al., 2004 | | | Laboratory | bulk SOA | Kalberer et al., 2004 | | |
| | | Laboratory | | Inuma et al., 2004 | | | Field, laboratory | bulk SOA, bulk WSOC | Kalberer et al., 2006 | | |
| | | Laboratory | | Gao et al., 2004 | | | Laboratory | bulk reaction solution | Holmes et al., 2007 | | |
| | | Laboratory | methanolic SOA extracts | Szmigielski et al., 2007 | | | Field, laboratory | | Facchini et al., 1999 | | |
| | ITMS | Field | water/ SEC | Romero et al., 2005 | | | Laboratory | bulk WSOC | Limbeck et al., 2003 | | |
| | IR | Laboratory | | Jang et al., 2002 | | | Laboratory | bulk SOA | Gross et al., 2006 | | |
| | LC-ESI-MS | Field | water/SPE (HLB) | Claeys et al., 2012 | | | Laboratory | bulk SOA | Zahardis et al., 2008 | | |
| | LC-MS-MS | Field | bulk WSOC | Stone et al., 2009 | | | FT-ICR-MS | Laboratory | bulk reaction solution | Altieri et al., 2008 | |
| | ESI-UHRMS | Field | water/SPE (HLB) | Lin et al., 2012a & 2012b | | | Chirality | ECD/VCD | Field | water/SPE (HLB) | Salma et al., 2010 |
| | UV/VIS | Field | water/ (XAD8) | Dinar et al., 2007 | | | Ozone uptake | | Field | 0.1 M NaOH/ IEC (HiTrap FF)/SPE (C18) | Baduel et al., 2011 |
| | | Field | water/SPE (HLB) | Salma et al., 2008a | | | Reactive oxygen species generation | | Field | water/SPE (HLB) | Lin et al., 2011a |
| | XPS | Field | water/SPE (HLB) | Song et al., 2012 | | | | | | | |

ESI-MS: electrospray ionisation mass spectrometry; (MA)LDI-MS: (matrix assisted) laser desorption/ionisation mass spectrometry; SEC: size exclusion chromatography; VPO: vapour pressure osmometry; UF: ultra filtration; ATOF: aerosol time-of-flight mass spectrometry; ESI-FTICR-MS: ESI-Fourier-transform ion cyclotron resonance MS; NMR: nuclear magnetic resonance spectrometry; ELSD: evaporative light scattering detection; ITMS: ion trap mass spectrometry; IR: infrared spectroscopy; OC: combustion methods applied to determine the total organic carbon concentration; VTDMA: volatility tandem differential mobility analyser; DMA: differential mobility analyser; RP-HPLC-FLD: reversed phase high pressure liquid chromatography with fluorimetric detection.

4 Sampling Sites

Austrian airborne PM₁₀ was collected at 23 three sites in Austria by the respective local authorities in a time frame from January 2004 to March 2006. Sites were located in the provinces of Vienna, Styria, Salzburg, Upper Austria, Lower Austria and Carinthia. Each set of sampling sites in the different regions consisted of urban and respective local background sites. Figure 5 gives an impression of the array of sampling sites that were selected from the air quality monitoring networks run by the respective local authorities. Nine sites are located north, seven east and seven south the Austrian alps, with varying climatic and topographic characteristics. All sampling sites were part of the projects AQUELLA Vienna, AQUELLA Salzburg, AQUELLA Graz (Bauer et al., 2006, Bauer et al., 2007a and 2007b), AQUELLA Lower Austria (Bauer et al., 2008b), AQUELLA Carinthia and AQUELLA Upper Austria (Bauer et al., 2008a; Jankowski et al., 2009b).

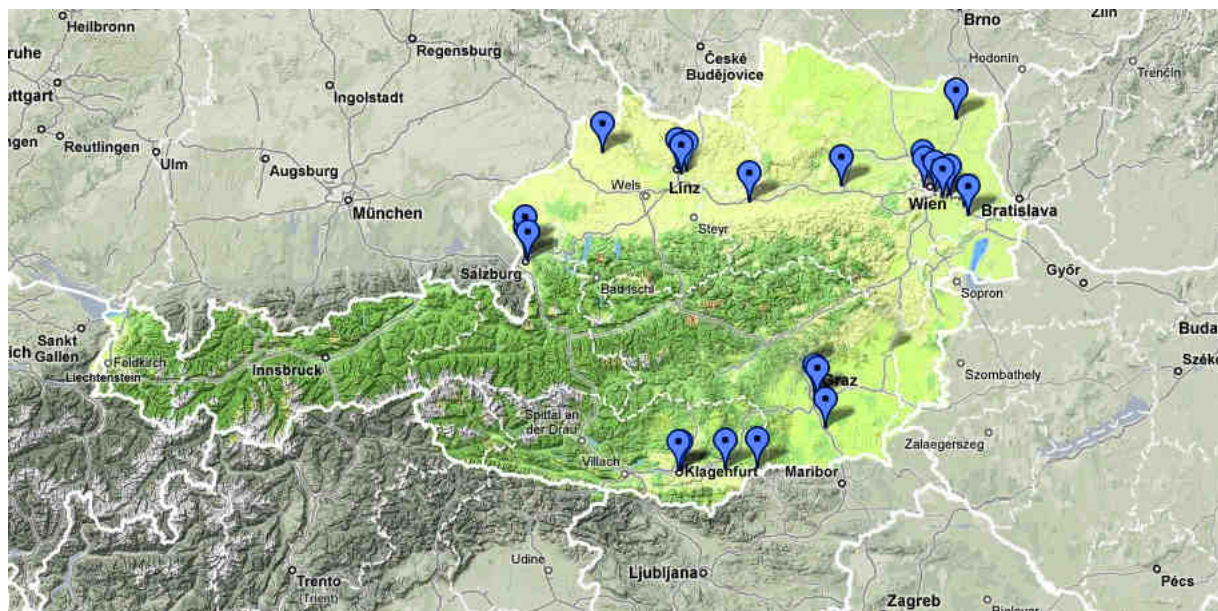


Figure 5: Sampling sites in Austria selected for the present work (based on Google Maps; supplemented with marks for sampling sites).

Climatic conditions (Slanar et al., 1985) in the regions of Vienna and the eastern part of Lower Austria are characterised by hot summers, rather mild winters and little precipitation (Pannonic climate). Farther west, in Salzburg and Upper Austria, a higher number of precipitation events and larger amounts of precipitation compared to the eastern part of Austria are recorded in a thirty-year average (Figure 6). The Illyric climate type is prevalent in Carinthia and Styria, which is characterised by cold winters, hot summers and rather large amounts of precipitation concentrated on a smaller number of precipitation days.

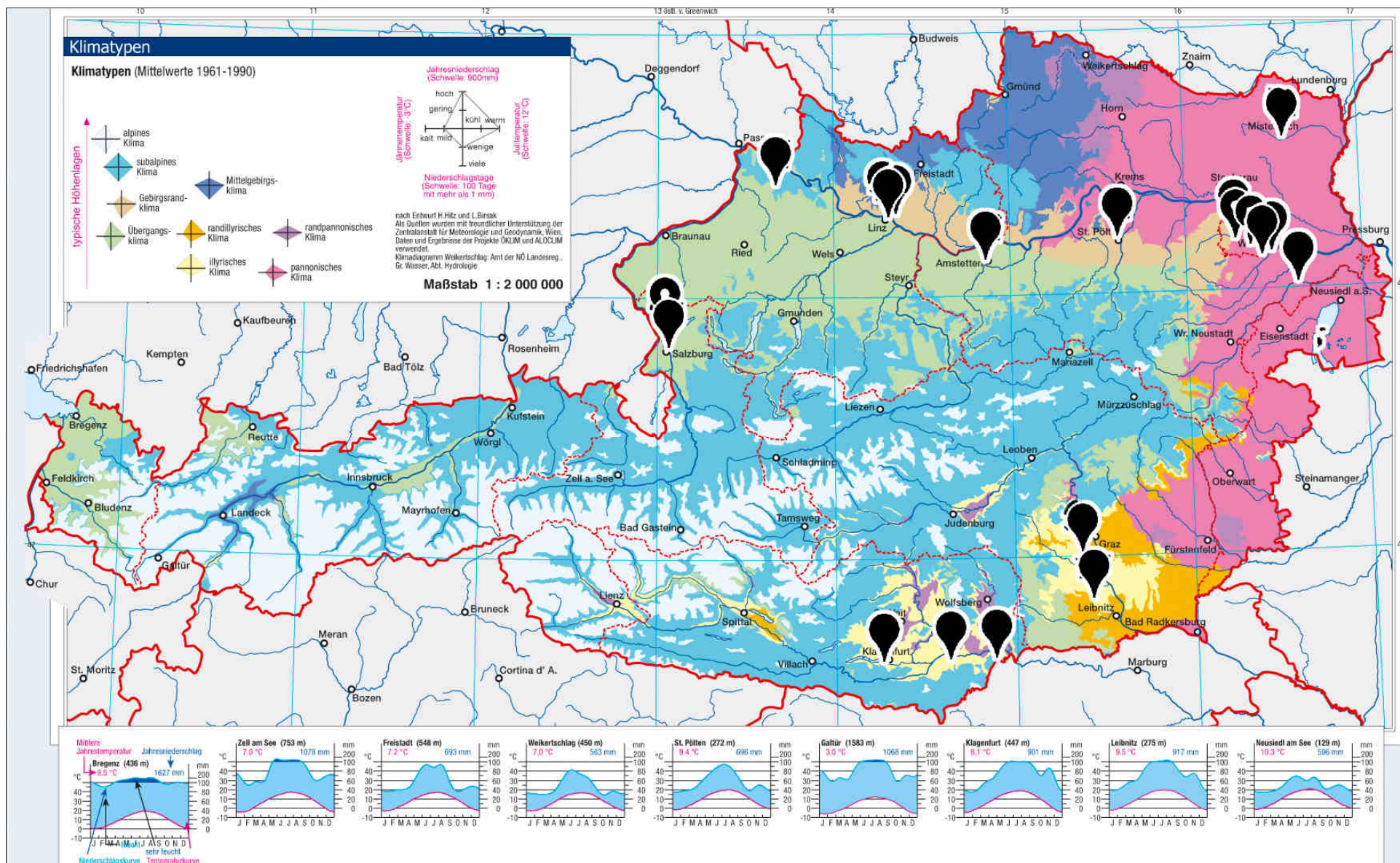


Figure 6: Prevalent climate types in Austria (based on Slanar et al., 1985; complemented with marks for sampling sites).

Vienna

Sampling sites in the Austrian capital Vienna are located in a northwest to southeast transect (Figure 7). Two sites, Schafbergbad (SCHA, 16° 18' 10.0"E, 48° 14' 9.2"N, 320 m a.s.l.) and Lobau (LOBA, 16° 31' 36.5"E, 48° 09' 45.4"N, 150 m a.s.l.) are located at the urban fringe of the city. The sampling site Schafbergbad (Figure 8) is situated in residential area whereas Lobau is in the area of the Donau-Auen National Park surrounded by woods and meadows in vicinity of a water course (Figure 9). The local surrounding of the intra-urban site Kendlerstraße (KEND, 16° 18' 39.2"E, 48° 12' 19.8"N, 230 m a.s.l.) is characterised by residential area and moderately impacted by traffic (Figure 8). The second urban site Rinnböckstraße (RINN, 16° 24' 28.0"E, 48° 11' 4.6"N, 160 m a.s.l.) is heavily impacted by the A23, which is with up to 170.00 vehicles per day (Asfinag, VCÖ, 2005), the most frequented Austrian road (Figure 9). Geographical coordinates, description of sampling sites and population figures are based on information from the Environment Agency Austria (Umweltbundesamt, 2009).



Figure 7: Sampling sites in Vienna. 1: Schafbergbad; 2: Kenderstraße; 3: Rinnböckstraße; 4: Lobau (based on Google Maps; supplemented with marks for sampling sites).



Figure 8: Sampling sites Schafbergbad (left) and Kenderstraße (right) (taken from Umweltbundesamt, 2009).



Figure 9: Sampling site Rinnböckstraße (left) and Lobau (right) (taken from Umweltbundesamt, 2009).

Graz

The two urban sites in Graz, provincial capital of Styria with 300.000 inhabitants, are Don Bosco (DONB, 15° 24' 59.8"E, 47° 03' 20.2"N, 358 m a.s.l.) and Graz Süd (GRAS, 15° 25' 59.0"E, 47° 02' 30.0"N, 342 m a.s.l.), with DONB being a heavily traffic impacted site and GRAS located in residential area. The local background site Bockberg (BOCK, 15° 29' 45.0" E, 46° 52' 17.0" N, 449 m a.s.l.) is situated 28 km south of Graz surrounded by farmland, vine yards and single houses (Figure 10, Figure 11, Figure 12, Figure 13) and most probably affected by the vicinity of a power plant and a motorway (Spangl et al., 2006). Geographical coordinates, description of sampling sites and population figures are based on information from the Environment Agency Austria (Umweltbundesamt, 2009).

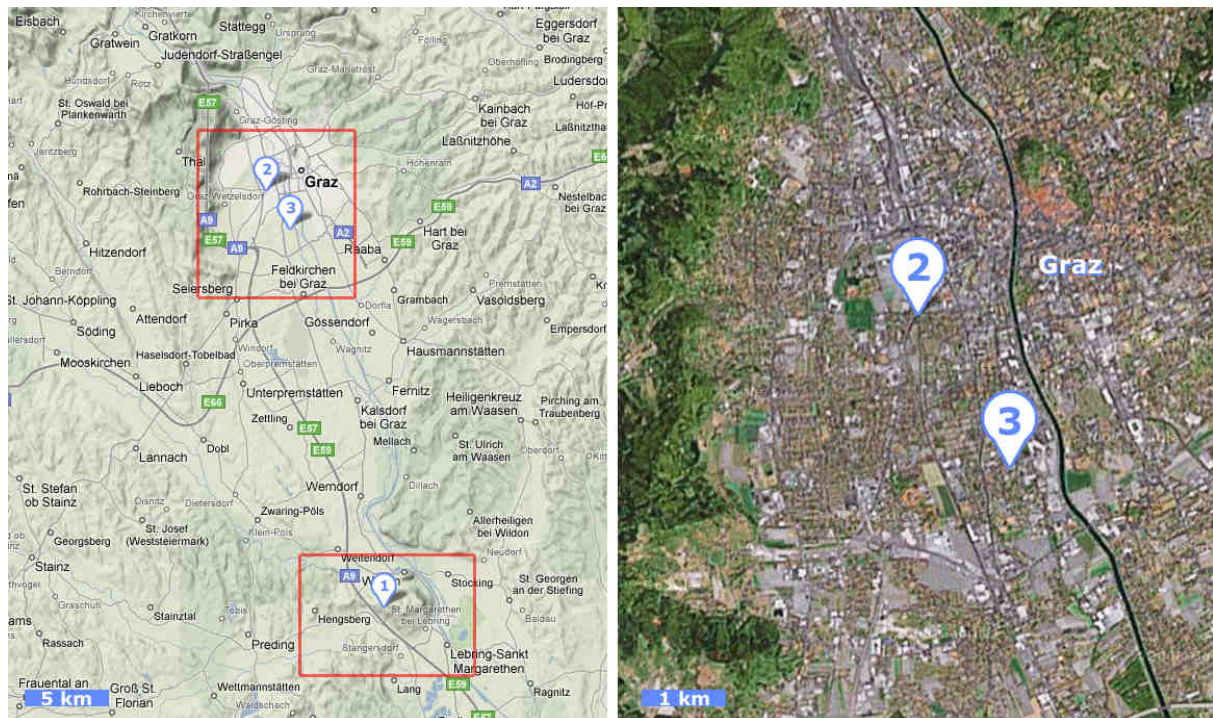


Figure 10: Sampling sites Graz. 1: Bockberg (background); 2: Don Bosco (urban); 3: Graz Süd (urban) (based on Google Maps; supplemented with marks for sampling sites).

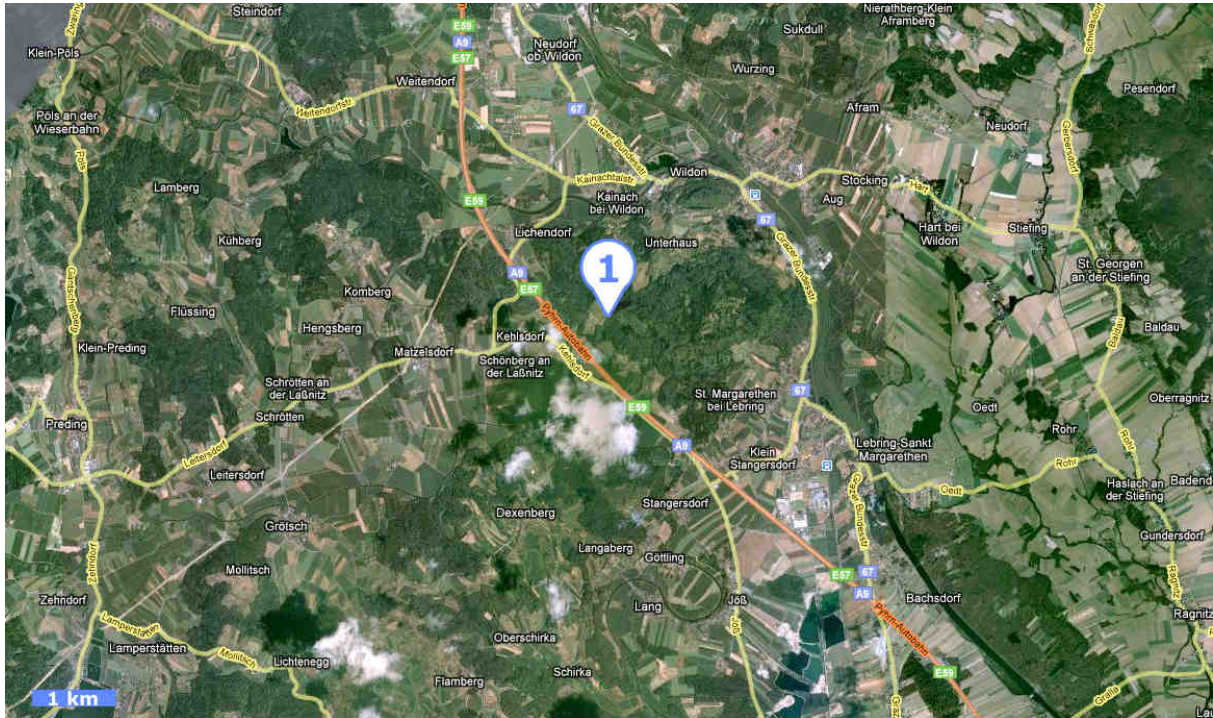


Figure 11: Background site Bockberg (based on Google Maps; supplemented with marks for sampling sites).



Figure 12: Sampling site Bockberg (left) and Graz Süd (right) (taken from Umweltbundesamt, 2009).



Figure 13: Sampling site Don Bosco (taken from Umweltbundesamt, 2009).

Salzburg

Sampling sites in the area of Salzburg (Figure 14, Figure 15 and Figure 16), the capital of the Austrian federal state Salzburg with 150.000 inhabitants, are located in a north-south transect. Rudolfsplatz (RUDO, 13° 03' 13.0"E, 47° 47' 51.0" N, 425 m a.s.l.) represents the traffic impacted inner urban site, while Lehen (LEHE, 13° 01' 51.0"E, 47° 49' 2.0"N, 420 a.s.l.) and Anthering (ANTH, 47°52' 53"E, 13°0' 43"N, 440 m a.s.l.) are the urban residential and the local background site, located several kilometres north of Salzburg's city centre, respectively. Geographical coordinates, description of sampling sites and population figures are based on information from the Environment Agency Austria (Umweltbundesamt, 2009). Geographical coordinates, description of sampling sites and population figures are based on information from the Environment Agency Austria (Umweltbundesamt, 2009).

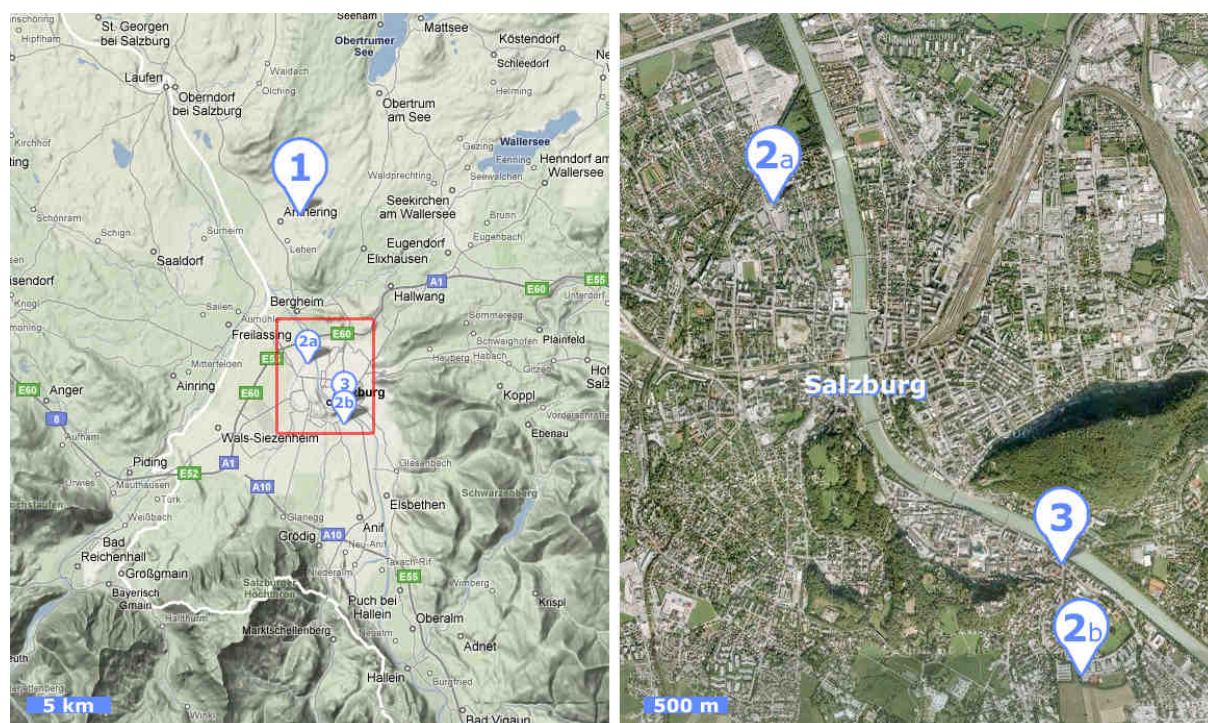


Figure 14: Sampling sites Salzburg. 1: Anthering (background); 2a: Lehen (urban); 2b: Freisaalweg; 3: Rudolfsplatz (urban) (based on Google Maps; supplemented with marks for sampling sites).

Sampling site Lehen was located in the district Lehen until 11th of September 2004 and subsequently moved to Freisaalweg on 14th September 2004. Old and new position and the respective immediate vicinity are depicted in Figure 14 and Figure 15.



Figure 15: Sampling site Lehen Fasangasse (left) and Freisaalweg (right) (taken from Umweltbundesamt, 2009).



Figure 16: Sampling site Rudolfsplatz (taken from Umweltbundesamt, 2009).

Carinthia

Sampling sites in the urban area of Klagenfurt and the Jauntal are arrayed in west-east transect, depicted in Figure 17. Samples were drawn from October 2004 to June 2005. Klagenfurt, with 95.000 inhabitants, is the capital of Carinthia, the most southern Austrian federal state. In the urban area of Klagenfurt the two sites with urban background and urban traffic impacted characteristics, are located in Koschatstraße (KOSCH, 14°17'50" E, 46°37'32" N,) and Völkermarkterstraße (VÖLKE, 14° 19' 10.6" E, 46° 37' 33.0" N, 445 m a.s.l., Figure 18 and Figure 21). The two rural sampling sites in Carinthia are located in Gurtschitschach (GURT), situated approximately 4 km south of the city of Völkermarkt (11.000 inhabitants) and Lavamünd (LAVA), 5 km from the centre of Lavamünd (3000 inhabitants), situated near the river Drau (Figure 19, Figure 20 and Figure 22). Geographical coordinates, description of sampling sites and population figures are based on information from the Environment Agency Austria (Umweltbundesamt, 2009).

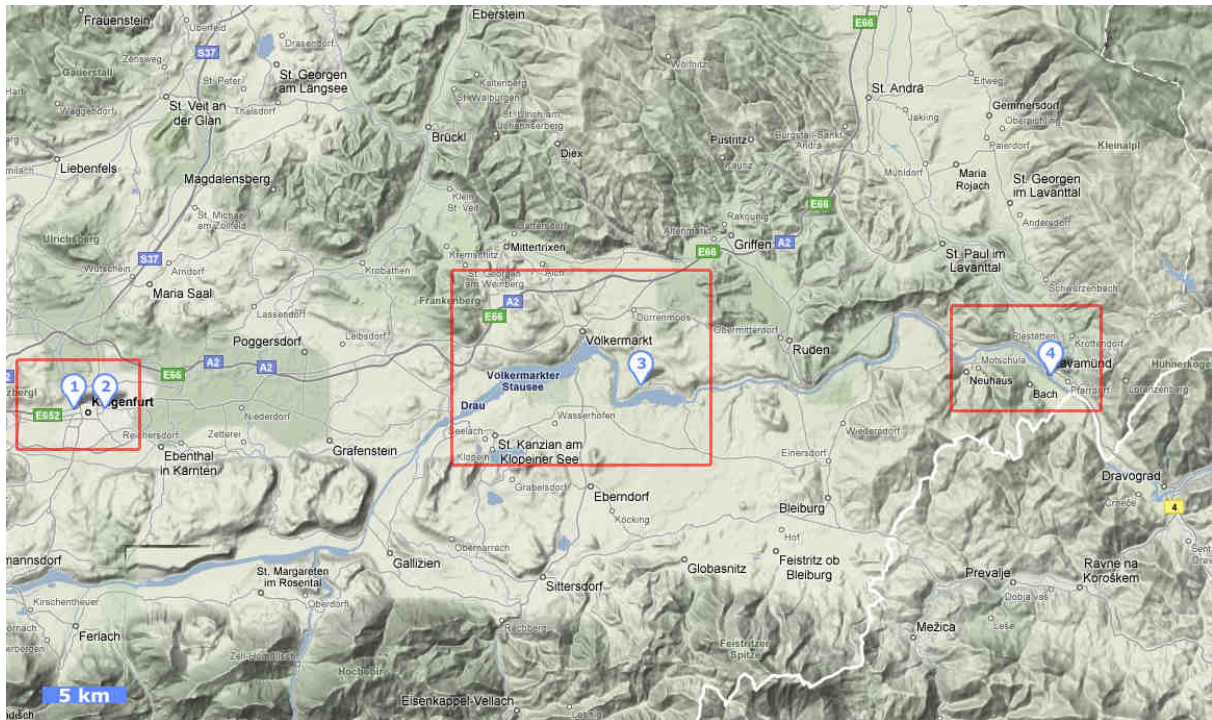


Figure 17: Sampling sites Carinthia. 1: Koschatstraße, 2: Völkermarkterstraße, 3: Gurtschitschach, 4: Lavamünd (based on Google Maps; supplemented with marks for sampling sites).

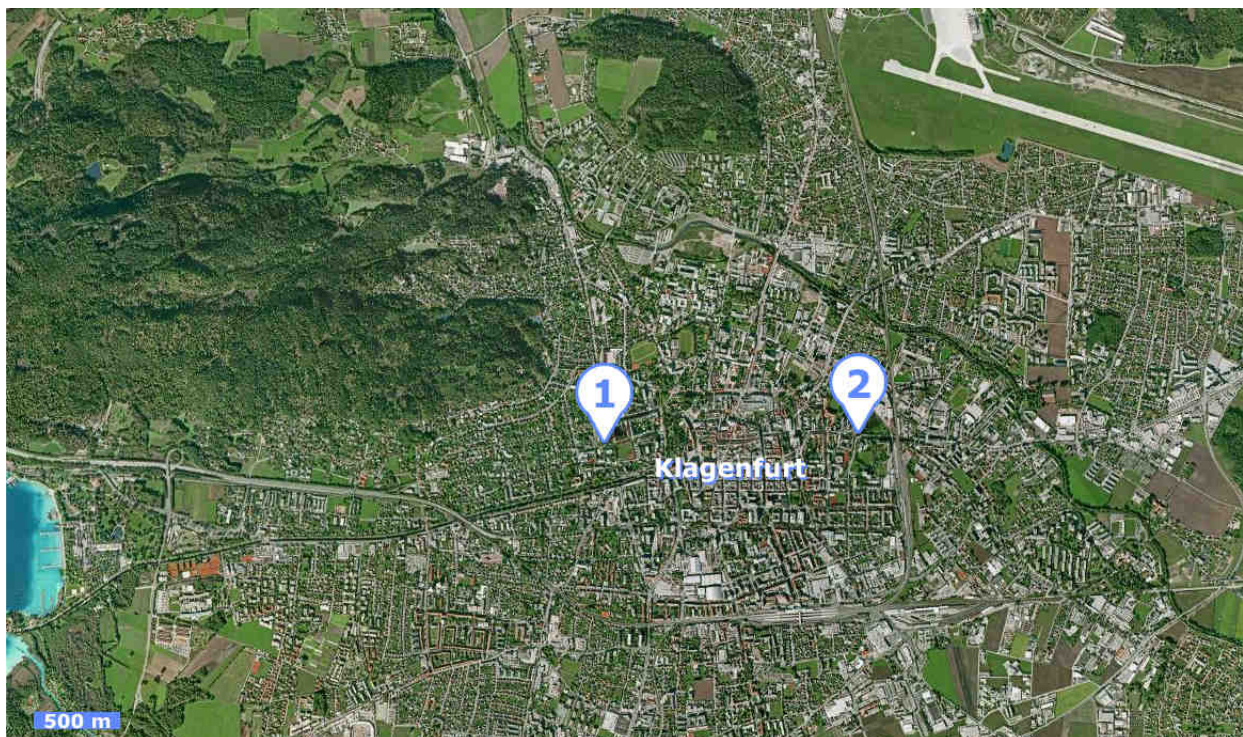


Figure 18: Urban sampling sites Klagenfurt. 1: Koschatstraße; 2: Völkermarkterstraße (based on Google Maps; supplemented with marks for sampling sites).

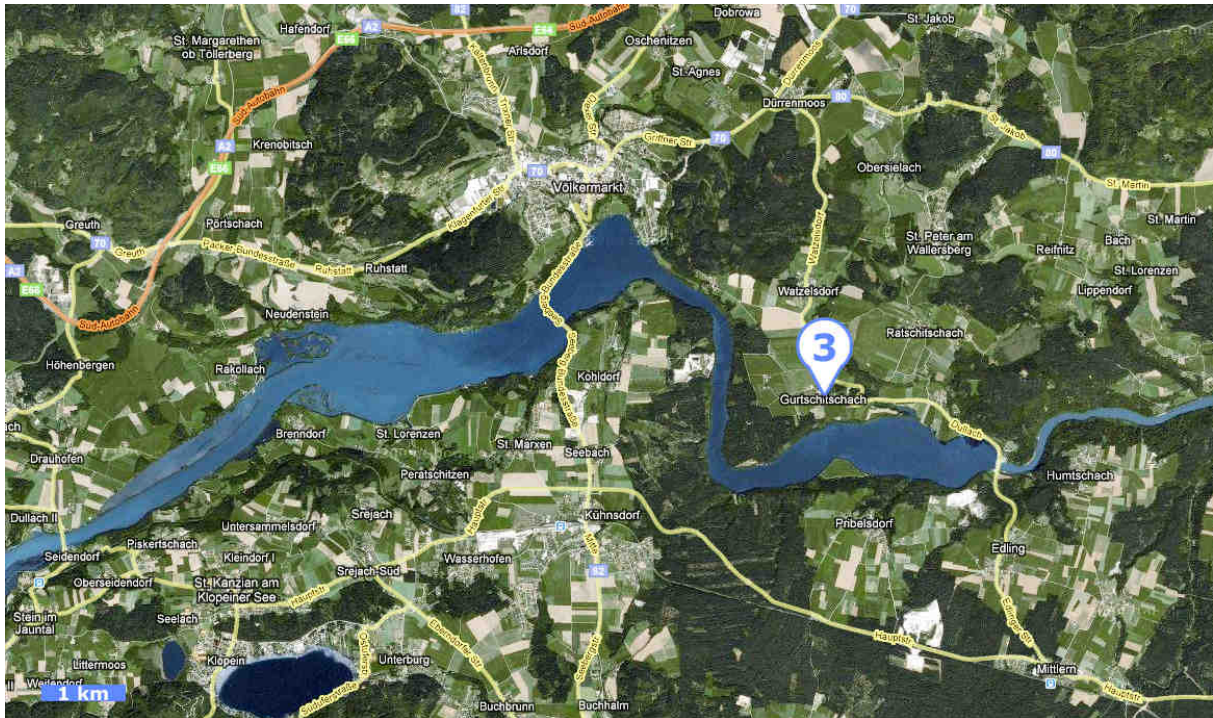


Figure 19: Regional surrounding Gurtschitschach (based on Google Maps; supplemented with marks for sampling sites).

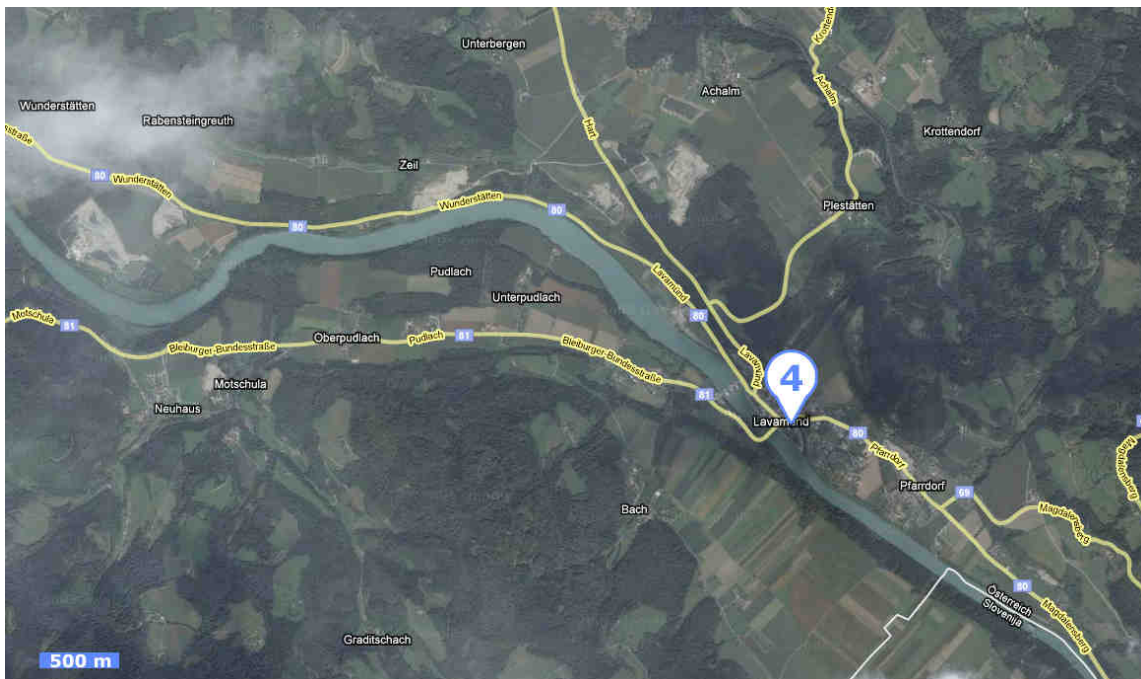


Figure 20: Regional surrounding Lavamünd (based on Google Maps; supplemented with marks for sampling sites).



Figure 21: Urban sampling sites Koschatstraße (left) and Völkermarkterstraße (right) (taken from Umweltbundesamt, 2009).

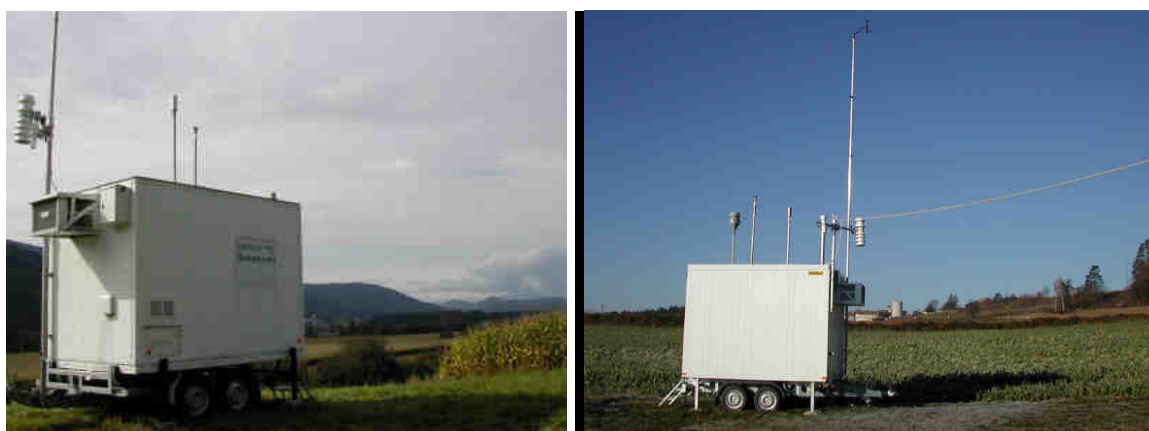


Figure 22: Rural sampling sites Lavamünd (left) and Gurtschitschach (right) (taken from Umweltbundesamt, 2009).

Lower Austria

Four out of five lower Austrian sampling sites are set up in a west-east transect. With Mistelbach being the station located slightly north, pictured in Figure 23. One urban site is situated in St.Pölten (STPÖ, $15^{\circ} 38' 3.0''$ E, $48^{\circ} 12' 45.0''$ N, 250 m a.s.l.), the capital of Lower Austria with 52.000 inhabitants. The second urban site is located in Schwechat (SCHW, $16^{\circ} 28' 28.0''$ E, $48^{\circ} 08' 42.0''$ N, 155 m a.s.l.) an urban municipality (16.500 inhabitants) merged with the southeast of Vienna. SCHW is influenced by Viennese emissions as well as industrial activities, such as the oil refinery situated 3 km northeast of the sampling site. Both sites are situated in urban residential area. Rural background sites are Amstetten (AMST, $14^{\circ} 52' 42.0''$ E, $48^{\circ} 07' 13.0''$ N, 270 m a.s.l.), Stixneusiedl (STIX, $16^{\circ} 40' 36.0''$ E, $48^{\circ} 03' 3.0''$ N, 240 m a.s.l.) and Mistelbach (MIST, $16^{\circ} 34' 50.0''$ E, $48^{\circ} 34' 43.0''$ N, 250 m a.s.l.). The immediate surroundings of the sites are shown in Figure 29 and Figure 30. Sampling took place from January to June 2005, except for Amstetten where sampling started in April 2005. Geographical coordinates, description of sampling sites and population figures are based on information from the Environment Agency Austria (Umweltbundesamt, 2009).

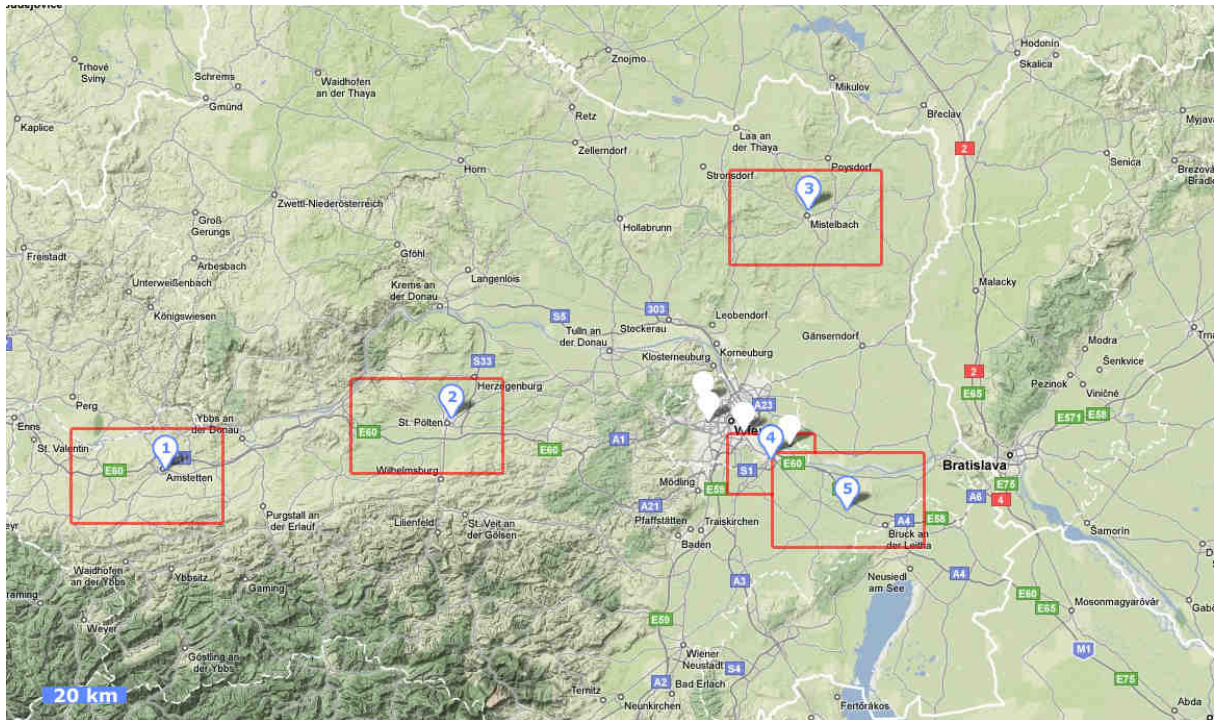


Figure 23: Sampling sites in Lower Austria. 1: Amstetten; 2: St.Pölten; 3: Mistelbach; 4: Schwechat; 5: Stixneusiedl (based on Google Maps; supplemented with marks for sampling sites).

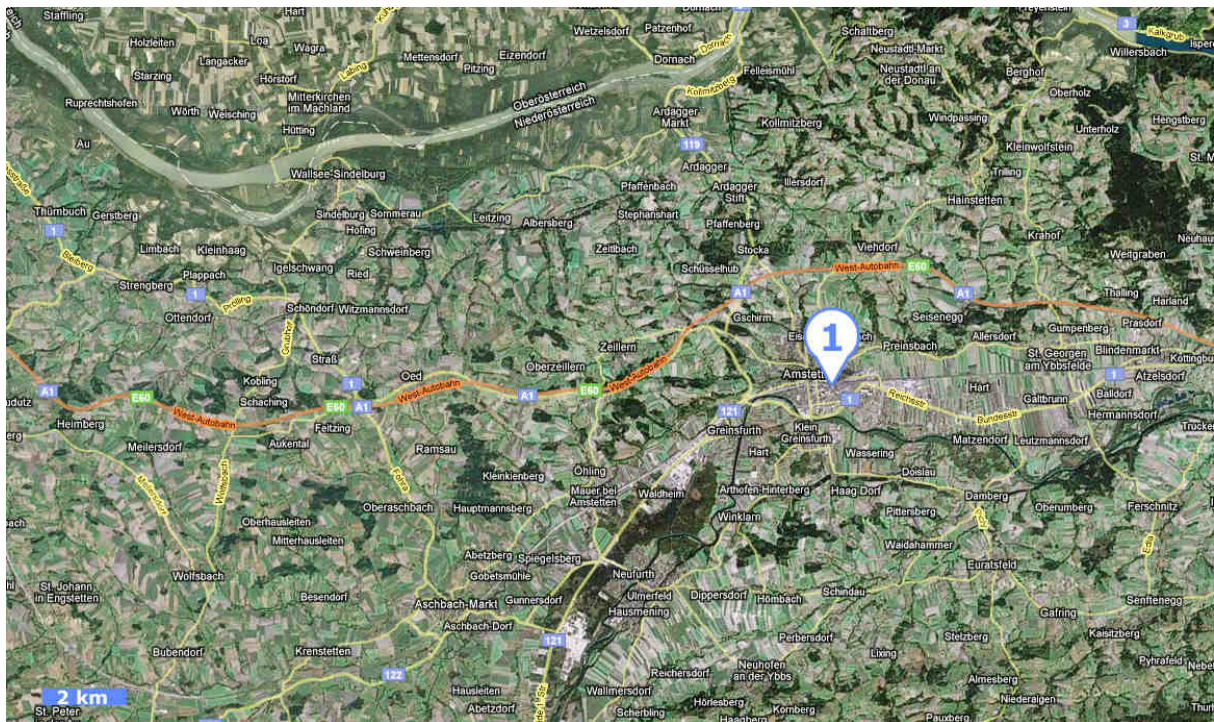


Figure 24: Regional surrounding of Amstetten (based on Google Maps; supplemented with marks for sampling sites).

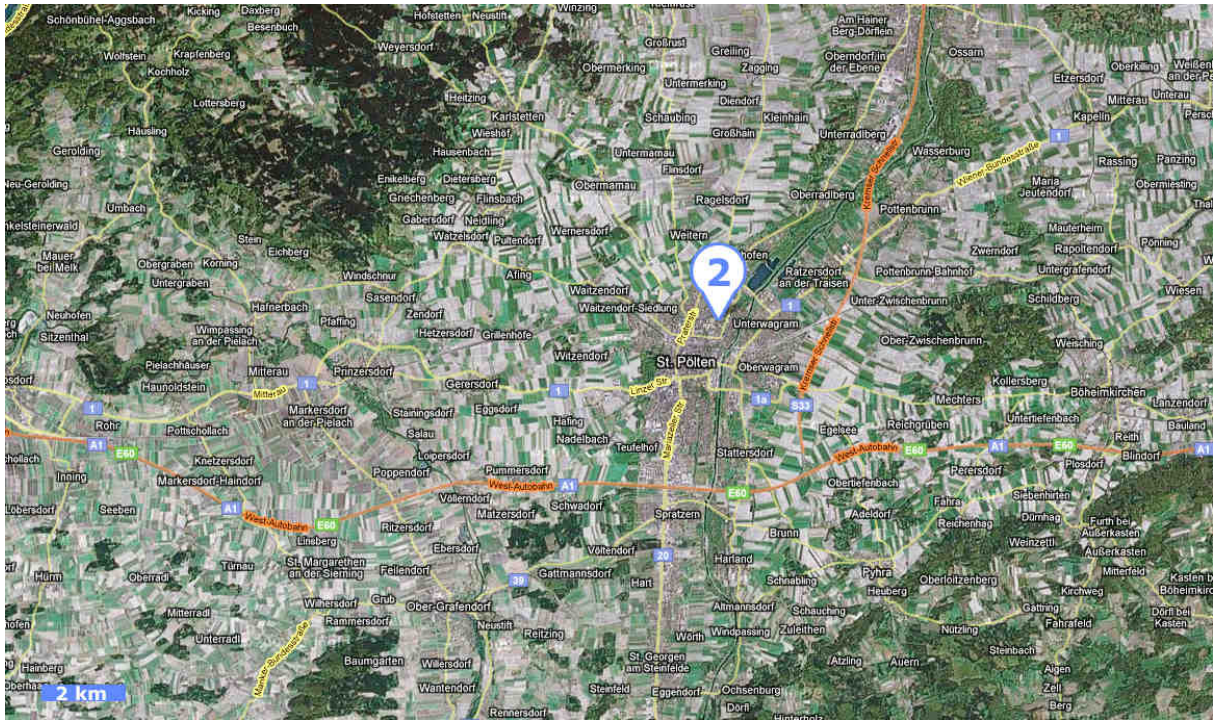


Figure 25: Regional surrounding of St.Pölten (based on Google Maps; supplemented with marks for sampling sites).

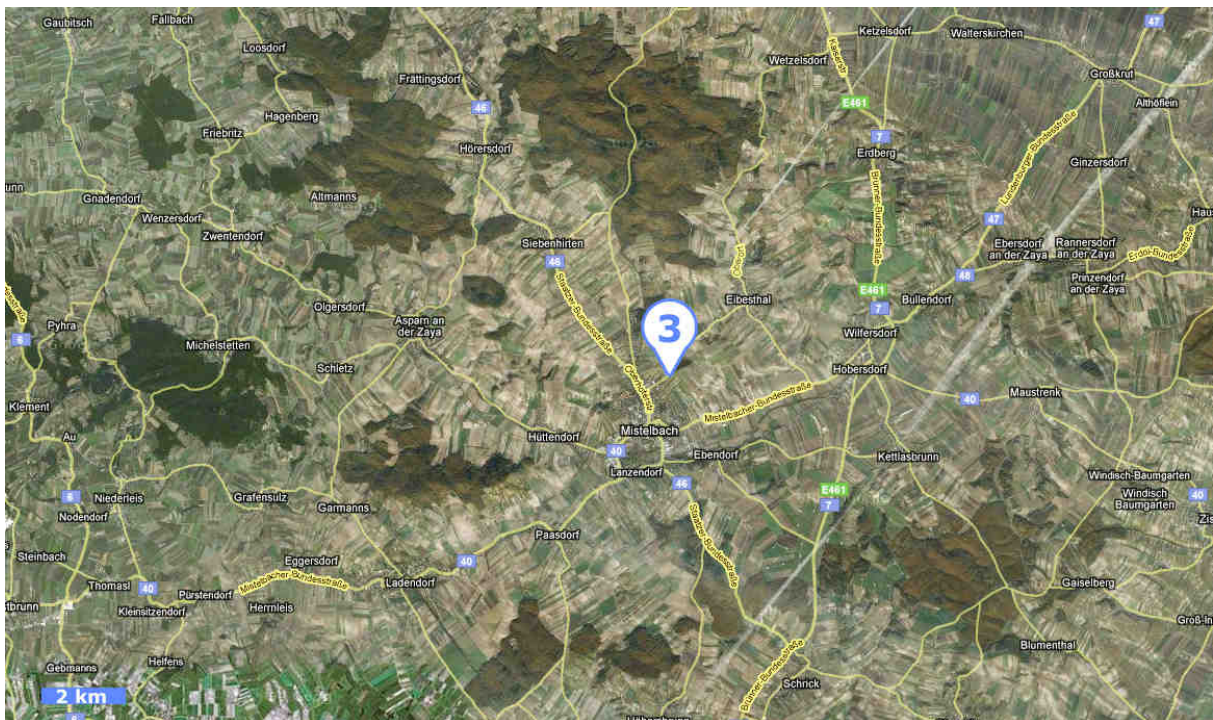


Figure 26: Regional surrounding of Mistelbach (based on Google Maps; supplemented with marks for sampling sites).

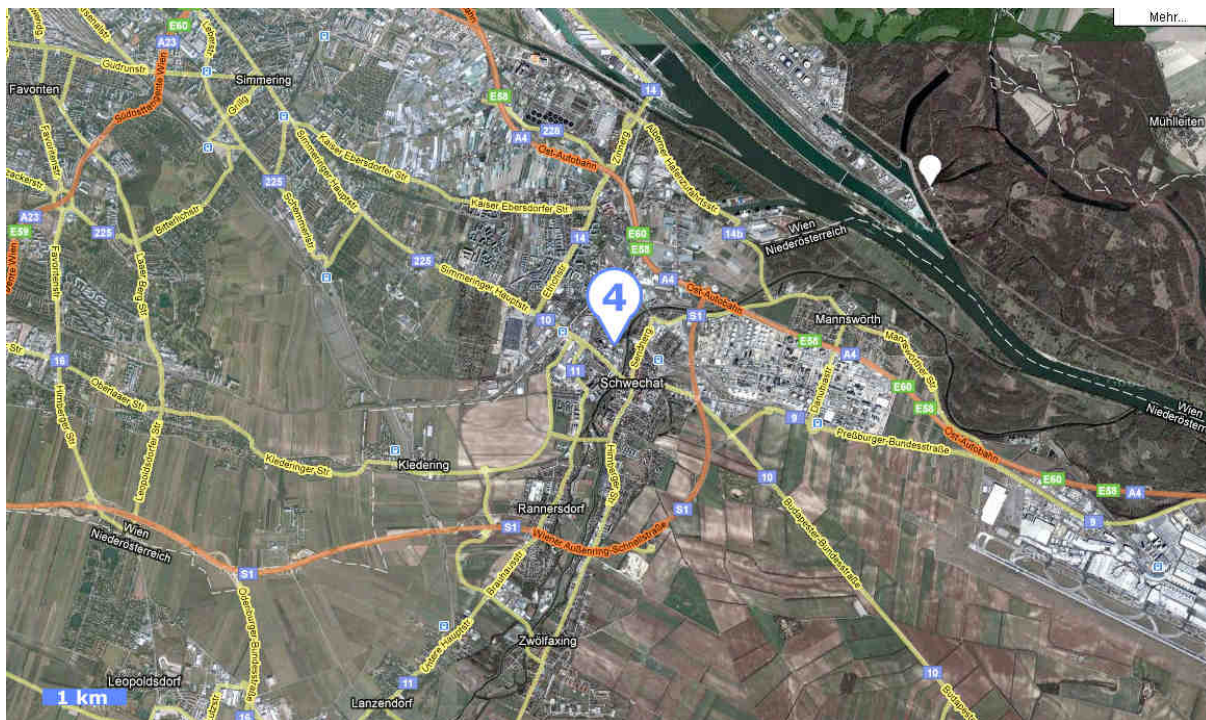


Figure 27: Regional surrounding of Schwechat (based on Google Maps; supplemented with marks for sampling sites).

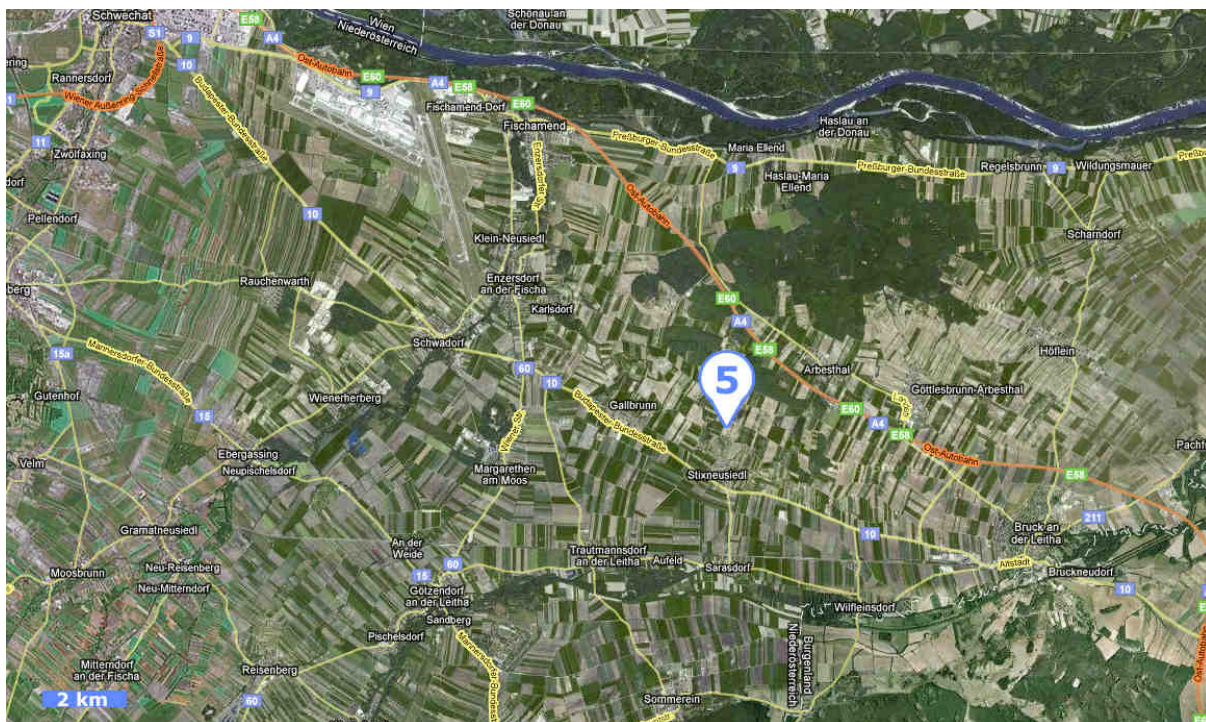


Figure 28: Regional surrounding of Stixneusiedl (based on Google Maps; supplemented with marks for sampling sites).



Figure 29: Sampling sites Schwechat (left) and Stixneusiedl (right) (taken from Umweltbundesamt, 2009).



Figure 30: Sampling sites St.Pölten (left), Mistelbach (middle) and Amstetten (right) (taken from Umweltbundesamt, 2009).

Upper Austria

The location of the four Upper Austrian sites is depicted in Figure 31. The regional background site Enzenkirchen is located about 50 km north west from Linz, the upper Austrian capital with 191.000 inhabitants, where the urban sites are located. Samples were drawn from April 2005 to March 2006.

The four sites chosen in this study are: Three urban sites (Figure 32, Figure 33, and Figure 34) and Enzenkirchen (ENZE, 13° 40' 16.1" E, 48° 23' 30.2" N, 525 m a.s.l., Figure 34 and Figure 35) as a rural background station 50km upwind. Figure 32 displays the three sampling sites in the city: Römerberg (RÖME, 14° 16' 58.0" E, 48° 18' 10.0" N, 262 m a.s.l.) a station next to a highly frequented road ending in a tunnel, Neue Welt (NEWE, 14° 18' 53.0" E, 48° 16' 28.0" N, 265 m a.s.l.) next to the industry area and a frequented road and Steyregg (STEY, 14° 21' 10.0"E, 48° 17' 25.0" N, 335 m a.s.l.) an elevated station at the urban fringe. A highway (A7, the so called "Mühlkreis-highway") with two lanes in each direction is crossing the city from the north to the south. The A7 ranks among one of the most frequented highways in Austria with a mean daily traffic volume of around 67.000 vehicles with up to 100.000 vehicles per day at working days in both directions (Asfinag, VCÖ, 2005). Beside the traffic emissions, Linz is also influenced by an industrialized area near the city centre. This area is situated between the A7 highway and the Danube and includes a steel producing industry, an area with different

companies for fine chemicals and a harbour with an industrialized zone. Geographical coordinates, description of sampling sites and population figures are based on information from the Environment Agency Austria (Umweltbundesamt, 2009).

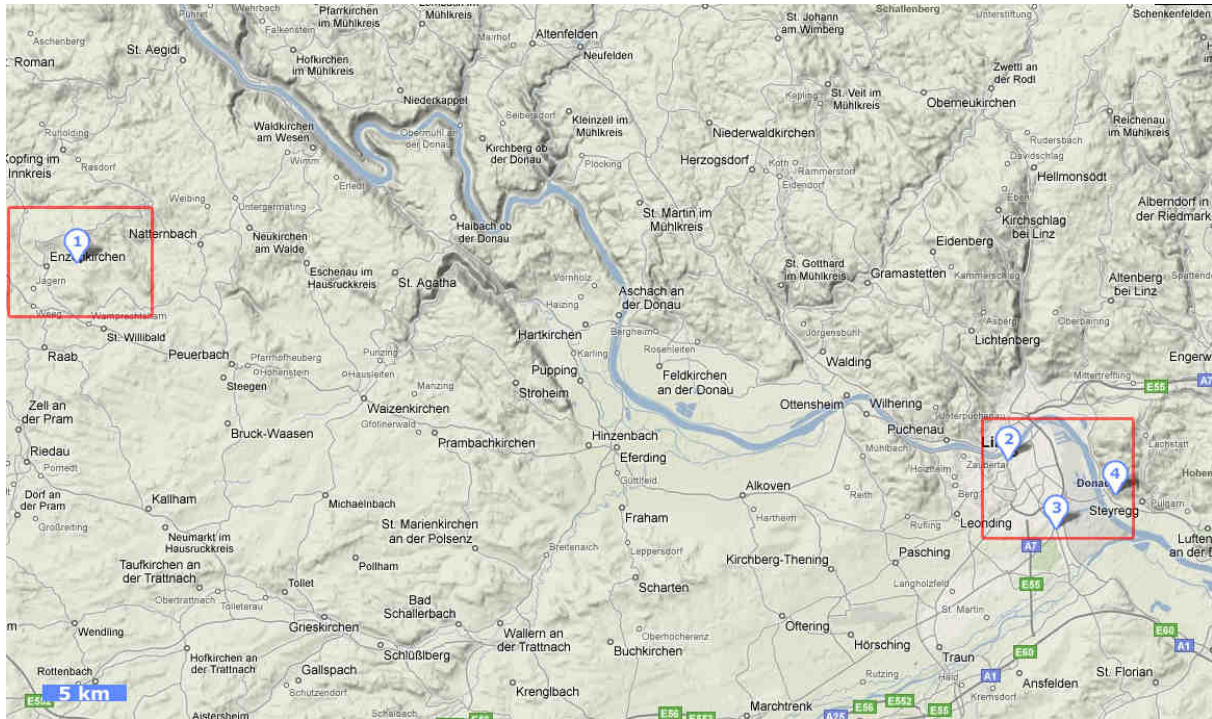


Figure 31: Sampling sites Oberösterreich. 1: Enzenkirchen. 2, 3, 4: urban sampling sites in Linz (Figure 32) (based on Google Maps; supplemented with marks for sampling sites).

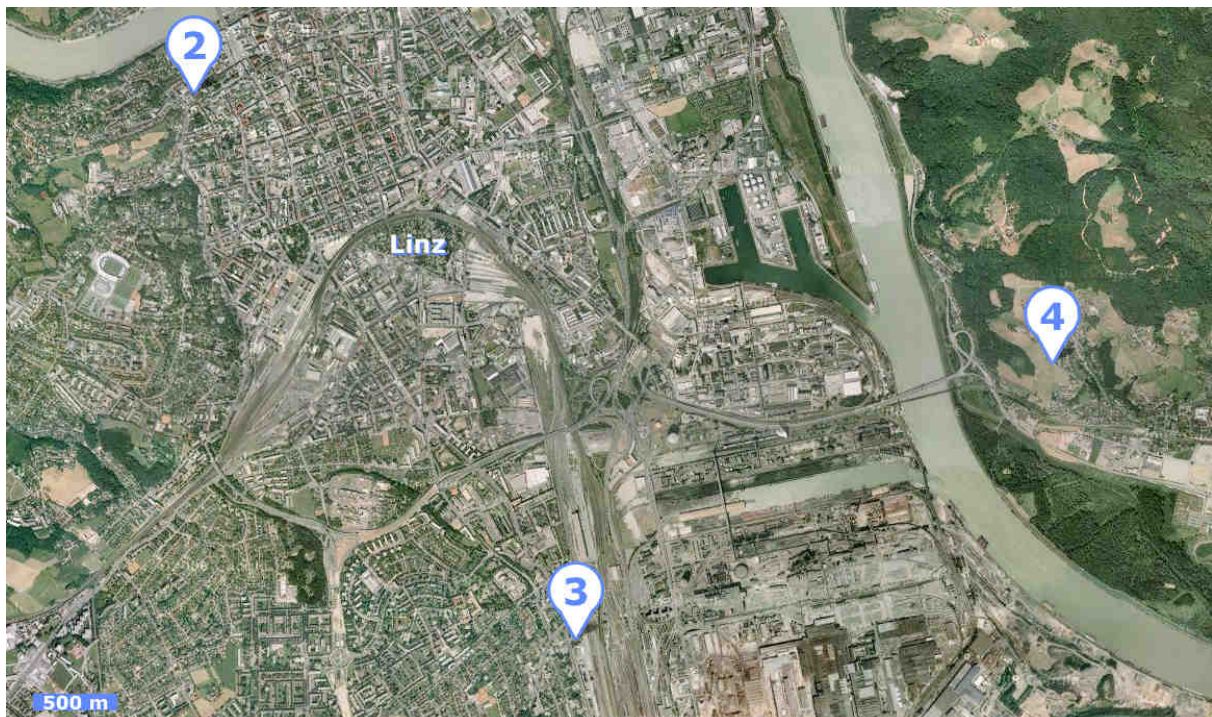


Figure 32: Sampling sites Linz. 1: Römerberg; 2: Neue Welt; 3: Steyregg (based on Google Maps; supplemented with marks for sampling sites).



Figure 33: Sampling site Römerbergtunnel (left) and Steyregg (right) (taken from Umweltbundesamt, 2009).



Figure 34: Sampling sites Neue Welt (left) and Enzenkirchen (right) (taken from Umweltbundesamt, 2009).

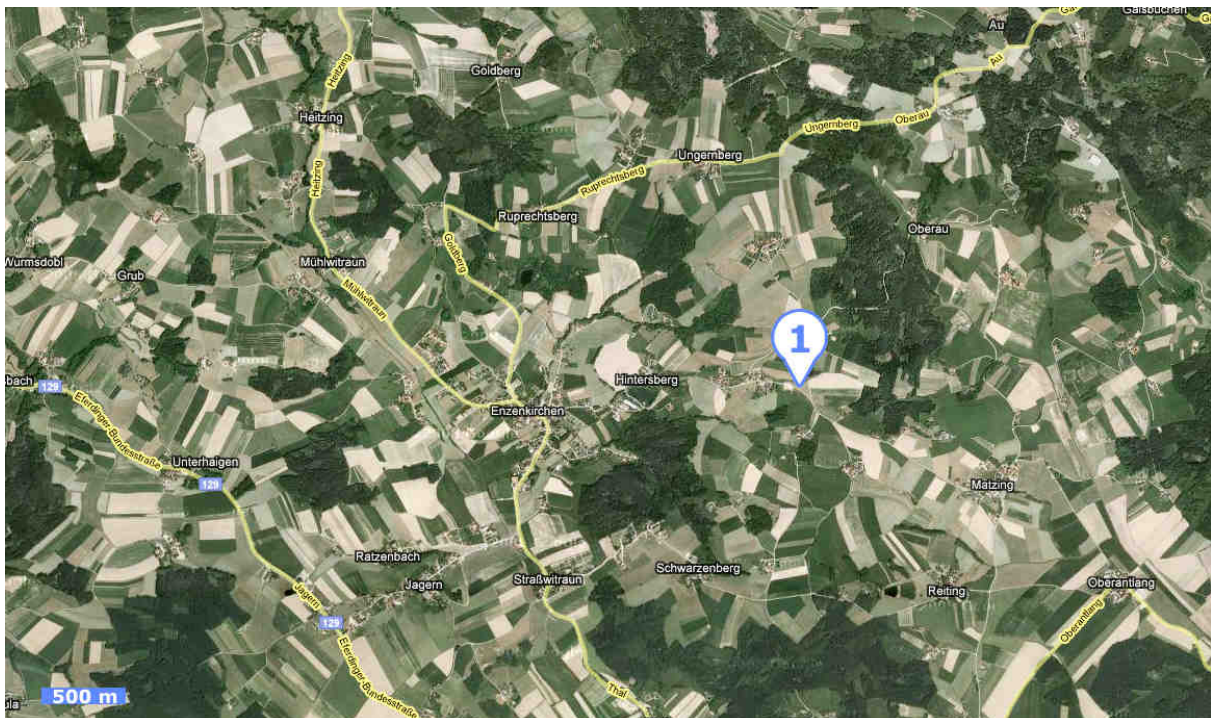


Figure 35: Background site Enzenkirchen (based on Google Maps; supplemented with marks for sampling sites).

Table 3: Overview of PM10 sampling sites investigated in the present work (compiled from information from Umweltbundesamt, 2009)

| Region | Name of sampling site | Acronym | Type of area | Type of station | Topography | Immediate vicinity | Local vicinity |
|---------------|-----------------------|---------|--------------|-----------------|---|--|---|
| Vienna | Schafbergbad | SCHAF | suburban | background | hill country | moderately frequented narrow road, park | residential area, loosely covered with buildings, woods, meadows |
| | Kendlerstraße | KEND | urban | background | plane at hill country margin | moderately frequented narrow road | residential area, densely covered with buildings, moderately frequented roads |
| | Rinnböckstraße | RINN | urban | traffic | plane | moderately frequented road | residential area, industrial zone, offices, heavily frequented road |
| | Lobau | LOBA | suburban | background | plane | park, meadow | farmland, wood, meadows, lakefront, single houses, moderately affected industrial area |
| Graz | DonBosco | DONB | urban | traffic | half-open basin at mountain margin | heavily used broad road, public building, meadow | office buildings, industrial and residential area, farmland, heavily frequented road |
| | Graz Süd | GRAS | urban | background | half-open basin at mountain margin | moderately frequented narrow road, meadow | lowly affected industrial area, residential area (loosely covered), moderately frequented road |
| | Bockberg | BOCK | rural | background | top of a hill | meadows | single houses, heavily frequented road, wood, meadows |
| Salzburg | Anthering | ANTH | rural | background | plane area, half-open basin mountain margin | farmland, meadows | single houses, wood, farmland |
| | Rudolfsplatz | RUDO | urban | traffic | plane area, half-open basin mountain margin | traffic island in a roundabout, heavily frequented road | city center, heavily frequented roads |
| | Lehen | LEHE | urban | background | plane area, half-open basin mountain margin | moderately frequented broad road | residential area, park, moderately frequented broad road |
| Carinthia | Koschatstraße | KOSCH | urban | background | bassin sorrounded by near low and high mountains | moderately frequented road, meadow | residential area, loosely covered with buildings, moderately to heavily frequented road, Park |
| | Völkermarkterstraße | VÖLKE | urban | traffic | bassin sorrounded by near low and high mountains | heavily frequented, broad road | office, industry, residential area, heavily frequented roads |
| | Gurtschitschach | GURT | rural | background | plane, broad valley , near low and high mountains | farmland, meadows | farmland, single houses |
| | Lavamünd | LAVA | rural | background | valley in low mountains | meadows | wood, meadows |
| Lower Austria | St.Pölten | STPÖ | urban | background | broad valley in hill country | park, public building, public building | office buildings, weakly impacted industrial area, residential area farmland, wood, meadows , moderately frequented road |
| | Mistelbach | MIST | rural | background | hill country | meadow, narrow weakly frequented road | meadow, farmland, rural residential area |
| | StixNeusiedl | STIX | rural | background | knowe in a plane | vine yard, meadows, farmaland | farmland, residential area (loosely covered), wood, meadows |
| | Schwechat | SCHWE | urban | industrial | plane | park, public building | airport, farmland, residential area (loosely covered), moderately impacted industrial area, heavily frequented road, wood, meadow |
| | Amstetten | AMST | suburban | background | plane at mountain margin | moderately frequented braod road | Office buildings, Industrial and residential area, moderately impacted industrial area, farmland, wood, meadow |
| Upper Austria | Römerberg | RÖME | urban | traffic | plane at the foot of hill | heavily frequented braod road | heavily frequented road, tunnel entrance, urban residential area |
| | NeueWelt | NEWE | urban | industrial | plane | heavily frequented broad road, tramway turningback, meadow | heavily frequented road, residential area, industrial area |
| | Steyregg | STEY | suburban | industrial | hill country, 80 m above the river danube | moderately frequented, narrow road, farmland and meadows | residential area, loosely covered with buildings, highly impacted industrial area, farmland |
| | Enzenkirchen | ENZE | rural | background | hill country | moderately frequented narrow road, meadows, farmland | farmland, moderately frequented road |

5 Sampling

5.1 Atmospheric PM₁₀

Austrian airborne PM₁₀ was collected at 23 three sites in Austria by the respective local authorities in a time frame from January 2004 to March 2006. All sampling sites were part of the projects AQUELLA Vienna, AQUELLA Salzburg, AQUELLA Graz (Bauer et al., 2006, Bauer et al., 2007a and 2007b), AQUELLA Lower Austria (Bauer et al., 2008b), AQUELLA Carinthia and AQUELLA Upper Austria (Bauer et al., 2008a; Jankowski et al., 2009b). The PM₁₀ samples were collected daily with high volume samplers (DHA-80, DIGITEL Electronic AG, Switzerland) on quartz fibre filters (Pallflex™ 2500QAT-UP, diameter 150 mm, PALL Life Sciences, USA) for 24-h sampling periods, with volumes of approximately 700 m³ per filter. The filters were conditioned for around 48 h in a clean room at a temperature of 20±1 °C and a relative humidity of 50±5% and were weighed before and after sampling. The gravimetric measurements were performed by the local authorities. The sampling periods of the respective sampling site are listed in Table 4.

The weighed filters were cut for the different analysis conducted in the scope of the AQUELLA project, where one eighth was apportioned for HULIS analysis. Filter sample pools for immission samples from the AQUELLA projects ranged from single days up to 31 days, according to meteorological episodes, much higher loadings on traffic impacted sampling sites compared to background sites, special emission events and according to PM₁₀ mass loadings (e.g. >50 µg/m³, <50mg/m³), respectively. The pooling was processed in a way which still enabled the calculation of monthly means of the respective analytes.

5.2 Source samples

Emission samples from various sources have been analysed for HULIS with the same method as applied for ambient samples (see section 6.1). Sampling procedures are described in detail elsewhere (Puxbaum et al., 2006; Schmidl et al., 2008a and 2008b). Briefly particles with an aerodynamic diameter smaller than µm (PM₁₀) were collected on quartz fibre filters via direct sampling in the “exhaust” stream (wood stove burning, cooking emissions, lawn mowing, vehicular exhausts) or via re-suspension of the collected bulk dust or soil samples (Jankowski et al., 2009a and 2009b). The preparation of emission and source samples and their analysis was part of the Aquellis IGL – project (Emissions of industry, craft and agriculture; Puxbaum et al., 2006), the project “Aquellis M” – PM₁₀ Aerosol Emissions of Mobile Sources, Source Profiles of Vehicle Emissions: Exhaust, Brake and Tire Abrasion Products for application in the CMB Model” (Jankowski et al., 2009a) and „AQUELLIS – FB– Combustion of solid fuels” (Schmidl et al., 2008c).

Table 4: Sampling periods and number of analysed pools (note that sampling was conducted daily, pools denote the temporal resolution)

| Region and site | Type of area | 2004 | | | | | | | | | | | | 2005 | | | | | | | | | | | | 2006 | | | Number of total analysed pools | |
|-----------------|---------------------|----------|-----|-----|-----|-----|-----|-----|-----|-----|-----|-----|-----|------|-----|-----|-----|-----|-----|-----|-----|-----|-----|-----|-----|------|-----|-----|--------------------------------|----|
| | | Jan | Feb | Mar | Apr | May | Jun | Jul | Aug | Sep | Oct | Nov | Dec | Jan | Feb | Mar | Apr | May | Jun | Jul | Aug | Sep | Oct | Nov | Dec | Jan | Feb | Mar | | |
| Vienna | Schafbergbad | Suburban | 14 | 2 | 4 | 6 | 1 | 1 | 1 | 1 | 1 | 8 | 5 | 5 | | | | | | | | | | | | | | | | 49 |
| | Kendlerstraße | Urban | 14 | 2 | 4 | 6 | 2 | 2 | 2 | 1 | 4 | 8 | 5 | 6 | | | | | | | | | | | | | | | | 56 |
| | Rinnböckstraße | Urban | 14 | 2 | 4 | 6 | 1 | 1 | 2 | 1 | 1 | 8 | 5 | 6 | | | | | | | | | | | | | | | | 51 |
| | Lobau | Suburban | 5 | 2 | 4 | 2 | 2 | 2 | 1 | 2 | 3 | 7 | 5 | 6 | | | | | | | | | | | | | | | | 41 |
| Graz | DonBosco | Urban | 9 | 3 | 4 | 3 | 2 | 2 | 2 | 2 | 3 | 4 | 4 | 3 | | | | | | | | | | | | | | | | 41 |
| | Graz Süd | Urban | 9 | 3 | 4 | 3 | 2 | 2 | 2 | 2 | 2 | 4 | 5 | 3 | | | | | | | | | | | | | | | | 41 |
| | Bockberg | Rural | 5 | 3 | 4 | 3 | 2 | 2 | 2 | 2 | 3 | 4 | 5 | 2 | | | | | | | | | | | | | | | | 37 |
| Salzburg | Anthering | Rural | 6 | 3 | 3 | 3 | 2 | 5 | 2 | 1 | 1 | 2 | 5 | 6 | | | | | | | | | | | | | | | | 39 |
| | Rudolfsplatz | Urban | 7 | 3 | 3 | 2 | 2 | 5 | 2 | 1 | 1 | 2 | 6 | 5 | | | | | | | | | | | | | | | | 39 |
| | Lehen | Urban | 6 | 3 | 3 | 3 | 4 | 4 | 2 | 1 | 1 | 2 | 3 | 2 | | | | | | | | | | | | | | | | 34 |
| Carinthia | Koschatstraße | Urban | | | | | | | | | | | | 2 | 3 | 4 | 5 | 2 | | | | | | | | | | | 18 | |
| | Völkermarkterstraße | Urban | | | | | | | | | | | | 2 | 3 | 4 | 4 | 2 | | | | | | | | | | | 17 | |
| | Gurtschitschach | Rural | | | | | | | | | | | | 2 | 3 | 4 | 5 | 2 | | | | | | | | | | | 18 | |
| | Lavamünd | Rural | | | | | | | | | | | | 2 | 3 | 4 | 4 | 2 | | | | | | | | | | | 17 | |
| Lower Austria | St.Pölten | Urban | | | | | | | | | | | | | 3 | 10 | 5 | 4 | 3 | 4 | | | | | | | | | 29 | |
| | Mistelbach | Rural | | | | | | | | | | | | | 3 | 10 | 5 | 4 | 2 | 4 | | | | | | | | | 28 | |
| | Stixneusiedl | Rural | | | | | | | | | | | | | 3 | 10 | 5 | 4 | 3 | 4 | | | | | | | | | 29 | |
| | Schwechat | Urban | | | | | | | | | | | | | 3 | 10 | 5 | 4 | 3 | 4 | | | | | | | | | 29 | |
| | Amstetten | Rural | | | | | | | | | | | | | - | - | - | 2 | 2 | 3 | | | | | | | | | 7 | |
| Upper Austria | Römerberg | Urban | | | | | | | | | | | | | | | | 4 | 6 | | 4 | | | 9 | 5 | 6 | 10 | 6 | 5 | 55 |
| | NeueWelt | Urban | | | | | | | | | | | | | | | | 4 | 6 | | 4 | | | 9 | 5 | 6 | 10 | 6 | 5 | 55 |
| | Steyregg | Suburban | | | | | | | | | | | | | | | | 4 | 6 | | 4 | | | 9 | 5 | 6 | 10 | 6 | 5 | 55 |
| | Enzenkirchen | Rural | | | | | | | | | | | | | | | | 4 | 6 | | 4 | | | 9 | 5 | 6 | 10 | 6 | 5 | 55 |

6 Analytical Methods

6.1 Extraction, Separation and Quantification of HULIS

The method is based on a two-step isolation procedure of HULIS and the subsequent HULIS carbon-specific detection with a dissolved organic carbon analyser (Limbeck et al., 2005; Neuberger, 2005 and Handler, 2003).

Sample preparation and isolation of HULIS

Aliquots of quartz fibre filters, discs with diameters between 0.5 and 12 mm were extracted with Milli-Q water and 0.1 M sodium hydroxide. Filter areas applied for extraction ranged between 7 and 15 cm². To gain complete extraction of the soluble species in particulate matter, extraction was performed consecutively with three times 3ml of water in a temperature controlled (23°C +/- 2 ° C) ultrasonic bath for twenty minutes and combined subsequently. Subsequently the procedure was repeated with 0.1 molar sodium hydroxide with the filter discs that were prior extracted with water. One filter sample yielded an aqueous and an alkaline extract, 9 ml each. The extracts were centrifuged to separate filter debris and insoluble particles. The clear supernatant was separated and adjusted to pH 2 with diluted nitric acid. Acidification of the extracts prior to solid phase extraction (SPE) converts the polyacidic organic compounds, which were usually present in their ionic form under neutral or basic conditions, into their protonated form, leading to a more hydrophobic behaviour. These conditions optimize the separation of HULIS from the aqueous solution during solid phase extraction (C18 (EC), Isolute, 221-0020-H). SPE cartridges are cleaned and pre-conditioned by flushing three times with 1 ml of methanol and rinsing with 10 ml of high-purity organic carbon free water. This is repeated three times, keeping approximately 0.5 ml of water in the cartridge after the last conditioning/cleaning run. After this step the prepared solutions are aspirated through the SPE column with a flow of ~2ml/min. The extract solution passing the SPE cartridge contains those compounds which were not retained on the column such as inorganic ions and organic compounds, which were still hydrophilic due to the presence of highly polar functional groups, such as short chain mono-carboxylic acids. The fraction adsorbed on the column contained HULIS and other polar organic compounds such as long-chain mono-carboxylic acids, aromatic alcohols, or aldehydes (Limbeck et al., 2005). The column then is rinsed with 2 ml of ultrapure water and sucked dry. The retained substances are then eluted with 0.2 ml of methanol and filled up to 2ml with a mixture of diluted sodium hydroxide and nitric acid to achieve a pH of ~3. These solutions were then applied to the second separation step on an ion exchange micro-column (Isolute SAX, IST 500-0020), integrated in a flow injection system (Figure 36 and Figure 37). The strong anion exchanger (SAX) in the microcolumn extracted HULIS and other analytes capable of

carrying a negative charge, whereas neutral compounds passed the column without retention. After sample loading (aliquots of 500 μl), a wash step with 0.01 mol/L nitric acid was performed, to separate anionic species bearing only one or two charges per molecule (e.g., mono- or dicarboxylic acids) from polycharged HULIS. Subsequently, the remaining fraction, assigned to humic-like substances, was eluted from the strong ion exchange (SAX) column with diluted NH_4OH (0.08 M) and directly introduced into the total organic carbon analyser.

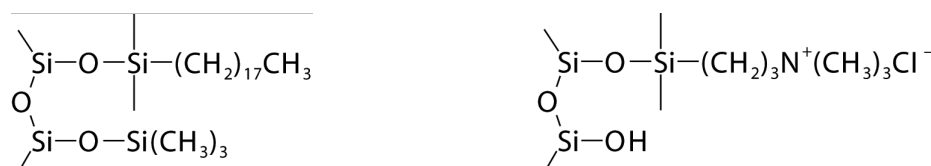


Figure 36: Chemical structure of the SPE (C18-EC, left) and the anion exchange sorbent (SAX, right) applied in the first and second isolation step, respectively (taken from <http://biotage.com/product-page>).

Instrumentation

The flow injection system for isolating HULIS from the remaining sample constituents consists of two six-port injection valves (VICI, Cheminert C22), two HPLC pumps (Merck Hitachi L-6000), and a peristaltic pump (Ismatec, Germany). For the ion exchange micro columns, Teflon tubes (inner diameter $\sim 1\text{mm}$, length $\sim 20\text{ mm}$) were filled with 20 μL of a strong ion exchanger (Isolute SAX, IST 500-0020) and sealed with porous teflon discs. The sample loop and the eluent loop had a volume of 500 μl and 750 μl , respectively. The diluted ammonia and nitric acid are pushed through the system with 0.6 ml/min by the two HPLC pumps. Connections between individual parts of the system were realised with Teflon tubes (inner diameter $\sim 0.7\text{mm}$) (Limbeck et al., 2005).

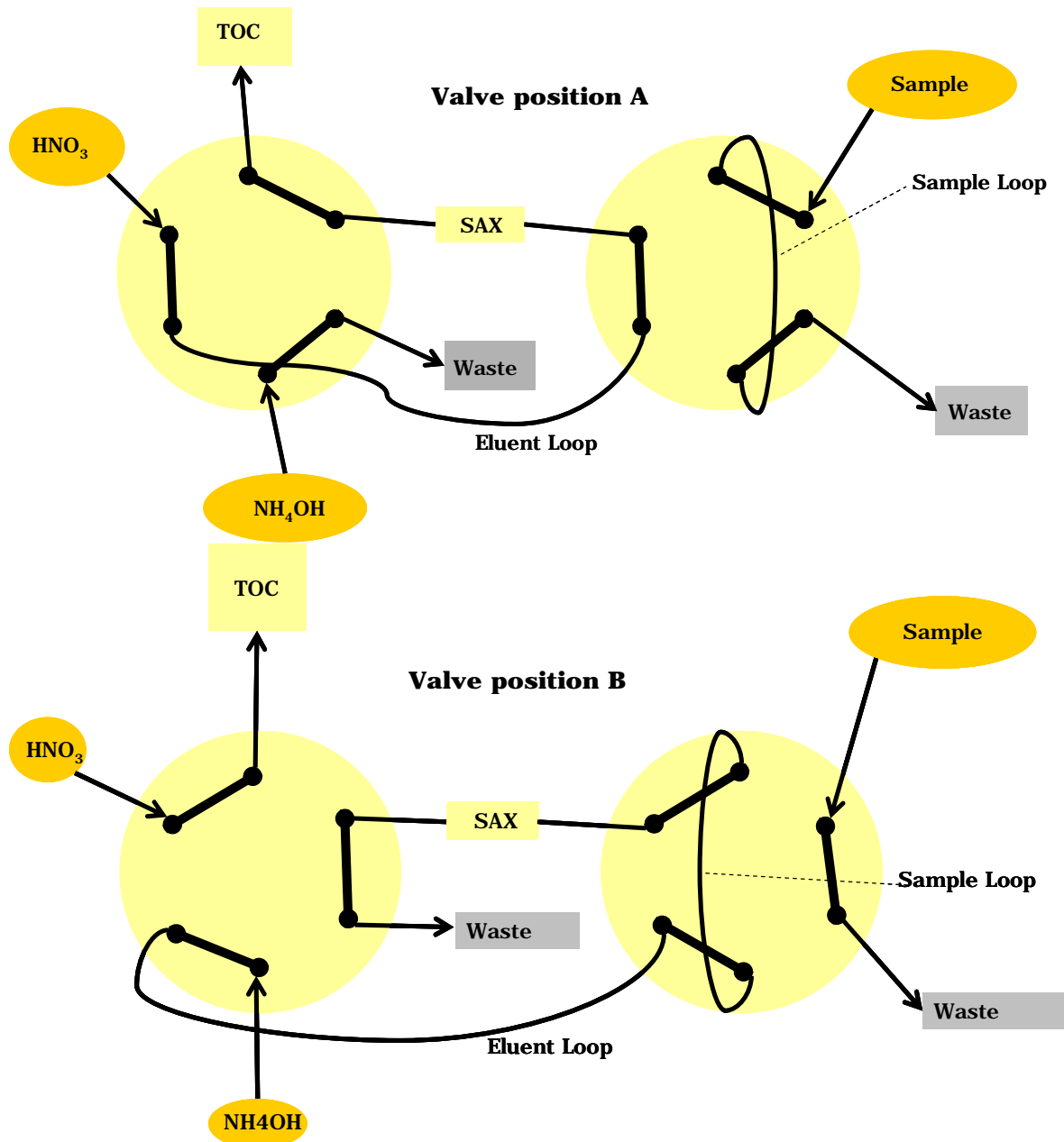


Figure 37: Flow injection manifold, developed by Limbeck et al. (2005); 2. Valve position A: fill/inject; Valve position B: load (after Neuberger, 2005).

The samples are injected in the sample loop (Valve position A, Figure 37), while the diluted nitric acid rinses the column and is subjected to the detection system. Subsequently valves are switched to position B (Figure 37) and diluted ammonia is pumped into the FI-system and moves the sample on the SAX-column and pushes the diluted nitric acid through the sample loop and over the sax column. After 175 s the valves switch back to position A, HULIS eluates are introduced in the combustion section of the TOC and nitric acid rinses the system. For the detailed operating sequence of the online FI-system see Limbeck et al. (2005).

The carbon content was determined with a Total Organic Carbon Analyser (GO TOC 100, Gröger & Obst) operating with a continuous flow rate of 0.6 ml/min, catalytic combustion at 800°C and a downstream non-dispersive infrared detector. The carrier gas is ambient air, pre-cleaned by three filters (activated charcoal, soda lime granulate and zinc, bronze grid filter) integrated in the TOC.

HULIS carbon quantification

HULIS carbon was quantified with an external 3-point calibration of diluted humic acid stock solutions. The standards are prepared and measured daily prior to HULIS carbon determination. The humic acid standard stock solution is prepared by dissolving ~0.05 g of humic acid (Fluka) in 50 ml of ultrapure, organic-free water which is kept in an ultrasonic bath for 30 minutes. Subsequently the solution is centrifuged and the clear supernatant is separated. The carbon content of the standard solution is determined with a dissolved organic carbon analyser (TOC 500, Shimadzu). Until further utilisation the standard stock solution was stored in a refrigerator. The calibration standards are prepared by adding 500 and 1000 µl of the humic acid standard solution to a mixture of diluted nitric acid and sodium hydroxide, to obtain identical matrix and pH conditions as for filter extracts. Blank calibration standards consisted solely of the diluted nitric acid sodium hydroxide mixture. The humic acid standards are subjected to the same protocol as the sample solutions and a calibration is processed at every day of measurement. Each standard and sample solution is aspirated into the sampling loop and analysed twice. Carbon dioxide signals obtained after the quantitative combustion of carbon containing fraction after the online separation step on an ion-exchange micro column, the HULIS fraction, were detected by a non-dispersive infra-red detector and recorded with the chromatographic software WINCHROM[®]/32 1.91.

6.2 Analytical Methods for other Species and Parameters

Analysis of other species and parameters were part of the AQUELLA and AQUELLIS projects, conducted by the AQUELLA-team. For details see Bauer et al., (2006, 2007a, 2007b, 2008a, 2008b, 2008c), Jankowski et al. (2009a and 2009b), Puxbaum et al. (2006) and Schmidl et al. (2008c).

6.2.1 Weighing and sample preparation

Gravimetric analysis was performed by the respective local authorities with a microbalance (Sartorius M5P with range up to 1 g reading to ±0.5 µg) after 48 h equilibration in an air-conditioned room (20±1 °C, 50±5% r.h.), following the European Standard 12341 (EN12341). For analysis of ions and carbon species, small discs, with 8 or 10 mm diameter, were stamped out of the quartz tissue filters with steel punches.

Larger filter sections were assigned for the analysis of polar and apolar analytes. Whole cellulose filters were used for the determination of trace metals by XRF and then by ICP.

6.2.2 Ions

The cations sodium, ammonium, potassium, magnesium and calcium were determined by isocratic cation chromatography. Aliquots of the loaded filters were taken and extracted ultrasonically in 12 mM methane sulfonic acid (MSA) which was also used as the chromatographic eluent. Filter blanks were treated in the same way as the samples. The determination was performed using a Dionex CS 12A cation-exchange column and a CG 12A guard column. The system is fitted with a CSRS Ultra II 4 mm auto-regenerated suppressor and a Dionex QIC conductivity detector with SRS controller (modified measurement setup as described by Löflund et al., 2001). Quantification was carried out using Chromeleon® 6.6 software. Calibration was performed by the direct injection of aqueous standard solutions made from 1000 mg/L parent solution (Aristar® sodium, ammonium, potassium, magnesium, calcium Standard, BHD Laboratory Supplies). The anions chloride, nitrate and sulphate were determined by isocratic anion chromatography. Filter discs of 10 mm Ø were taken as sample and blank aliquots and extracted ultrasonically in ultra-pure Milli-Q water. Calibration was carried out with aqueous standard solutions made from 1000 mg/L parent solutions (CertiPUR®, chloride, nitrate and sulphate standard, Merck).

6.2.3 Cellulose

Aliquots were taken and extracted with 0.05M citric acid solution (pH = 4.8) in an ultrasonic bath. Cellulose was saccharified to glucose by the action of two enzymes: a “Trichoderma reesei” cellulase and an “Aspergillus Niger” cellobiase. Subsequently the glucose content was determined photometrically (Unicam 5625 UV/Vis Spectrometer) using a modified test-combination (Boehringer Mannheim GmbH/R-Biopharm). To calculate the amount of plant debris, cellulose is multiplied by a factor of 2 (Puxbaum and Tenze-Kunit, 2003).

6.2.4 Carbon Analysis

Total carbon (TC) was determined by combustion of all material on the filter, in oxygen, at 1000 °C and measurement of the resulting CO₂ by non-dispersive IR photometry (NDIR, Maihak). Elemental carbon (EC) was determined in the same apparatus on material previously heated in oxygen at 340°C to burn off the organic matter (Cachier et al., 1989) and additionally, as a check, it was also determined for a number of samples by the modified thermo-optical temperature gradient method (Puxbaum, 1979; Schmid et al., 2001). Carbonate carbon, was determined by the thermo-optical temperature gradient method as the last form of carbon to be released as CO₂ at temperatures higher than 550

°C. Organic carbon (OC) was calculated by subtracting elemental and carbonate carbon from total carbon.

Qualitative investigations on the thermal stability of isolated ambient HULIS and solid humic acid as well as their aqueous and alkaline extracts was performed with a thermal-optical transmission method with linear temperature program, originally described by Puxbaum, 1979, with the modification of a simultaneous laser transmission measurement and NDIR detection of the CO₂ (Schmid et al., 2001a). HULIS was isolated as described in detail in chapter 6.1. The HULIS isolates (in a matrix of diluted ammonium hydroxide) were dropped on quartz fibre filters discs with a diameter of 12mm and dried in an exsiccator over silica gel at room temperature for about 2 hours. After drying filters showed slight colouration from bright yellow to light brown. A sample punch of the quartz fibre filter was placed in a horizontal furnace FROK 200/50/1000 (AHT Austria) at room temperature in oxygen and then heated in O₂ (4.8) to 800°C at a rate of 20°C/ min. A manganese oxide catalyst heated to 700°C converts the carbonaceous gases to CO₂, which is continuously measured using an NDIR analyzer (Maihak UNOR 6N). During the heating procedure the transmittance of a laser beam through the filter punch is recorded. The change of the transmittance gives information about charring phenomena of the organic carbon leading to increased blackness of the filter. In case of the HULIS isolates the initial colouration of the filter samples was too weak to result in evaluable laser signals.

6.2.5 Anhydrosugars, Sugars and Sugar Alcohols

5 punches of 8mm diameter were taken from the quartz fibre filter and extracted in Milli-Q water with the aid of ultrasonic agitation. After centrifugation the aqueous phase was separated with HPLC and analyzed with electrochemical (amperometric) detection. Quantification is based on external standards. The apparatus for the determination of sugars, anhydrosugars and sugar alcohols consists of a Dionex pump model GP50, coupled to a Rheodyne 9740 sample injection valve to a Carbopac PA 10 guard column, followed by a Carbopac PA10 analytical column. Gradient elution was accomplished with 1mL min⁻¹ diluted sodium hydroxide, starting at 30mM sodium hydroxide (88Vol% Milli-Q water and 12Vol% of 250mM NaOH) increasing to 40mM. The electrochemical detection was performed by a Dionex ED 40 electrochemical detector with a gold indicator electrode (P/N 060139) and a pH electrode (P/N 046333) as reference, both from Dionex (Caseiro et al., 2007).

6.2.6 Metals

For the analysis of metals ICP-OES, GF-AAS and XRF were applied. The analysis with XRF was performed with a Philips 1480 wavelength-dispersive X-Ray fluorescence spectrometer, fitted with a rhodium target X-Ray tube ($K = 0,616\text{\AA}$). The tube was set at

50kV and takes a current of 40mA. The flow proportional detector was operated with 10% v/v methane in argon PR-gas, obtained from Messer-Griesheim, Austria. NIST Standard Reference Material® 2709 San Joaquin Soil was used for calibration. Additionally calibration curves were validated with a material containing bush branches and leaves from the China National Analysis Centre for Iron and Steel, standard NCS DC73349. For ICP-OES and GF-AAS one or two filters of mixed cellulose esters were solubilised by aqua regia digestion with hydrofluoric acid in a microwave oven. The determination of the elements magnesium, calcium, vanadium, chromium, manganese, iron, copper, zinc, strontium, cadmium, barium, titanium, nickel and cobalt was performed with ICP-OES (Perkin-Elmer Sciex ELAN, CEM detection), for the determination of lead, arsenic and antimony a GF-AAS (Perkin-Elmer model 370 fitted with graphite furnace model HGA 74 and autosampler model AS1) was used. As a reference for ICP-HRMS NIST Standard Reference Material® 1646a Estuarine Sediment was taken (Handler et al., 2008).

6.2.7 Organic Trace Components

For the determination of apolar organic tracers the filters were spiked with the deuterated recovery standards tetracosane and benzo[a]pyrene and then extracted twice with the help of ultrasonic agitation in 5mL of cyclohexane. The combined extracts were evaporated to 200µL, after adding the internal standard 1-bromopentadecane the samples were analyzed by GC-MS using a HP-6890 gas chromatograph equipped with a pre-column of deactivated fused silica (1m x 0.32mm) and an analytical column (capillary, DB-5 MS – 95% dimethyl-, 5% phenylsiloxane, 30m x 0.25mm, ID 0.25µm film). Splitless mode was used and detection was carried out with a mass spectrometer HP-5973 (70eV) in ion-scan mode (Kotianova et al., 2008).

For the determination of polar organic tracers the filters were spiked with internal standards (12-bromododecanoic acid, 1-bromopentadecane) and the extraction was carried out with the help of ultrasonic agitation in a mixture of 5mL methanol and 150µL acetone. After extraction the organic acids were derivatised to their methyl esters and extracted with cyclohexane. Analysis was carried out with a HP-5890 GC-MS fitted with two capillary columns (95% dimethyl-, 5%phenylsiloxane, 30m x 0.25mm, ID 0-25µm film) in splitless mode. The gas flow from the first column was led to a flame ionisation detector (FID), the flow from the other column was fed to a mass spectrometer HP-5971-A (70eV) running in ion-scan mode.

6.2.8 Gaseous compounds

Ozone and SO₂ were measured by the respective local authorities and data was kindly provided by the Environment Agency Austria (Umweltbundesamt).

7 A three City Study: Seasonal Behaviour and possible Origin of atmospheric HULIS

7.1 Introduction

A growing body of literature is giving account on ambient HULIS levels in particulate matter from urban, rural, marine and continental and biomass burning impacted environments all around the globe (see section 3). The vast majority of these studies investigated the water-soluble fraction of HULIS although it has been evidenced that the alkaline soluble fraction roughly doubles the amount of HULIS_{WS} in atmospheric aerosol (Feczko et al., 2007). Thus HULIS_{AS} plays an important role if aiming at organic mass closure and might even play a more important role in atmospheric photochemistry than HULIS_{WS} due to their higher absorption coefficients in UV (Baduel et al., 2009). To the best of our knowledge up till now, only one study covered complete seasonal cycles of both fractions (Feczko et al., 2007) and nothing is reported about the seasonality of HULIS_T (as sum of HULIS_{WS} and HULIS_{AS}) in urban environments.

The present study investigates the atmospheric abundance of HULIS_T and seasonal variations in urban and rural environments throughout a full seasonal cycle. Furthermore a dilution tracer is established to assess the influence of meteorological unfavourable dispersion conditions on the winter enrichment of HULIS_T. Investigations of correlating co-determined aerosol constituents and HULIS_T allow conclusions on potential sources contributing to atmospheric HULIS levels. Finally quantification of HULIS_T in source emission samples was processed to HULIS/tracer-source ratios (HTSR). Together with atmospheric tracer levels these ratios were used to estimate potential primary emissions of HULIS from wood stoves, diesel vehicles and cooking emissions.

7.2 Experimental

HULIS analysis (isolation, quantification and recording of thermograms) was conducted in the scope of the present work. Analysis of other species and parameters were conducted by the AQUELLA-team and taken from the AQUELLA data base. Results of HULIS analysis are parts of the publications from Schmidl et al. (2008a and 2008b), Wonaschütz et al. (2009) and the AQUELLA/AQUELLIS project reports (Bauer et al., 2006, 2007a, 2007b, 2008a, 2008b, 2008c; Jankowski et al., 2009a and 2009b; Puxbaum et al., 2006, Schmidl et al., 2008c).

7.2.1 Ambient Aerosol Samples

Daily PM₁₀ sampling was conducted from January to December 2004 at ten sites in the area of the three cities Vienna, Graz and Salzburg, with 1.7 million, 300.000 and 150.000 inhabitants (Umweltbundesamt, 2009), respectively. The three cities are located between 200 and 300 km away from each other. Samples were collected with high volume

samplers (DHA-80, DIGITEL Elektronik AG, Switzerland) on quartz fibre filters (Pallflex™ 2500QAT-UP, diameter 150 mm, PALL Life Sciences, USA) for 24 h sampling periods, with volumes of approximately 700 m³ per filter. The filters were conditioned for around 48 h in a clean room at a temperature of 20±1 °C and a relative humidity of 50±5% and weighed before and after sampling. Sampling and weighing at all sites was conducted by the respective local authorities. Sampling sites in the Austrian capital Vienna are located in a northwest to southeast transect. Two sites, Schafbergbad (SCHA, 16° 18' 10.0"E, 48° 14' 9.2"N, 320 m a.s.l.) and Lobau (LOBA, 16° 31' 36.5"E, 48° 09' 45.4"N, 150 m a.s.l.) are located at the urban fringe of the city. The sampling site Schafbergbad is situated in residential area whereas Lobau is in the area of the Donau-Auen National Park surrounded by woods and meadows in vicinity of a water course. The local surrounding of the intra-urban site Kendlerstraße (KEND, 16° 18' 39.2"E, 48° 12' 19.8"N, 230 m a.s.l.) is characterised by residential area and only moderately impacted by traffic. The second urban site Rinnböckstraße (RINN, 16° 24' 28.0"E, 48° 11' 4.6"N, 160 m a.s.l.) is heavily impacted by the A23, which, with 170.00 vehicles per day (Asfinag, VCÖ, 2005), is the most frequented Austrian road. The two urban sites in Graz are Don Bosco (DONB, 15° 24' 59.8"E, 47° 03' 20.2"N, 358 m a.s.l.) and Graz Süd (GRAS, 15° 25' 59.0"E, 47° 02' 30.0"N, 342 m a.s.l.), with DONB being a heavily traffic impacted site and GRAS located in residential area. The local background site Bockberg (BOCK, 15° 29' 45.0" E, 46° 52' 17.0" N, 449 m a.s.l.) is situated 28 km south of Graz surrounded by farmland, vine yards and single houses. The highway A9 passes in only several hundred meters distance and most likely the site BOCK is as well influenced by emissions from the power plants Werndorf and Mellach (Spangl et al., 2006).

In Salzburg Rudolfsplatz (RUDO, 13° 03' 13.0"E, 47° 47' 51.0" N, 425 m a.s.l.) represents the traffic impacted inner urban site, while Lehen (LEHE, 13° 01' 51.0"E, 47° 49' 2.0"N, 420 a.s.l.) and Anthering (ANTH, 47°52' 53"E, 13°0' 43"N, 440 m a.s.l.) are the urban residential and the local background site, located several kilometres north of Salzburg's city centre, respectively. For detailed information about sites, pictures and maps see chapter 4.

Regarding their geographical characteristics each of the three cities is situated in a basin, though with different surroundings. The Vienna basin ranks amongst the better ventilated areas in Austria. Accumulation of air mass at the hill country in the west and northwest of the city, the Wienerwald, only occurs during periods of weak airflow from eastern direction and inversion situations. Topographical influence is considered to be of inferior importance concerning accumulation of pollutants (Bauer et al., 2006). Contrasting in Graz the topographical conditions play a major role concerning the enrichment of particulate matter. The leaside of the basin concerning eastern or western winds, which would enhance ventilation with cleaner air mass, and its pronounced drawdown against

the hinterland support conditions for frequent occurrence of stable inversions and thus the enrichment of air pollutants (Bauer et al., 2007b). Salzburg is freely accessible for air currents from northwest. The elevated surrounding causes a pack up of air mass streaming from northern direction which frequently causes rainfall and depletion of PM10 (Bauer et al., 2007a). Although stable inversions layers in Salzburg are possible, in general Atlantic air masses and higher wind speeds cause efficient dilution of pollutants (Spangl et al., 2006).

7.2.2 Source Samples

Emission samples from various sources have been analysed for HULIS with the same method as applied for ambient samples (see section 6.1). Sampling procedures and experimental set up were part of the AQUELLIS projects and are described in detail elsewhere (Puxbaum et al., 2006; Schmidl et al., 2008a and 2008b; Jankowski et al., 2009a). Briefly PM10 samples were drawn in the exhaust stream of diesel vehicles, wood stoves and cooking activities. Bulk soil or dust samples, collected at construction sites, a vine yard, a chicken house and dust stemming from a carpentry and harvesting activities were re-suspended and the PM10 fraction was collected on quartz fibre filters.

7.2.3 Extraction, Isolation and Quantification of HULIS

Extraction, isolation and quantification of HULIS are described in detail in section 6.1. Briefly, aliquots of quartz fibre filters were extracted with water, obtained from a Millipore ultrapure water system (Milli Q-plus 185), and subsequently with 0.1 molar sodium hydroxide. A scheme of the whole process is depicted in Figure 38.

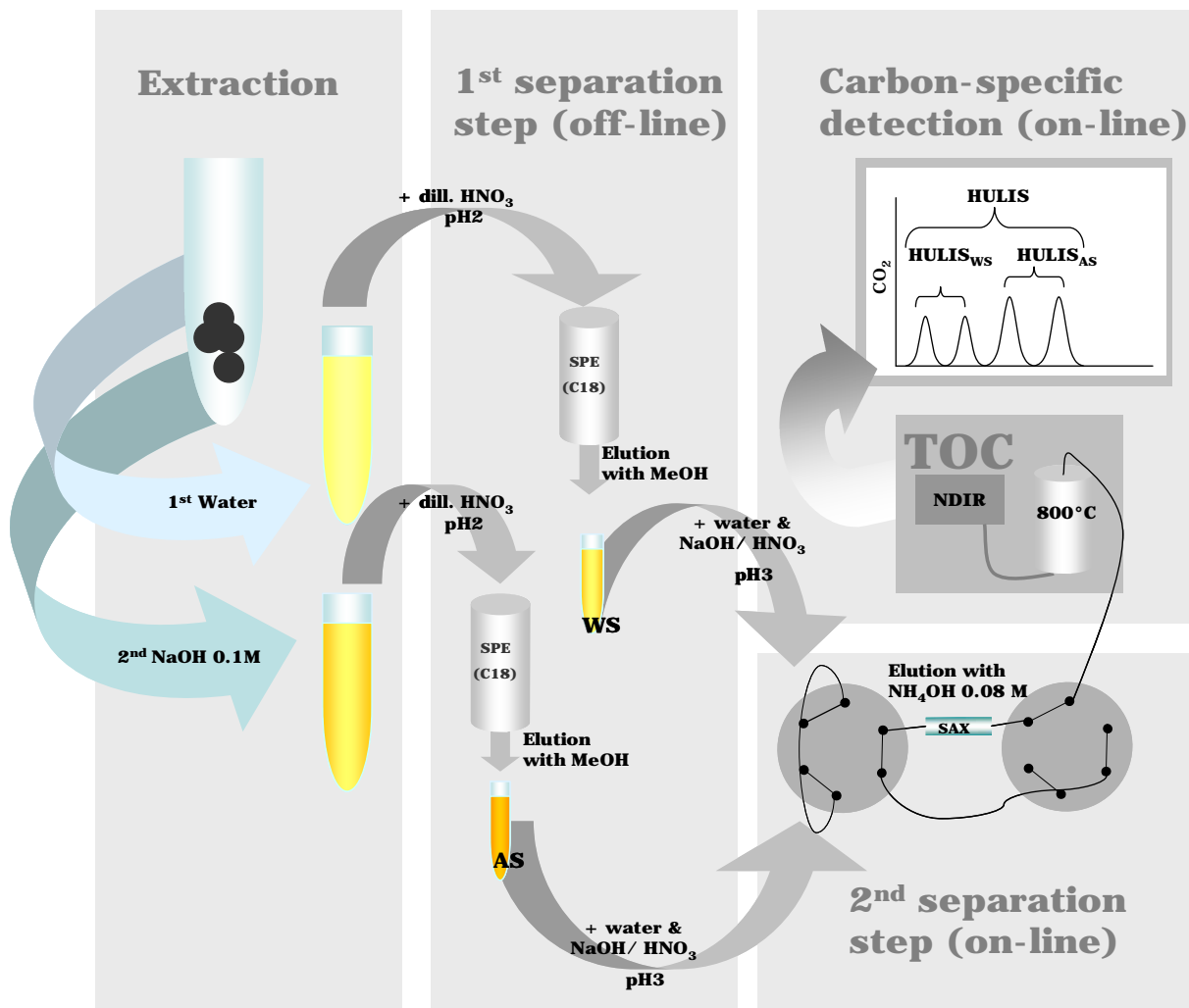


Figure 38: Scheme of extraction, isolation and quantification of HULIS; 1: Solid phase extraction; 2: Online separation with an ion-exchange micro column integrated in a flow injection system; 3: Carbon specific detection with dissolved organic carbon analyser.

The aqueous and alkaline extracts were acidified with diluted nitric acid to a pH of two. Insoluble particles and filter debris was separated via centrifugation. The clear solutions were then subjected to the first separation step on a SPE cartridge (Isolute, C18 (EC)). The effluent contained inorganic ions and hydrophilic organic compounds such as short-chain monocarboxylic acids). The adsorbed fraction, HULIS and other aerosol constituents such as long-chain monocarboxylic acids, aromatic alcohols or aldehydes (Limbeck et al. 2005), was eluted with 200 µl methanol and filled up to a final volume of 2ml with a mixture of diluted sodium hydroxide and nitric acid to achieve a pH of ~3. 500 µl of this solution are subjected to the second (on-line) separation step on a strong anion

exchanger (Isolute SAX) integrated in a flow injection system. Neutral compounds passed the column without retention, whereas HULIS and other compounds capable of carrying a negative charge were retained on the column. Species bearing only one or two charges per molecule were removed in a washing step with diluted nitric acid and subsequently HULIS was eluted with 0.08 M ammonium hydroxide and directly introduced into a total carbon analyser (GTOC 100, Gröger & Obst) that operates with continuous flow. Evolving carbon dioxide was detected with a non-dispersive infrared detector (Siemens Ultramat 5E).

7.2.4 Determination of other Species and Parameters

Determination of other species and parameters are described in section 6.2.

7.3 Results

7.3.1 Analytical Performance

The method and its statistical characteristics were described by Limbeck et al. (2005). The authors reported an LOD and LOQ of 1.0 and 1.6 mg of HULIS C/L referred to a sample volume of 5ml, respectively. The reproducibility given as the relative standard deviation was determined at a humic acid standard concentration level of 11.8 mg/L and was determined using humic acid standards. A value of 4.3 % was reported. Excellent linearity and ($r^2=0.999$) between signal and response was evidenced in a range from 3-23.7 mg of C/L. A major advantage of this method is the high selectivity of this method (see interference study reported by Limbeck et al., 2005 and Baduel et al., 2009) which is achieved by the application of two separation principles-one by polarity one by acidity-and a compound independent quantification method.

However, since extraction of filter material was performed with water and sodium hydroxide, instead of solely water extraction, and extraction volumes were slightly adopted (Neuberger, 2005), the analytical performance was re-evaluated in the scope of the present work (Table 5). A set of field blanks from atmospheric samples were subjected to the isolation and quantification protocol. No increase of the blank signal was observed from these measurements. The limit of detection (LOD) and limit of quantification (LOQ) were determined from the blank signal of the calibration standard (n=12). LOD and LOQ were calculated as the amount of analyte necessary to yield a peak area equal to the sum of the blank signals plus three and six times the standard deviation of the blank signals, respectively. Referred to the applied extraction volume of 9ml the LOD and LOQ was 0.3 $\mu\text{g C/mL}$ and 1 $\mu\text{g C/mL}$, respectively. Ambient LOD and LOQ were estimated assuming an average filter portion of 14 cm^2 and a sampled air volume of $\sim 700 \text{ m}^3$ and were 0.05 and 0.15 $\mu\text{g HULIS carbon/m}^3$, respectively. Reproducibility at mid calibration range was 2.5

%. The reproducibility for the whole procedure, including extraction, tested with a real sample (n=5) was 5.5 %, given as relative standard deviation.

Table 5: Analytical characteristics

| LOD | | | LOQ | | | Reproducibility | |
|----------------------------------|-------------------------------------|--------------------------------------|----------------------------------|-------------------------------------|--------------------------------------|-----------------|------------|
| [$\mu\text{g C}$] ^o | [$\mu\text{g C/mL}$] ⁺ | [$\mu\text{g C/m}^3$] [*] | [$\mu\text{g C}$] ^o | [$\mu\text{g C/mL}$] ⁺ | [$\mu\text{g C/m}^3$] [*] | [%] | |
| 3 | 0.3 | 0.05 | 9 | 0.9 | 0.15 | MCR | PROC |
| | | | | | | 2.5 | 5.5 |

^o μg carbon referred to absolute amount in filter extracts/calibration standards, ⁺referred to 9mL sample volume; ^{*}calculated with an average filter portion ($\sim 14 \text{ cm}^2$) and an average sampled air volume ($\sim 700 \text{ m}^3$); MCR: repeatability in mid-calibration range with humic acid standards; PROC: procedure repeatability with real aerosol samples including extraction.

The linear range of the calibration between detected signal and carbon loading showed excellent linearity ($R^2=0.998$; $n=6$) up to 270 μg carbon (referred to sample volumes prior to SPE extraction of ~ 6 -10ml and 2ml of normalised sample volume after SPE extraction, respectively). An absolute HULIS carbon load of 130 μg (referred to extracts prior to SPE extraction) was the highest observed load during all the conducted analysis, thus the testified linear range was never exceeded.

7.3.2 HULIS Carbon Quantification and Humic Acid Standard

For HULIS quantification external calibrations with dilutions of the humic acid stock solutions, which were subjected to the same isolation protocol as the filter samples, were processed every day to compensate analyte losses on the analytical columns. The method was optimised by Limbeck et al. (2005) towards minimum solvent (methanol) amounts yielding maximum recovery after the SPE (C18) separation step, since the organic solvent has to be removed in the subsequent separation step, prior carbon specific detection. Tests and optimisation on the recovery of humic acid were performed and estimated to be $\sim 70\%$ (Limbeck et al., 2005). Most studies reported in literature investigated the water soluble fraction of HULIS and utilise fulvic acid as standard/reference material. The latter is mainly because of the smaller molecular weight of FA than HA (Reemtsma et al., 2003; Shinozuka et al., 2004) and the fact that the majority of previous studies did this too. In the present work both, the water soluble and alkaline fraction of atmospheric HULIS are investigated. In analogy to terrestrial and aquatic humic substances the alkaline fraction might be of higher molecular weight and/or lower acidity (Graber and Rudich, 2006; Fooker, 1999) and aqueous extracts of HA were chosen to be a more appropriate standard than FA. It is crucial that the HA acid standard shows the same behaviour during the extraction steps to avoid systematic errors in the determination of atmospheric HULIS levels. Because dramatically varying pH ranges of resulting extracts after the different steps made it unsuitable to apply UV/VIS

spectrometric methods, we decided to apply a more direct approach. Solid humic acid and alkaline and aqueous extracts were investigated with a thermal-optical method with linear temperature programme (TLT) and compared to HULIS isolates from an urban environment in winter. The thermal behaviour of HULIS might not provide detailed structural information but allows qualitative comparison of volatility/thermal stability of fractions of HULIS (e.g. Duarte et al., 2008; Cheng et al., 2012). The normalised thermograms of solid humic acid and humic acid dissolved in 0.1 M NaOH (Figure 39) show very similar thermal characteristics with a smaller peak evolving at $\sim 300^{\circ}\text{C}$ and the major one at $\sim 450^{\circ}\text{C}$, coherent with the definition of humic acid being soluble in strong bases. The aqueous HA extract conversely shows a peak maximum at 300°C and unresolved shoulders at $\sim 350^{\circ}\text{C}$ and $\sim 420^{\circ}\text{C}$, showing that less refractory material is present in the water extracts, thus, following the logic of humic substances, representing smaller molecular weights. Comparison with HULIS_{AS} extracts from ambient urban PM10 showed stunning general resemblance (Figure 40) concerning the peak features. The major peak evolving at 300°C appears to be almost congruent. The regions of the two unresolved shoulders appear to be stretched to higher temperatures for the isolated HULIS. This effect is likely due to the absence of anions such as K^+ and Na^+ which are removed during the isolation protocol and reported to catalyze the combustion of refractory organic material at lower temperatures (Mayol-Bracero et al., 2002; Hoffer et al., 2006b). The signal below 200°C might either stem from traces of eluant leftovers or from low volatile compounds co-eluting with HULIS. The former might result in signals stemming from methanol (boiling point 65°C) and/or ammonium carbonate (thermal decomposition starting at 58°C), since concentrated NH_4OH solutions are known to absorb carbon dioxide formed by the sorption of ambient carbon dioxide. Isolation of HULIS from ambient samples for the thermal characterization was slightly adopted to gain larger amounts of HULIS isolates and the second separation step was accomplished on an SAX cartridge instead of sample introduction into the flow injection system. Thus the likeliness for a signal stemming from ambient carbon dioxide during HULIS quantification is much lower due to the drastically reduced eluant exposition to ambient air. However, the application of an external calibration with blank and HA standards, subjected to the isolation procedure, exclude systematic errors stemming from eluant interactions. Beside eluant interferences stemming from the up-scaled preparative HULIS isolation, co-eluting interfering substances with relatively high volatility, present in atmospheric aerosol, could generate carbon dioxide signals below 200°C . Although the present method is highly selective, as evidenced in interference studies (Limbeck et al., 2005; Baduel et al., 2009) and no quantifiable amounts of tested substances were detected, traces of aromatic acids with melting points between 125°C and 217°C could contribute to these features. However, the steep increase of evolving carbon dioxide, peaking at $\sim 300^{\circ}\text{C}$, the low amount of high volatile species (less than 10% of the carbon

evolves below 200°C) and the high resemblance of the thermograms from ambient HULIS and aqueous dissolved HA clearly show the high selectivity of the method, thus purity of HULIS isolates, and the suitability of water soluble HA as a calibration standard for carbon-specific calibration.

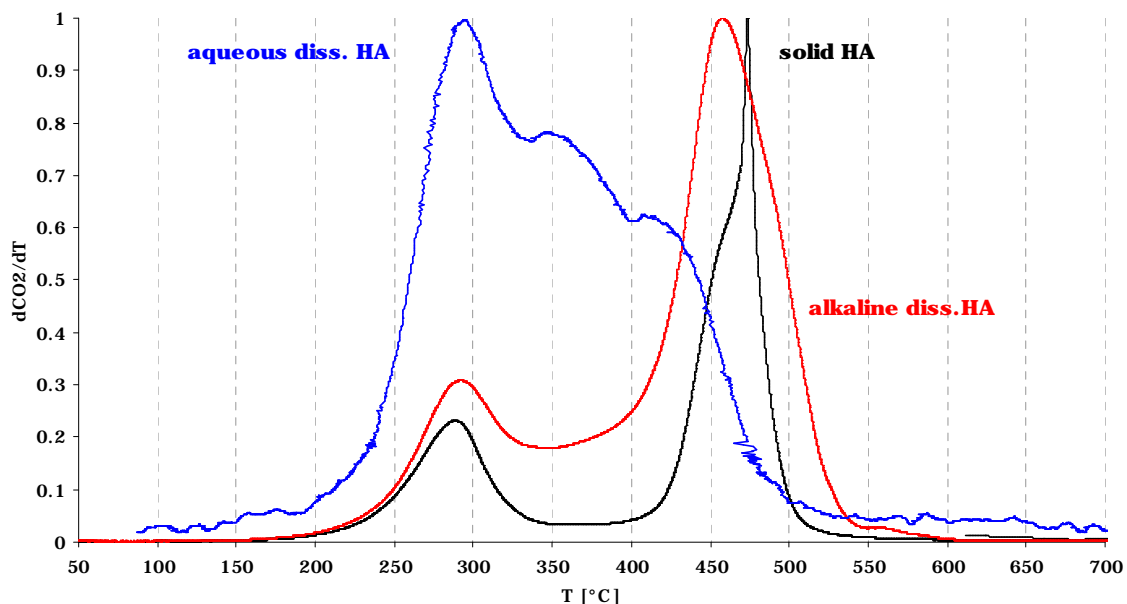


Figure 39: Thermograms of solid and aqueous and alkaline dissolved humic acid.

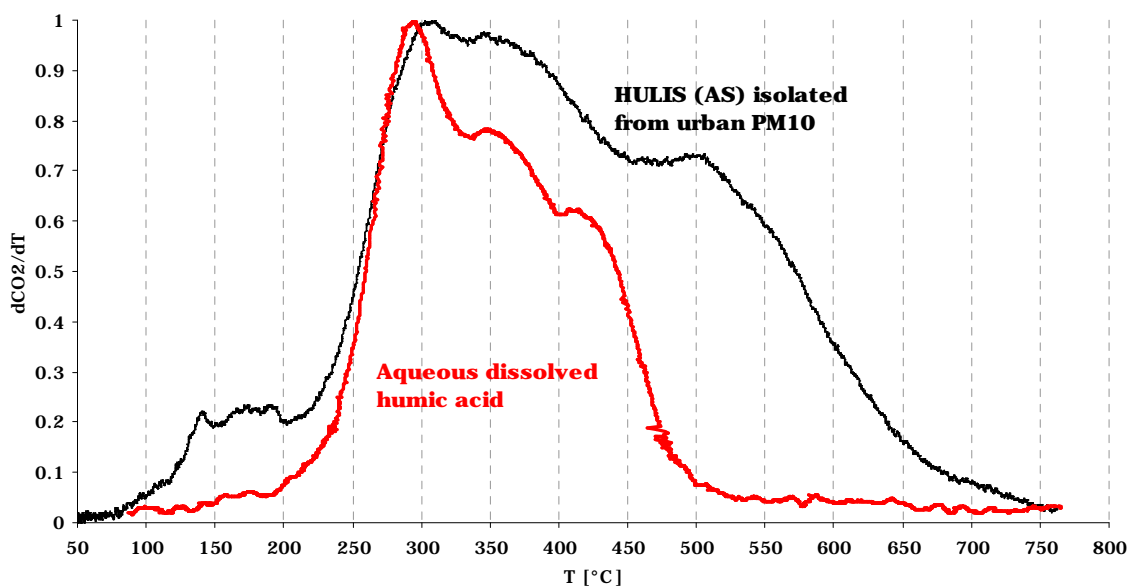


Figure 40: Thermograms from HULIS_{AS} isolated from urban PM10 in winter and aqueous dissolved humic acid standard.

7.3.3 Comments on recent Comparisons of Methods for Isolation, Separation and Quantification of HULIS

Although substantial progress has been made in studying ambient HULIS, there is still a lack of understanding, to which extent the applied isolation/separation protocols reported in literature cover the same group of compounds (Graber and Rudich, 2006; Kalberer et al., 2006). Isolation and separation of HULIS with the methods reported in literature are based on different characteristics such as their size, polarity or acidity (Table 1 and Table 2). Thus comparison of the different methods is highly desirable though scarce. Reported comparisons investigated recovery rates of ambient WSOC gained with different SPE columns, though without tests on standard compounds or interference tests (Varga et al., 2001) and an interference study conducted for two methods based on separation with HPLC and quantification with TOC and UV, respectively (Mancinelli et al., 2007). More recently Baduel et al. (2009) compared their method based on the separation on a weak anion exchanger (DEAE) with the method applied in the present work. A study on the different fractions isolated with the most common SPE techniques was reported by Fan et al. (2012) including a test on potentially interfering substances.

The comparison of the two methods by Baduel et al. (2009) was based on carbon-specific quantification and investigations of absorbance characteristics of the water and alkaline soluble HULIS fractions isolated with the DEAE and C18-SAX protocol, respectively. The results gave some interesting insights on the characteristics of the gained fractions but do not allow the conclusions the authors draw from this observations, as is explained in the following. They reasoned their major conclusion that the present isolation protocol (C18+SAX) would discriminate towards smaller or less aromatic molecules, based on the observations of UV/VIS absorbances, not taking in account the dramatic differences of pH ranges in the investigated samples. Following their reported methodical approach the derived HULIS extracts from both methods were subjected to UV/VIS measurements directly after elution from the column, which means that the pH for the HULIS fraction derived with C18+SAX and DEAE had a pH of ~11 and ~7, respectively (Figure 41). Furthermore the aqueous humic and fulvic acid standard solutions were as well in a neutral pH range, like all samples and standards subjected to the DEAE isolation protocol. As the authors mentioned themselves, amongst others, the absorbance of a substance is dependent on the pH of the sample matrix (Baduel et al., 2009).

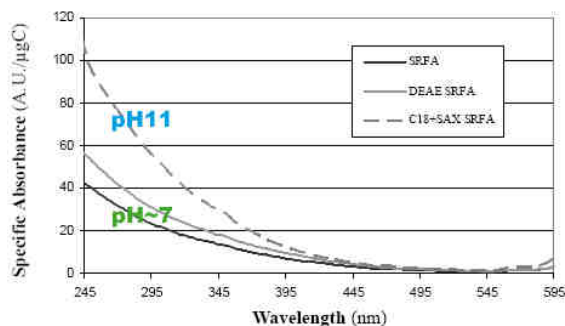


Fig. 2. Impact of the DEAE and C₁₈+SAX extraction protocols on the UV spectrum of a SRFA standard solution. Specific absorbance is in arbitrary unit (AU) of absorbance per μg carbon extracted.

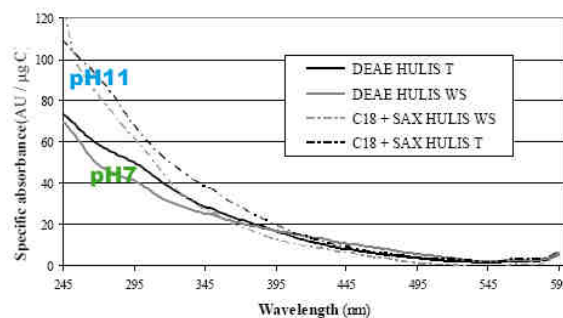


Fig. 3. Comparison of typical Water Soluble and Total HULIS spectra resulting from DEAE and C₁₈+SAX extraction procedures for an actual atmospheric sample. Specific absorbance is in arbitrary unit (AU) of absorbance per μg carbon extracted.

Figure 41: taken from Baduel et al., 2009, complemented by indication of pH regimes.

Investigating the pH dependence of the UV absorbance of different humic acids, Chen et al. (2011) examined the spectral curve slopes between 275-295 nm and 350-400 nm. Absorbances at wavelengths beyond 300nm are widely used to investigate the presence of aromatic compounds, like phenolic derivatives, benzoic acids, polyenes and polycyclic aromatic hydrocarbons (e.g. Salma et al., 2008) and the ratio of absorbances at 250 nm and 360 nm ($E_2:E_3$) was calculated to estimate the molecular weight of chromophoric dissolved organic matter and HULIS (Chen et al., 2011, Dinar et al., 2006). Chen et al. (2011) evidenced that no linear dependency exists between pH and absorption of HA, thus even the comparison of the E_2/E_3 ratios in different pH regimes, as conducted by Baduel et al., 2009, does not allow conclusions on differences and/or similarities of the two methods. Furthermore they concluded that the present method discriminates towards smaller molecules when observing lower concentrations for the C₁₈+SAX HULIS_{WS} fraction. This argumentation seems not coherent since the HULIS_T fractions obtained by the two methods showed quite good agreement. Due to their assumptions HULIS_T being a fraction of higher molecular weight and/or higher aromaticity, the size discrimination should be even more pronounced in this fraction. In fact the HULIS_T concentrations in ambient samples they found nearly equivalent for both methods. From investigations of thermal characteristics of humic acid standards and HULIS isolates we found no indication for the favoured extraction of smaller molecules for the C₁₈+SAX method (see 7.3.2). A reason for the about two times higher HULIS_{WS} levels for the DEAE method (Baduel et al., 2009) might be the presence of interfering water-soluble aerosol constituents. Baduel et al. (2009) did not report tests on any organic di- or triacids, which can contribute significantly to ambient WSOC (Limbeck et al., 2001; Fisseha et al., 2006). Fan et al. (2012) overcame this lack of knowledge and found that the DEAE method is not interfered by diacids of relatively small molecular weight such as lactic and succinic acid, but higher molecular weight acids are recovered in the HULIS fraction, in

case of 3,5-Dihydroxy-benzoic acid, even quantitatively. Reported atmospheric abundance of di- and triacids, oxalic acid being in the fore (Limbeck et al., 2001; Fisseha et al., 2007), occur in magnitudes that would explain the higher HULIS_{WS} levels derived by the DEAE method. The higher dispersion of ambient HULIS levels obtained with the C18+SAX protocol, as observed by Baduel et al, 2009, on the one hand might be the result of the manual collection of the samples (Baduel et al., 2009), which offers possibility of ambient carbon dioxide to be incorporated in the ammonia containing sample matrix and on the other hand the inaccurate implementation of the method. Following their methodology section the wash step with nitric acid after the sample injection on the SAX column was not applied. This wash step was shown to remove major potential interfering atmospheric aerosol constituents (see interference study in Limbeck et al., 2005) and it's skipping leads to more instable results. Conclusively the reproducibility we determined for the present work was 2.5% and 5.5 %, determined with humic acid standards in mid-calibration range and PM10 samples (thus including extraction), being smaller than the ones reported by Baduel et al. (2009). However, their comparison on method characteristics regarding the two methods is not fully comparable as they e.g. used a higher volume of methanol for eluting the absorbed fraction from the C18 column, on an absolute and relative scale (which causes higher matrix interactions at the anion exchange column) and they did not apply the wash step at the SAX column (causing more uncertainties in ambient concentrations). Furthermore Baduel et al. (2009) used a different approach for estimating the LOD. Two times the standard deviation from the blank signal, yielded in a lower LOD, compared to that processed by Limbeck et al. (2009) and the present work which both processed 3 and 9 times the blank signal for calculations of the LOD and LOQ, respectively. Baduel et al. (2009) collected samples manually prior to carbon quantification, which potentially enables a higher amount of ambient carbon dioxide to be absorbed by the ammonium hydroxide sample matrix, leading to lower reproducibility. To which extent the higher recovery of SRFA and HA standard solutions of the DEAE protocol compared to the C18+SAX method stems from irreversible interactions on the resins or the actual accomplishment of operative steps e.g. the influence of accurate pre-conditioning of the resins as conducted in the present work and by Limbeck et al. (2005), remains to be elucidated. Summarizing, we can not share their (Baduel et al., 2009) concern that our C18+SAX isolation protocol and the application of aqueous dissolved humic acid as correction standard vastly overestimates atmospheric HULIS concentrations due to the following:

- Thermal characterization of aqueous dissolved HA showed very good resemblance with isolated ambient HULIS, from which we conclude HA being a suitable calibration standard.
- Several extensive mass/source closure studies of ambient Austrian PM10 (e.g. Bauer et al., 2006; Bauer et al., 2007a and Bauer et al., 2007b) did not yield

overestimations of organic matter, on the contrary, as expected, a part of the organic fraction relieved unexplained indicating that measured atmospheric HULIS levels are unlikely affected by large positive systematic errors.

- Good agreement of atmospheric HULIS levels and their contribution to OC observed in the present study and values reported in literature was found, even considering that the present work covers the total HULIS fraction (as sum of water and alkaline soluble HULIS) and the vast majority of reported investigations focused solely on the water soluble fraction of HULIS (Table 1).

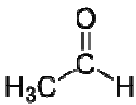
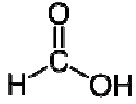
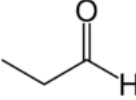
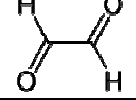
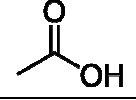
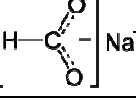
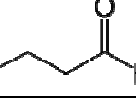
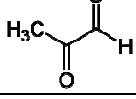
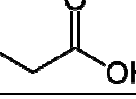
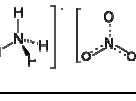
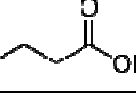
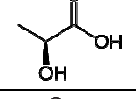
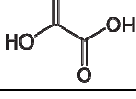
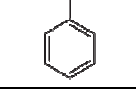
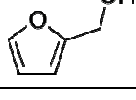
However, both the DEAE and the C18+SAX protocols are very suitable to measure HULIS carbon concentrations accurately down to low levels, with the C18+SAX method being less influenced by potential interfering aerosol constituents than the DEAE protocol, as shown in the following.

Fan et al. (2012) compared four isolation methods of HULIS based on solid phase extraction with different resins. Beside hydrophilic-lipophilic balanced resins (HLB), diethylaminoethyl (DEAE) resins and hydrophobic cross linked polystyrene copolymer resins (XAD) they investigated ENVI-18 (polymeric bond octadecyl functional groups) resins, which uses the same separation principle as the first separation step (SPE, C18) applied in the present work. Fan et al. (2012) found similar recoveries for SRFA and HA, though on a lower level for the latter, for all the four methods. The low recoveries for the aqueous HA standard appearing in the range of 30-60% stem most likely from the application of Pahokee peat humic acid (PPHA), which has different characteristics than marine HA or FA acid (Reemtsma et al., 2003; Shinozuka et al., 2004). This would imply for the present work that the majority of decrease in recovery is caused by the C18 step what is in general in agreement with the separation principal of the C18 resin. Lower losses of the analyte can be expected on the SAX column, which retains the analytes capable of bearing three or more negative charges, properties all of which assigned to the whole HULIS fraction. Comparing the results for recoveries for SRFA obtained by Fan et al. (2012) for the C18 step and Baduel et al. (2009) for C18+SAX step, the former found that C18 recovers SRFA quantitatively whereas the latter found only 50% of initial SRFA concentration after the C18+SAX procedure. This would mean that the separation on the SAX column would be the reason for the low extraction yields of the fulvic acid standard, what is contradicting the suggested size discrimination of the C18+SAX method proposed by Baduel et al. (2009). Furthermore it is not likely that the above mentioned SAX column discriminates towards size, since its separation principle relies on the acidity of the subjected analytes. Straight forward comparison of recovery rates of HA was not possible since the studies used PPHA and HA (Fluka), respectively. Also, Fan et al. (2012) showed that the separation on the C18 (ENVI-18) resin in their work did not change the UV/VIS characteristics of the applied standard (SRFA) while the DEAE protocol led to changes for standard and ambient WSOC, for the latter being much

more pronounced and over a wide range of wavelengths. Further conclusions and comparison might be speculative since applied methodologies were, at least partly, not adopted accurately by Fan et al. (2012), compared to the originally reported methods by the respective authors. However Fan et al. (2012) found recovery rates of WSOC varying significantly between 20 and 70% for the same aerosol sample extracted with different resins. An interference test showed that all four methods are heavily interfered by the presence of aromatic acids and partly by phenols and di-carboxylic acids (ENVI-18, HLB XAD). Unfortunately levoglucosan, occurring in vast amounts in biomass burning impacted areas, and oxalic acid, both of which can occur at comparable atmospheric levels as HULIS, were not subjected to the method comparison. Table 6 juxtaposes interference studies conducted by the authors of the respective methods and complemented with reported comparisons processed by other groups. The selectivity of each of the methods was tested with about 20 substances, but as can be seen on first glance, only partly covering the same set of analytes. Concluding, it can be stated that the present method (C18+SAX) is beneath the most extensively tested methods and most selective protocols, regarding preparative methods actually the most selective protocol, reported in literature. To reach higher comparability of the respective methods and avoiding diverging adoption of isolation protocols, processing the protocols in different groups, to minimize the influence of actual differences in method adoptions, is highly desirable. An inter-laboratory test on the same set of aerosol samples, a fixed set of substances for interference tests and the use of identical standard fulvic and humic acids would furthermore help to raise the understanding of similarities and differences of HULIS isolated with different types of isolation/separation protocols.


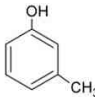
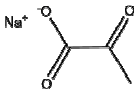
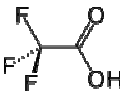
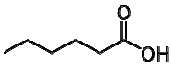
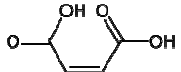
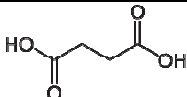
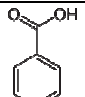
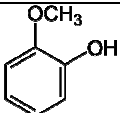
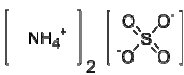
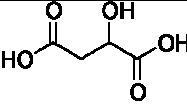
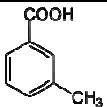
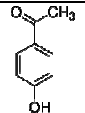
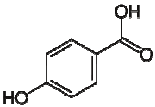
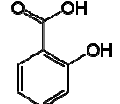
7 A three City Study: Seasonal Behaviour and possible Origin of atmospheric HULIS

Table 6: Summary of recently reported interference studies, part I

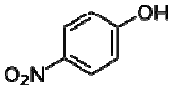
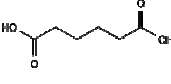
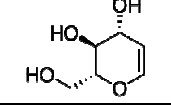
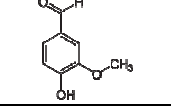
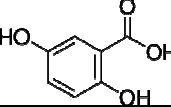
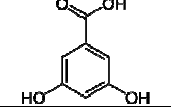
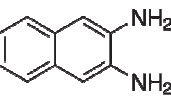
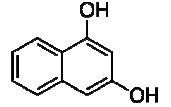
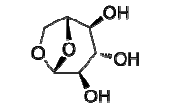
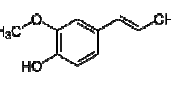
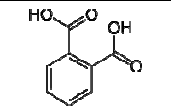
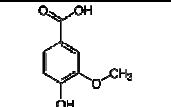
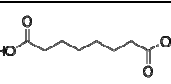
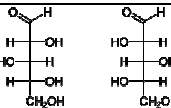
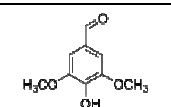
| Common/IUPAC name | Structure | Molecular mass [g/mol] | Limbeck et al., 2005 ^a | Emmenegger et al., 2007 ^b | Mancinelli et al., 2007 ^c | Baduel et al., 2009 ^d | Lin et al., 2010 ^a |
|---|---|------------------------|-----------------------------------|--------------------------------------|--------------------------------------|----------------------------------|-------------------------------|
| Acetaldehyde/ Ethanal |  | 44 | - | - | 0 | - | - |
| Formic acid |  | 46 | - | 0 | - | - | - |
| Propanal |  | 58 | -/(0) | - | - | 0 | - |
| Glyoxal/ Ethandial |  | 58 | - | - | 0 | -/ [<5] | - |
| Acetic acid |  | 60 | 0 | 0 | - | -/[0] | 0 |
| Sodium formate |  | 68 | - | - | 0 | - | - |
| Butyraldehyde/ Butanal |  | 72 | -/(0) | - | - | 0 | - |
| Methylglyoxal/ 2-oxopropanal |  | 72 | -/(0) | - | - | 0 | - |
| Propionic acid/ Propanoic acid |  | 74 | - | 0 | - | - | - |
| Ammonium nitrate |  | 80 | -/(0) | 0 | - | 0* | - |
| Butyric acid/ Butanoic acid |  | 88 | - | 0 | - | - | - |
| Lactic acid/ 2-Hydroxypropanoic acid |  | 90 | CT | 0 | - | -/[0] | - |
| Oxalic acid/ ethanedioic acid |  | 90 | 0 | 0 | - | - | 0 |
| Phenol |  | 94 | 0/(0) | 0 | X | 0 | <5 |
| Furfuryl alcohol/ 5-Hydroxymethylfuran |  | 98 | - | - | 0 | - | - |

7 A three City Study: Seasonal Behaviour and possible Origin of atmospheric HULIS

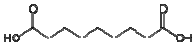
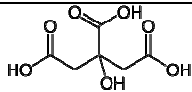
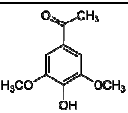
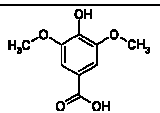
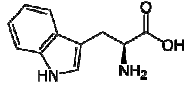
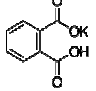
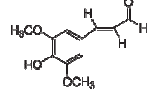
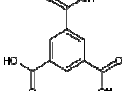
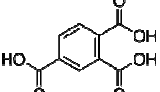
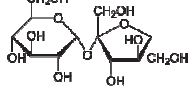
Table 6: Summary of recently reported interference studies. part II

| Common/IUPAC name | Structure | Molecular mass [g/mol] | Limbeck et al., 2005 ^a | Emmenegger et al., 2007 ^b | Mancinelli et al., 2007 ^c | Baduel et al., 2009 ^d | Lin et al., 2010 ^a ^e |
|---|---|------------------------|-----------------------------------|--------------------------------------|--------------------------------------|----------------------------------|--|
| Valeric acid/ Pentanoic acid |  | 102 | - | 0 | - | - | - |
| m-Cresol/ 3-Methylphenol |  | 108 | - | - | 0 | - | - |
| Sodium pyruvate |  | 110 | - | - | 0 | - | - |
| Trifluoroacetic acid/ 2,2,2-Trifluoroethanoic acid |  | 114 | - | 0 | - | - | - |
| Caproic acid/ Hexanoic acid |  | 116 | - | 0 | - | - | - |
| Maleic acid/ 2-Butenedioic acid |  | 116 | - | - | 0 | - | - |
| Succinic acid/ butanedioic acid |  | 118 | 0 | 0 | - | -/[0] | <5 |
| Benzoic acid |  | 122 | -/(0) | - | - | 0 | <5 |
| Guaiacol/ 2-methoxyphenol |  | 124 | - | - | - | -/[<5] | <5 |
| Ammonium sulfate/ Diazanium sulfate |  | 132 | - | 0 | - | - | - |
| Malic Acid/ hydroxybutanedioic acid |  | 134 | - | 0 | - | - | <5 |
| m-Tuloic acid/ 3-Methylbenzoic acid |  | 136 | - | - | - | - | <5 |
| 4-Hydroxyacetophenon |  | 136 | - | - | - | -/[<5] | - |
| 4-Hydroxybenzoic acid |  | 138 | CT | 0 | - | - | 15 |
| Salicylic acid/ 2-Hydroxybenzoic acid |  | 138 | -/(0) | - | - | 0 | - |

7 A three City Study: Seasonal Behaviour and possible Origin of atmospheric HULIS

| Common/IUPAC name | Structure | Molecular mass [g/mol] | Limbeck et al., 2005 ^a | Emmenegger et al., 2007 ^b | Mancinelli et al., 2007 ^c | Baduel et al., 2009 ^d | Lin et al., 2010 ^a ^e |
|---|---|------------------------|-----------------------------------|--------------------------------------|--------------------------------------|----------------------------------|--|
| 4-Nitrophenol |  | 139 | - | - | 0 | - | - |
| Adipic acid/ hexanedioic acid |  | 146 | 0 | 0 | - | - | - |
| D-Glucal/ 1,5-Anhydro-2- deoxy-D-arabino- hex-1-enitol |  | 146 | - | - | 0 | - | - |
| Vanillin/ 4-Hydroxy-3- methoxybenz- aldehyde |  | 152 | -(0) | - | X | 0 | <5 |
| 2,5- Dihydroxybenzoic acid |  | 154 | CT | - | - | - | - |
| 3,5-Dihydroxy- benzoic acid |  | 154 | - | - | - | -/[98.5] | - |
| 2,3, Diamino- naphthalene |  | 158 | -(0) | - | - | 0 | - |
| 1,3-Dihydroxy- naphthalene |  | 160 | CT | - | - | - | - |
| Levoglucosan/ (1R,2S,3S,4R,5R)- 6,8- Dioxabicyclo[3.2.1] |  | 162 | 0/(0) | - | - | 0 | <5 |
| Iso-eugenol/ 2-Methoxy-4-(1- propenyl)phenol |  | 164 | - | - | - | - | <5 |
| Phthalic acid/ benzene-1,2- dicarboxylic acid |  | 166 | 0 | X | - | -/[18.1] | 46 |
| Vanillic acid/ 4-Hydroxy-3- methoxybenzoic acid |  | 168 | - | - | - | - | 26 |
| Suberic acid/ octanedioic acid |  | 174 | - | - | - | -/[15.5] | 39 |
| Xylose/ D-Xylose |  | 180 | - | - | - | - | 6 |
| Syringaldehyde/ 4-Hydroxy-3,5- dimethoxybenzal- dehyde |  | 183 | -(0) | - | - | 0 | - |

7 A three City Study: Seasonal Behaviour and possible Origin of atmospheric HULIS

| Common/IUPAC name | Structure | Molecular mass [g/mol] | Limbeck et al., 2005 ^a | Emmenegger et al., 2007 ^b | Mancinelli et al., 2007 ^c | Baduel et al., 2009 ^d | Lin et al., 2010 ^{a,e} |
|---|---|--------------------------|-----------------------------------|--------------------------------------|--------------------------------------|----------------------------------|---------------------------------|
| Azelaic acid/ nonanedioic acid |  | 188 | - | - | - | - | 47 |
| Citric acid/ 2-hydroxypropane-1,2,3-tricarboxylic |  | 192 (210 monohydrate) | 0 | 0 | X | - | - |
| Acetosyringone/ 4'-Hydroxy-3',5'-dimethoxyacetophenone |  | 196 | - | - | - | - | <5 |
| Syringic acid/ 4-hydroxy-3,5-dimethoxybenzoic acid |  | 198 | - | - | - | - | 59 |
| Tryptophan/ 2-Amino-3-(1H-indol-3-yl)propanoic acid |  | 204 | - | - | 0 | - | - |
| Potassium phthalate |  | 204 | - | - | 0 | - | - |
| Sinapinaldehyde/ 3,5-Dimethoxy-4-hydroxycinnamaldehyde |  | 208 | - | - | - | - | 46 |
| Trimesic acid/ 1,3,5-Benzene-tricarboxylic acid |  | 210 | - | - | - | - | 54 |
| 1,2,4-Benzenetri-carboxylic acid |  | 210 | - | - | 0 | - | - |
| Sucrose |  | 342 | - | - | - | -/[<5] | 13 |

^a not specified which nitrate was investigated (Baduel et al., 2009); 0...not detected in HULIS fraction;

-...not investigated; []...investigated by Fan et al. (2012); Numbers denote percentages of recovery.

^a / this study; ()...investigated by Baduel et al., 2009; CT...detected in the HULIS fraction (beyond LOQ)

^b X...recovered in HULIS fraction, without indication of quantitative recovery.

^c Mancinelli et al. (2007) presented a method for separating neutral WSOC constituents, mono- and di-acids and a polyacidic fraction (PA); results given in this table refer to the PA fraction.

7.3.4 Atmospheric Abundance, spatial Variation and seasonal Patterns of HULIS_T in Austrian PM₁₀

Annual averaged HULIS_T related carbon (HULIS in the present work, is the sum of water and alkaline soluble HULIS fractions, HULIS_{WS} and HULIS_{AS}, respectively) levels occurred in a comparable order of magnitude at the ten sites in a range from 0.46 (background site ANTH, Salzburg) to 1.24 $\mu\text{g}/\text{m}^3$ (urban traffic impacted site DONB, Graz). With values between 0.74 and 0.96 $\mu\text{g}/\text{m}^3$ Vienna positions itself between Graz (0.79 - 1.24 $\mu\text{g}/\text{m}^3$) on the higher and Salzburg (0.46 - 0.79 $\mu\text{g}/\text{m}^3$) on the lower side, in terms of annual averaged HULIS_T related carbon (HULIS_T C) levels (Figure 42).

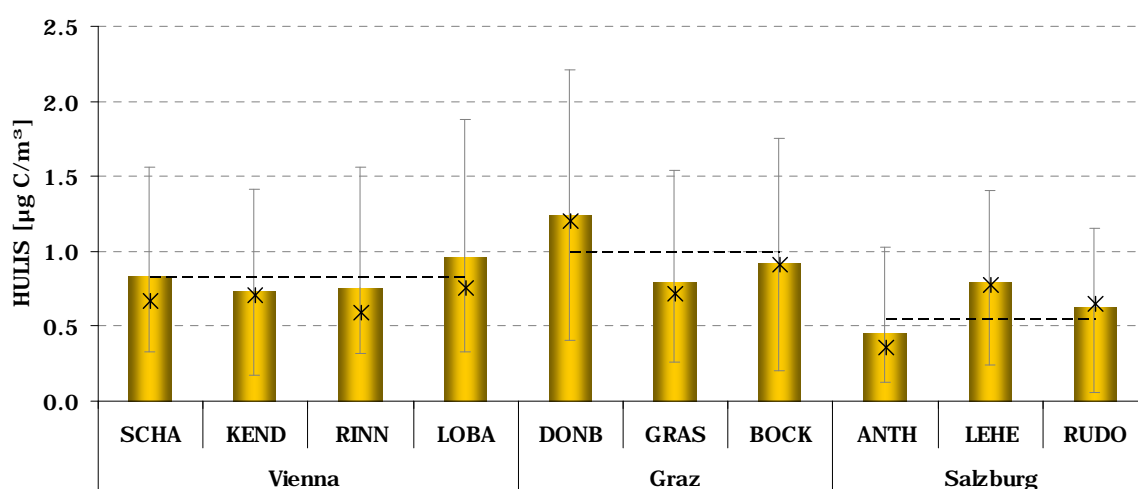


Figure 42: Annual averages of HULIS_T concentrations, Vienna, Graz and Salzburg, 2004. Bars: minimum and maximum monthly averages; Stars: median concentrations; dotted line: regional median.

Table 7: HULIS concentrations ($\mu\text{g C}/\text{m}^3$) Vienna, Graz and Salzburg 2004; winter: December-February; spring: March-May; summer: June-August; fall: September-November^a

| HULIS [$\mu\text{g C}/\text{m}^3$] | Vienna | | | | Graz | | | Salzburg | | |
|---|--------|------|------|------|------|------|------|----------|------|------|
| | SCHA | KEND | RINN | LOBA | DONB | GRAS | BOCK | ANTH | LEHE | RUDO |
| Average | 0.84 | 0.74 | 0.76 | 0.96 | 1.24 | 0.79 | 0.92 | 0.46 | 0.79 | 0.63 |
| Median | 0.67 | 0.71 | 0.59 | 0.76 | 1.20 | 0.72 | 0.91 | 0.36 | 0.78 | 0.65 |
| Min | 0.33 | 0.18 | 0.32 | 0.33 | 0.40 | 0.26 | 0.20 | 0.12 | 0.24 | 0.06 |
| Max | 1.56 | 1.42 | 1.56 | 1.88 | 2.21 | 1.54 | 1.76 | 1.03 | 1.40 | 1.15 |
| Spring | 0.84 | 0.63 | 0.70 | 0.89 | 1.26 | 0.80 | 0.96 | 0.49 | 0.79 | 0.62 |
| Summer | 0.48 | 0.46 | 0.43 | 0.50 | 0.66 | 0.45 | 0.56 | 0.28 | 0.36 | 0.41 |
| Fall | 0.89 | 0.78 | 0.73 | 1.04 | 1.34 | 0.86 | 0.69 | 0.44 | 1.02 | 0.59 |
| Winter | 1.13 | 1.09 | 1.17 | 1.42 | 1.72 | 1.05 | 1.47 | 0.62 | 1.00 | 0.82 |
| Winter/ summer | 2.3 | 2.4 | 2.7 | 2.8 | 2.6 | 2.4 | 2.6 | 2.2 | 2.8 | 2.0 |

^a Minima and maxima from monthly averages.

One emission source that is strongly linked to the atmospheric abundance of HULIS is biomass burning (e.g. Duarte et al., 2005b; Samburova et al., 2005b; Feczko et al., 2007; Hopkins et al., 2007; Samburova et al. 2007; Schmidl et al., 2008a und 2008b; Lin et al., 2010a und 2010b; Claeys et al., 2012). The impact of wood smoke on the regions

investigated in the present work was reported by Caseiro et al. (2009). They found organic matter stemming from wood smoke in winter to appear three and two times higher in the region of Graz compared to Vienna and Salzburg, respectively. Interestingly HULIS levels do not follow this trend (Figure 43) even though significant correlation with the biomass burning tracer levoglucosan was observed at all ten sites (see detailed discussion in section 7.3.9). This suggests that additional sources or atmospheric conditions affect the emission and formation of HULIS. Similar observations were reported by Stone et al. (2009) at North American sampling sites.

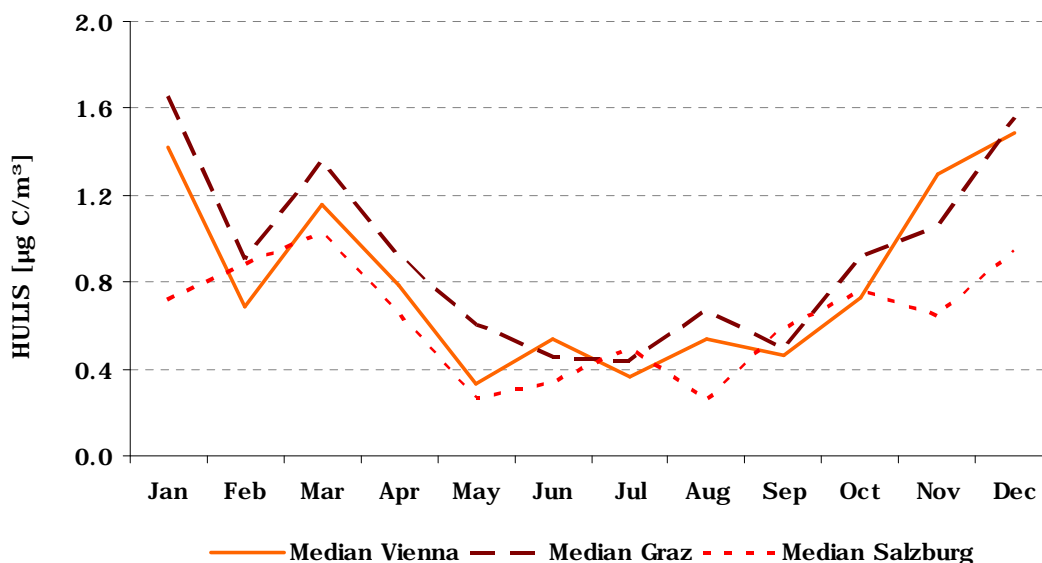


Figure 43: Regional median HULIS levels in Vienna and the regions of Graz and Salzburg.

Seasonal averaged HULIS carbon concentrations revealed lowest concentrations in summer ($0.28 - 0.66 \mu\text{g}/\text{m}^3$) and highest in winter time ($0.62-1.72 \mu\text{g}/\text{m}^3$) regarding the ten sampling sites in Vienna and the regions of Graz and Salzburg (Table 7, Figure 44, Figure 45 and Figure 46). The winter/ summer ratio appears quite similar at the different sites in Vienna, Graz and Salzburg ranging from 2 to 2.8 times higher HULIS_T carbon levels in winter. The winter enrichment of HULIS_T points to higher source strength of HULIS and/or its precursors in winter. It can be excluded that plain accumulation, due to unfavourable dispersion conditions such as inversion and lowered mixing layer heights, is mainly responsible for wintry HULIS maxima, as discussed in detail in subchapter 7.3.7. The discovered seasonal behaviour of atmospheric HULIS, with summer minima and winter maxima, was as well observed at background sites in Portugal (Aveiro) and Hungary (K-puszta), a rural coastal site with maritime influence and a continental site, respectively (Feczko et al., 2007), with winter/summer ratios for HULIS_T of 3 and 2.8 for the continental and the rural maritime site, respectively. Averaged annual HULIS carbon levels of $1.26 \mu\text{g}/\text{m}^3$ (Aveiro) and $1.68 \mu\text{g}/\text{m}^3$ (K-puszta) are reported, exceeding the highest annual average observed in the present study at the urban traffic impacted site in Graz ($1.24 \mu\text{g}/\text{m}^3$).

Figure 44, Figure 45 and Figure 46 display the seasonal variations of atmospheric HULIS_T levels in Vienna, Graz and Salzburg.

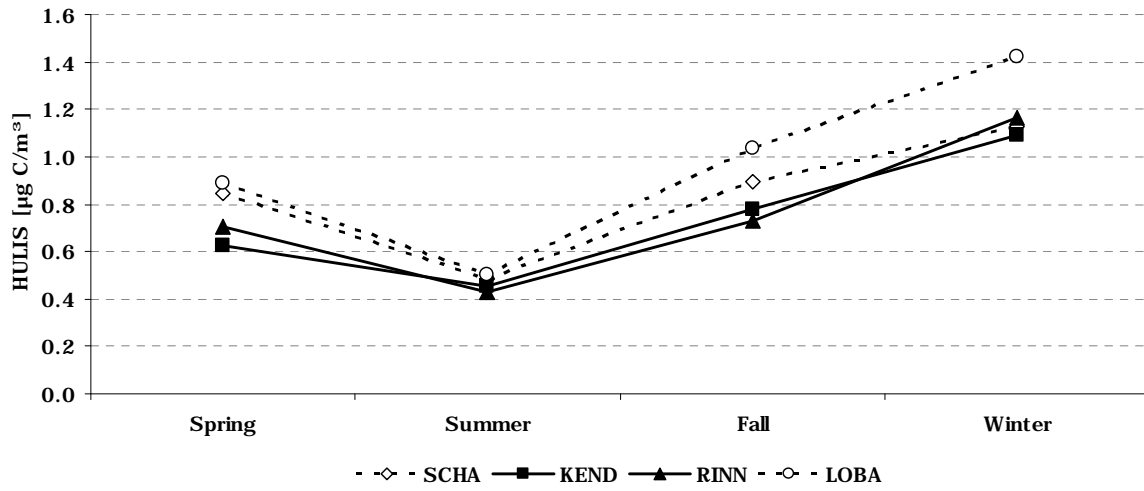


Figure 44: Seasonal averaged HULIS carbon concentrations, Vienna 2004.

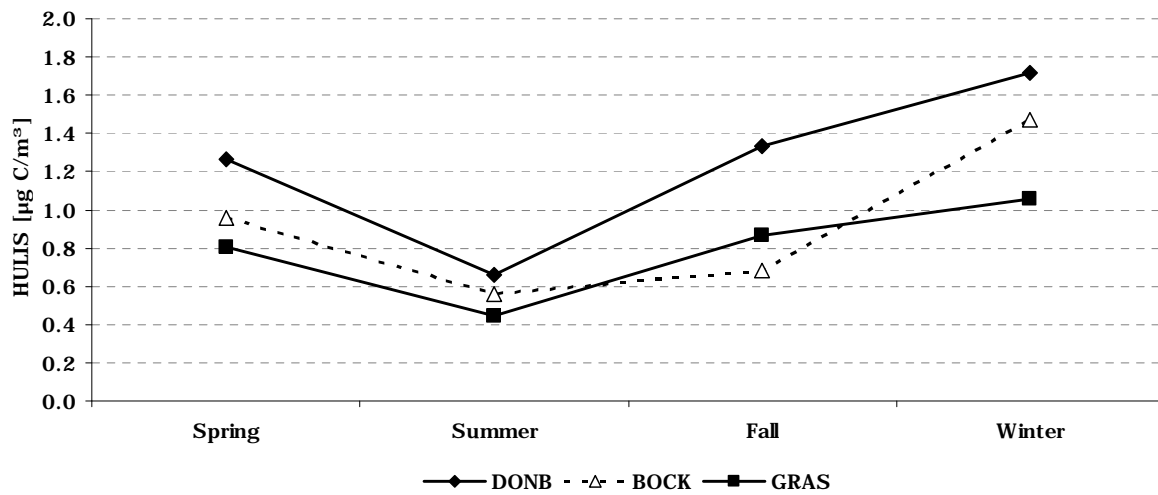


Figure 45: Seasonal averaged HULIS carbon concentrations, Graz 2004.

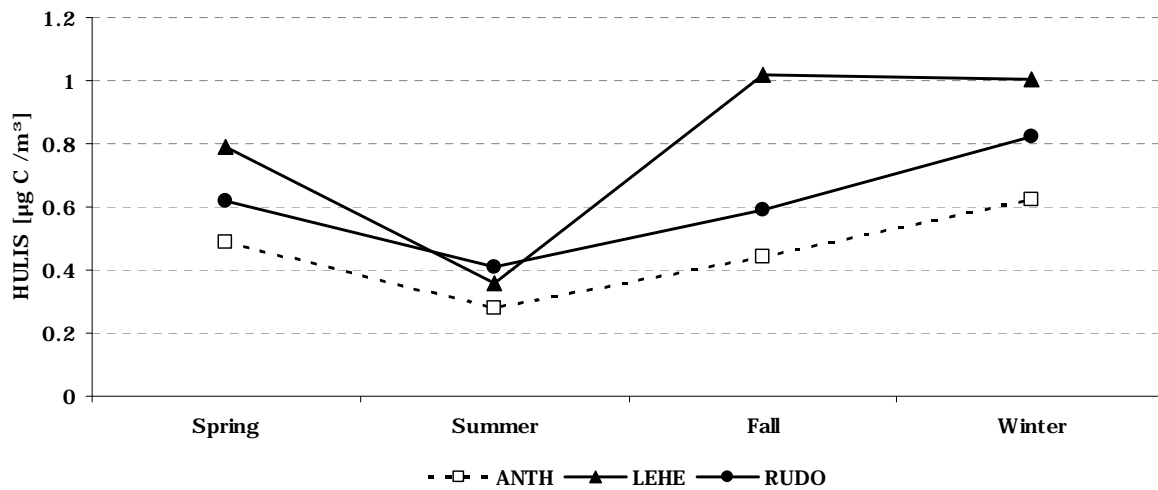


Figure 46: Seasonal averaged HULIS carbon concentrations, Salzburg 2004.

Concerning Vienna (Figure 44), highest seasonal averaged HULIS_T levels occurred at the background site LOBA with ~25 % higher HULIS carbon levels in winter and summer, and ~50% higher levels in spring and fall, compared to the intra-urban sites RINN and KEND. As mentioned above lowest values for all sites were found in summer (0.43-0.50 µg C/m³) and maximised in winter (1.09-1.42 µg C/m³), whereas spring and fall revealed intermediate levels. The sites in the area of Graz and Salzburg qualitatively showed the same seasonal devolution. In Graz the urban, traffic impacted site DONB showed maximum HULIS_T carbon levels (Figure 45), whereas in Salzburg the urban residential site LEHE revealed highest HULIS carbon levels, with the exception of summer, where concentration levels were found at very similar heights.

Comparison of the three cities during the winter months revealed highest HULIS_T carbon levels at the traffic impacted site DONB (Graz) with 1.72 µg C/m³ HULIS_T on winter average, followed by 1.47 and 1.42 µg/m³ HULIS_T carbon at the background sites BOCK and LOBA, respectively and the urban sites (RINN, KEND, SCHA, GRAS and LEHE) within a narrow range of 1.0-1.17 µg C/m³. Lowest winter averages were found at RUDO and ANTH (0.82 and 0.62 µg/m³), the traffic impacted urban site and the respective background site in Salzburg. HULIS_T summer levels occurred in similar heights in the three regions. Differences between the sampling sites, regarding the HULIS_T level, in all three regions, get smaller during summer and maximise in fall, as visualised in Figure 47, by the use of the relative standard deviation as a proxy for spatial HULIS spreads.

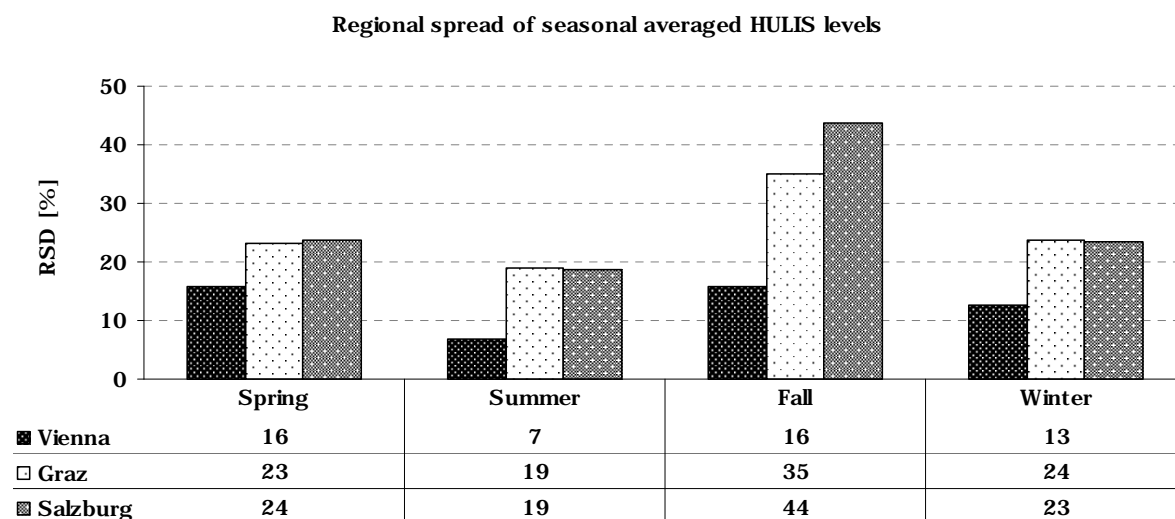


Figure 47: Regional spread (as relative standard deviations (RSD)) of seasonal HULIS levels in Vienna, Graz and Salzburg.

Each region showed the most homogenous HULIS levels during summer with a RSD between 7 and 19 %. More pronounced differences occurred during fall with an RSD of 16, 35 and 44 % in Vienna, Graz and Salzburg, respectively. This might point to a stronger impact of local sources during the heating period and transition month on the occurrence

of HULIS. Differences between HULIS levels in Vienna are lower about a factor of 2 (in terms of RSD) throughout the year compared to Graz and Salzburg. Reasons for that might be the better ventilation of the Vienna Basin (Spangl et al., 2006), as well as lower impact of local sources of HULIS and/or its precursors, while topographical characteristics play a minor role (Figure 48).

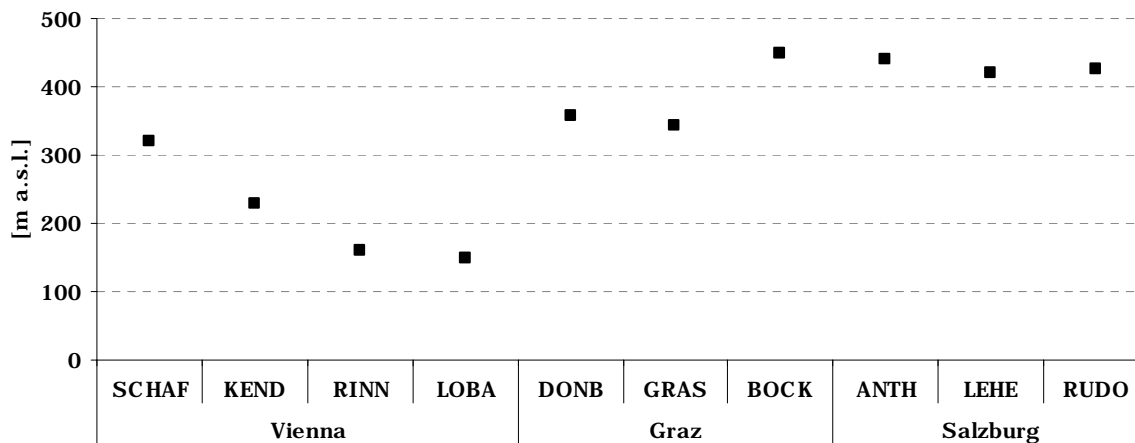


Figure 48: Meter above sea level of the sampling sites in Vienna, Graz and Salzburg

7.3.5 Contributions of HULIS_T to PM10 and Organic Carbon

To estimate the contributions of HULIS_T matter to PM10, a proxy factor of 1.9 (Krivácsy et al. 2001, Kiss et al. 2002, Lin et al. 2010a) is applied to convert HULIS_T carbon to HULIS_T related organic matter. On annual average HULIS_T contribute to PM10 in the range of 3.8 (RUDO, Salzburg)-8.9 (LOBA, Vienna) % at the ten sites in Vienna and the regions of Salzburg and Graz. Annual averages of HULIS_T contributions to PM10 and HULIS_T carbon to organic carbon (OC), median and seasonal averages are summarized in Table 8.

Table 8: Contributions of HULIS_T to PM10 and HULIS_T carbon to OC in Vienna, Graz and Salzburg, 2004; Winter: December-February; Spring: March-May; Summer: June-August; Fall: September to November

| | | Vienna | | | | Graz | | | Salzburg | | |
|----------------|-------------------|--------|------|------|------|------|------|------|----------|------|------|
| | | SCHA | KEND | RINN | LOBA | DONB | GRAS | BOCK | ANTH | LEHE | RUDO |
| HULIS/PM10 [%] | Average | 7.9 | 5.3 | 4.4 | 8.9 | 5.5 | 4.5 | 8.3 | 5.6 | 7.6 | 3.8 |
| | Median | 7.6 | 5.1 | 4.0 | 7.9 | 4.9 | 4.3 | 8.4 | 5.1 | 6.9 | 4.2 |
| | Min | 5.0 | 1.7 | 2.8 | 4.6 | 3.1 | 1.5 | 2.3 | 2.1 | 3.5 | 0.5 |
| | Max | 13.1 | 8.3 | 7.4 | 15.9 | 9.2 | 6.7 | 14.6 | 9.5 | 14.1 | 5.2 |
| | Spring | 7.5 | 4.0 | 3.7 | 8.6 | 5.7 | 4.8 | 8.6 | 4.7 | 7.4 | 3.2 |
| | Summer | 7.1 | 5.2 | 3.9 | 7.0 | 5.0 | 4.2 | 7.4 | 5.1 | 5.4 | 3.7 |
| | Fall | 8.8 | 5.8 | 4.6 | 10.1 | 6.3 | 5.0 | 6.7 | 6.4 | 11.5 | 3.8 |
| | Winter | 8.0 | 6.2 | 5.5 | 9.9 | 5.0 | 3.9 | 10.2 | 6.2 | 6.3 | 4.4 |
| | Winter/ summer | 1.1 | 1.2 | 1.4 | 1.4 | 1.0 | 0.9 | 1.4 | 1.2 | 1.2 | 1.2 |
| HULIS C/OC [%] | Average | 27.0 | 17.2 | 15.1 | 28.9 | 14.3 | 10.1 | 23.5 | 19.6 | 24.4 | 11.1 |
| | Median | 26.1 | 16.9 | 12.4 | 28.1 | 13.7 | 10.3 | 22.0 | 18.0 | 21.3 | 11.9 |
| | Min | 14.8 | 6.0 | 10.3 | 10.0 | 7.8 | 2.9 | 7.2 | 6.7 | 9.4 | 1.9 |
| | Max | 43.2 | 26.2 | 25.1 | 49.7 | 21.5 | 17.0 | 44.6 | 40.8 | 57.5 | 15.3 |
| | Spring | 30.9 | 16.4 | 15.2 | 30.8 | 14.8 | 11.6 | 28.3 | 22.4 | 25.5 | 9.2 |
| | Summer | 21.7 | 15.1 | 12.5 | 19.3 | 15.6 | 11.8 | 20.2 | 14.6 | 14.9 | 11.5 |
| | Fall | 30.4 | 18.2 | 15.8 | 32.0 | 14.2 | 10.6 | 16.4 | 18.2 | 38.3 | 12.8 |
| | Winter | 25.1 | 19.1 | 16.9 | 33.7 | 12.6 | 6.9 | 29.3 | 23.0 | 18.8 | 11.0 |
| | Winter/ summer | 1.2 | 1.3 | 1.4 | 1.7 | 0.8 | 0.6 | 1.5 | 1.6 | 1.3 | 0.9 |

^a Minima and maxima from weighed monthly averages.

In Vienna and Graz higher relative average fractions in PM10 occurred at the background sites in a narrow range of 7.9 – 8.9 %, whereas the inner city sites in Vienna and Graz revealed lower HULIS to PM10 shares between 4.4 and 5.5 %. Compared to the sites in Vienna and Graz the background site in Salzburg (ANTH) showed an annual average HULIS_T to PM10 share of 5.1% similar to the inner city sites in Vienna and Graz. The traffic impacted site in Salzburg (RUDO) revealed lower shares to PM10, consistent with observations in Graz and Salzburg while highest HULIS_T carbon to PM10 contributions appeared at the urban residential site LEHE (where there should be mentioned that the high values are influenced by the high HULIS_T fall levels at that site, where sampling was conducted only on 34 out of 92 days, thus are not fully representative).

The importance of achieving better understanding of sources, formation pathways and structure of humic-like substances as major constituents of ambient aerosol gets even more accented if one looks to their share to total organic carbon. HULIS_T carbon

contributes substantially to particulate organic carbon (OC) from 10.1% (Urban residential site GRAS, Graz) up to 28.9% (Background site LOBA, Vienna; Figure 49).

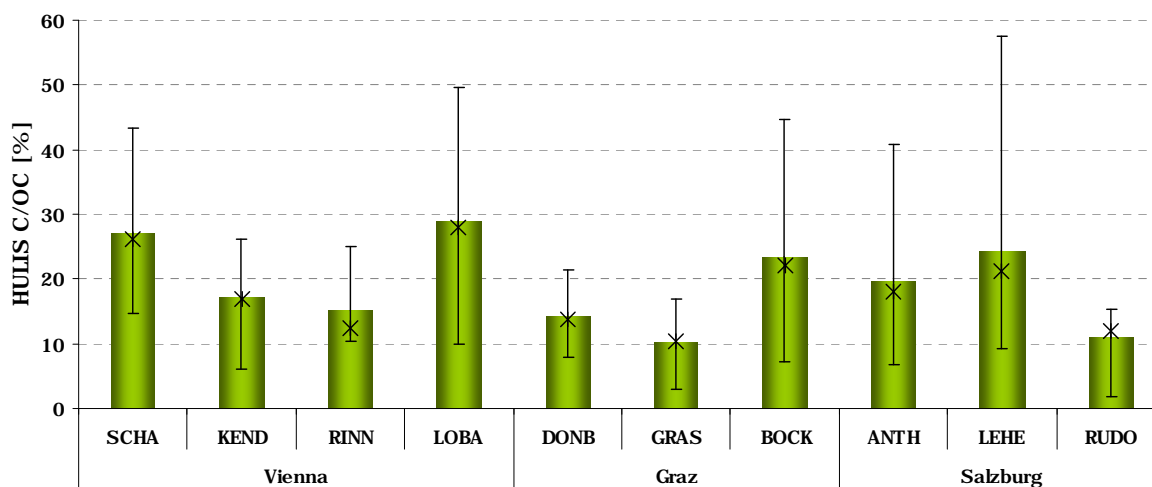


Figure 49: HULIS_T C contribution to OC, annual averages, Vienna, Graz and Salzburg, 2004. Bars: minimum and maximum monthly averages; Stars: median concentrations.

The background sites in Vienna and the region of Graz reveal highest annual averaged shares of HULIS carbon to OC within a narrow range of 23.5-28.9 %, being almost a factor of two higher compared to corresponding inner city sites. In Salzburg the urban residential site (HULIS/OC= 38.3 %), reveals HULIS_T C to OC contributions two times higher than the urban traffic impacted site, respectively. Taking into account that the average at the site LEHE is not fully representative (due to only one third available samples during fall) the shares to OC are about a factor of 2 higher at the background sites compared to the inner city sites. The fraction of HULIS_T carbon contributing to OC (annual average) at the background sites is in remarkable agreement with values determined for continental (K-pusztá, Hungary) and maritime (Aveiro, Portugal and Azores) background sites where contributions of 24.2, 26.2 and 23.2% (Feczko et al., 2007) were observed and seem to be characteristic shares for HULIS_T C to OC for background sites at lower tropospheric levels.

In general HULIS carbon shares of OC showed no distinct seasonality. Seasonal resolution of HULIS contribution to OC in Vienna revealed lower contributions at the intra-urban sites KEND and RINN (12.5-19.1%) as well as lower seasonal differences compared to the urban fringe sites SCHA and LOBA (19.3-33.7%), displayed in Figure 50. Concerning the two intra-urban sites the traffic impacted site RINN showed lowest HULIS_T C to OC contributions quite constantly 2% lower than the intra-urban residential site KEND. All four sites in Vienna showed minimum contributions during the summer month. Maximum shares to OC occurred during winter at RINN, KEND and LOBA. The site SCHA showed maximum contributions in spring and fall (30.9 and 30.4 %), possibly pointing to stronger

potential HULIS/HULIS precursor sources such as emissions from biomass space heating during transition month.

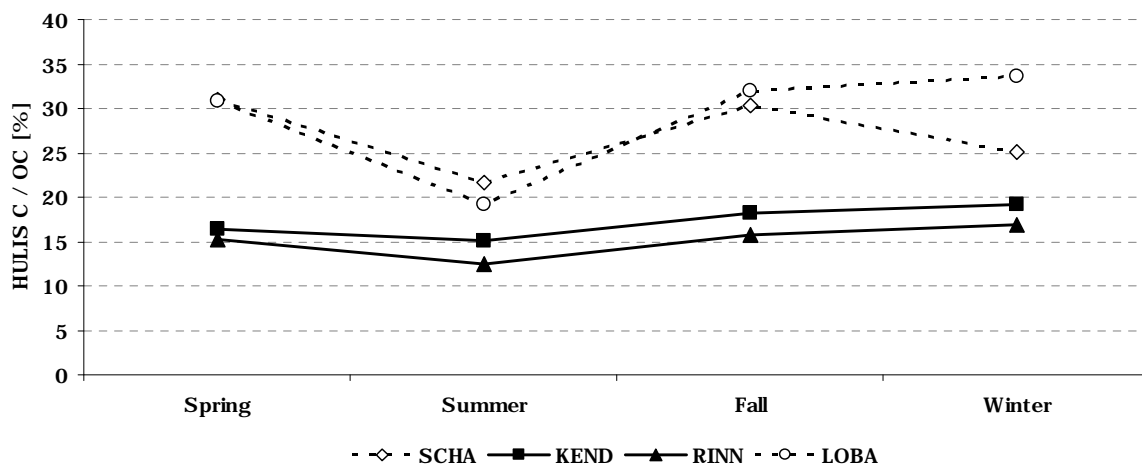


Figure 50: HULIS_T C contribution to OC, seasonal averages, Vienna 2004.

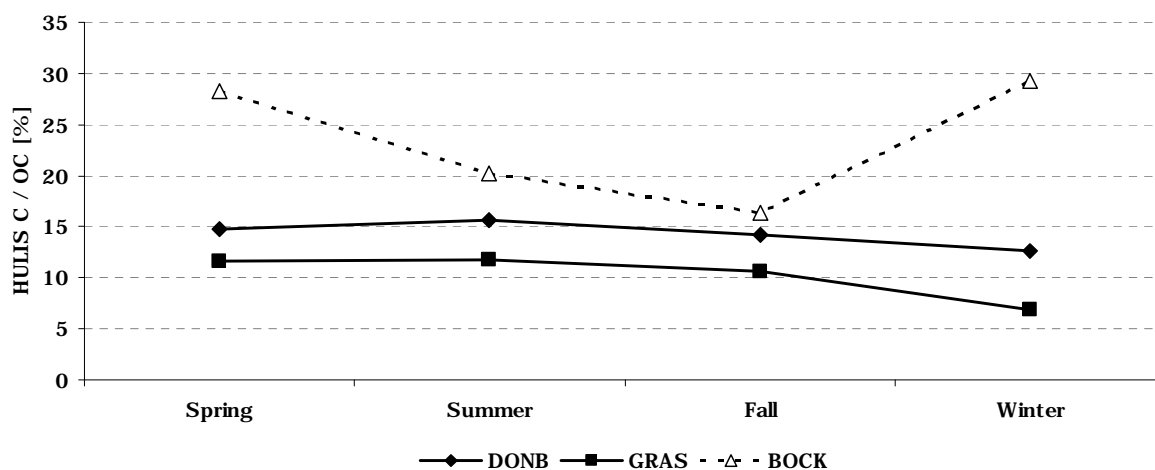


Figure 51: HULIS_T C contribution to OC, seasonal averages, Graz 2004.

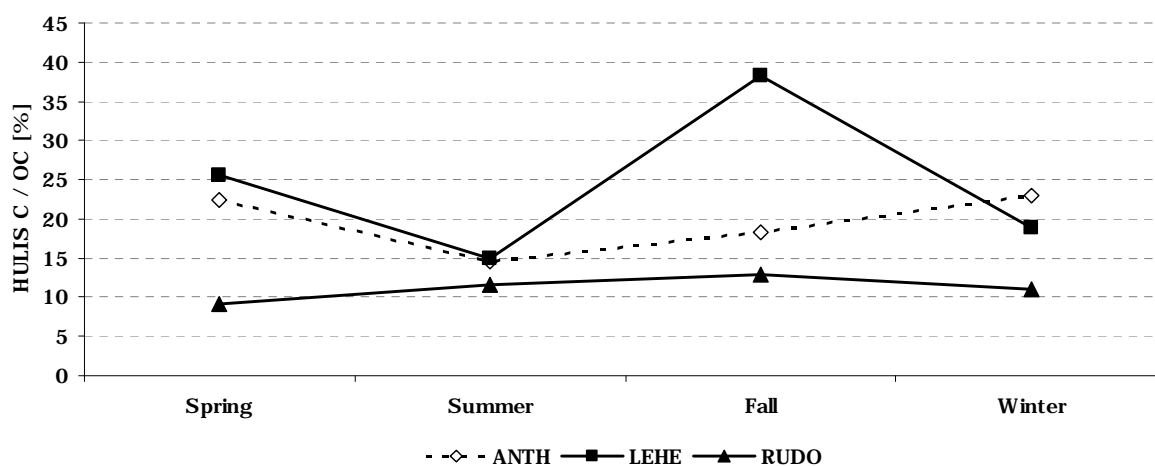


Figure 52: HULIS_T C contribution to OC, seasonal averages, Salzburg 2004.

At the sites in the region of Graz the two urban sites as well show a parallel devolution concerning the HULIS_T C to OC share and lower values as the background site BOCK (Figure 52). In contrary to Vienna the urban residential site GRAS revealed lowest values with 2-6 % lower values compared to the traffic impacted site DONB. The urban sites show slight maxima in summer (15.6 and 11.8%) and minima during winter (12.6 and 6.9%) whereas at the background site BOCK maxima occurred in spring and winter where OC consisted almost up to one third of HULIS_T carbon.

In the region of Salzburg the trend to lower OC shares and smaller seasonal changes continues for the traffic impacted site RUDO, although minima occurred in spring and maxima during fall. The urban residential site LEHE revealed values and a slope more like the background site ANTH where HULIS carbon to OC shares in the range of 14.6-25.5% occurred, except for fall where contributions of 38 % formed a distinct maximum (RUDO: 9.2-12.8% HULIS_T C/OC), which is not fully representative due to the fact that only one 34 out of 92 daily samples were sampled by the local authorities during fall. As at the background site in Graz, maxima occurred in spring and winter in ANTH (22.4 and 23 %). Summarizing observations concerning the share of HULIS carbon to OC at Vienna, Graz and Salzburg a trend for higher shares at the background sites LOBA (Vienna), BOCK (Graz) and ANTH (Salzburg) with maxima during spring and winter gets visible. The background site SCHA, situated in residential area at the fringe of Vienna, revealed highest HULIS carbon to OC shares in spring and fall. Water-soluble HULIS was reported to contribute to OC with 6-31% at a Swiss (Samburova et al., 2005b) and with 14 % at a maritime (El Haddad et al., 2011) urban background site, what is in good agreement with the present results.

7.3.6 Water and alkaline soluble Fractions of HULIS

Literature provides only poor information on the alkaline soluble fraction of atmospheric HULIS. To the best of our knowledge no investigations on seasonal behaviour (in terms of full seasonal cycles) of this fraction in urban environments have been published so far. A study of Feczko et al. (2007) focused on HULIS_T levels at six background sites in Europe. In that study HULIS_T was defined as sum of water and alkaline extracted HULIS, which is the same approach as used in the present work. Baduel et al. (2009) investigated HULIS_T and HULIS_{WS} with UV-spectrometric methods. HULIS_T in the study of Baduel et al. (2009) was the alkaline soluble fraction which-by definition (e.g. Stevenson et al., 1994)- included the water soluble fraction as well. Contrasting, Feczko et al. (2007) and the present work performed subsequent water and alkaline extraction of the filter samples. However, UV-spectrometric analysis of the alkaline one-step extracted HULIS showed a slight enrichment of aromatic and high molecular weight compounds compared to the water extracted HULIS (Baduel et al., 2009). Overall the differences between the two fractions seemed rather small (Baduel et al., 2009). An experiment on the photochemical aging of HULIS_T by oxidation in the presence of ozone showed that HULIS_T get more hydrophilic (Baduel et al., 2011). Both studies (Feczko et al., 2007; Baduel et al., 2009) observed HULIS_{WS} accounting for roughly 50 % of HULIS_T.

In the present work, HULIS_{WS} contributed 55% ±5% to HULIS_T in the majority of the sample pools at the ten sampling sites (Table 9). That is in good agreement with the shares of 44 – 47 % observed by Feczko et al. (2007) at continental background sites. The relative share of HULIS_{WS} did not show any seasonality, as well observed by Feczko et al. (2007), or a clear trend to occur preferred on urban or rural sites. No general difference was found between episodes with high and low PM10 burdens. Correlations between HULIS_{WS} and the HULIS_T (defined as the sum of the water and alkaline soluble HULIS fraction) are significant at all sites and the slopes are found in a narrow range of 1.39-1.74 (Table 9). A small number of sample pools showed strongly diverging HULIS_{AS} shares, which, with one exception, are all occurring in January or November. Restraining these sample pools from correlation calculations lead to significant rises of R² at the sites in Vienna and Graz (Table 9). As mentioned in the previous section, PM10 was sampled daily, but analyses were conducted on pooled filter samples. The filters were pooled either according to episodes (meteorological episodes, significant higher urban PM10 burdens or special events) or after the level of pollution (>50 µg/m³, <50µg/m³) as described in detail in Bauer et al. (2006, 2007a and 2007b). Slopes of the correlation trend lines therefore do not exactly reflect the overall HULIS_{WS} shares. However, plotting HULIS_{WS} against HULIS_T revealed differences between the three cities (Figure 53, Figure 54, and Figure 55). Salzburg showed rather uniform behaviour between the sites and no

strong deviations from the mean of HULIS_{WS} shares, whereas a few samples showed strongly diverging HULIS composition in Graz and Vienna. For further investigations samples with rather high HULIS_T and high HULIS_{AS} shares were chosen.

Table 9: Correlations between HULIS_T (defined as sum of HULIS_{WS} und HULIS_{AS}; y, µg C/m³) and HULIS_{WS} (x, µg C/m³)

| Sampling site | Characteristic | Entire samples | HULIS _{WS} / HULIS _T [%] | Without high HULIS _{AS} samples* |
|---------------|----------------|---|--|---|
| Vienna | SCHAF | urban fringe $y=1.41x+0.2$ $R^2=0.61$ | 51 | $R^2=0.89$ |
| | KEND | urban $y=1.48x+0.10$ $R^2=0.93$ | 58 | $R^2=0.92$ |
| | RINN | urban $y=1.69x+0.10$ $R^2=0.72$ | 49 | $R^2=0.87$ |
| | LOBA | urban fringe $y=1.61x+0.05$ $R^2=0.94$ | 57 | $R^2=0.95$ |
| Graz | DONB | urban $y=1.74x-0.03$ $R^2=0.79$ | 60 | $R^2=0.93$ |
| | GRAS | urban $Y=1.60x+0.08$ $R^2=0.72$ | 55 | $R^2=0.93$ |
| | BOCK | rural $y=1.39x+0.16$ $R^2=0.73$ | 56 | $R^2=0.92$ |
| Salzburg | ANTH | rural $y=1.59x+0.03$ $R^2=0.96$ | 60 | - |
| | LEHE | urban $y=1.41x+0.21$ $R^2=0.77$ | 50 | - |
| | RUDO | urban $y=1.50x+0.11$ $R^2=0.90$ | 56 | - |

*correlation of HULIS_{WS} and HULIS_T, restraining sample pools with stongly diverging HULIS_{AS} shares from calculations

Aerosol composition of aerosol and meteorology were investigated in Vienna, Graz and Salzburg in the scope of the AQUELLA projects to elucidate the sources contributing to PM10 and causing high PM10 episodes (Bauer et al., 2006; Bauer et al. 2007a; Bauer et al., 2007b). Meteorological data compiled in the studies of Bauer et al. (2006 and 2007) was taken for analysing sample pools with high HULIS_{AS} shares in the present work.

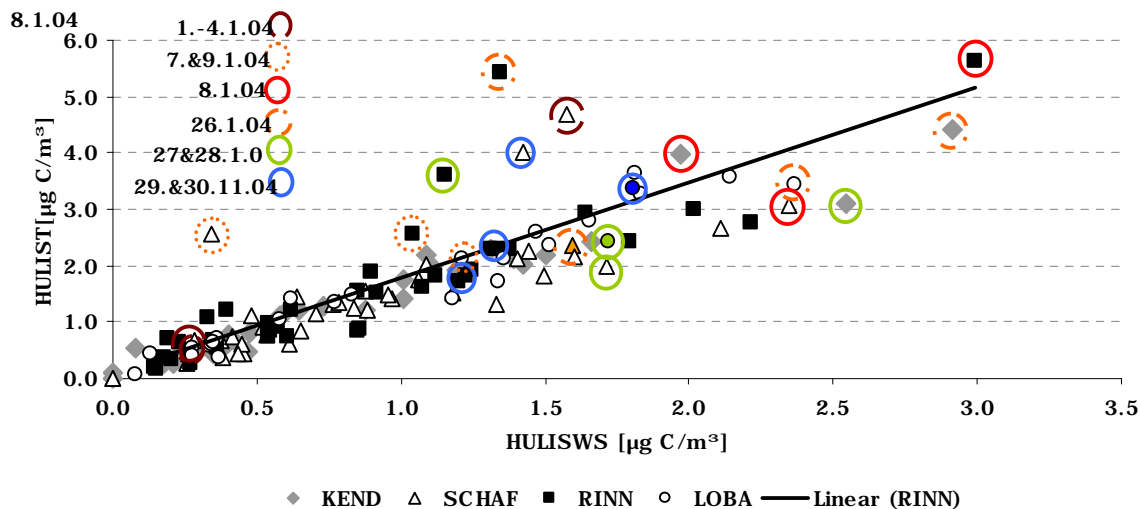


Figure 53: Correlation between HULIS_{WS} and HULIS_r, Vienna.

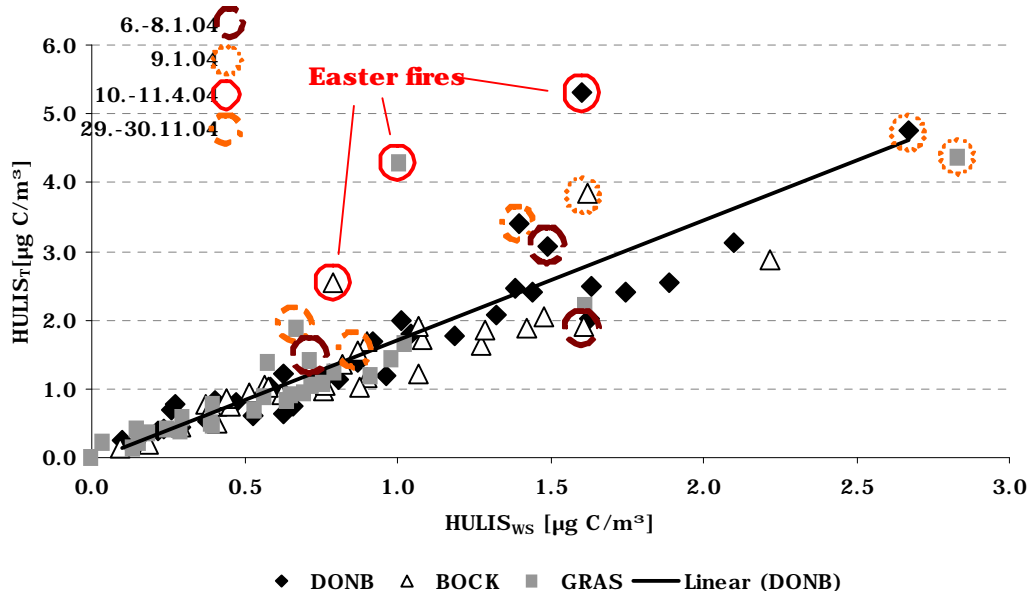


Figure 54 : Correlation between HULIS_{WS} and HULIS_r, Graz.

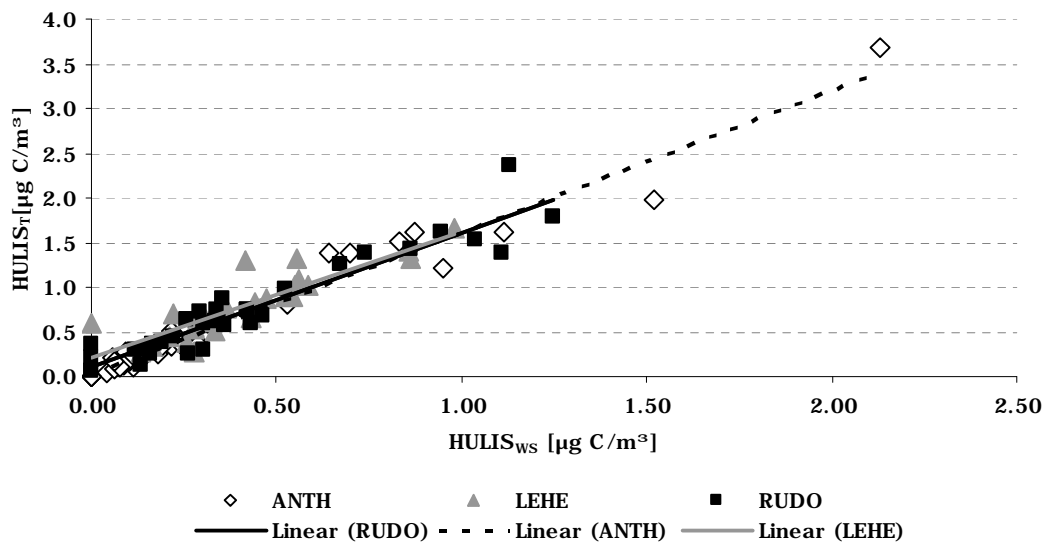


Figure 55: Correlation between HULIS_{WS} and HULIS_r, Salzburg.

In Vienna high shares of HULIS_{AS} (or low HULIS_{WS}) occurred at four episodes in January and one in November, either at the urban traffic impacted site RINN or at the slightly elevated urban fringe site SCHAF. The latter is situated on the urban fringe 100 and 150 m higher than KEND and RINN or LOBA (Umweltbundesamt, 2009), respectively, and is partly lying above the upper limit of inversion layers (Bauer et al., 2006). Comparing meteorological data with HULIS composition revealed that the occurrence of high HULIS_{AS} shares resembles to three different types of meteorological situations connected to different PM10 burdens.

Table 10: Meteorological characteristics and PM10 burden at high relative HULIS_{AS} periods in Vienna; ND...no data; surface wind directions, inversion situation, dominating PM10 sources are from Bauer et al. (2007a)

| Sampling site | Sampling date | Episode 1 | Episode 2.1 | Episode 2.2 | Episode 3.1 | Episode 3.2 | Episode 4 |
|---------------|---|--|---|---|---|---|--|
| | | 1.-4.1. 2004 | 7. & 9.1. 2004 | 8.1.2004 | 26.1.2004 | 27. & 28.1. 2004 | 29. & 30.11. 2004 |
| SCHAF | HULIS _{WS} [$\mu\text{g C/m}^3$] | 1.57 | 0.34 | 2.35 | 1.59 | 1.71 | 1.42 |
| | HULIS _T [$\mu\text{g C/m}^3$] | 4.68 | 2.55 | 3.05 | 2.35 | 1.97 | 4.02 |
| | HULIS _{WS} /HULIS _T [%] | 34 | 13 | 77 | 68 | 87 | 35 |
| KEND | HULIS _{WS} [$\mu\text{g C/m}^3$] | 0.29 | 1.39 | 1.97 | 2.91 | 2.55 | 1.31 |
| | HULIS _T [$\mu\text{g C/m}^3$] | 0.47 | 2.14 | 3.99 | 4.40 | 3.09 | 2.29 |
| | HULIS _{WS} /HULIS _T [%] | 63 | 65 | 49 | 66 | 83 | 57 |
| RINN | HULIS _{WS} [$\mu\text{g C/m}^3$] | 0.26 | 1.04 | 2.99 | 1.34 | 1.16 | 1.12 |
| | HULIS _T [$\mu\text{g C/m}^3$] | 0.41 | 2.57 | 5.62 | 5.42 | 3.61 | 1.83 |
| | HULIS _{WS} /HULIS _T [%] | 64 | 41 | 53 | 25 | 32 | 61 |
| LOBA | HULIS _{WS} [$\mu\text{g C/m}^3$] | | | | 2.37 | 1.72 | 1.81 |
| | HULIS _T [$\mu\text{g C/m}^3$] | | no samples | | 3.44 | 2.43 | 3.35 |
| | HULIS _{WS} /HULIS _T [%] | | | | 69 | 71 | 54 |
| | PM10 [$\mu\text{g/m}^3$] | All sites ~20 | RINN & KEND ~70/ SCHAF~60/ LOBA ~50 | RINN & KEND ~105/ SCHAF~80/ LOBA~65 | RINN >95/ SCHAF, KEND, LOBA ~80 | RINN 70/ KEND ~60/ SCHAF & LOBA ~55 | RINN ~70/ KEND~ 60/ SCHAF & LOBA~50 |
| | Surface wind direction/inversion | NW-W/no | OSO-SSO/yes | SO/yes | SO/yes | SSO-NNW/no | ND/ ND |
| | Dominating PM10 sources | mixed | inorganic secondary/ wood smoke | inorganic secondary/ wood smoke | inorganic secondary/ wood smoke | inorganic secondary/ wood smoke | mixed |
| | Characteristic | High rel. HULIS _{AS} at SCHAF (UF-BG) | Mixed | | High rel. HULIS _{AS} at RINN (U-T) | | High rel. HULIS _{AS} at SCHAF (UF-BG) |

Type 1 (episode 1 and 4), occurring at the first days of January and late November (Table 10), is characterised by highest HULIS_T levels and HULIS_{AS} contributions at the urban fringe site SCHAF, and lower levels at both urban sites. PM 10 levels at all sites in Vienna were below 30 $\mu\text{g/m}^3$ and moderately between 70 and 50 mg/m^3 , respectively, connected to influences from air masses from western/north-western Europe (Bauer et al., 2006; Spangl et al, 2006). Lowest PM10 levels at SCHAF make it unlikely that a strong primary source at SCHAF is responsible for both, high HULIS_T levels and HULIS_{AS} shares. Meteorological data (appendix, Figure 96) showed that fog events took place in both episodes during daytime reducing the intensity of solar radiation. SCHAF, due to its

elevation, might be unaffected by fog layers and enhanced photochemical activity and a higher formation rate could lead to higher absolute HULIS levels. High shares of HULIS_{AS} to the total HULIS fractions of 65 and 66% for both episodes and lower, quite uniform shares below 40% at the urban sites potentially link higher shares of HULIS_{AS} to freshly formed HULIS.

Type 2 (episodes 2.1 and 2.2) are influenced by air masses from southeast and an inversion lower than 500 m. Regarding the HULIS_{AS} shares this meteorological episode reflect a mixed episode with highest HULIS_{AS} shares at the fringe site SCHAF (87%) on the 7th and 9th of January and lower at the urban sites, with comparable HULIS_T levels at the three sites. On January 8th PM10 burdens peak with over 100 µg/m³ at both urban sites and lower at the fringe sites. HULIS_T levels follow this trend whereas higher HULIS_{AS} shares occur at the urban sites (~50%) compared to 30% at the elevated fringe site (SCHAF). Local photochemical formation of HULIS during these three days is rather unlikely since fog and precipitation were recorded for this period (Bauer et al., 2006). Strong differences might reflect the inversion situation and the partly decoupled sampling site SCHAF from urban PM10. However, since the pools do not reflect chronological order, straight forward conclusions on the aging process of HULIS are not possible.

Type 3 (episode 3.1 and 3.2), took place on January 26th and 27th to 28th and was characterised by highest HULIS_T levels and HULIS_{AS} contributions at the urban traffic impacted site RINN and lower at KEND, SCHAF and LOBA. PM10 levels were high (>50µg/m³) at all sites, highest at RINN. All three days were impacted by air masses from southeast Europe. On 26th an inversion in the height of 500-700m and high fog (Bauer et al., 2006) prohibited dilution of particulate matter and diminished insolation, respectively. HULIS_{AS} shares at RINN on 26th were remarkably high with 75% and uniformly low at SCHAF, KEND and LOBA (~30%), suggesting a dominant HULIS source at RINN due to higher HULIS_T and relative HULIS_{AS} levels. On 27th and 28th the inversion disbanded accompanied with slightly decreasing PM10 levels. Wind direction changed from southeast to northwest and the air masses from southeast traversed Vienna a second time (backward trajectories in Bauer et al., 2006). Coherently relative HULIS_{WS} levels increased considerably at SCHAF and KEND and slightly at RINN and LOBA. Still RINN showed highest HULIS_{AS} shares with 75% compared to 30% at the other Vienna sites, pointing to a dominant source.

In the region of Graz three meteorological episodes showed most diverging of HULIS composition (Table 11).

Table 11: Meteorological characteristics and PM10 burden at high relative HULIS_{AS} periods in Graz; ND...no data; surface wind directions, inversion situation, dominating PM10 sources are from Bauer et al. (2007a)

| Sampling site | Sampling date | Episode 1.1 | Episode 1.2 | Episode 2 | Episode 3 |
|----------------------------------|---|---|--|---|---|
| | | 6.-8.1. 2004 | 09.01. 2004 | 10.-11.4. 2004 | 29.-30.11. 2004 |
| DONB | HULIS _{WS} [µg C/m ³] | 1.49 | 2.67 | 1.60 | 1.40 |
| | HULIS _T [µg C/m ³] | 3.07 | 4.75 | 5.32 | 3.40 |
| | HULIS _{WS} /HULIS _T [%] | 49 | 56 | 30 | 41 |
| GRAS | HULIS _{WS} [µg C/m ³] | 0.71 | 2.83 | 1.01 | 0.67 |
| | HULIS _T [µg C/m ³] | 1.40 | 4.37 | 4.28 | 1.88 |
| | HULIS _{WS} /HULIS _T [%] | 51 | 65 | 23 | 36 |
| BOCK | HULIS _{WS} [µg C/m ³] | 1.61 | 1.62 | 0.79 | 0.87 |
| | HULIS _T [µg C/m ³] | 1.89 | 3.85 | 2.53 | 1.55 |
| | HULIS _{WS} /HULIS _T [%] | 85 | 42 | 31 | 56 |
| PM10 [µg/m ³] | | DONB & GRAS~75/BOCK 45 | DONB & GRAS~110/BOCK~90 | DONB 104/GRAS~90/B OCK~50 | DONB~75/GRAS~65/BOCK~40 |
| Surface wind direction/inversion | | SSO-SO/yes | S/no | calm/ slight inversion | NNO-O/yes |
| Dominating PM10 sources | | inorganic secondary/ wood smoke | inorganic secondary/ wood smoke | inorganic secondary/ Easter fires | wood smoke/ vehicular emissions |
| Characteristic | | low rel. HULIS _{AS} rural site | high rel. HULIS _{AS} rural site | high rel. HULIS _{AS} all sites | high rel. HULIS _{AS} urban sites |

Contrasting to Vienna highest absolute HULIS levels in these episodes were always found at the urban traffic impacted site DONB. Lowest HULIS_{WS} shares occurred in episodes with inversion, decoupling the background site BOCK from urban emissions (Table 11). Episode 1.1 from 7th to 9th January was characterised by a very stable inversion and air masses transported by surface near wind from the southeast, which are typically connected to long-range transported inorganic secondary aerosol and partly biomass smoke (Bauer et al., 2007a; Spangl et al., 2006). A very stable inversion layer trapped the secondary components and locally emitted PM in the Graz basin, reflected in higher urban and lower rural PM10 levels. HULIS_T levels at BOCK are rather high and consist of 85% HULIS_{WS} indicating local sources, thus freshly formed HULIS of minor importance. Contrasting the urban sites, impacted by a strong inversion, show HULIS_{WS} shares of ~50%, pointing to mixed influence of regional or long-range transported HULIS and local formation and/or emission. On the 9th of January (episode 1.2) the strong inversion disbanded and surface near wind from south transports heavily PM10 loaded air masses to the city, as can be seen on very high PM10 burdens at the background and urban sites. HULIS_T levels are raised to similar heights at all three sites. The major increase at

the urban sites is caused by HULIS_{WS} coherently leading to higher HULIS_{WS} shares than the days before. At BOCK the HULIS_{WS} levels remain on a constant level while HULIS_{AS} causes the major increase. Another filter pool that showed rather low HULIS_{WS} shares was sampled on 10th and 11th of April (episode 2) where traditional Easter fires caused explicitly high PM10 burdens in urban Graz (~100 µg/m³) and were doubling the PM10 levels at BOCK (Wonaschütz et al., 2009; Bauer et al., 2007a). The HULIS_T levels followed this trend. The HULIS_{WS} contribution was comparable low at the three sites with values between 23 und 31%, reflecting the regional influence of the open fires and confirms the consideration of low relative HULIS_{WS} levels of about 30% being typical for freshly emitted or formed HULIS.

Episode 3 (November 29th and 30th) is characterised by moderately high PM10 burdens and a strong inversion layer, similar to the situation in episode 1.1 in January. In contrast to episode 1.1 the dominating surface wind direction was NNE. Due to the strong inversion these air masses had no major influence on the urban sites. Chemical analyses (Bauer et al., 2007a) showed considerably low contributions of inorganic secondary aerosol and strong local contributions of vehicular emissions and wood smoke. These observations are in line with the lower HULIS_{WS} contributions at the urban sites in episode 3 compared to episode 1. Higher relative shares of HULIS_{WS} at BOCK reflect the higher share of long-range transport air masses connected to higher abundance of secondary inorganic aerosol at BOCK.

A multitude of factors, such as topographical situations and meteorological conditions, the source region and trajectory of air masses and the strength and type of emission sources influence the quantity and quality of atmospheric particulate matter and pose a multidimensional puzzle (Pöschl, 2005; Spangl et al., 2006). Results from combining observations of HULIS levels and composition with meteorological conditions from periods with well understood origin and chemical composition of PM10 from the AQUELLA project (Bauer et al., 2006, 2007a and 2007b), indicate that the relation of HULIS_{WS} and HULIS_{AS} is linked to the age of HULIS, as HULIS_{WS} shares to the total fraction of HULIS of about 30% and beyond were observed at a heavily biomass burning impacted episode in Styria. Meteorological observations and source composition would as well support spatial and temporal variations of HULIS compositions in Vienna. Since the average contributions are remarkably similar in the three investigated regions and neither seasonal trends nor tendency for favoured enrichment of one of the fractions at sites with urban or rural characteristics, respectively, were observed, the type of source seems to be of minor importance for the ratio of HULIS_{AS} and HULIS_{WS}. However, since the present data consists of sample pools with highly varying temporal resolution and the two HULIS fractions were analysed separately for about 80% of the samples, further investigations would be necessary, to gain more information on the variation of HULIS composition. It is possible that the appearance of the alkaline soluble HULIS is linked to other sources

than their water soluble counterparts. In the case of the investigated sites at the three cities however it seems that the atmospheric age is of higher importance.

7.3.7 Meteorological Influence on the Seasonality of HULIS_T

As discussed in section 7.3.6, beside emissions of air pollutants, thus their actual source strength, meteorological conditions have a major influence on immission concentrations (e.g. Bauer et al., 2006). Dilution and transport in the atmosphere as well as chemical transformation and removal of particulate matter are directly affected by various meteorological influencing factors (Pöschl, 2005). For primary emitted pollutants (in case of particulate matter e.g. Si, Ca, EC, heavy metals, levoglucosan) unfavourable dispersion conditions, such as stable temperature layers and low wind speeds, result in high immission concentrations near to the surface (Spangl et al., 2006). Generally spoken summer months are characterised by better atmospheric mixing due to higher solar radiation leading to better mixing of surface near layers and thus to more rapid dilution of pollutants. High-pressure conditions in winter are connected to specifically unfavourable weather conditions, especially if connected to import of cold, continental air masses (Spangl et al., 2006). Air masses passing regions in Mideast and Eastern Europe with high emissions enable long range-transport over several hundred kilometres and adversely influence immission concentrations in Austria. In contrast oceanic air masses are linked to better dispersion conditions with higher wind speeds. Even if passing regions with high emissions in Western and central Europe they are taking along relatively low amounts of pollutants leading to lower shares of long range transported PM₁₀ (Spangl et al., 2006). Concentration levels of secondarily formed aerosol are highly impacted by meteorological conditions. The time period available for their formation as well as accumulation plays a major role for their atmospheric abundance (Gelencsér, 2004).

One way to assess the influence of meteorological phenomena on immission concentrations is to introduce a dilution tracer (Limbeck et al., 2004; Lukacs et al., 2007). Such an aerosol component can be a primarily emitted analyte of known origin with constant source strength throughout a seasonal cycle. Thus its concentration is to large extents varying according to the atmospheric dilution potential. Limbeck et al. (2004) established palladium as a tracer for atmospheric dilution at two heavily traffic impacted sampling sites in Carinthia and Salzburg. They assigned about 20% of the concentration increase of PM₁₀ and EC in the cold season to meteorological unfavourable dispersion conditions and between 22 and 50 % to higher source strength and formation rates.

The present work processes data from elemental carbon to establish a dilution tracer. Elemental carbon in atmospheric aerosol is in general the result of incomplete combustion of fossil or biogenic fuel. In Europe the transport sector is accountable for the major part of EC emission. Together with residential combustion of coal and bio fuel these sectors are responsible for over 90% of EC emissions (Bond et al., 2004). In Vienna, Graz and

Salzburg coal plays a minor role concerning residential heating, only used by 1 and 3% of the households (Statistics Austria, 2004). Whereas this is the case as well for wood in Vienna (1%), 25 % of the households in Styria and 20% in Salzburg use wood for domestic heating purposes (Figure 57, based on data from Statistics Austria, 2004). The low impact of oil or coal combustion in the urban Vienna region was as well confirmed by investigating the seasonality of trace metals related to these sources (Puxbaum et al., 2004) and by investigating enrichment factors and “urban impact” of mineral components and trace metals. It was confirmed that arsenic, a main tracer for coal combustion, at inner city sites in Vienna is mainly stemming from regional sources outside the city or long range transports (Limbeck et al., 2004). Following the results of these studies (Puxbaum et al., 2004; Limbeck et al., 2004; Bond et al., 2004) and considerations based on fuel types used in Austria (Statistics Austria, 2004), elemental carbon emitted by diesel engined cars (EC_D) poses a suitable atmospheric dilution tracer at traffic impacted urban sites- constant source strength of EC_D provided. EC_D was calculated from measured EC by subtracting the EC shares stemming from wood combustion after:

$$EC_D = EC - EC_W \text{ (Bauer et al., 2006)} \quad \text{Equation 1}$$

$$EC_W = PM_{10W} * 0.15 \text{ (factor derived by Schmidl et al. 2008a)} \quad \text{Equation 2}$$

$$PM_{10W} = \text{levoglucosan} * 10.7 \text{ (factor derived Schmidl et al. 2008a)} \quad \text{Equation 3}$$

$$EC_D = EC - 1.6 \times \text{levoglucosan} \text{ (Bauer et al., 2006 and references therein)} \quad \text{Equation 4}$$

The factors for converting levoglucosan levels in ambient air to the mass of wood smoke (PM_{10W}) and EC stemming from wood combustion (EC_W) were derived by Schmidl et al. (2008a) by establishing emission profiles for closed stoves stoked with wood types commonly used in Austria. This approach does not allow the differentiation between EC stemming from diesel vehicles and other fossil fuel combustion sources such as industrial coal combustion. Therefore only the urban traffic impacted sites were included in these considerations because emissions from the transport sector are responsible for the largest part of atmospheric EC levels (Puxbaum et al., 2004; Limbeck et al., 2004; Bond et al., 2004).

Urban traffic impacted sites were selected from Vienna, Graz and Salzburg, where EC and levoglucosan data for an entire seasonal cycle was available. Monthly averages of EC_D revealed quite symmetric devolution of EC_D in Vienna and Graz with lower EC_D values in summer and higher during the cold month, reflecting the lower dilution potential of the atmosphere (Figure 56). The site in Salzburg (RUDO) showed a steady increase of monthly averaged EC_D , thus might implicate a change of source strength and therefore was restrained from calculations.

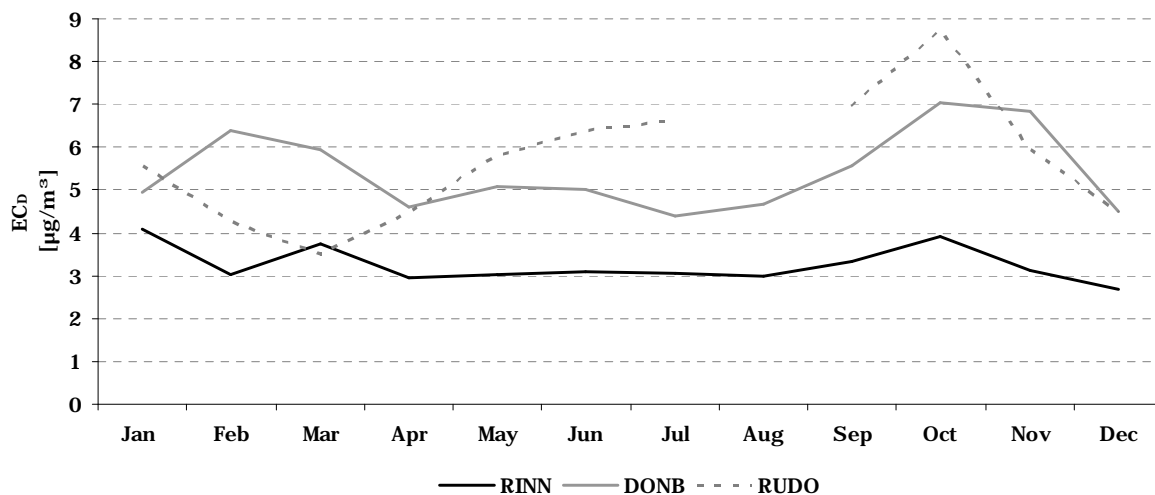


Figure 56: Calculated elemental carbon stemming from diesel vehicles (EC_D), monthly averages, urban traffic impacted sites, Vienna, Graz and Salzburg, 2004.

7 A three City Study: Seasonal Behaviour and possible Origin of atmospheric HULIS

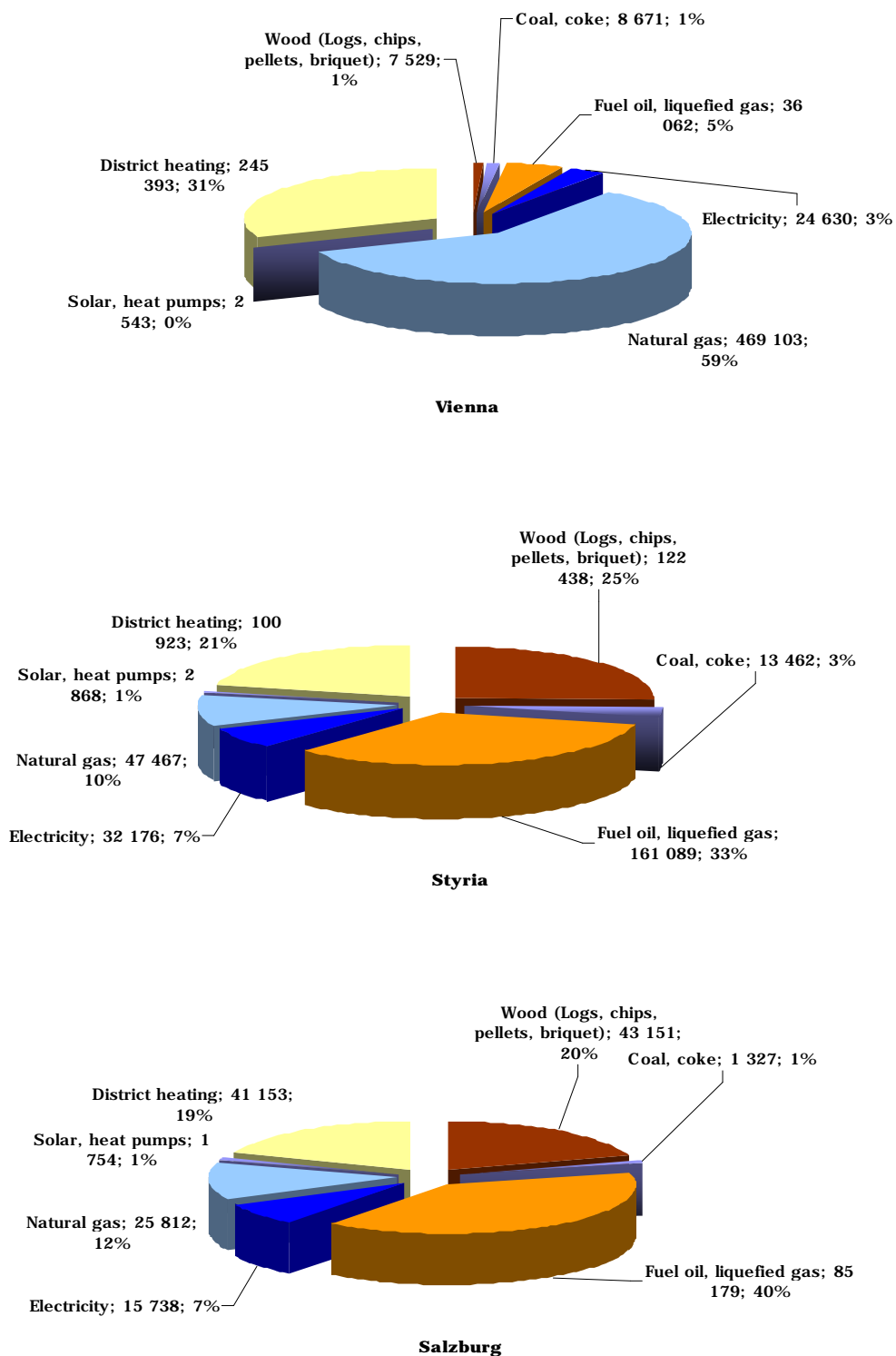


Figure 57: Fuel types used for domestic heating, 2004; numbers....absolute number of households using the respective heating type (based on data from Statistics Austria, 2004; statistik.at/web_de/statistiken/energie_und_umwelt/energie/energieeinsatz_der_haushalte/index.html).

EC concentrations were enriched in winter about a factor of 1.2 and 1.4, for the site in Vienna and Graz, respectively (Table 12).

Table 12: Ambient concentrations of elemental carbon, levoglucosan and HULIS_T at two traffic impacted sites in Vienna and Graz, 2004

| Urban traffic impacted sites | | | | | | |
|--|-------------|--------|---------------------|-----------|--------|---------------------|
| | Vienna-RINN | | | Graz-DONB | | |
| | Summer | Winter | Winter/summer ratio | Summer | Winter | Winter/summer ratio |
| EC [$\mu\text{g}/\text{m}^3$] | 3.10 | 3.79 | 1.2 | 4.78 | 6.69 | 1.4 |
| Levoglucosan [$\mu\text{g}/\text{m}^3$] | 0.03 | 0.32 | 11.7 | 0.05 | 0.88 | 17.0 |
| EC _D [$\mu\text{g}/\text{m}^3$] * | 3.05 | 3.27 | 1.1 | 4.70 | 5.28 | 1.1 |
| HULIS [$\mu\text{g C}/\text{m}^3$] | 0.43 | 1.17 | 2.7 | 0.66 | 1.72 | 2.6 |

* EC_D was calculated after Bauer et al. (2006).

Wintry HULIS levels increased by 172 and 161 % at the urban traffic impacted sites in Vienna and Graz. After normalisation of HULIS_T concentrations with EC_D concentrations, the calculated winter increase of 154 % (RINN) and 132 % (DONB) reflects the contribution of source emissions for HULIS_T and their precursor substances and higher formation rates. Only a minor part of the increase can be attributed to unfavourable meteorological conditions (Table 13).

Table 13: Assignment of measured winter increase of HULIS_T concentration to higher source emissions/ formation rates and meteorological influences

| Increase of HULIS concentrations (Summer-winter) | | |
|---|-------------|-----------|
| | Vienna-RINN | Graz-DONB |
| Total increase [%] | + 172 | + 161 |
| Source emissions/ formation rates [%] | + 154 | + 132 |
| Meteorological changes [%] | + 18 | + 29 |

Expressed as share to the winter enrichment factor, meteorological aspects only contributed to the overall HULIS_T increase with 7% at RINN (Vienna) and 13% at DONB (Graz) (Figure 58). Higher influence of meteorological conditions on winter enrichment of HULIS in Graz consistently reflects the topographical and meteorological situation in the two regions, Vienna being a better ventilated area and Graz situated in a basin with frequently occurring inversion episodes during the cold seasons (for details see Bauer et al., 2006 and 2007a).

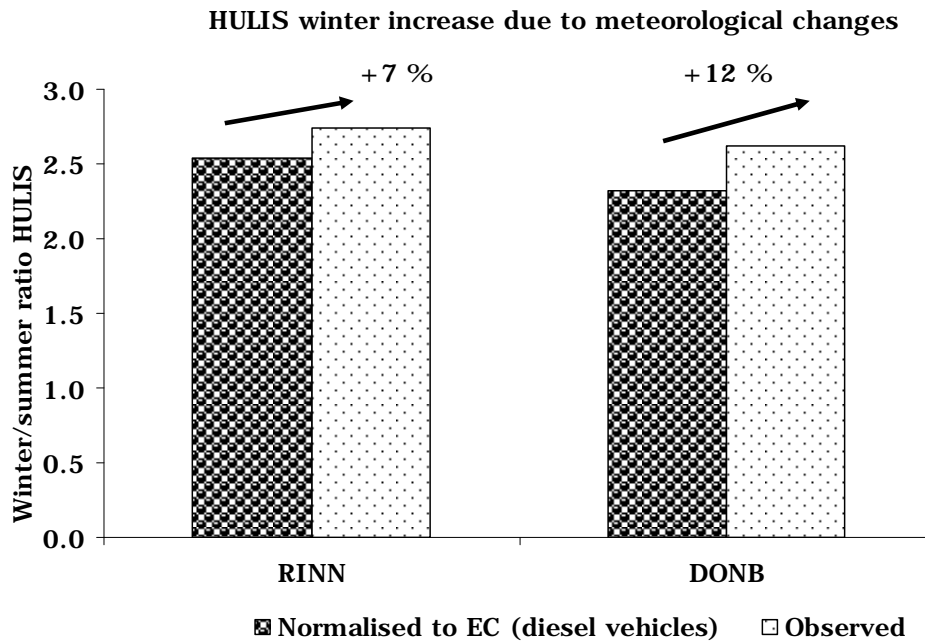


Figure 58: Influence of meteorological conditions on winter enrichment of HULIS_T at the urban traffic impacted sites in Vienna and Graz.

The meteorological impact on winter enrichment of EC was as well estimated with the same approach to prove its suitability. Observed EC levels increased by 22 and 44 %, where approximately one third can be assigned to meteorological changes (Table 14). The main increase during the cold season after this approach resulted from wood smoke, which contributes to wintry EC levels with 15 and 32 %. These results are in excellent agreement with the results from Limbeck et al. (2004) who assigned one third of the EC winter increase at a traffic impacted site in Salzburg to meteorological changes by using palladium as dilution tracer. The approach to use EC_D as a proxy for atmospheric dilution potential thus seems suitable for the traffic near sites in Vienna and Graz.

Table 14: Assignment of measured winter increase of EC levels to higher source emissions and meteorological influences; Meteorological changes calculated from EC_D winter/summer ratio

| Increase of EC concentrations (Summer-winter) | | |
|--|-------------|-----------|
| | Vienna-RINN | Graz-DONB |
| Total increase [%] | +22 | +44 |
| Source emissions | +15 | +32 |
| Meteorological changes [%] | +7 | +12 |

7.3.8 Estimations on the primary Emissions of HULIS_T

As reviewed by Graber and Rudich (2006), potential origins of HULIS in the atmosphere are manifold, including primary terrestrial (Simoneit, 1980) and marine sources (Cini et al., 1994; Cini et al. 1996) and biomass burning (Mukai and Ambe, 1986; Facchini et al., 1999; Zappoli et al., 1999; Mayol-Bracero et al., 2002; Schmidl et al., 2008 b). Most of the studies concerning the origin of atmospheric HULIS have proposed secondary formation pathways (condensation, reaction, oligomerisation etc.) via heterogeneous (Kalberer et al., 2004, Limbeck et al., 2003; Iinuma et al., 2004; Jang et al., 2002) and multiphase (Gelencsér et al., 2002 and 2003; Hoffer et al., 2004) reactions including precursors and formation pathways such as polar, low molecular weight degradation products of organic debris in soil and other anthropogenic sources, aromatic mono/diacids, terpenes, 1,3,5-Trimethylbenzene, glyoxal and acid catalyzed reactions on soot to name a few. Since a variety of possible precursor and formation mechanism for atmospheric HULIS are reported in literature it is a common position that HULIS might be of primary as well as of secondary origin. This subchapter presents estimations of possible primary HULIS_T emissions based on quantification of HULIS and main and unique tracer components analysed in immission and source samples. HULIS carbon (as sum of HULIS_{AS} and HULIS_{WS}) contributions in PM₁₀ samples from vehicular exhaust, emissions from small stoves operated with various fuels, cooking fumes, open fire and redispersed dust and soil samples have been quantified. A HULIS/tracer-source ratio (HTSR), together with ambient tracer levels, was processed to estimate potential primary emissions of HULIS. The experimental set-up, sampling, weighing and analysis of other species than HULIS_T were conducted and published by the authors listed in (Table 15, Table 16) in the scope of the AQUELLA/AQUELLIS projects.

7.3.8.1 HULIS abundance in source emissions and the establishing of HULIS-tracer source ratios (HTSR)

To our best knowledge the present work is the first reported in literature that utilises ratios of HULIS and selected tracer compounds in source emissions to estimate primarily emitted HULIS in airborne PM₁₀. As Gelencsér (2004) summarised and discussed, primary aerosol particles are generally understood to be those particles which are released directly from various sources and emission processes. Due to internally or externally mixed particles e.g. stemming from condensing of semi-volatile species on inorganic or organic particles the actual definition is not as simple as that. Traditionally, in addition to particulate organic matter, primary organic aerosols were understood to be those which are released into the gas phase by the sources then partition into the aerosol phase without undergoing gas-phase chemical reactions in the atmosphere. Conversely, compounds which are no released directly but formed in photochemical reactions from precursor prior to partitioning into the aerosol phase are considered to be secondary

aerosol components (Gelencsér, 2004 and references therein). Emissions from combustion processes pose an exception if secondary processes are very fast and take place seconds away from the combustion. In that case the formed particles are as well considered of primary origin. In the present work primarily emitted HULIS ($HULIS_{prim}$) is defined as the amount of HULIS derived from multiplying HULIS tracer source ratios (HTSR) with ambient tracer concentrations. PM10 sampling for solid fuel combustion (Schmidl et al., 2008c), vehicular exhaust (Jankowski et al., 2009a and 2009b) and cooking emissions (Puxbaum et al., 2006) was conducted in a time frame from 60 seconds (solid fuel) up to several minutes (vehicular emissions and cooking). Sampling in all combustion experiments included the dilution and cooling of the exhaust to minimize sampling artefacts. Sampling thus represents conditions that are coherent with the definitions of primarily emitted particles and pose a good fundament on estimations on primarily emitted $HULIS_T$.

$HULIS_T$ related carbon was quantified in samples from combustion experiments (biomass, coal, waste, open air burning), soil and street dust and dust from construction sites, cooking activities, vehicular exhaust (diesel and gasoline engined vehicles) and dusts emitted by farming and craft activities (for details on sampling see section 5.2 and references therein). Contributions of $HULIS_T$ carbon to PM10 from source emissions are displayed in Table 15 and Table 16 and gave some interesting findings. Highest contributions of $HULIS_T$ carbon to PM10 have been observed in samples from garden fires (~20 %) whereas emissions from wood combustion in closed stoves consisted of $HULIS_T$ carbon in comparatively low but considerable quantities (0.6 to 9.8 %). Emissions from coal combustions and cooking activities revealed $HULIS_T$ carbon contributions to total PM10 of ~6 % and from below the LOD up to 0.7 %, respectively. The relatively high amount of $HULIS_T$ carbon in emissions from barbecuing of 7.3 % is explained by the use of wood char coal as fuel and was not integrated in the HULIS-tracer source ratio (HTSR) calculations. Vehicular exhaust from diesel fuelled cars showed $HULIS_T$ carbon contributions of 0.9 and 0.8 % to PM10. Surprisingly high $HULIS_T$ carbon contributions were discovered in vehicular emissions from diesel vehicles without particle filters (1.3-13.4 %) and of gasoline engined cars (6.7%) (Jankowski et al., 2009a). The detection of $HULIS_T$ in diesel vehicular emissions was a rather surprising finding since its atmospheric abundance up till now is mostly connected to biomass burning and the secondary formation of various gaseous precursors (Graber and Rudich, 2006). However, the high shares of $HULIS_T$ in PM10 from particle filter equipped diesel vehicles and gasoline-engined cars is inline with the findings of Jankowski et al. (2009a) were samples of both vehicle types showed surprisingly resembling thermograms, revealing high shares of non-volatile organic material. Recently, Mladenov et al. (2011) found that the water-soluble fraction of diesel soot was absorbing in the UV range between 250 and 300 and had fluorescent properties, which made them suggest that fossil fuel burning should be

included in considerations about sources of atmospheric WSOC in winter time. Mimicking diesel engine conditions Adelhelm et al. (2008) investigated the formation of large nitrated or oxygenated and polar reaction products of PAH with m/z ratios up to 650. These rather polar compounds are increasingly investigated since oxygenated PAHs are considered to be more toxic than their parent PAHs, because of their direct mutagenic potential, whereas PAHs require enzymatic activation (Walgraeve et al., 2010 and references therein). In contrast to PAHs, which are emitted directly from combustion processes, the sources of oxygenated PAHs emission in the atmosphere can be both, direct introduction and tropospheric conversion of PAHs or other precursor molecules. Direct emission of both gaseous and PM associated oxygenated PAHs proceeds through incomplete combustion processes of a wide variety of materials. Major sources are the combustion of domestic waste and biomass and plant. They are also constituents of diesel particulate emissions and are emitted during gasoline combustion, production of charcoal and coal burning (Walgraeve et al., 2010). Although reports on their physical and chemical properties are scarce, their polarity, molecular weight and aromatic structure make them possible candidates for a subgroup of HULIS and/or their precursors.

The abundance of HULIS_T in emissions from anthracite and lignite combustions appeared in considerable heights appearing at similar levels as in emissions from experiments with wood types commonly used in Austria for space heating (Table 15). As discussed in section 7.3.7 coal plays a minor role in domestic heating in Austria (Figure 57), but lignite and anthracite are still of major importance in energy production. Figure 59 displays a (non-exhaustive) map of coal power plants in Europe. Concerning that immediate Austrian neighbouring countries still cover substantial fractions of their energy demand with coal power plants, coal combustion very likely poses a non-negligible source for HULIS_T.

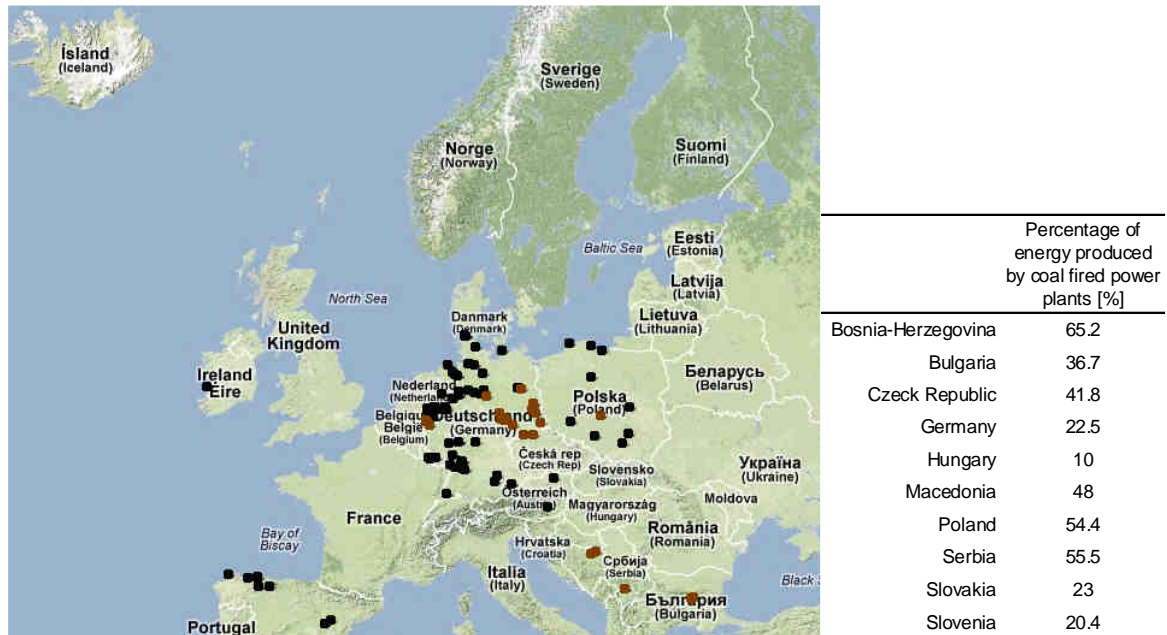


Figure 59: Non-exhaustive map of anthracite- (black spots) and lignite-fired (brown spots) power plants (from www.wikienergy.de; ©2013 GeoBasis DE/BG and Google ©2009) (left) and percentage of energy produced by coal power plants in selected European countries (source: International Energy Agency (IEA): Energy Statistics Division 08/2011, © OECD/IEA; British Petroleum (BP): Statistical Review of World Energy 2011) (right).

7 A three City Study: Seasonal Behaviour and possible Origin of atmospheric HULIS

Table 15: Contribution of HULIS carbon to PM10 from source emissions, part 1

| Source type | Details | HULIS C | | Reference | |
|--------------------|----------------------------|--------------------|--------|-----------------------|---|
| | | % PM10 | n* | | |
| Biomass combustion | Tiled stove | Beech | 2.6 | 8 | Puxbaum et al., 2006 Schmidl et al., 2008a |
| | | Spruce | 1.1 | 10 | |
| | | Briquet | 3.0 | 6 | |
| | | Oak | 5.8 | 4 | |
| | | Larch | 0.6 | 3 | |
| | | Painted fence | 0.8 | 3 | |
| Coal combustion | | Brown coal | 5.3 | 1 | Schmidl et al., 2008c |
| | | Black coal | 5.7 | 2 | |
| Biomass combustion | Stove A | Beech | 4.4 | 1 | |
| Waste burning | | Beverage carton | 10.0 | 1 | |
| | | Waste paper | 2.7 | 2 | |
| Biomass combustion | Stove B | Hornbeam | 3.5 | 2 | |
| | | Beech | 2.9 | 3 | |
| | | Briquet | 2.0 | 1 | |
| | | Ash tree | 1.7 | 2 | |
| | | Oak | 1.3 | 1 | |
| | Stove C | Oak | 4.7 | 2 | |
| | | Briquet | 3.5 | 2 | |
| | | Beech | 6.1 | 1 | |
| | | Pear | 9.8 | 2 | |
| | | Cherry tree | 7.7 | 2 | |
| | | Elder | 5.3 | 2 | |
| | | Maple | 5.1 | 2 | |
| | | Mulberry | 5.8 | 2 | |
| | | Birch | 9.4 | 1 | |
| | | Peach | 6.9 | 1 | |
| | | Alder | 4.5 | 2 | |
| | | Sweet chestnut | 6.7 | 2 | |
| | | Pine | 2.3 | 2 | |
| | | Leaves (open-air) | Burn 1 | 21.2 | 1 |
| Burn 2 | 18.5 | | 1 | Schmidl et al., 2008c | |
| Vehicular exhaust | Diesel vehicle without DPF | Passenger car | 0.9 | 4 | Jankowski et al., 2009a |
| | | Light duty vehicle | 0.8 | 1 | |
| | Diesel vehicle with DPF | Passenger car | 13.4 | 1 | |
| | | Light duty vehicle | 1.3 | 1 | |
| | Gasoline | Passenger car | 6.7 | 1 | |

n*...number of samples

Table 16: Contribution of HULIS carbon to PM10 from source emissions, part 2

| Source type | Details | HULIS C | | Reference | |
|--------------------|-------------|------------------------------------|-------|-----------|----------------------|
| | | % PM10 | n* | | |
| Cooking | Roasting | Pork, sunflower oil | 0.1 | 1 | Puxbaum et al., 2006 |
| | | Pork, rapeseed oil | 0.2 | 3 | |
| | | Pork, without oil | 0.1 | 2 | |
| | Frying | Schnitzel sunflower oil | <LOD | 1 | |
| | | Schnitzel rapeseed oil | 0.5 | 2 | |
| | Barbecue | Mixed meet blends | 7.3 | 1 | |
| | Deep-frying | French fries sunflower oil | < LOD | 1 | |
| | | French fries rapeseed oil | 0.7 | 3 | |
| Farming | Soil | Vineyard | <LOD | 1 | |
| | | Chicken house | 1.5 | 2 | |
| | Dust | Oat harvest | < LOD | 1 | |
| | | Lawn mowing | < LOD | 2 | |
| Crafts | Carpentry | Suction dust | 0.4 | 1 | |
| | | Workshop dust | < LOD | 1 | |
| | | Polishing dust | 0.4 | 1 | |
| | | Paint dust | < LOD | 2 | |
| | | Wood dust, grinding | < LOD | 1 | |
| | | Wood dust, power house | 0.4 | 1 | |
| Construction sites | Vienna | Dust, A21 Gieshübel bridge, Vienna | 0.5 | 2 | |
| | | Dust, U2, Ausstellungsstrasse | 0.2 | 1 | |
| | | Saw dust, Ausstellungsstrasse | 0.7 | 1 | |
| | | Dust, U1, Kagranerplatz | 0.1 | 1 | |
| | | Cement, U1, Kagranerplatz | < LOD | 1 | |
| | | Dust, Elektroititut | < LOD | 1 | |

n*...number of samples

Cooking activities are known to constitute a very efficient aerosol source (Rogge et al., 1991) and can pose a non-negligible source of atmospheric particulate matter (Bauer et al., 2006; Srimuruganandam et al., 2012). HULIS_T carbon was found in relatively low amounts in PM10 from cooking emissions. Similarly low levels were found in dusts from wood-processing business and construction sites.

The estimations on primary HULIS levels in ambient atmosphere from HTSR require a unique or main tracer for a specific source and the main contribution of this source to atmospheric tracer levels. The considerations in the following lead to selection of diesel vehicle exhausts, domestic wood stove emissions and cooking activities for investigations on primary HULIS estimations.

On-road and off-road transport together with residential heating (biomass and coal) are responsible for more than 90% of elemental or black carbon emissions in Europe (Bond et al., 2004). Within the transport sector diesel vehicles are the major EC source. As discussed in section 7.3.7 residential heating in Vienna with solid fuels is of minor importance, where 1% of the households use wood or coal for residential heating. In Graz

and Salzburg wood comprises 25 and 20% and coal 1 and 3%, respectively, of the domestic heating fuels in 2004 (Statistics Austria, 2004). Ambient EC levels stemming from diesel vehicle emissions are gained by subtracting EC stemming from wood smoke with:

$$ECD = EC - 1.6 \times \text{levoglucosan} \quad (\text{Bauer et al., 2006 and references therein}) \quad \text{Equation 4}$$

and are further processed for the estimations on primarily emitted HULIS by diesel vehicles ($HULIS_{\text{Prim, DVE}}$). Due to uncertainties of the coal combustion tracer arsenic in source samples EC could not be corrected for EC stemming from coal combustion thus EC_D may partly cover EC stemming from residential coal combustion. Whereas residential coal combustion for the before mentioned reasons is of minor importance, industrial activities such as steel or energy production might contribute to ambient EC levels. Especially emissions from coal power plants in Eastern Europe, not equipped with state-of-the-art fuel gas cleaning technology, might influence EC levels via the long-range transport of air masses. Calculated primary emissions stemming from diesel vehicles therefore pose a lower estimate.

Ratios of HULIS carbon and EC in samples of vehicular exhaust varied between 0.012 and 1.94. Lowest factors occurred in emissions from diesel vehicles without particle filters whereas factors in emissions from particle filter equipped vehicles and gasoline vehicles were higher by several orders of magnitude. Due to the composition of the Austrian car fleet (details in Jankowski et al., 2009a), which consists of 50 % diesel vehicles which in 2004 to a large majority were not equipped with particle filters (ARBÖ, 2004), the HTSR of 0.015 was chosen for calculations. To our best knowledge no other study reported direct quantification of $HULIS_T$ in vehicular exhaust, but calculations from ratios of $HULIS_T$ carbon and EC from immission samples from a tunnel study reported by El Haddad et al. (2009) revealed very good agreement with the factor in the present study. Factors calculated from results from El Haddad et al. (2009) in PM10 and PM2.5 were 0.02 and 0.015, respectively.

For estimating the contribution of wood smoke to primary HULIS emissions, source ratios of HULIS carbon and levoglucosan appearing in exhausts from stoves were chosen, since it can be assumed that most particulate matter, thus levoglucosan signals, related to wood combustion is generated by tiled wood stoves for domestic heating in Austria (Figure 61). Larger biomass fuel plants for district heating and cogeneration plants are almost exclusively equipped with precipitators or other dust collector units with efficiency factors above 90 % concerning particles smaller than 10 μm (Scheuch, 2013; FGW, 2011). Even if the relative share of wood consumption as split logs for domestic heating decreases from 50 % to 36 % (Figure 61), the absolute wood consumption for this purpose stagnates, thus domestic heating still being the dominant levoglucosan source in Austria.

The so calculated contributions of biomass burning though might underestimate primary HULIS, taking in account that the HULIS levoglucosan ratios from wood stove emissions (HTSR=0.33) and garden leave burning (HTSR=9.32) show dramatic differences. Also higher ratios are found in open wood burning (1-2.0) as calculated from Mayol-Bracero et al. (2002). Open fires in and outside Austria (Figure 60) may as well raise locally primary HULIS levels during the warmer season compared to calculated values. HULIS carbon to levoglucosan ratios in wood stove emissions appeared to be lower for softwoods (HTSR average =0.22) than for hardwoods (HTSR average=0.59). According to this, a weighed HTSR average for wood stove emissions was calculated, considering a softwood:hardwood ratio in Austrian domestic fuel use of approximately 70:30 (Schmidl et al., 2008a).

As mentioned before, HTSR obtained from coal combustion (with the main tracer arsenic) turned out to be not suitable for primary HULIS estimations resulting in levels about four times higher than total HULIS concentrations, since arsenic compounds emitted by coal combustion could not be fully and reproducibly captured on the filters due to their rather high volatility (Pacyna, 1987; Bauer et al., 2006). Since nonanal, a tracer for cooking emissions (e.g. Bauer et al., 2007a and references therein), was analysed only in a small set of samples, cooking emissions were not involved in the general considerations on the seasonality of HULIS_{Prim}. Though, punctual insights on possible primary emissions of HULIS from cooking activities revealed small, though non-negligible, contributions.

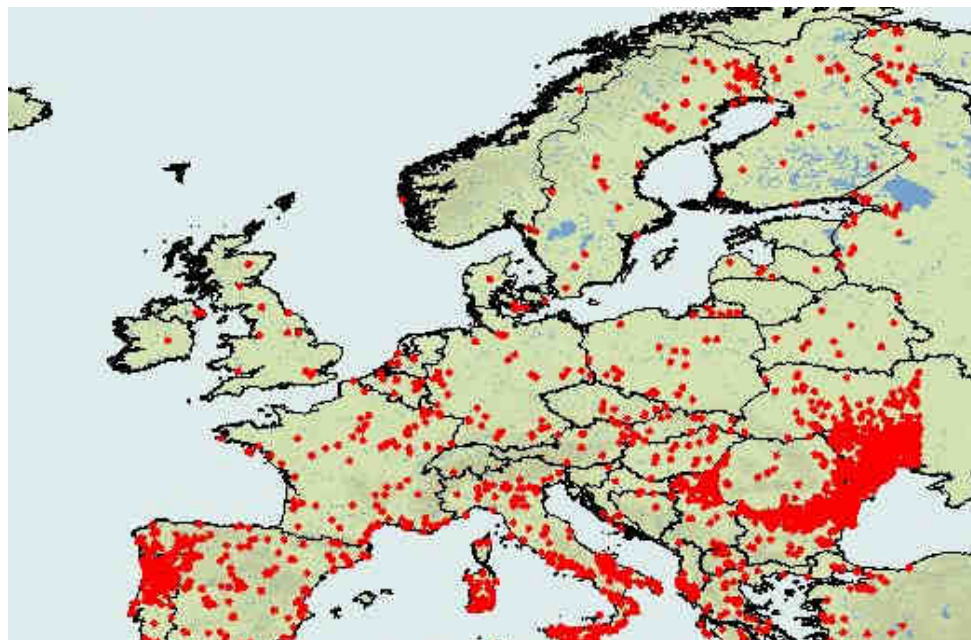


Figure 60: Open fires detected by MODIS fire monitoring satellites, July 2005 (from: <http://firemaps.geog.umd.edu>).

7 A three City Study: Seasonal Behaviour and possible Origin of atmospheric HULIS

Table 17: HULIS-Tracer source ratios (HTSR), bold numbers were applied for estimations on primary HULIS emissions

| Source type | HTSR | Tracer |
|------------------------------|---------------------------------|--------------|
| Wood combustion (stove) | 0.33 | Levoglucosan |
| Leave burning (open fire) | 9.32 | Levoglucosan |
| Coal combustion | $2.65 * 10^3$ | As |
| Diesel vehicles (without PF) | 0.015 | EC* |
| Cooking | $5.84 * 10^3$ | Nonanal |

* ambient levels of EC were corrected by subtraction of EC stemming from wood combustion and resulting EC_D levels were used for ambient estimations of $HULIS_{Prim}$

Derived HTSRs are depicted in Table 17 and ambient levels of $HULIS_{Prim}$ were calculated after $c_{HULIS, primary} = HTSR \times c_{Tracer, ambient}$ (Equation 5).

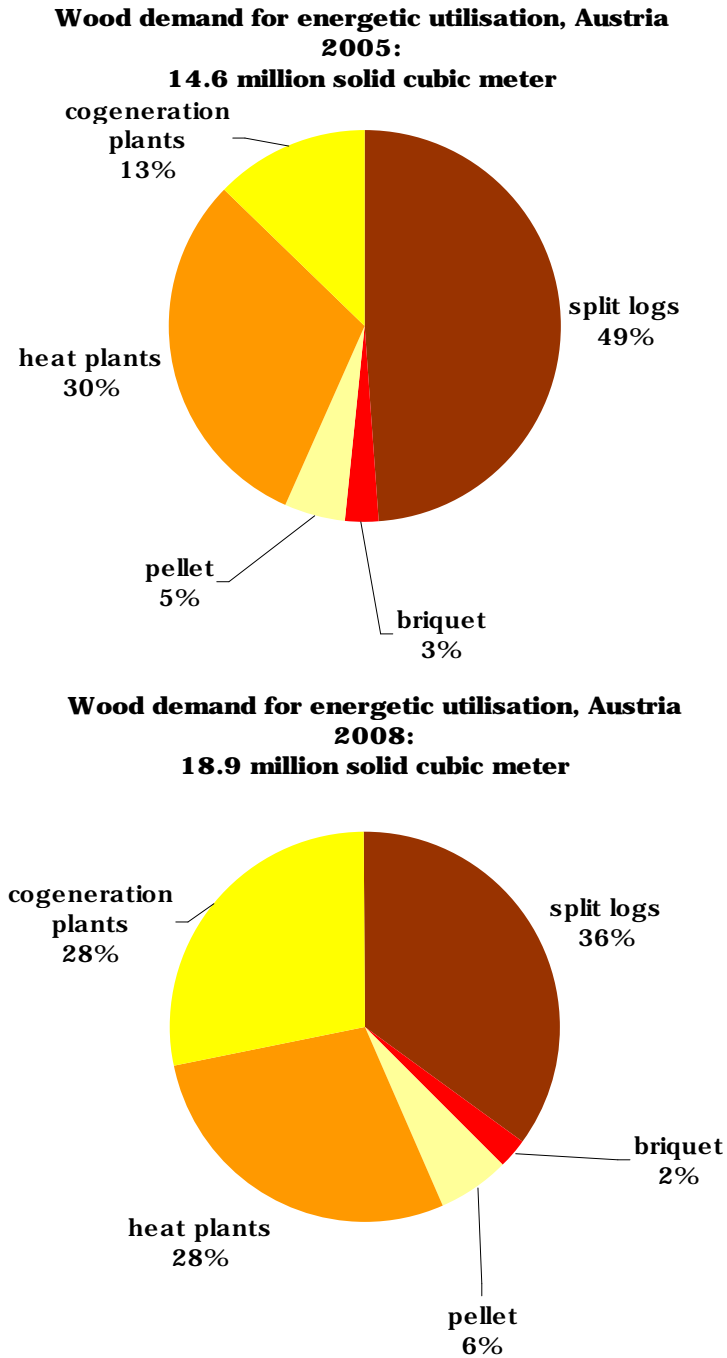


Figure 61: Wood demand for energetic use, Austria 2005 and 2008 (from <http://lebensministerium.at>).

7.3.8.2 Estimations on HULIS_T emitted primarily by Diesel Vehicles, Wood Stoves and Cooking Activities

Potential primary emissions of HULIS_T by diesel engined cars (HULIS_{Prim,DVE}) and wood stoves (HULIS_{Prim,WSE}) were calculated on seasonal averages. The main tracer for cooking emissions, nonanal (Bauer et al., 2006 and references therein), was analysed in a smaller set of samples and is not included in annual and seasonal averages. However, where existing data allowed the calculation of monthly averages of HULIS_T directly emitted by emissions from cooking activities (HULIS_{Prim,COO}), contributions to total HULIS_T ranged between 0.2 and 3 % in Vienna, Graz and Salzburg. In single sample pools cooking emissions could contribute up to 7 % (Figure 62) to measured ambient HULIS_T levels.

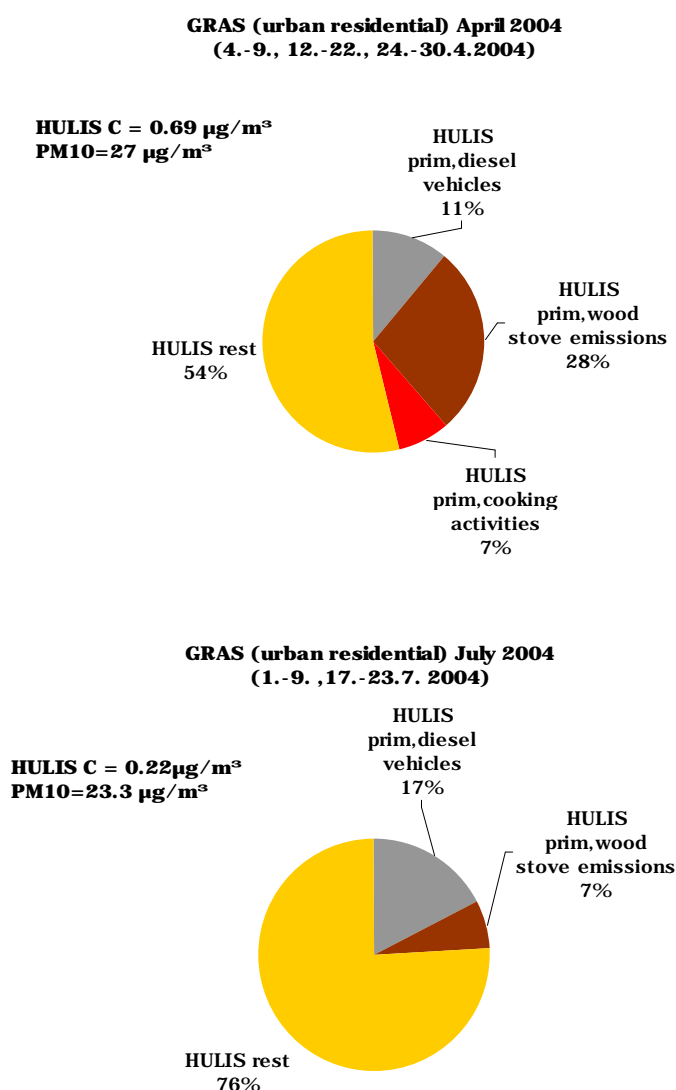


Figure 62: Calculated contributions of primarily emitted HULIS_T; HULIS_{rest} is the difference of HULIS_{measured} and the sum of HULIS_{Prim,WSE+DVE}

Primary HULIS emissions from diesel vehicles, cooking activities and wood stove emissions can contribute up to 46% of measured ambient $HULIS_T$ levels at the urban residential site in Graz in April. In July still considerable contributions of 24% were estimated.

Concerning Vienna and the regions of Graz and Salzburg, annual averaged contributions of calculated primary HULIS emitted by wood stoves and diesel engine vehicles ($HULIS_{prim,WSE+DVE}$) to total HULIS (measured) ranged from 7 % at the urban fringe sites in Vienna to 25 % at the heavily traffic impacted site in Salzburg, depicted in Figure 63. Comparison of the three cities revealed lowest $HULIS_{prim,WSE+DVE}$ contributions in Vienna (7-14%) and almost 2 times higher contributions in Graz and Salzburg with 13-23 % and 12-25 %, respectively. Highest contributions of $HULIS_{prim,WSE+DVE}$ were found at urban traffic impacted sites in Vienna and Salzburg and the urban residential site in Graz. In Vienna and the urban traffic impacted sites in Graz (DONB) and Salzburg (RUDO), HULIS primarily emitted by diesel vehicles contributed in similar or higher fractions as HULIS primarily emitted from wood stoves. The urban residential and rural sites in Salzburg and Graz revealed 2 to 3 times higher relative shares of $HULIS_{prim,WSE}$ to total HULIS.

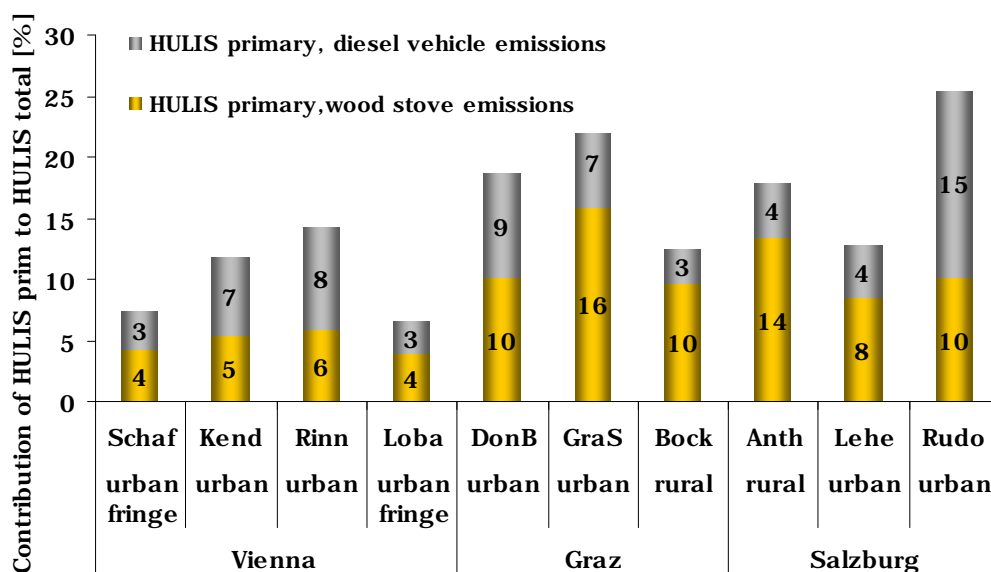


Figure 63: Annual averaged contributions of calculated primary HULIS from wood stove emissions ($HULIS_{prim,WSE}$) and Diesel vehicle emissions ($HULIS_{prim,DVE}$) to measured total HULIS; Vienna, Graz and Salzburg 2004.

Seasonal averages (Figure 64) reveal that up to one third of atmospheric HULIS might be of primary origin, with maximum values occurring during fall or winter.

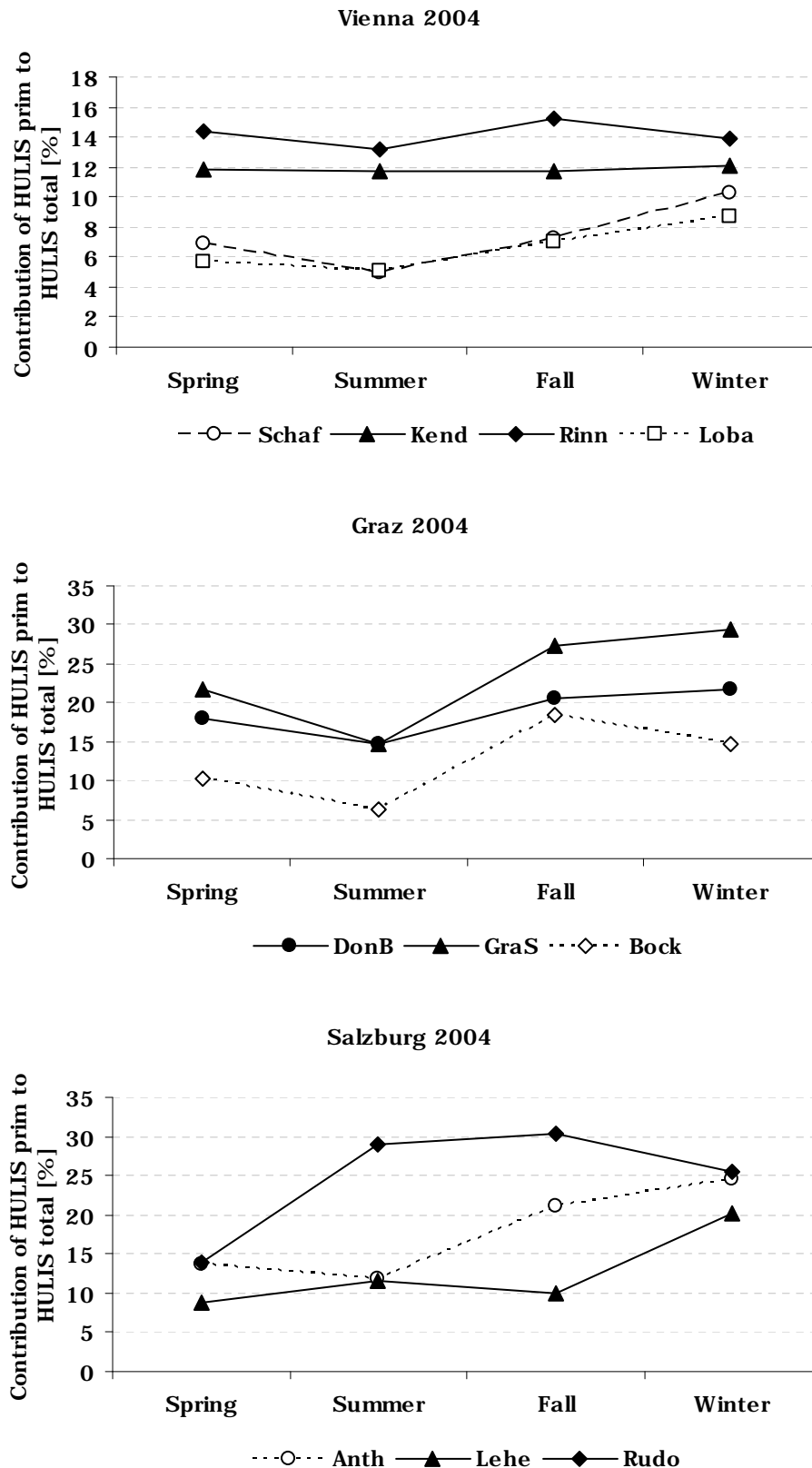


Figure 64: Contributions of primarily emitted HULIS by wood stoves and diesel vehicles (calculated) to HULIS_T (measured) in Vienna, Graz and Salzburg 2004; solid squares: urban sites; open squares: urban fringe or rural sites.

Vienna, Graz and Salzburg 2004

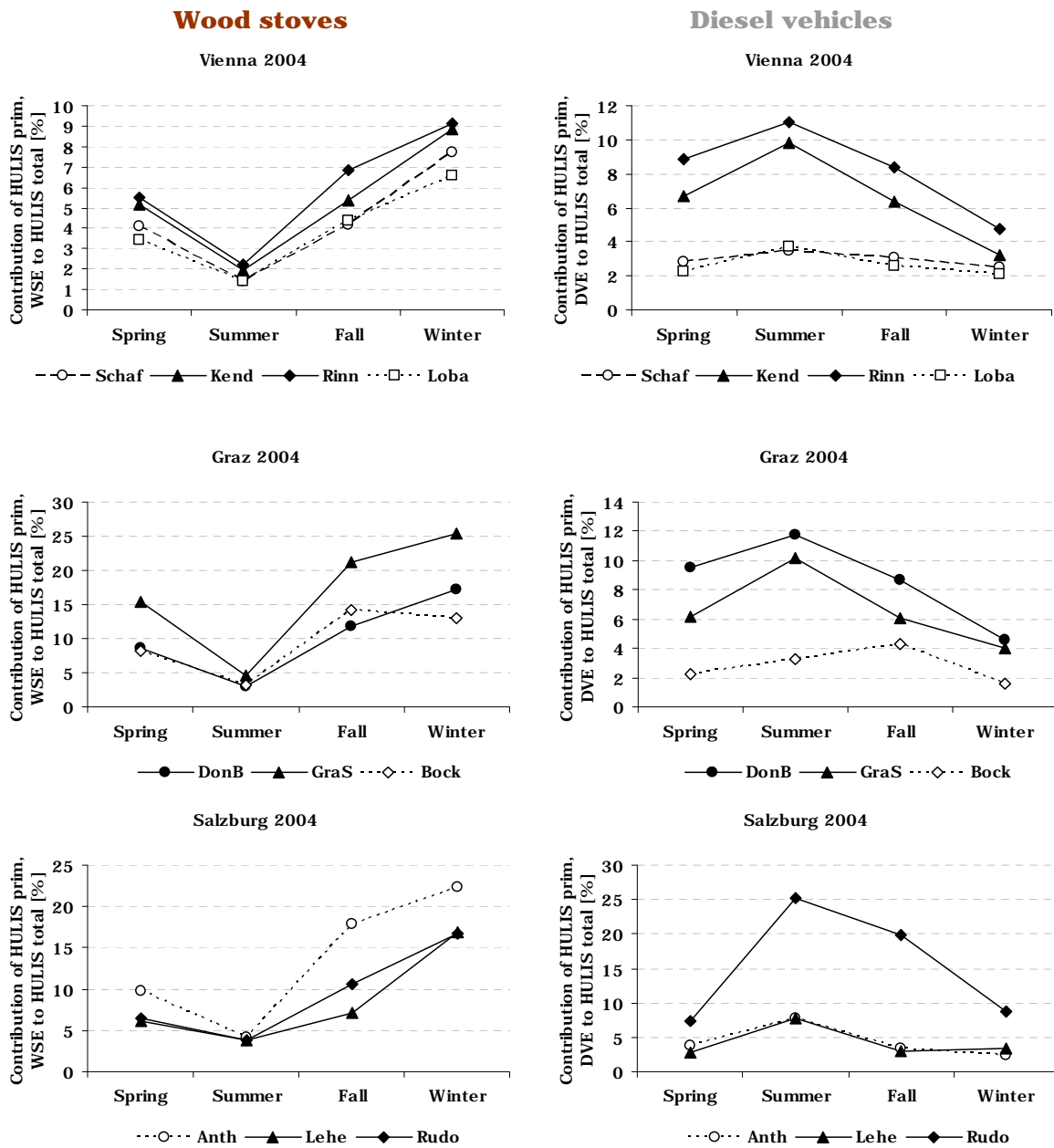


Figure 65: Seasonality of contributions from HULIS primary (calculated) to total HULIS (measured) from wood stove emissions (left column) and diesel vehicle emissions (right column), Vienna, Graz and Salzburg 2004.

Distinguishing between $HULIS_T$ emitted primarily by diesel vehicles and wood stoves (Figure 65), one can see that seasonal behaviour of calculated HULIS shares from the two investigated primary HULIS sources is diametrically opposed. $HULIS_{prim, WSE}$ shares minimize during summer with equal or less than 5% at all sites and show maxima in winter and/or fall with values from 6 to 30 %. Opposed to summer minima of $HULIS_{prim, WSE}$, shares of HULIS emitted primarily by diesel engines, rise during summer month with more distinct maxima for the urban traffic impacted sites compared to urban fringe or rural sites. These observations lead to the assumption that vehicle exhaust, or

more general spoken fossil fuel burning is responsible for a quite considerable fraction of HULIS in summer, only concerning primary contributions. Absolute calculated primary HULIS levels show, analogue to the seasonal behaviour of the tracers levoglucosan and elemental carbon stemming from diesel vehicles applied for calculation, distinct seasonality for $HULIS_{prim, WSE}$ and constant levels of $HULIS_{prim, DVE}$, exemplarily depicted in Figure 66 for an urban and an urban fringe site in Vienna.

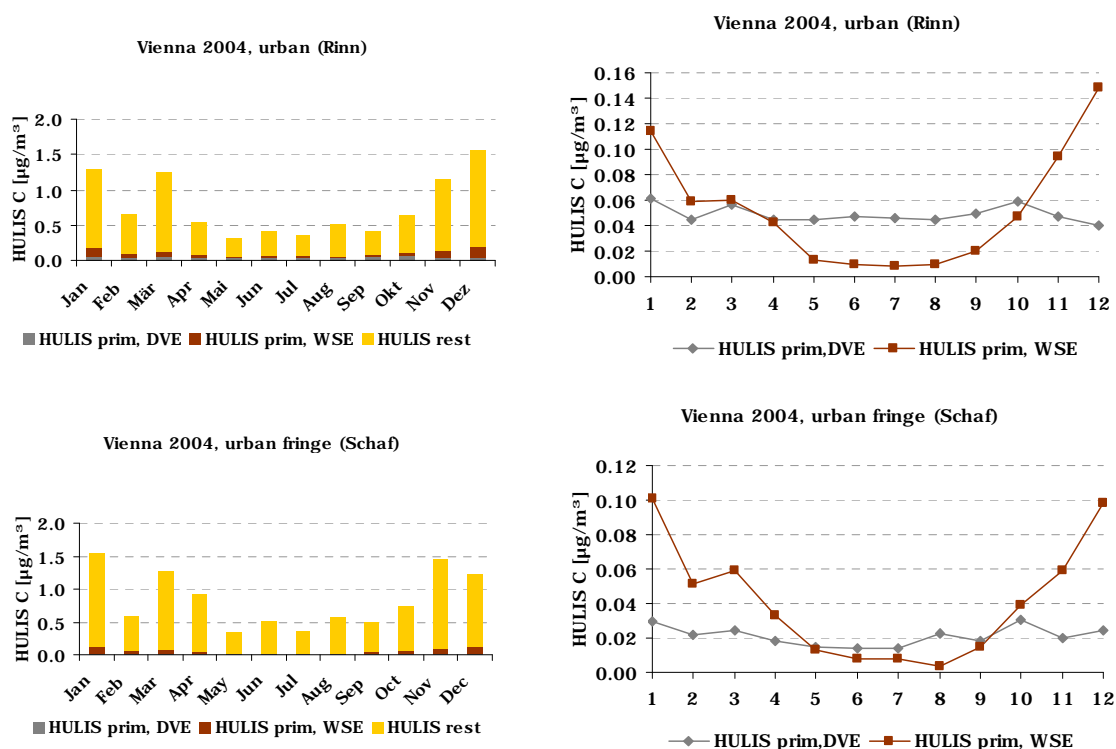


Figure 66: Absolute levels of calculated $HULIS_{prim, WSE}$ and $HULIS_{prim, DVE}$; $HULIS_{rest}$: $HULIS_{measured} - HULIS_{prim, WSE+DVE}$; Vienna 2004.

Based on results from the present and the following subchapter, HULIS quantification in source emission samples and seasonal resolved correlation analysis, respectively, Figure 67 depicts semi-quantitative estimations on the source apportionment of $HULIS_{Rest}$ (the difference between measured HULIS carbon and calculated primary contributions). Relative primary shares at the urban residential and the rural site in Styria are two times higher in winter than in summer. 30 % of the winter average at the urban traffic impacted site could be explained by primary emissions from wood stoves and diesel vehicles, wood stoves with 25 % being far more dominant. Potential contributors in winter to $HULIS_{Rest}$ are emissions from coal combustion, to lower extents other stationary and mobile fossil combustion sources, and secondary formation from fossil precursors as well as from wood combustion. As quantification of HULIS in source samples in this chapter and correlation analysis in the following chapter suggest, fossil fuel combustion might be of equal importance as wood combustion for the atmospheric occurrence of

HULIS. By considering shifts in source strengths and types in summer, beside anthropogenic sources, the secondary formation from biogenic precursors plays very likely an important role, whereas the impact of wood smoke diminishes and secondary formation plays a more important role than primary emissions of HULIS. Qualitatively the same might be valid for rural or background sites, though with even more pronounced secondary nature of HULIS. These considerations are as well in line with findings from Kleindienst et al. (2010) who determined 50 % of the OC in an urban environment to be fossil based and still 20 % at a rural site in North America. The authors reported ratios between secondary and primary aerosol of 1:2, 1:1 and 2:1 in urban, suburban and rural areas, respectively, what in analogy to HULIS as well supports the proposed source contributions in the present work.

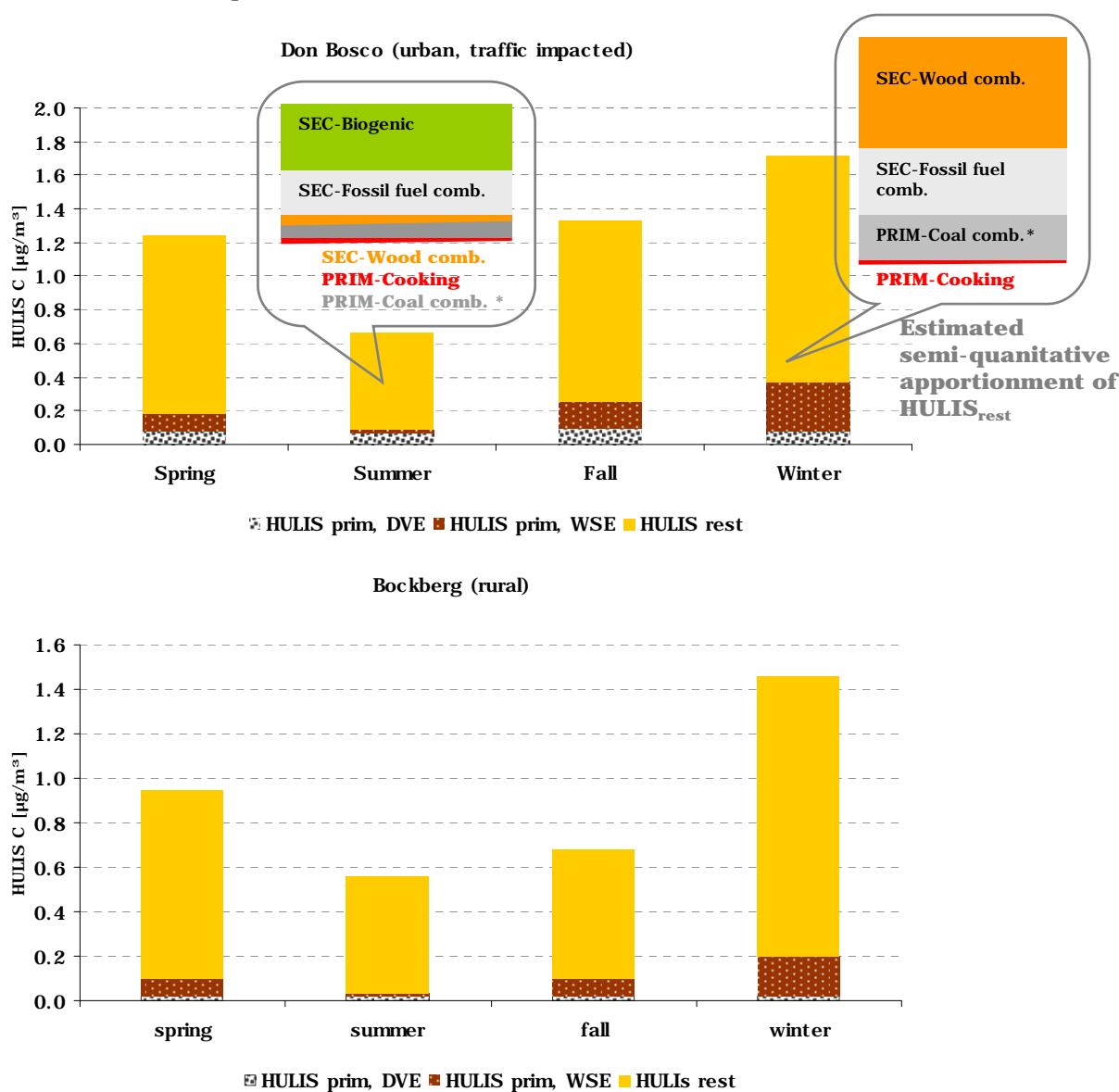


Figure 67: Seasonal averages of calculated HULIS_{prim, WSE} and HULIS_{prim, DVE}; HULIS_{rest}: HULIS_{measured} - HULIS_{prim, WSE+DVE} and semi-quantitative estimated apportionment of HULIS_{rest} based on findings from the present work.

7.3.9 Seasonal resolved Correlation Analysis

Immission concentrations of particulate matter carry a complex mixture of information including meteorological conditions, atmospheric transport phenomena, source strengths and formation rates. Correlations with selected aerosol species can provide information on possible origins, comprising the way a respective species is linked to HULIS_T (e.g. same main source, transport, same formation pathway etc.). To avoid correlations stemming mainly from same seasonal behaviour, data was investigated seasonally resolved. Correlations of HULIS and other aerosol constituents were investigated from the pools individual data during the seasons. Since the scope of the AQUELLA projects was the investigation of sources responsible for exceedances of the PM10 limit of 50 µg/m³, almost exclusively occurring during the cold season (Bauer et al., 2006, 2007a and 2007b), the largest set of observations with higher temporal resolution is available for winter (n=9-22) for the respective sites. Additionally to particulate analytes data for SO₂ and Ozone were available for some sites, measured by the local authorities, compiled and kindly provided as daily means by Environment Agency Austria. Daily averages were calculated according the respective sample pools. Species selected for correlation analyses are summarised in Table 18.

Table 18: Species selected for correlation analyses with HULIS_T

| | Analyte | Characteristic source | References |
|-------------------------|--|---|------------------------|
| Particulate species | Elemental carbon | Combustion processes | |
| | Pb | Fossil fuel combustion | |
| | Sb | Brake abrasion | |
| | As | Coal combustion | |
| | Pd | Catalyst-equipped vehicles | |
| | Si | Soil/street dust | Bauer et al., 2006; |
| | Sulfate | | Simoneit et al., 1999; |
| | Nitrate | | Puxbaum and Tenze |
| | Oxalate | Secondary aerosol | Kunit, 2003; |
| | Ammonium | | Cass, 1998; |
| | Potassium | Biomass combustion/ soil | Limbeck et al., 2009; |
| | Levoglucosan | Biomass combustion | Gelencsér, 2005 (and |
| | Cellulose | Plant debris | references therein) |
| | Benzo(ghi)perylene | Fossil fuel combustion/ vehicle exhaust | |
| Benzo(de)anthracen-7-on | Fossil fuel combustion/ natural gas combustion | | |
| Nonanal | Cooking activities | | |
| Gaseous species | Sulfurdioxide | Fossil fuel combustion | |
| | Ozone | | |

Only a few studies reported in literature provide information on correlations of atmospheric HULIS and other particulate aerosol constituents. Feczko et al. (2007) reported significant correlations of HULIS_T (determined with the same method as in the present work) and levoglucosan and fine potassium at three European background sites

(two low-level sites in Hungary and Portugal, respectively and one mid tropospheric site in Austria in Europe, considering the whole set of data gained during two years. Fine K and HULIS (determined by a method based on a separation step on diethylaminoethyl (DEAE) cellulose and subsequent UV/VIS detection (Okochi et al., 2008)) in dew water sampled in 21 one days in August and July 2005 in a suburban city near Tokyo, revealed good correlation as well. Samburova et al. (2005a) quantified HULIS_{WS} at an urban site in Zürich, surrounded by moderately frequented roads, office and apartment buildings, in August 2002 (10 samples) and February/March 2003 (13 samples), with a method based on size exclusion and subsequent UV detection (Samburova et al., 2005b). They investigated levels of ozone, levoglucosan and oxalic acids on potential correlations with HULIS concentrations. They found ozone correlated positively to the maximum molecular HULIS weight and oxalic acid with HULIS_{WS} concentrations. Levoglucosan (the authors remarked that only four data pairs were available for HULIS and levoglucosan during the campaign in February and March) in winter samples from downtown Zürich did not show significant correlation. They suggested photochemical activity to promote higher concentrations of HULIS on the base of significant correlations of HULIS and oxalic acid. A more recent study linked correlation of HULIS_{WS} with K⁺ in winter and oxalic acid in summer to be biomass burning and secondary formation, respectively, to be major HULIS sources (Baduel et al., 2010). Lin et al. (2010b) found good correlation of HULIS_{WS} with ammonium, oxalate, nitrate, sulfate, potassium and the atmospheric oxidants O₃ and NO₂ what as well indicates biomass burning and secondary formation contributing to atmospheric HULIS_{WS} levels. However neither investigation on the correlation of HULIS_T nor the inclusion of metals and polar organic compounds in correlation was reported so far. The present work overcomes the lack of data for HULIS_T on full seasonal cycles at urban and corresponding background sites and moreover provides the possibility to investigate relations between main and unique tracer substances and the atmospheric occurrence of HULIS_T. The sites in Vienna, a rather well ventilated area, and Graz, with very unfavourable dispersion conditions, were chosen for wintry correlation analysis. A considerable amount of aerosol species correlated significantly with HULIS_T [Table 19; 95 % significance levels for correlation coefficients were calculated individually for each aerosol species according to the number of data pairs (degree of freedom: f=number of observations-2)].

Table 19: Correlation coefficient among HULIS_T and major aerosol constituents/tracer components in PM10 (Dec-Feb)*

| Correlation coefficients winter | Vienna | | | | Graz | | |
|------------------------------------|--------------|--------------|--------------|---------------|---------------|--------------|---------------|
| | SCHA | KEND | RINN | LOBA | BOCK | DONB | GRAS |
| EC | 0.872 | 0.850 | 0.794 | 0.678 | 0.920 | 0.114 | 0.027 |
| Si | -0.194 | -0.082 | -0.271 | ND | 0.059 | 0.053 | ND |
| NH ₄ ⁺ | 0.878 | 0.605 | 0.888 | 0.800 | 0.956 | 0.803 | 0.905 |
| K ⁺ | 0.868 | 0.703 | 0.863 | 0.820 | 0.893 | 0.841 | 0.549 |
| NO ₃ ⁻ | 0.849 | 0.777 | 0.902 | 0.756 | 0.910 | 0.857 | 0.854 |
| SO ₄ ²⁻ | 0.900 | 0.624 | 0.902 | 0.681 | 0.927 | 0.771 | 0.900 |
| Oxalate | 0.803 | 0.815 | 0.865 | 0.667 | 0.888 | 0.819 | 0.952 |
| Cellulose | -0.063 | 0.472 | 0.467 | 0.074 | 0.744 | 0.099 | 0.077 |
| Levogluconan | 0.886 | 0.801 | 0.739 | 0.926 | 0.710 | 0.754 | 0.447 |
| Benzo(de)anthracen-7-on | 0.651 | 0.653 | 0.677 | 0.494 | 0.803 | 0.581 | 0.120 |
| Benzo(ghi)perylene | 0.803 | 0.696 | 0.734 | 0.669 | 0.711 | 0.336 | -0.107 |
| Nonanal | 0.241 | 0.431 | 0.026 | 0.014 | LP | LP | 0.650 |
| Pb | 0.810 | 0.642 | 0.823 | ND | 0.968 | 0.774 | ND |
| Pd | 0.067 | -0.353 | -0.078 | ND | 0.147 | 0.531 | ND |
| As | 0.580 | 0.223 | 0.587 | ND | 0.563 | 0.331 | ND |
| Sb | 0.631 | 0.128 | 0.239 | ND | 0.624 | -0.143 | ND |
| SO ₂ | 0.715 | ND | 0.539 | 0.296 | -0.268 | 0.305 | -0.001 |
| Ozone | ND | ND | ND | -0.694 | -0.737 | ND | -0.516 |

*Bold numbers denote significance on a 95% confidence level; ND...no data available of respective species; LP...most or all tracer levels below limit of detection

Correlation of species does not stringently mean that they share common sources. As discussed in a previous chapter, especially in winter inversion layers can lead to co-variations of species from any sources blocked under the inversion. Strong correlation of HULIS_T with EC, diesel vehicles being the major source in urban PM, at the Vienna sites might on one hand reflect a mutual source or the influence of unfavourable dispersion conditions. To exclude meteorological co-variations of species a period with frequently occurring inversions was examined on correlations of PM10 and EC as well as HULIS and EC. Strong inversions were observed on eight days in January (Bauer et al., 2006). Correlations of EC with PM10 and HULIS_T carbon with EC (n=14) were significant in January with R²=0.80 and R²=0.75, respectively. Restraining sample pools which involved the observations of strong inversion layers resulted in an increase of correlation (n=7) for EC with PM10 (R²=0.92) and HULIS_T C with EC (R²=0.89), respectively. If the co-variation was mostly induced meteorologically, restraining these periods from calculations would result in lower correlation coefficients. As the opposite was observed, we conclude that the present data set is applicable for considerations on possible origins of HULIS_T. Figure 71 and Figure 70 depict winter correlation plots for the four sites in Vienna, gained from the

pools individual data from December to February. Significant linear correlations (bold numbers denote correlation coefficients significant on a 95% confidence level) are summarised in Table 19. HULIS_T C levels vs. selected species for all investigated sites from Vienna are depicted in one plot, whereas correlations coefficients were calculated for each site separately. Values under the limit of detection are as well depicted in correlation plots and included in calculating the correlation coefficient. Good significant correlations occurred at all sites for secondary species (NH₄⁺, NO₃⁻, SO₄²⁻, oxalate), primarily emitted tracers for wood combustion (levoglucosan and K⁺) and species which are primarily emitted by combustion of fossil or biogenic fuels (EC, benzo(ghi)perylene). Surprisingly, significant correlations were as well observed for benzo(de)anthracene-7-on and lead, both clearly related to fossil fuel combustion. The former is strongly linked to combustion of natural gas and was found to dominate the PAH fraction in diesel vehicle emissions, together with benzo(ghi)perylene (Gelencsér, 2004; Bauer et al., 2006). These findings are in agreement with the quantification of HULIS carbon in samples from coal combustion as well as in vehicular exhausts (see section 7.3.8.1). Since the vast majority of previous studies focused on the water-soluble fraction of HULIS, analysis of metal data requires different sampling substrates (e.g. Handler et al., 2008), thus additional filter sampling, and EC inventories identified domestic wood combustion as major particle source it is not surprising that fossil combustion was not considered to be a potentially important source for atmospheric HULIS. The resuspension of plant debris or street dust or soil does not seem to play a role in the atmospheric abundance of HULIS since no correlation of HULIS and cellulose or silicium was observed at neither of the sites. Significant positive correlation was as well not observed for nonanal, an apolar organic compound related to cooking activities, at the Vienna sites. Correlation with arsenic, a tracer substance for coal combustion, was positive at the three Vienna sites (no metal data for LOBA available), though reaching the level of significance only for the fringe site SCHAF and the traffic impacted site RINN. The rather low correlation levels (r=0.580 at SCHAF, r=0.587 at RINN) and the non-uniformity in Vienna most likely appears because of the rather high volatility of arsenic compounds (they can appear in the atmosphere in PM as well as in the gas phase), and resulting analytical uncertainties.

The sites in Styria as well showed significant correlation at all sites for NH₄⁺, NO₃⁻, SO₄²⁻, oxalate, levoglucosan and lead. Benzo(ghy)perylene and Benzo(de)anthracen-7-on showed correlations with HULIS at BOCK, whereas rather low correlation coefficients between HULIS and Benzo(de)anthracen-7-on at DONB were observed. PAHs seem not to be linked to HULIS at the residential site GRAS. Regarding the specific source related tracers, levoglucosan is not the highest correlated tracer at neither of the three sites.

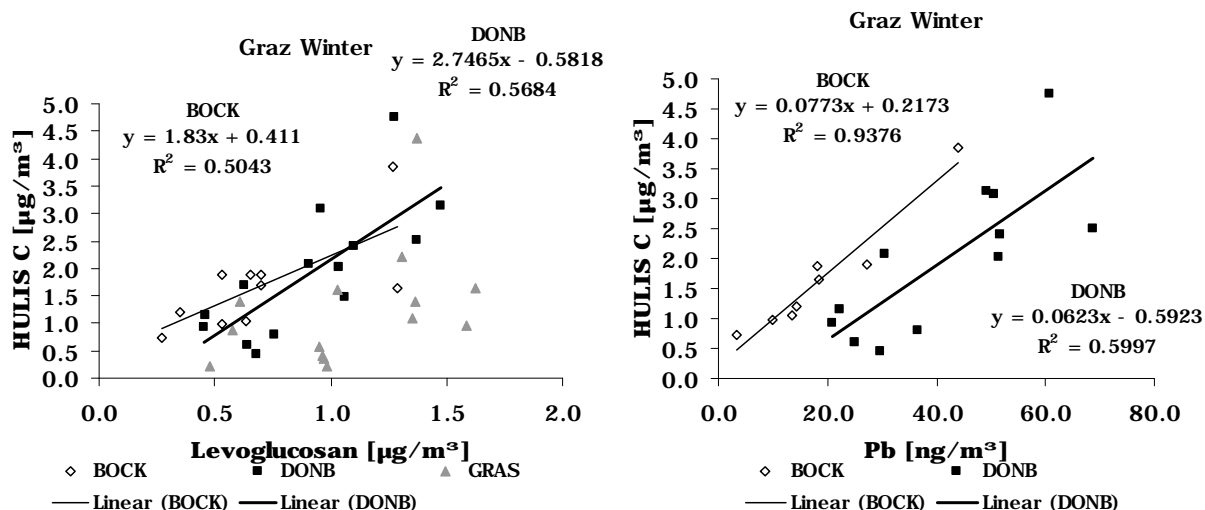


Figure 68: Correlation of HULIS_T carbon and levoglucosan (left) and lead (right) in Styria (December-February).

Compared to levoglucosan, lead is correlated on a distinctive higher level at BOCK and similarly at DONB (no metal data available for GRAS), whereas cooking emissions seem to have more influence on HULIS_T levels than biomass smoke. In general, fossil fuel combustion related aerosol species, are stronger linked to atmospheric HULIS_T levels at the rural background site BOCK (Figure 68), what points to air masses regional or long-range transported from source regions that are strongly impacted by fossil fuel burning are the dominant influence at the background site BOCK. Strongest correlation on the urban sites was observed for HULIS_T and secondary species. Most of these correlations were weaker than those observed at BOCK. This indicates that additional to long range transported HULIS_T, several local sources might contribute to HULIS_T levels at the inner city sites. The only species significantly negative correlated to HULIS was ozone. Ozone data was available only for the background site LOBA in Vienna and GRAS and BOCK, the urban residential and background site in Styria, and all three sites showed a negative trend. The relation between ozone and HULIS_T (defined as sum of HULIS_{AS} and HULIS_{WS}) and HULIS_{AS} at the urban site GRAS, respectively, is represented better by a potential than a linear function, whereas the background sites show a rather linear negative correlation (Figure 69). For HULIS_{AS} at GRAS the negative correlation gets even more pronounced, and a second slope with a higher HULIS offset gets visible, mainly consisting of data pairs from the Vienna site LOBA. These findings indicate photochemical degradation of HULIS being active in winter, which is in agreement with the findings of Baduel et al. (2011) who found carbon losses of alkaline soluble HULIS of about 30% after three hours of ozonisation and UV irradiation. HULIS_{AS} plotted against ozone levels at background sites seem to follow a rather potential slope whereas HULIS_{WS} at the same sites follow a more linear negative trend (Figure 69).

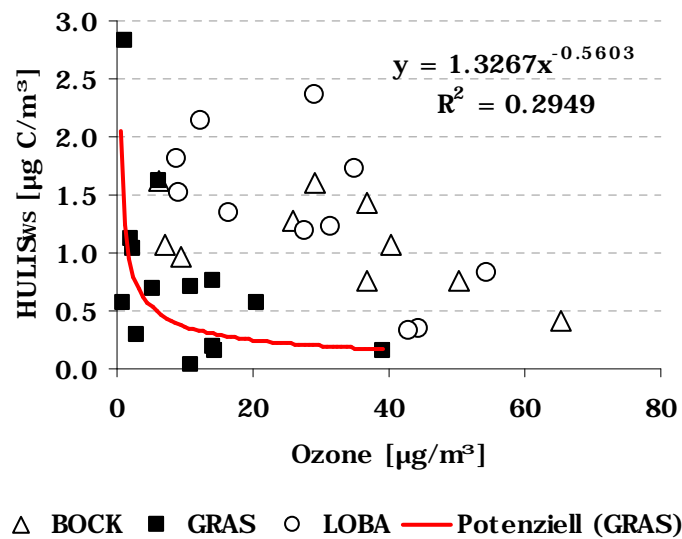
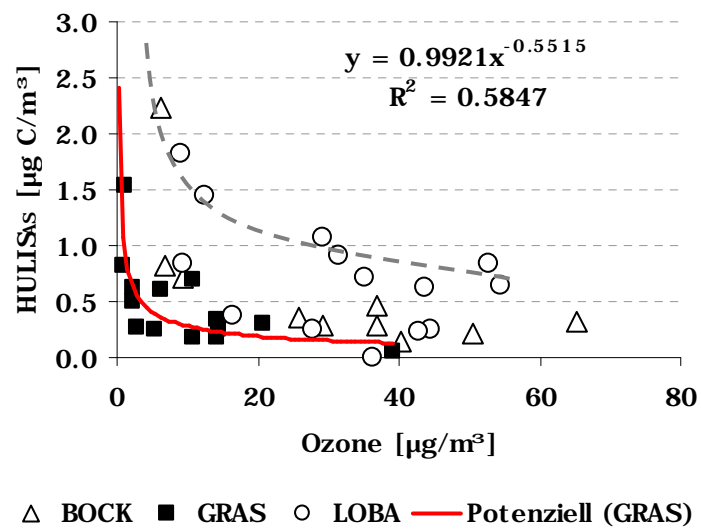
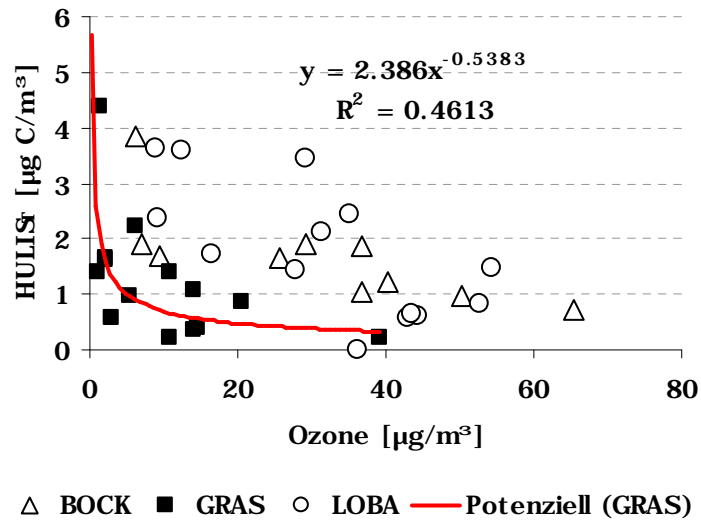


Figure 69: Atmospheric levels of ozone and HULIS_T (top), HULIS_{AS} (middle) and HULIS_{WS} (bottom) in winter samples at urban (solid squares) and open circles and triangles; red lines denote actual correlation function; grey line was added to guide the eye.

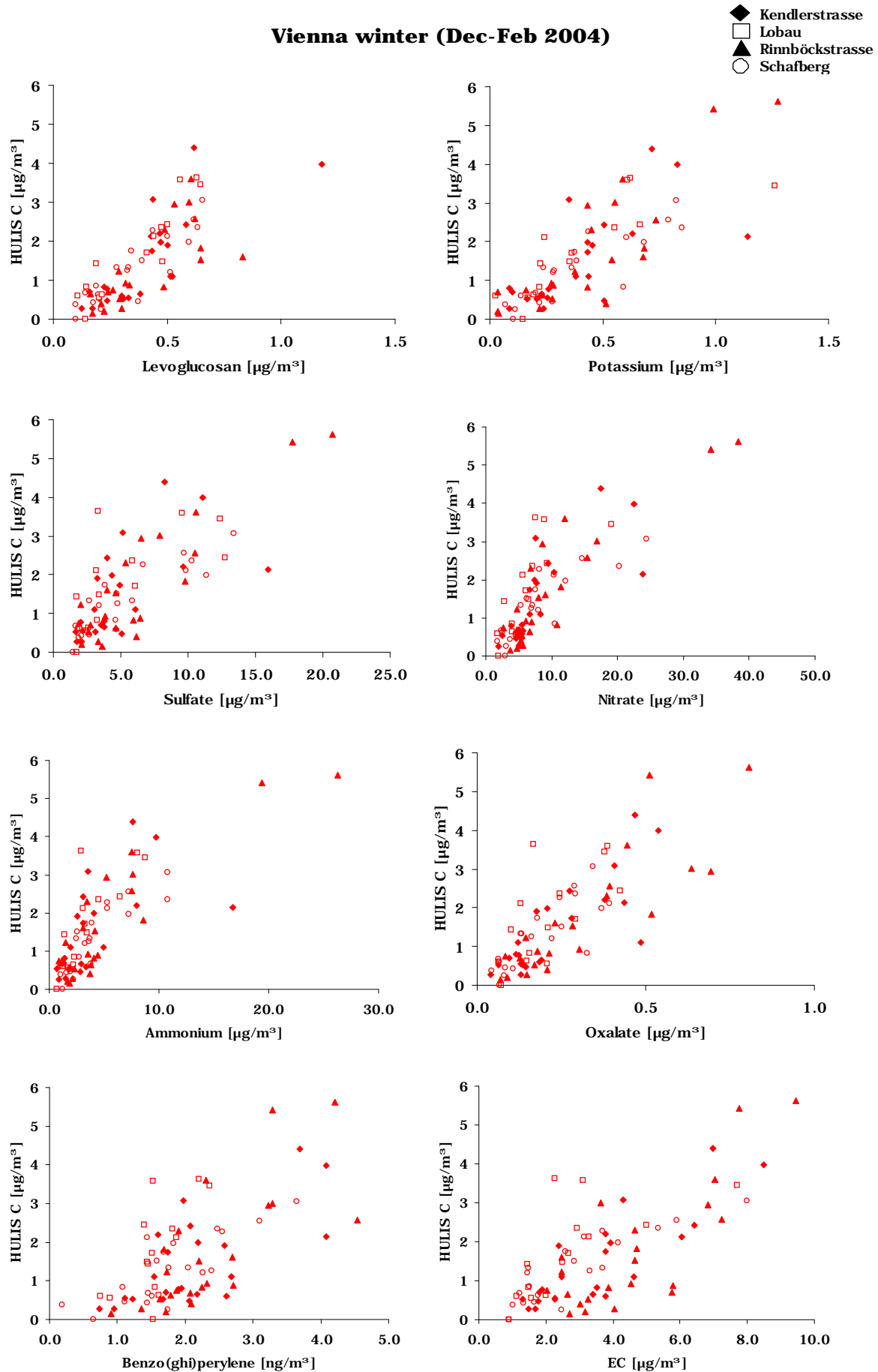


Figure 70: Correlation of HULIS_T carbon and aerosol species from the AQUELLA database (winter); **red:** significant linear correlation on a 95% confidence level.

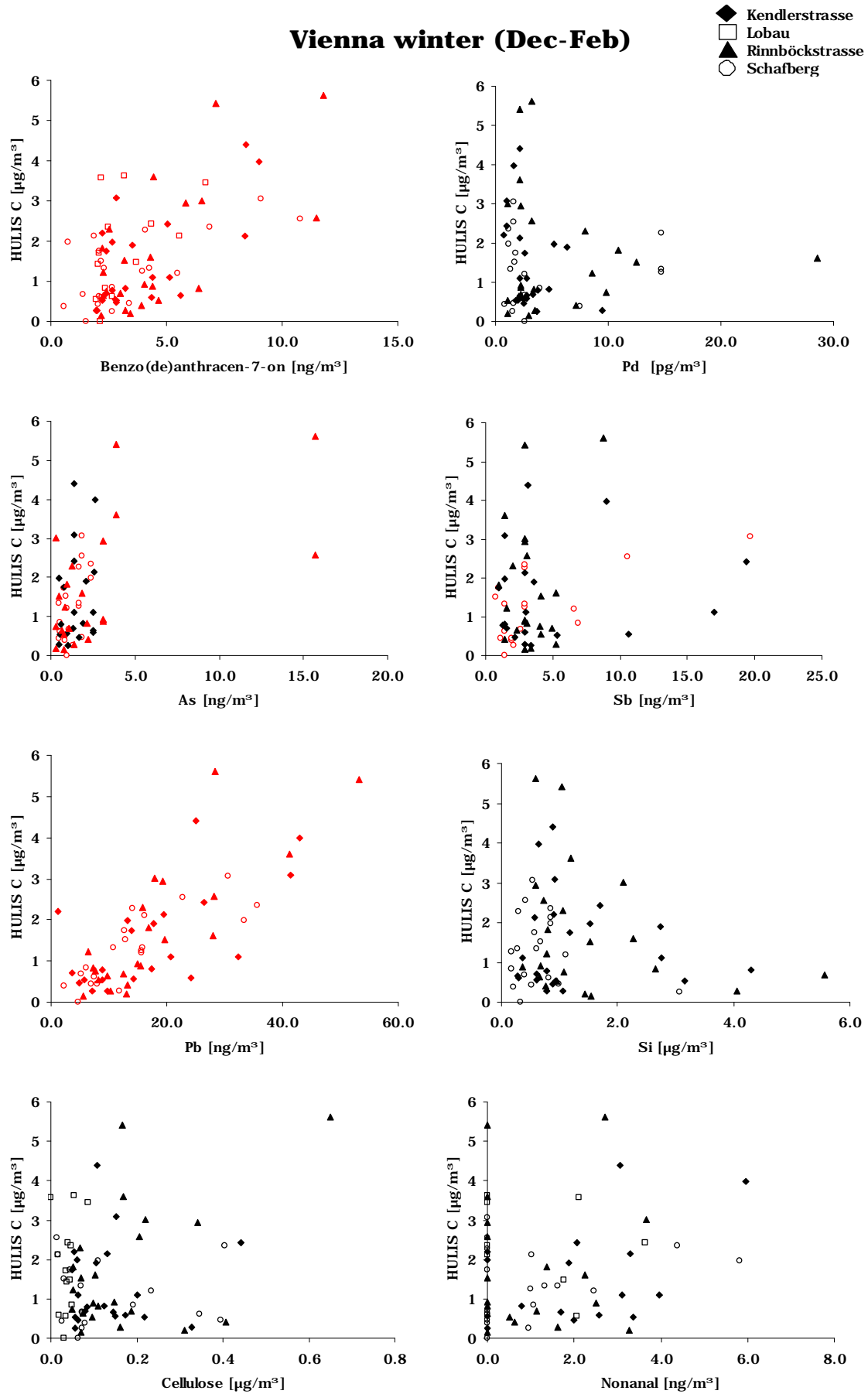


Figure 71: Correlation of HULIS_T carbon and aerosol species from the AQUELLA database (winter); **red:** significant linear correlation on a 95% confidence level.

Table 20: Correlation coefficient of HULIS_T and major aerosol constituents/tracer components in PM₁₀ at three sites in Styria (Jun-Aug)*

| Correlation coefficients (Summer) | Graz | | |
|--------------------------------------|--------------|--------------|--------------|
| | BOCK | DONB | GRAS |
| EC | -0.448 | 0.944 | 0.680 |
| Si | ND | 0.438 | 0.238 |
| NH ₄ ⁺ | 0.925 | 0.680 | 0.861 |
| K ⁺ | 0.972 | 0.492 | 0.717 |
| NO ₃ ⁻ | 0.961 | 0.644 | 0.747 |
| SO ₄ ²⁻ | 0.917 | 0.750 | 0.844 |
| Oxalate | 0.960 | 0.870 | 0.869 |
| Cellulose | 0.468 | 0.235 | -0.645 |
| Levoglucosan | 0.894 | -0.108 | 0.832 |
| Benzo(de)anthracen-7-on | ND | ND | ND |
| Benzo(ghi)perylene | ND | ND | ND |
| Nonanal | ND | ND | ND |
| Pb | ND | -0.254 | -0.318 |
| Pd | ND | -0.149 | ND |
| As | ND | 0.575 | -0.467 |
| Sb | ND | -0.569 | 0.485 |
| SO ₂ | -0.429 | 0.090 | 0.336 |
| Ozone | -0.107 | --- | 0.035 |

*Bold numbers denote significance on a 95% confidence level; ND...no data available

Temporal resolution was lower during the summer month with 15 to 30 sampling days accounting to one sample pool. No data for polar organic species was available (Bauer et al., 2007a). In Vienna investigations did not allow investigations on HULIS_T correlations with other species due to too low numbers of data pairs. However, a small set of sample pairs (n=4-6) in Graz allows some insight on possible summer sources of HULIS_T (Table 20). Correlations patterns at the urban traffic impacted site (DONB) point to different sources being of importance than at the urban and regional background site, respectively. Strongest correlation at DONB with EC (r=0.944) and a lack of such with levoglucosan or K⁺ indicates that fossil fuel combustion, especially diesel vehicle emissions as major source in summer, can contribute to ambient HULIS_T levels. Primary emissions or secondary formation, e.g. via the oxidation of soot (Decesari et al., 2002), are both thinkable pathways. Weaker but still significant and good correlations with oxalate and sulfate suggest secondary processes to be included in the ambient occurrence of HULIS_T in summer. Unfortunately no data for tracer for biogenic gaseous emissions was available, but it is likely that biogenic precursor, simply due to their ubiquitous abundance as well play a role (Gelencsér, 2004). The urban residential site GRAS and the background site BOCK showed correlations with the secondary aerosol species and levoglucosan. Ratios of HULIS_T carbon and levoglucosan are three to six times higher in summer than in winter,

what indicates other sources than domestic wood stove emissions to be active in summer (see Table 23). Plausible summer sources for wood smoke are forest fires commonly occurring during warmer periods in Europe (see Figure 60, section 7.3.8.1). Correlation patterns at the three sites suggest impact of regionally or long-range transported biomass burning aerosol in the region of Graz and additional local contribution of vehicular emissions at the urban site DONB constituting major HULIS sources. The lack of data in the summer months for metals, polar organic compounds and a tracer for biogenic gaseous emissions does not allow insights on potential other sources such as industrial coal burning, cooking or secondary biogenic formation. The latter commonly suggested constituting a major summer source for HULIS and likely at least partly operative at most environments due to the high source strength of biogenic VOC (Gelencsér et al., 2004). Since fossil fuel combustion was shown to contribute to wintry HULIS levels due to strong positive correlations with lead (Table 19), with coal power plants as most likely source in Europe, it can be assumed that fossil fuel combustion influences atmospheric HULIS levels rather constantly throughout the year.

7.4 Discussion

Annual average HULIS_T levels occurred in comparable heights in the three regions and ranged from 0.46 µg C/m³ to 1.24 µg C/m³. Regarding the ten sampling sites in the three regions, HULIS_T did not reveal a distinct general trend to be more present at urban or background sites. Highest HULIS_T levels occurred at the suburban sites in Vienna, a traffic impacted site in Graz and an urban residential site in Salzburg. The seasonal devolution of atmospheric HULIS_T levels qualitatively was the same in the three cities, with minima in summer and maxima during winter. Concentrations in winter were 2.0 to 2.8 times higher than in summer. The concentrations in summer turned out to occur in a narrower range in and have a bigger spread in fall, what points to higher impact of local emissions at the latter. Contributions of HULIS_T to PM₁₀ and OC occurred between 3.8 and 8.9 % and 10.1 and 28.9 %, respectively. Higher values appeared at the background sites. Inner-city sites showed generally very stagnant relative HULIS concentrations throughout the year in Vienna and Graz. Contributions of HULIS_T C to OC at the five background and urban fringe sites and the urban sites were 25±5% and 14±3%, respectively. HULIS_{WS} contributed to HULIS_T with 55% ±5% in the majority of the sample pools at the ten sampling sites. Results from combining observations of HULIS_T levels and composition with meteorological conditions from periods with well understood origin and chemical composition of PM₁₀ from the AQUELLA project, might point to a linkage of the relative abundance of HULIS_{WS} and HULIS_{AS} and the age of HULIS, since HULIS_{WS} shares to the total fraction of HULIS of about 30% and beyond were observed at a heavily biomass burning impacted episode in Styria. Meteorological observations and

source composition would as well support spatial and temporal variations of HULIS_T composition in Vienna.

The application of a dilution tracer at two urban traffic impacted sites revealed that unfavourable meteorological conditions in the cold season are of minor importance to the HULIS_T winter enrichment, accounting only with 7 and 12 % at the traffic impacted sites in Vienna and Graz, respectively, thus additional sources and/ or higher formation rates being actually responsible for the observed winter enrichment.

HULIS_T in source emissions from wood, lignite and anthracite combustion, diesel vehicular emissions and cooking revealed contributions to PM₁₀ in the range of 1-7%, 4-5%, 0.9-1.3% and up to 0.7%, respectively. Highest relative HULIS_T levels occurred in emissions from open leaf burning (~20% of PM₁₀). The amount in diesel vehicular exhaust is quite surprising since the occurrence of atmospheric HULIS_T was closely connected to biomass burning and the formation from various gaseous precursors. These results indicate that combustion of fossil fuels, especially mobile sources and coal combustion can not be ignored in considerations on the potential sources of HULIS_T. Processing ratios of HULIS_T and unique or main tracers in source emissions on ambient tracer levels revealed that, on annual average, up to 25% of HULIS carbon could be of primary origin emitted by diesel vehicles and wood stoves.

The findings from investigating source emission samples are confirmed in observations from correlations of HULIS_T (as sum of HULIS_{AS} and HULIS_{WS}) and other aerosol species in Vienna and the region of Graz. Averaged correlation coefficients from species that correlated significantly at all sites revealed that in Vienna wintry secondary formation is an important pathway. Precursors are potentially stemming from fossil as well as biomass combustion.

Strong significant correlation with lead, a primary pollutant strongly connected to coal combustion, was observed at the sites in Vienna and Graz (Table 21). Lead showed even better correlation with HULIS_T than levoglucosan at the Styrian sites. At the urban sites additional local sources such as diesel vehicle emissions and cooking activities can contribute to atmospheric HULIS_T abundance. Furthermore the regional or long-range transport of air masses has a major influence on HULIS_T levels. At all sites where ozone data was available, significant negative correlation, more pronounced at the urban site compared to background sites, points to effective degradation processes being at work in winter.

Table 21: Regional averaged correlation coefficients for HULIS_T in wintry PM10 (averages from species which are correlated significantly on a 95% confidence level at each site in the respective region)

| Species correlated significantly at all sites in Vienna | Regional averaged correlation coefficients (winter) | Species correlated significantly at all sites in Styria | Regional averaged correlation coefficients (winter) |
|---|---|---|---|
| Levoglucosan | 0.838 | NH ₄ ⁺ | 0.888 |
| NO ₃ ⁻ | 0.821 | Oxalate | 0.886 |
| K ⁺ | 0.814 | NO ₃ ⁻ | 0.874 |
| EC | 0.798 | Pb | 0.871 |
| NH ₄ ⁺ | 0.793 | SO ₄ ²⁻ | 0.866 |
| Oxalate | 0.787 | K ⁺ | 0.761 |
| SO ₄ ²⁻ | 0.777 | Levoglucosan | 0.637 |
| Pb* | 0.758 | Ozone | -0.626 |
| Benzo(ghi)perylene | 0.726 | | |
| Benzo(de)anthracen-7-on | 0.619 | | |
| Ozone* | -0.694 | | |

*Ozone data was available for the urban fringe site LOBA (Vienna) and BOCK (rural background) and GRAS (urban residential); Pb data was available for three sites in Vienna (SCHAF, RINN, KEND) and two in Graz (BOCK and DONB)

Correlation patterns occurring in summer in the region of Graz suggest forest or open agricultural fires as a “background” source and local impact of diesel-vehicles to be of importance. Primary emissions and secondary formation are both possible. Biogenic secondary contributions could not be investigated due to the lack of an appropriate tracer, but of course can not be excluded as potential source of HULIS_T.

8 HULIS over Austria- Spatial and temporal Variations of HULIS_T and Wood Smoke

The atmospheric abundance of HULIS is reported in a growing amount of literature. Most studies focus on the investigation of the water-soluble fraction of HULIS (Table 1 and Table 2, based on summaries from Krivácsy et al., 2008 and Kalberer, 2006). Due to our best knowledge only one study covered the seasonality of HULIS_T (Feczko et al., 2007), where full seasonal cycles of water and alkaline-soluble fractions were investigated at six continental background sites in Europe. Atmospheric abundance of HULIS_T, in the present work defined as the sum of water and alkaline extracts of HULIS, HULIS_{WS} and HULIS_{AS}, respectively, and spatial and seasonal distribution as well as contributions of HULIS_T to OC and PM₁₀ at 23 Austrian sampling sites are compared in the present section. Furthermore the importance of biomass smoke for the atmospheric occurrence of HULIS_T at the different sites is assessed by comparison of HULIS_T with the wood smoke tracer levoglucosan. If not explicitly denoted otherwise the term HULIS and HULIS_T are used interchangeably.

8.1 Experimental

For description of sampling sites, sampling and chemical analysis see sections 4, 5 and 6. HULIS quantification was conducted in the scope of the present work. Analysis of other species and parameters were conducted by the AQUELLA-team and taken from the AQUELLA data base. Results of levoglucosan and/or HULIS analysis are parts of the publications from Caseiro et al. (2009), Schmidl et al. (2008a and 2008b), Wonaschütz et al. (2009) and the AQUELLA/AQUELLIS project reports (Bauer et al., 2006, 2007a, 2007b, 2008a, 2008b, 2008c; Puxbaum et al., 2006, Schmidl et al., 2008c).

8.2 Results

8.2.1 Atmospheric Abundance

Averaged HULIS_T concentrations (Figure 72) appeared in a range of 0.46 -1.61 $\mu\text{g C}/\text{m}^3$, the former occurring at a rural background site in Salzburg (ANTH) and the latter at an urban site in Lower Austria (SCHW), which most likely is influenced by the vicinity of Vienna and potentially as well by emissions of an oil refinery located in about 3 km distance of the site Spangl et al., 2006; Bauer et al., 2006).

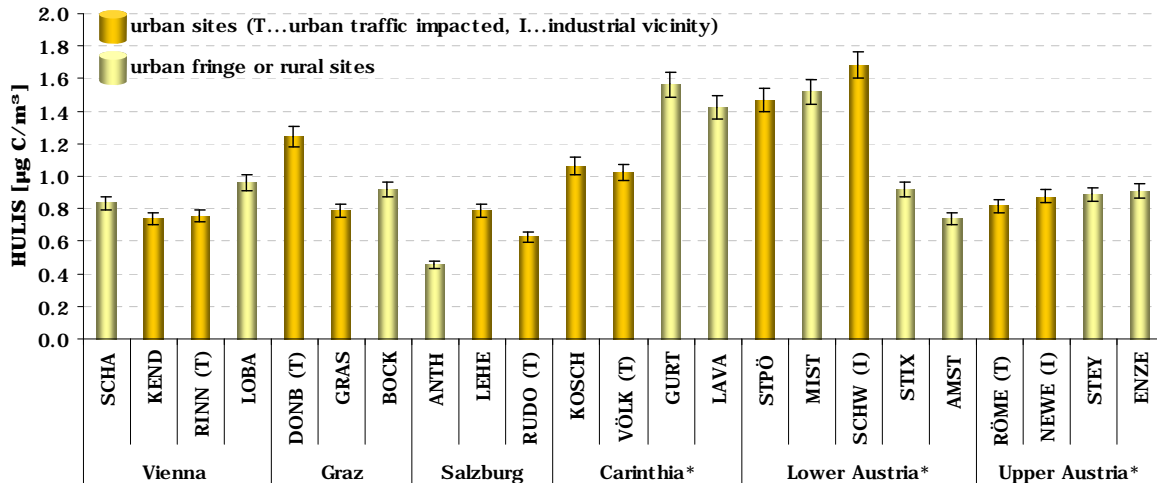


Figure 72: (Quasi-) annual average HULIS_T carbon levels in Austrian PM10; Vienna, Graz and Salzburg 12 month average; *Carinthia: November& December 2004, January-March & July 2005; Lower Austria: January-June 2005 (AMST April-June 2005); Upper Austria: April, May, June, October-December 2005, January-March 2006); bars indicate analytical uncertainty.

The abundance of atmospheric HULIS_T did not show a trend to occur preferred at sites with specific characteristics. Regarding the respective regions HULIS levels at background sites were slightly higher or similar than the respective urban sites (Vienna, Upper Austria) and markedly lower (Salzburg) or higher (Carinthia). In Lower Austria HULIS levels at two background sites (STIX, AMST) were markedly lower and similar (MIST) to the urban sites, respectively.

8.2.2 Seasonal Variations

HULIS_T showed similar seasonal devolution at the 23 sites. HULIS_T levels were lower and found in a narrower range during the warm season compared to late fall and winter month (Figure 73). Monthly averaged HULIS levels appeared in a range of 0.06-2.66 $\mu\text{g C}/\text{m}^3$.

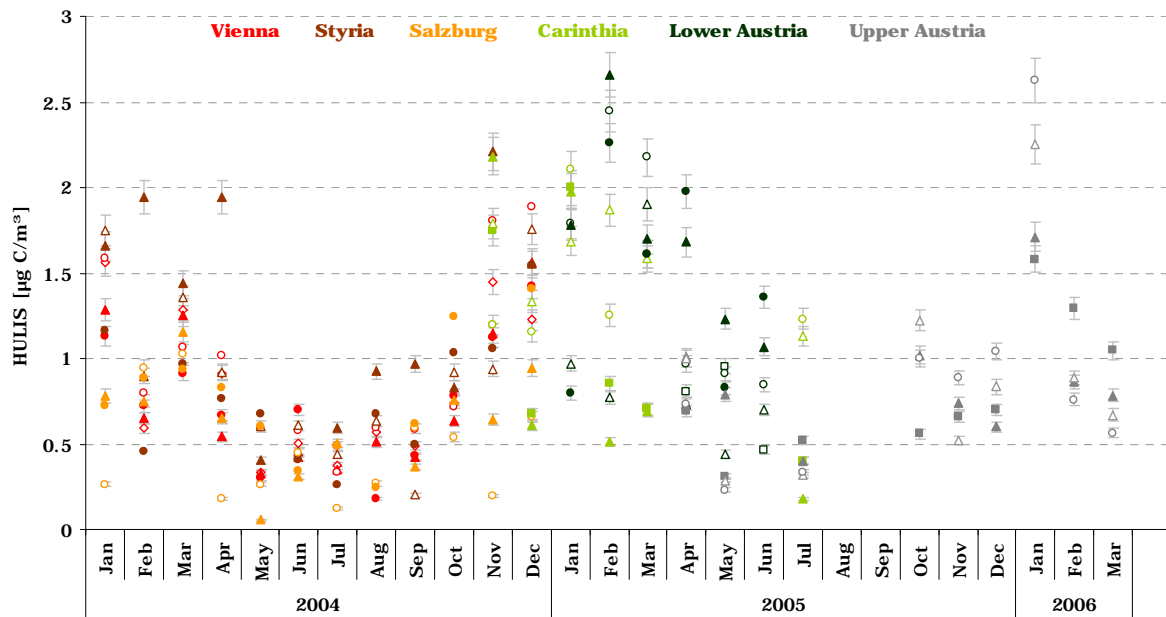


Figure 73: Seasonal cycles for HULIS_T (as sum of water and alkaline extractable HULIS) at the AQUELLA sites

The majority of the 23 sampling sites showed minima and maxima in fall or winter (Figure 74) with a winter enrichment factor in the range of 2-4. Only four sites did show almost no seasonality. Two background sites in Carinthia and the urban site in the capital of Lower Austria (STPÖ) showed no or very weak seasonality at a rather high HULIS_T level of $1.4 \pm 0.3 \mu\text{g C/m}^3$ compared to summerly HULIS_T levels found in a range of $0.28\text{--}0.70 \mu\text{g C/m}^3$ at 18 out of the 23 sites. A rural background site showed rather constant levels throughout the year on a lower level ($0.9 \pm 0.2 \mu\text{g C/m}^3$). This either indicates a source emitting HULIS or its precursors throughout the year, or a summer source with equal strength as biomass burning is in winter. Such emission sources with strong and constant source strength could be provided by industrial activities such as the paper industry, coal power plants or oil refinery would come into question. Emissions from the latter could be contributing to the emission or formation to atmospheric of HULIS_T as discussed in section 7.3.9. and 7.3.8.1. The sites LAVA and STPÖ are likely influenced by the emissions of industrial paper manufacturing (PRTR registry, Umweltbundesamt, 2013). Emissions from the combustion of large amounts of lignin containing solutions, a by-product in industrial paper manufacturing, may contribute to atmospheric HULIS_T levels on a regional scale. Such emissions would contain lignin break-down products and no levoglucosan signal, due to the beforehand separated cellulose. A further difference between the sites in Carinthia and Lower Austria and the other regions is that the spread of HULIS levels is quite high in the investigated summer month. In Carinthia background sites show four times higher HULIS_T concentrations compared to the urban sites in Klagenfurt in July. At the urban sites in Lower Austria in June, HULIS concentrations are 2 and 3 times higher than at the background sites (AMST).

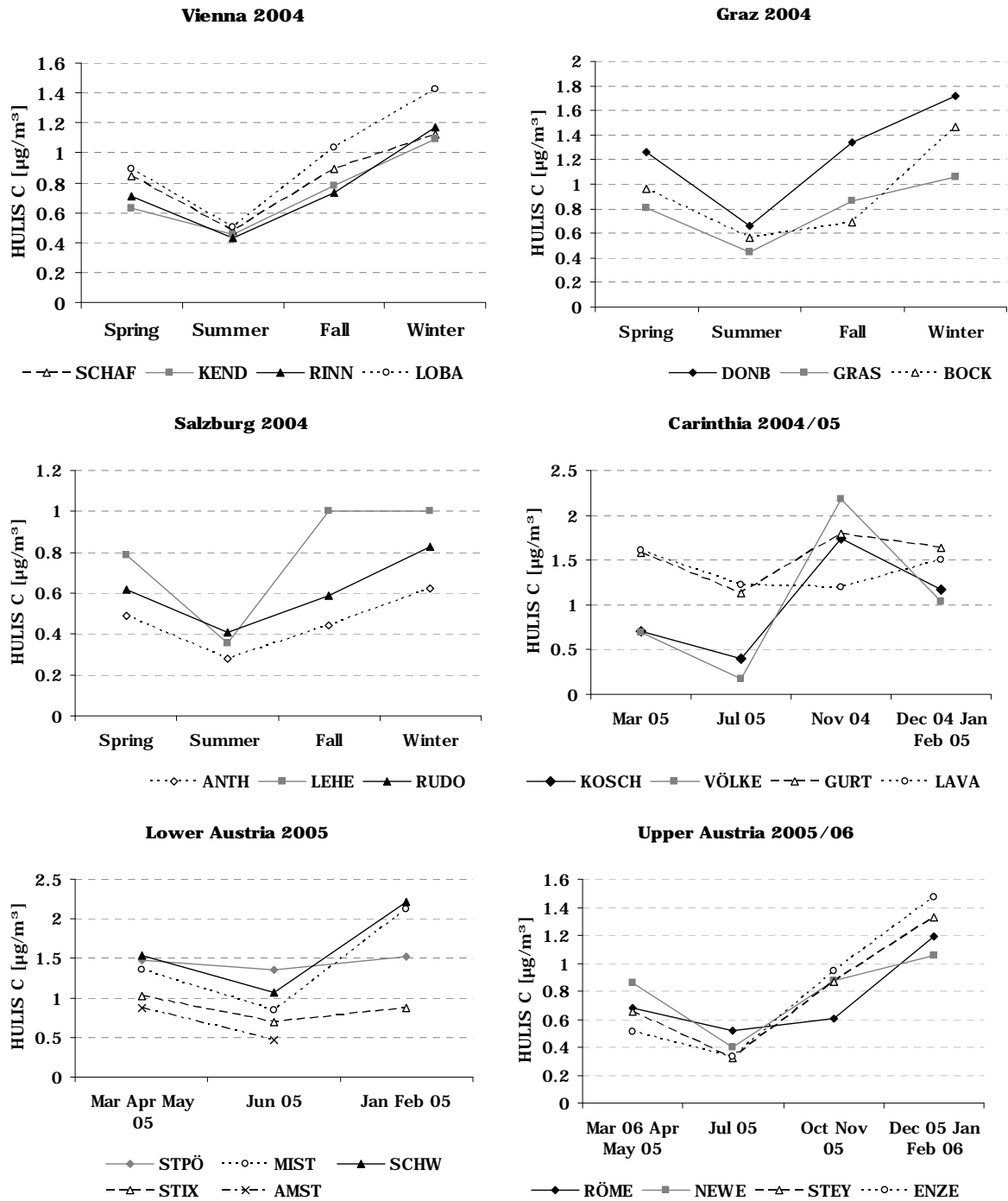


Figure 74: Seasonality of HULIS_T at 23 sites in Austria. Broken lines...rural or suburban sites; solid lines...urban sites.

8.2.3 Contributions of HULIS_T Carbon to OC and HULIS_T to PM10

Average contributions (annual average in Vienna, Graz and Salzburg, six month average for Carinthia and Lower Austria, nine month average for Upper Austria) of HULIS_T carbon at the 23 sites varied between 9 and 44 % (Figure 75). As mentioned in the previous sub-section averages pose 12-month averages (Vienna, Graz and Salzburg), 6 month averages (Carinthia and Lower Austria) and 9-month averages (Upper Austria) and therefore are not fully comparable, but should give a general impression on the abundance of HULIS_T in Austrian PM10.

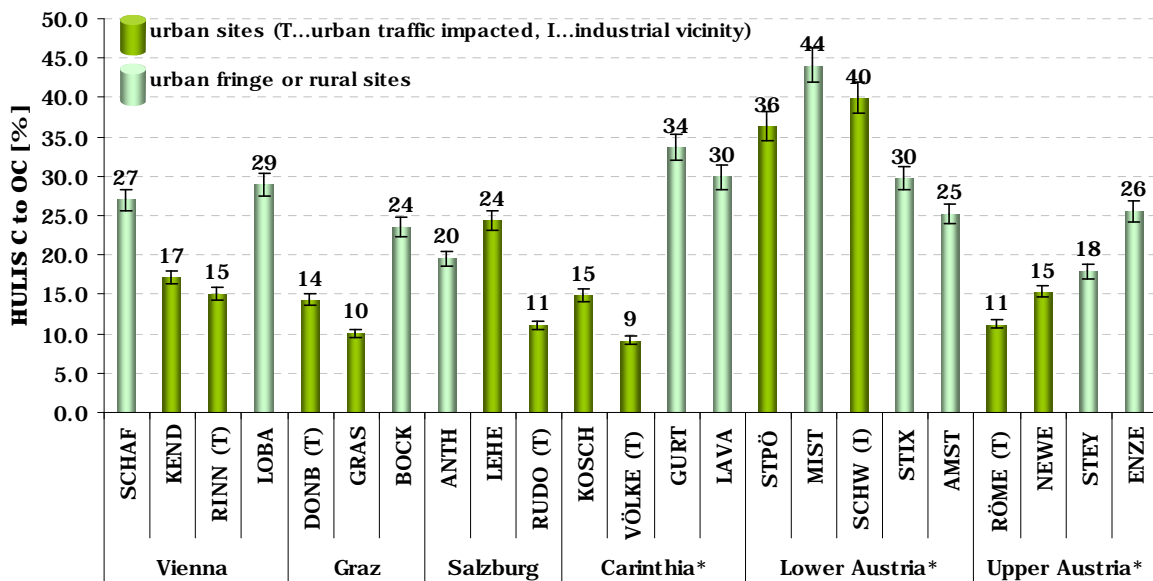


Figure 75: (Quasi-) annual average of HULIS_T carbon shares to OC in Austrian PM10; Vienna, Graz and Salzburg 12 month average; *Carinthia: November& December 2004, January-March & July 2005; Lower Austria: January-June 2005 (AMST April-June 2005); Upper Austria: April, May, June, October-December 2005, January-March 2006); bars indicate analytical uncertainty of HULIS carbon quantification.

The seasonal summarised contribution of HULIS_T C to OC at the urban traffic impacted sites (RINN, DONB, RUDO, RÖME, VÖLKE) in Vienna, Graz, Salzburg and Upper Austria ranged from 5.2-20.5% (Table 22 and Figure 98). Background and urban fringe sites revealed OC contributions from 8.9-52.8%. The share of HULIS_T carbon is roughly two times higher at the background sites compared to the respective urban sites. In Lower Austria HULIS_T generally contributed to OC in very high shares. At the site SCHW and MIST shares of around 40% and higher occurred throughout the sampling month. In June all Lower Austrian sites exceeded 40%. Even higher values were found at Carinthian background sites GURT and LAVA with HULIS_T C to OC ratios of 48.4 and 52.8%, respectively. Comparable results were reported by Feczko et al. (2007) who found relative fractions of HULIS_T carbon (as well defined as sum of HULIS_{AS} and HULIS_{WS}) in OC accounting for 15.4-26.3% at six continental background sites. HULIS_{WS} (in terms of

carbon) was reported to contribute to OC in ranges from 5-40% at an urban site in Vienna (Limbeck et al., 2005), 6-31% at an urban (Samburova et al., 2005b) and 10-33% at a suburban site in Zürich (Emmenegger et al., 2007) and from 12.7-22% at sites with varying characteristics in France (Baduel et al., 2010), what is good accordance with results from the present study considering that HULIS_{AS} roughly doubles the water soluble fraction.

To assess the contribution of HULIS to PM₁₀, HULIS related carbon was converted to organic matter. HULIS OC/ OM factors are reported in the range of 1.81-2.04 (Kiss et al., 2002; Krivácsy et al., 2002; Salma et al., 2007 and 2010; Lin et al., 2010a). A proxy factor of 1.9 was chosen to convert HULIS carbon to HULIS related OM in the present work. Average contributions of HULIS to PM₁₀ appeared in a range of 3.5-13 % (Figure 76). Note that averages are 12 month (Vienna, Graz and Salzburg), 9 month (Upper Austria) and 6 month averages (Lower Austria and Carinthia), respectively.

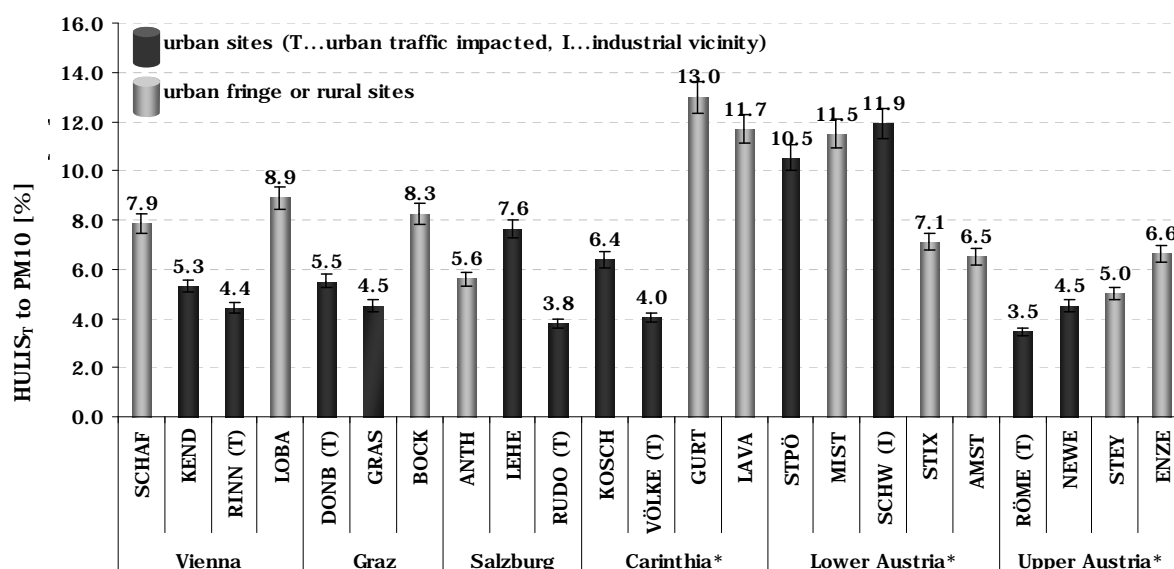


Figure 76: (Quasi-) annual average of HULIS_T contributions to PM₁₀; Vienna, Graz and Salzburg 12 month average; *Carinthia: November& December 2004, January-March & July 2005; Lower Austria: January-June 2005 (AMST April-June 2005); Upper Austria: April, May, June, October-December 2005, January-March 2006); bars indicate analytical uncertainty of HULIS carbon quantification.

8 HULIS over Austria- Spatial and temporal Variations of HULIST and Wood Smoke

Table 22: Seasonal averages of HULIS_T C and contributions to OC and PM10 at the 23 Austrian sampling sites

| | | Spring | Summer | Fall | Winter | Min | Max | Winter/ | |
|---------------|----------|-----------------|-----------------|-----------------|-----------------|--------------------|------|---------|-----|
| | | (Mar, Apr, May) | (Jun, Jul, Aug) | (Sep, Oct, Nov) | (Dec, Jan, Feb) | (monthly averages) | | summer | |
| Vienna | SCHA | 0.84 | 0.48 | 0.89 | 1.13 | 0.33 | 1.56 | 2.3 | |
| | KEND | 0.63 | 0.46 | 0.78 | 1.09 | 0.18 | 1.42 | 2.4 | |
| | RINN | 0.70 | 0.43 | 0.73 | 1.17 | 0.32 | 1.56 | 2.7 | |
| | LOBA | 0.89 | 0.50 | 1.04 | 1.42 | 0.33 | 1.88 | 2.8 | |
| | SCHA | 30.9 | 21.7 | 30.4 | 25.1 | 14.8 | 43.2 | 1.2 | |
| | KEND | 16.4 | 15.1 | 18.2 | 19.1 | 6.0 | 26.2 | 1.3 | |
| | RINN | 15.2 | 12.5 | 15.8 | 16.9 | 10.3 | 25.1 | 1.4 | |
| | LOBA | 30.8 | 19.3 | 32.0 | 33.7 | 10.0 | 49.7 | 1.7 | |
| | SCHA | 7.5 | 7.1 | 8.8 | 8.0 | 5.0 | 13.1 | 1.1 | |
| | KEND | 4.0 | 5.2 | 5.8 | 6.2 | 1.7 | 8.3 | 1.2 | |
| | RINN | 3.7 | 3.9 | 4.6 | 5.5 | 2.8 | 7.4 | 1.4 | |
| | LOBA | 8.6 | 7.0 | 10.1 | 9.9 | 4.6 | 15.9 | 1.4 | |
| Styria | DONB | 1.26 | 0.66 | 1.34 | 1.72 | 0.40 | 2.21 | 2.6 | |
| | GRAS | 0.80 | 0.45 | 0.86 | 1.05 | 0.26 | 1.54 | 2.4 | |
| | BOCK | 0.96 | 0.56 | 0.69 | 1.47 | 0.20 | 1.76 | 2.6 | |
| | DONB | 14.8 | 15.6 | 14.2 | 12.6 | 7.8 | 21.5 | 0.8 | |
| | GRAS | 11.6 | 11.8 | 10.6 | 6.9 | 2.9 | 17.0 | 0.6 | |
| | BOCK | 28.3 | 20.2 | 16.4 | 29.3 | 7.2 | 44.6 | 1.5 | |
| | DONB | 5.7 | 5.0 | 6.3 | 5.0 | 3.1 | 9.2 | 1.0 | |
| | GRAS | 4.8 | 4.2 | 5.0 | 3.9 | 1.5 | 6.7 | 0.9 | |
| | BOCK | 8.6 | 7.4 | 6.7 | 10.2 | 2.3 | 14.6 | 1.4 | |
| | Salzburg | ANTH | 0.49 | 0.28 | 0.44 | 0.62 | 0.12 | 1.03 | 2.2 |
| | | LEHE | 0.79 | 0.36 | 1.02 | 1.00 | 0.24 | 1.40 | 2.8 |
| | | RUDO | 0.62 | 0.41 | 0.59 | 0.82 | 0.06 | 1.15 | 2.0 |
| ANTH | | 22.4 | 14.6 | 18.2 | 23.0 | 6.7 | 40.8 | 1.6 | |
| LEHE | | 25.5 | 14.9 | 38.3 | 18.8 | 9.4 | 57.5 | 1.3 | |
| RUDO | | 9.2 | 11.5 | 12.8 | 11.0 | 1.9 | 15.3 | 0.9 | |
| ANTH | | 4.7 | 5.1 | 6.4 | 6.2 | 2.1 | 9.5 | 1.2 | |
| LEHE | | 7.4 | 5.4 | 11.5 | 6.3 | 3.5 | 14.1 | 1.2 | |
| RUDO | | 3.2 | 3.7 | 3.8 | 4.4 | 0.5 | 5.2 | 1.2 | |
| Carinthia | | KOSCH | 0.71 | 0.40 | 1.75 | 1.17 | 0.40 | 2.00 | 2.9 |
| | | VÖLKE | 0.69 | 0.18 | 2.18 | 1.03 | 0.18 | 2.18 | 5.8 |
| | | GURT | 1.58 | 1.13 | 1.79 | 1.63 | 1.13 | 1.87 | 1.4 |
| | LAVA | 1.61 | 1.23 | 1.19 | 1.50 | 1.15 | 2.10 | 1.2 | |
| | KOSCH | 10.3 | 19.3 | 24.3 | 11.8 | 7.5 | 24.3 | 0.6 | |
| | VÖLKE | 8.0 | 5.2 | 20.5 | 7.1 | 4.9 | 20.5 | 1.4 | |
| | GURT | 33.1 | 48.4 | 38.2 | 27.6 | 21.5 | 48.4 | 0.6 | |
| | LAVA | 29.4 | 52.8 | 27.0 | 23.4 | 18.4 | 52.8 | 0.4 | |
| | KOSCH | 4.5 | 5.3 | 11.3 | 5.8 | 3.5 | 11.3 | 1.1 | |
| | VÖLKE | 2.9 | 1.7 | 9.3 | 3.4 | 1.7 | 9.3 | 2.0 | |
| | GURT | 11.6 | 16.0 | 16.2 | 11.4 | 9.7 | 16.2 | 0.7 | |
| | LAVA | 10.4 | 16.1 | 12.0 | 10.6 | 8.0 | 16.1 | 0.7 | |
| Lower Austria | STPÖ | 1.47 | 1.36 | --- | 1.53 | 0.80 | 2.26 | 1.13 | |
| | MIST | 1.35 | 0.85 | --- | 2.12 | 0.85 | 2.45 | 2.50 | |
| | SCHW | 1.54 | 1.07 | --- | 2.22 | 1.07 | 2.66 | 2.08 | |
| | STIX | 1.02 | 0.70 | --- | 0.87 | 0.44 | 1.90 | 1.25 | |
| | AMST | 0.88 | 0.46 | --- | --- | 0.46 | 0.95 | --- | |
| | STPÖ | 36.9 | 52.6 | --- | 27.6 | 17.0 | 52.6 | 0.5 | |
| | MIST | 41.3 | 45.6 | --- | 47.3 | 30.1 | 55.5 | 1.0 | |
| | SCHW | 38.6 | 43.9 | --- | 39.8 | 28.7 | 49.1 | 0.9 | |
| | STIX | 31.1 | 48.0 | --- | 18.8 | 9.9 | 48.0 | 0.4 | |
| | AMST | 30.5 | 14.5 | --- | --- | 14.5 | 36.8 | --- | |
| | STPÖ | 10.3 | 13.7 | --- | 9.3 | 6.5 | 13.7 | 0.7 | |
| | MIST | 10.0 | 9.3 | --- | 14.8 | 6.5 | 15.9 | 1.6 | |
| SCHW | 11.0 | 10.5 | --- | 14.1 | 8.0 | 14.6 | 1.3 | | |
| STIX | 7.2 | 7.3 | --- | 6.8 | 3.7 | 10.8 | 0.9 | | |
| AMST | 7.6 | 4.3 | --- | --- | 4.3 | 9.7 | --- | | |
| Upper Austria | RÖME | 0.68 | 0.52 | 0.61 | 1.19 | 0.31 | 1.58 | 2.3 | |
| | NEWE | 0.86 | 0.40 | 0.88 | 1.06 | 0.40 | 1.71 | 2.6 | |
| | STEY | 0.65 | 0.32 | 0.87 | 1.32 | 0.29 | 2.25 | 4.1 | |
| | ENZE | 0.51 | 0.33 | 0.94 | 1.47 | 0.23 | 2.63 | 4.5 | |
| | RÖME | 12.4 | 9.6 | 9.2 | 11.9 | 8.2 | 15.7 | 1.2 | |
| | NEWE | 21.5 | 8.6 | 14.8 | 11.8 | 8.6 | 25.8 | 1.4 | |
| | STEY | 19.2 | 8.9 | 18.0 | 19.5 | 8.9 | 33.3 | 2.2 | |
| | ENZE | 22.4 | 11.0 | 30.3 | 30.4 | 11.0 | 43.6 | 2.8 | |
| | RÖME | 3.3 | 2.6 | 3.0 | 4.2 | 2.0 | 4.9 | 1.6 | |
| | NEWE | 5.6 | 2.8 | 4.5 | 4.0 | 2.7 | 6.9 | 1.4 | |
| | STEY | 4.7 | 2.3 | 5.6 | 5.8 | 2.3 | 9.1 | 2.5 | |
| | ENZE | 4.9 | 3.6 | 7.7 | 8.7 | 3.3 | 13.6 | 2.4 | |

8.2.4 Wood Smoke and HULIS_T - Comparison of atmospheric Abundance of HULIS_T and Levoglucosan

Here we report temporal evolution and spatial variations of HULIS_T carbon/levoglucosan ratios at 23 sampling sites in Austria (Table 23). The winter average, calculated from two and three month averages, respectively, ratios of HULIS_T carbon and levoglucosan occurred in a rather narrow range of 1.1- 5.9 whereas summer averages were higher at all sites and showed higher dispersion with values between 6.4 and 69.6. Calculation of HULIS_T C/ levoglucosan ratios from data reported by Puxbaum et al. (2007) and Feczko et al., (2007) for two continental background sites resulted in comparable values, for both seasons. The two sites in Portugal and Hungary showed ratios of 1.7 and 4.6 on winter average and 26 and 50 on summer average (Table 23). Mayol-Bracero et al. (2002) quantified a water-soluble polyacidic fraction that is assumed to correspond to the water extractable fraction of HULIS to large extents (Graber and Rudich, 2006), and levoglucosan in ambient PM_{2.5} during a major biomass event in Brazil. Resulting ratios ranged between 1.0 and 2.0, also being surprisingly similar to winter ratios in the present work, considering that burning of grazing land, wood, refuse and charcoal were involved in this burning event in Brazil, all of which types of combustion that are normally not considered to be the main source of central European biomass smoke, since most countries forbid the practice of garden waste burning common in past years (Schmidl et al., 2008b). However, once a year traditional Easter fires, very wide spread in southern Austria, resulting in PM₁₀ levels exceeding 100 µg/m³ (Bauer et al., 2007a; Wonaschütz et al., 2009) allow the open-air burning of wood and green waste. Such a period was observed in April 2004 in the region of Graz, with relatively high levels of HULIS between 2.53 -5.32 µg C/m³ and levoglucosan levels in the range of 1.16-2.06 µg/m³, resulting in HULIS carbon and levoglucosan ratios from 2.08-2.78. The ratios derived from literature data as well as the ratios in Austrian PM₁₀ in the present work are higher than those observed in emissions from combustion of wood in stoves commonly used for space heating. The average ratio, weighed according the Austrian fuel wood consumption, in the wood stove emission was 0.33 in a range of 0.11-0.68. Open burning of leaves on the contrary, leads to ratios of HULIS carbon and levoglucosan of 9.32 (Schmidl et al., 2008b).

8 HULIS over Austria- Spatial and temporal Variations of HULIST and Wood Smoke

Table 23: Summary of HULIS_T carbon and levoglucosan ratios in fine particulate matter and source emissions, calculated and compiled from recent literature^a, the AQUELLA and AQUELLIS project reports and related publications and the present work^b

| Ambient observations | Conditions | Resolution | Levoglucosan | | HULIS C | | HULIS C/levoglucosan | | Summer /winter | Ratios calculated from | | | | | | | |
|------------------------|---|---|----------------------|----------------------|----------------------|----------------------|----------------------|-------------------------|----------------|------------------------|---|------------|--|-------------|--|------|--|
| | | | [µg/m ³] | [µg/m ³] | [µg/m ³] | [µg/m ³] | | | | | | | | | | | |
| Brazil | Rondonia, pasture site | Open fires (wood, pasture, charcoal), PM2.5 | 12-46 hours | 3.2 (1.5-6.9) | | 5.26 (2.8-12.2) | | 1.6 (1.0-2.0) | | --- | Mayol-Bracero et al., 2002 ^a | | | | | | |
| European background | Azoren Aveiro, Portugal K-Pusztá, Hungary Sonnblick, Austria Puy de Dôme, France Schauinsland, Germany | PM 2.5 | Seasonal average | Winter | Summer | Winter | Summer | Winter | Summer | | | | | | | | |
| | | | | 0.006 | 0.002 | 0.047 | 0.117 | 7.8 | 58.5 | 7.5 | | | | | | | |
| | | | | 1.3 | 0.03 | 2.18 | 0.78 | 1.7 | 26 | 15.3 | | | | | | | |
| | | | | 0.65 | 0.02 | 3 | 1 | 4.6 | 50 | 10.9 | | | | | | | |
| | | | | 0.01 | 0.01 | 0.042 | 0.296 | 4.2 | 29.6 | 7.0 | | | | | | | |
| | | | | 0.02 | 0.007 | 0.19 | 0.54 | 9.5 | 77.1 | 8.1 | | | | | | | |
| | | | | 0.03 | 0.01 | 0.39 | 0.24 | 13 | 24 | 1.8 | | | | | | | |
| Wood stove emissions | Source emission | PM10 | n= 11 | --- | | --- | | 0.33^c | | --- | | | | | | | |
| Open air leave burning | Source emission | PM10 | n=2 | --- | | --- | | 9.32 | | --- | | | | | | | |
| Styria, Easter fires | DONB (urban) GRAS (urban) BOCK (background) | PM10 (Easter fire) | 2-day average | 1.91 | | 5.32 | | 2.78 | | --- | | | | | | | |
| | | | | 2.06 | | 4.28 | | 2.08 | | --- | | | | | | | |
| | | | | 1.16 | | 2.53 | | 2.18 | | --- | | | | | | | |
| Vienna | SCHA (urban fringe) KEND (urban) RINN(urban) LOBA (urban fringe) | PM10 | Seasonal average | Winter | Summer | Winter | Summer | Winter | Summer | | | | | | | | |
| | | | | 0.25 | 0.02 | 1.13 | 0.48 | 4.4 | 25.5 | 5.7 | | | | | | | |
| | | | | 0.29 | 0.02 | 1.09 | 0.46 | 3.7 | 26.5 | 7.2 | | | | | | | |
| | | | | 0.32 | 0.03 | 1.17 | 0.43 | 3.6 | 15.4 | 4.3 | | | | | | | |
| | | | | 0.28 | 0.02 | 1.42 | 0.50 | 5.0 | 23.9 | 4.8 | | | | | | | |
| Graz | DONB (urban) GRAS (urban) BOCK (background) | PM10 | Seasonal average | 0.88 | | 0.05 | | 1.72 | | 0.66 | | 1.9 | | 12.6 | | 6.5 | |
| | | | | 0.97 | | 0.06 | | 1.05 | | 0.45 | | 1.1 | | 8.1 | | 7.5 | |
| | | | | 0.55 | | 0.05 | | 1.47 | | 0.56 | | 2.7 | | 10.6 | | 4.0 | |
| Salzburg | ANTH (background) LEHE (urban) RUDO (urban) | PM10 | Seasonal average | 0.32 | | 0.03 | | 0.62 | | 0.28 | | 1.9 | | 9.6 | | 5.0 | |
| | | | | 0.53 | | 0.04 | | 1.00 | | 0.36 | | 1.9 | | 9.3 | | 4.9 | |
| | | | | 0.43 | | 0.04 | | 0.82 | | 0.41 | | 1.9 | | 10.0 | | 5.2 | |
| Carinthia* | KÖSCH (urban) VÖLKE (urban) GURT (background) LAVA (background) | PM10 | Seasonal average | 0.81 | | 0.03 | | 1.17 | | 0.40 | | 1.4 | | 11.7 | | 8.5 | |
| | | | | 0.74 | | 0.02 | | 1.03 | | 0.18 | | 1.4 | | 11.6 | | 9.0 | |
| | | | | 0.63 | | 0.03 | | 1.63 | | 1.13 | | 2.6 | | 34.3 | | 12.4 | |
| | | | | 0.84 | | 0.03 | | 1.50 | | 1.23 | | 1.8 | | 45.5 | | 23.2 | |
| Lower Austria* | STPÖ(urban) MIST(background) SCHW (urban) STIX (background) AMST (background) | PM10 | Seasonal average | 0.44 | | 0.04 | | 1.53 | | 1.36 | | 3.4 | | 37.7 | | 11.1 | |
| | | | | 0.40 | | 0.02 | | 2.12 | | 0.85 | | 5.2 | | 37.6 | | 7.2 | |
| | | | | 0.38 | | 0.02 | | 2.22 | | 1.07 | | 5.9 | | 68.7 | | 11.7 | |
| | | | | 0.42 | | 0.01 | | 0.87 | | 0.70 | | 2.1 | | 69.6 | | 28.3 | |
| | | | | --- | | 0.06 | | --- | | 0.46 | | --- | | 7.6 | | --- | |
| Upper Austria* | RÖME (urban) NEWE (urban) STEY (urban fringe) ENZE (background) | PM10 | Seasonal average | 0.59 | | 0.04 | | 1.19 | | 0.52 | | 2.0 | | 14.5 | | 7.3 | |
| | | | | 0.54 | | 0.06 | | 1.06 | | 0.40 | | 2.0 | | 6.4 | | 3.2 | |
| | | | | 0.57 | | 0.05 | | 1.32 | | 0.32 | | 2.3 | | 6.9 | | 2.8 | |
| | | | | 0.56 | | 0.04 | | 1.47 | | 0.33 | | 2.6 | | 9.1 | | 3.0 | |

^a HULIS from Mayol-Bracero et al., 2002 is originally termed polyacidic fraction, assumed to overlap with chemical and physical properties of HULIS_{WS} to a large extent, though in this case the different terms are used interchangeably; numbers in parenthesis give minimum and maximum values occurring on daily base during the sampling period (9 days).

^b HULIS_T quantification and calculations of ratios were conducted in the scope of the present work; results of levoglucosan and/or HULIS_T analysis are parts of the publications from Caseiro et al. (2009), Schmidl et al. (2008a and 2008b), Wonaschütz et al. (2009) and the AQUELLA/AQUELLIS project reports (Bauer et al., 2006, 2007a, 2007b, 2008a, 2008b, 2008c; Puxbaum et al., 2006, Schmidl et al., 2008c).

^c factor calculated according to Austrian fuel wood consumption; for detailed description and discussion see section 7.3.8.1.

* Vienna, Graz and Salzburg: winter averages (January, February, December 2004)) and summer averages (June – August 2004); winter averages: Carinthia: December 04 to February 05; Upper Austria: December 05 to February 06, Lower Austria: January and February 05. Summer averages: Carinthia and Upper Austria: July 05; Lower Austria: June 05.

These observations confirm that secondary formation and contribution from sources with different emission patterns contribute to atmospheric HULIS levels. Seasonal averaged HULIS carbon and levoglucosan ratios in Vienna, Graz and Salzburg maximise in summer with values 4-7 times higher than in winter. Intermediate values occurred during transition month (Figure 77) lying closer to winter than to summer values. As mentioned before, seasonal averages observed in the present work were found to be in remarkable agreement with ratios calculated from Puxbaum et al. (2007) and Feczko et al. (2007). The winter ratios for two low level background sites with comparable levoglucosan levels as found in Austria were 1.7 and 4.6 for the rural maritime site Aveiro (Portugal) and the continental site K-Pusztá. The lower factor at the site in Portugal, closer to anthropogenic emission sources, shows more resemblance with the sites in Salzburg and Graz, which showed higher levoglucosan levels in 2004 (Caseiro et al., 2009) than the Vienna sites. The winter average ratio at the more remote site at K-Pusztá Hungary (4.6) fits very well in the observed winter range at the Vienna sites (3.6-5).

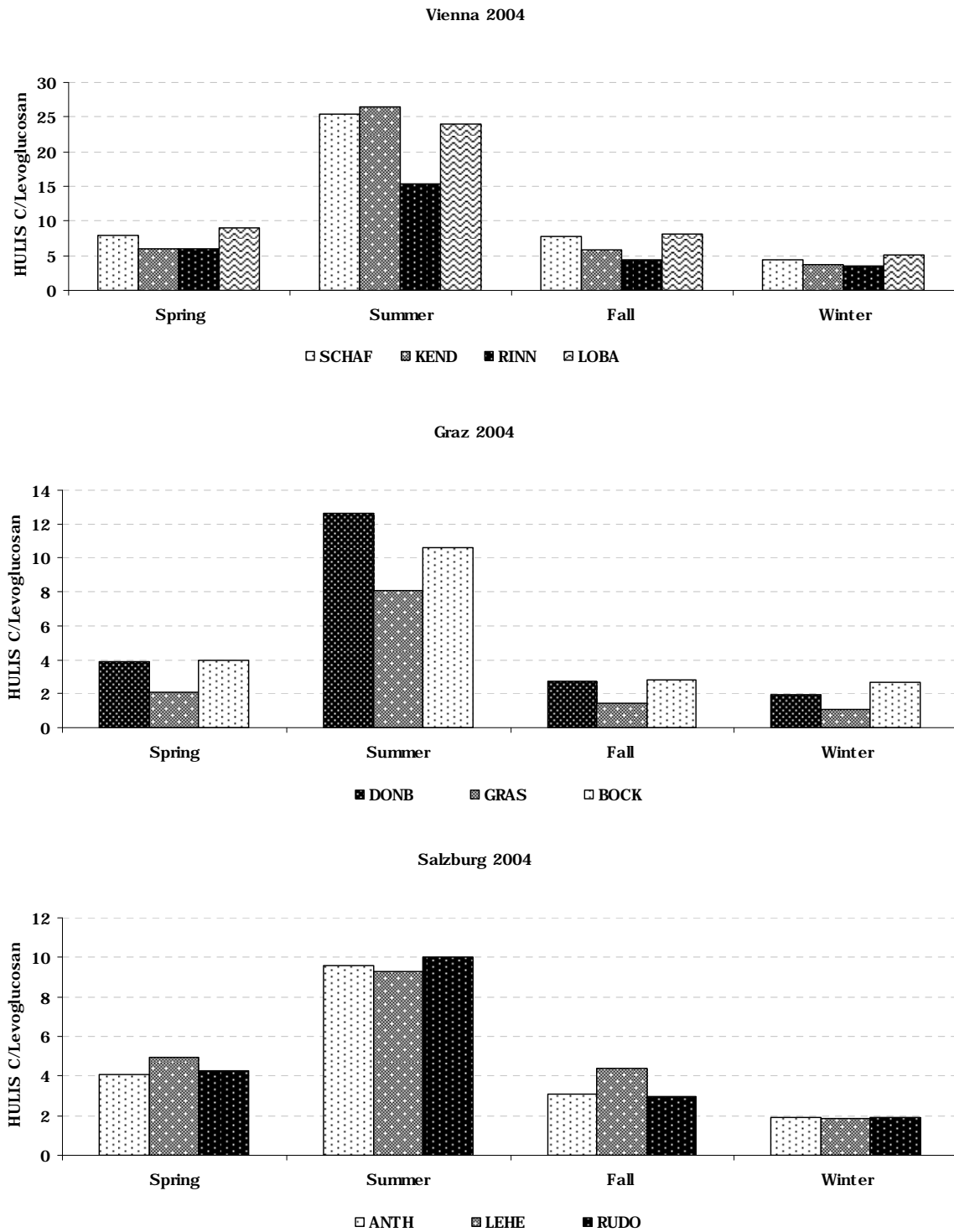


Figure 77: HULIS_T C/Levoglucosan ratios Vienna, Graz and Salzburg, 2004.

Devolution of HULIS_T carbon to levoglucosan ratios over the sampling periods in Carinthia, Lower Austria and Austria (depicted in Figure 78, Figure 79 and Figure 80) show as well significantly lower HULIS_T carbon to levoglucosan ratios during the cold month and a significant increase during summer month.

Carinthia 2004/2005

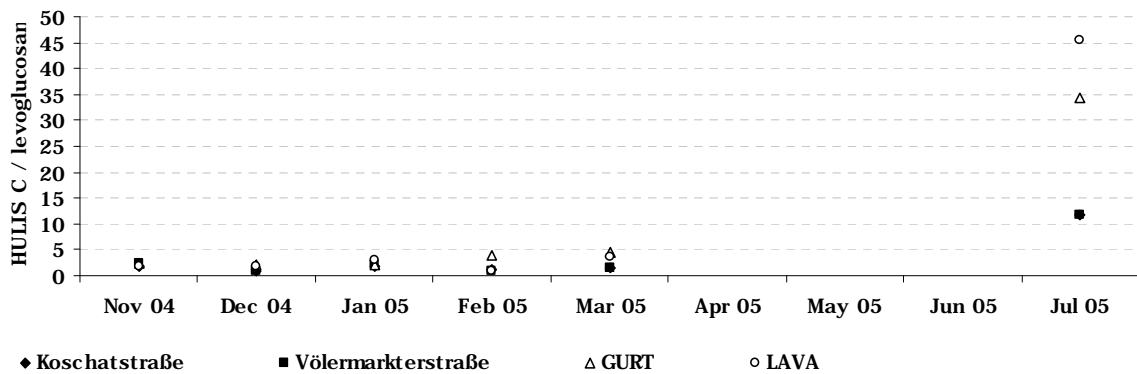


Figure 78: Monthly averaged HULIS carbon to levoglucosan ratios (a.u.), Carinthia.

Lower Austria 2005

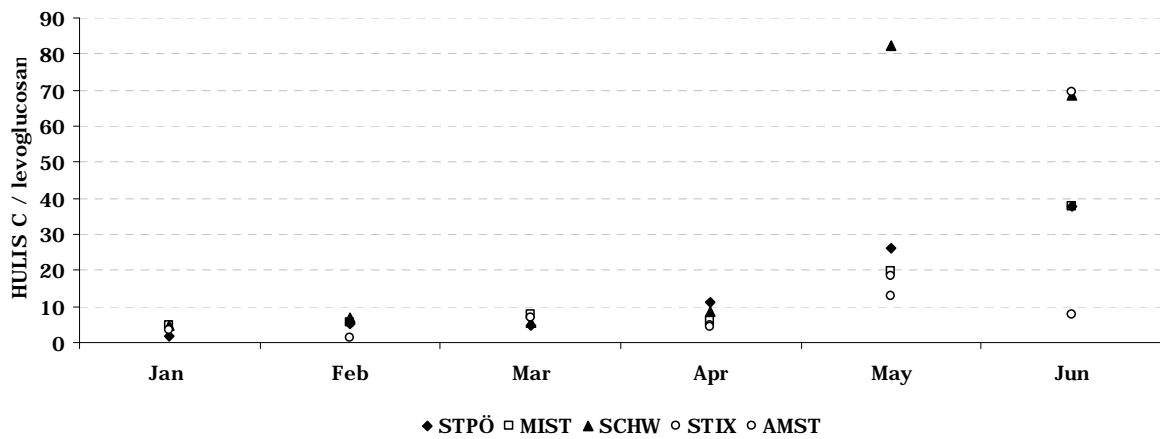


Figure 79: Monthly averaged HULIS carbon to levoglucosan ratios (a.u.), Lower Austria, 2005.

Upper Austria 2005/2006

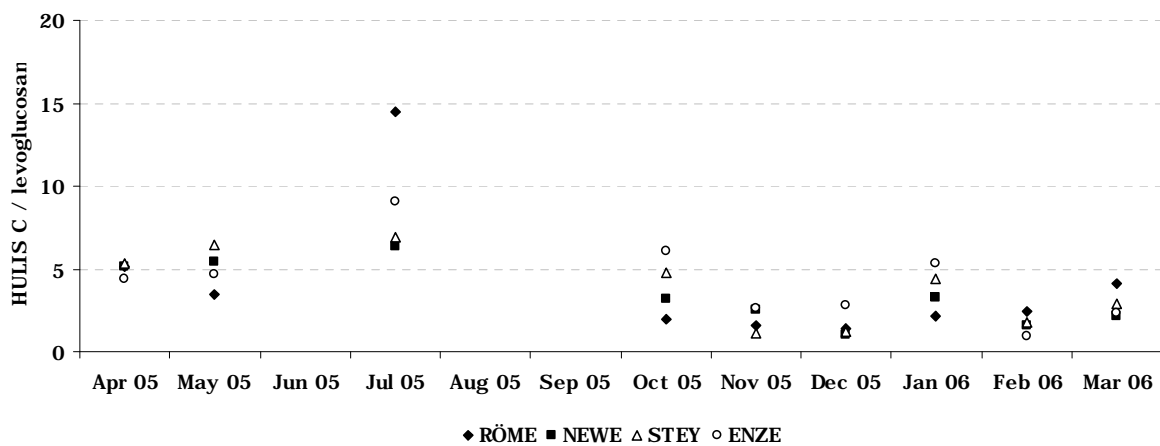


Figure 80: Monthly averaged HULIS_T carbon to levoglucosan ratios (a.u.), Upper Austria, 2005.

Wintry HULIS C/levoglucosan ratios ranged from 1.4 to 2.6 (Carinthia), 2.1-5.9 (Lower Austria) and 2-2.6 (Upper Austria). Carinthian and Upper Austrian winter ratios compare very well with those of Graz and Salzburg whereas the higher ratios observed in Lower Austria fit well to Viennese HULIS carbon/levoglucosan ratios. Enhanced HULIS/levoglucosan ratios during summer at all the investigated sites in the range of 6.4-69.6 in Austria, indicate a change of source types responsible for levoglucosan emissions as well as additional HULIS/ HULIS precursor sources and higher formation rates in summer. Beside long range transported aerosol impacted by open fires, primary emissions from fossil fuel combustion, these summer origins can be formation from gaseous biogenic or anthropogenic precursors (Baduel et al., 2010; Salma et al., 2010). However, the seasonal appearance of HULIS_T C/levoglucosan ratios most likely reflects the influence of biomass burning for space heating during winter and transition month on HULIS levels at most sites.

Wintry HULIS_T C/levoglucosan ratios furthermore revealed a trend (with the exception of the site STIX) for higher values in Eastern Austrian regions (3.4 -5.9) and lower in western and southern Austria (1.1-2.7) (Figure 82). Summer ratios showed generally the same trend where one should note that Lower Austria, Upper Austria and Carinthian summer values only consist of an weighed one month average whereas Vienna, Graz and Salzburg summer HULIS_T C/levoglucosan ratios include the entire summer period (June-August). Winter ratios showed a tendency to be higher at the background and suburban sites, respectively, in Vienna, Salzburg, Carinthia and Upper Austria. In Salzburg HULIS C/levoglucosan winter ratios showed equal values at all three sites, whereas Lower Austrian sites showed highest values at a traffic impacted site (Schwechat, impacted by emissions from Vienna) and a background site (Mistelbach).

Significant correlation of HULIS_T and levoglucosan was observed for most, but not all, sites in winter. We observed significant and good correlation for the sites in Vienna ($r \sim 0.74-0.93$) and Salzburg ($r \sim 0.70-0.88$). Correlations were lower, though still significant, at the sites in Graz ($r \sim 0.45-0.75$) although the region of Graz is higher impacted by biomass smoke (Caseiro et al., 2009), what again indicates, that biomass smoke is an important source for HULIS or their precursor but additional conditions have influence on the atmospheric appearance of HULIS_T. Similar levels of levoglucosan as observed in Graz, occurred in Carinthia, where significant but rather weak correlation was observed at the urban site. In Lower Austria HULIS_T carbon and levoglucosan were only weakly, or in case of STPÖ, not correlated significantly, although visually two main “branches” of HULIS carbon and levoglucosan ratios appeared, indicating the influence of different air masses (Figure 81). A ratio of HULIS_T C and levoglucosan of ~ 2 and ~ 4 , the former more typical for the background site STIX and the latter for the sites STPÖ, MIST and SCHW, appears to be typical during winter month.

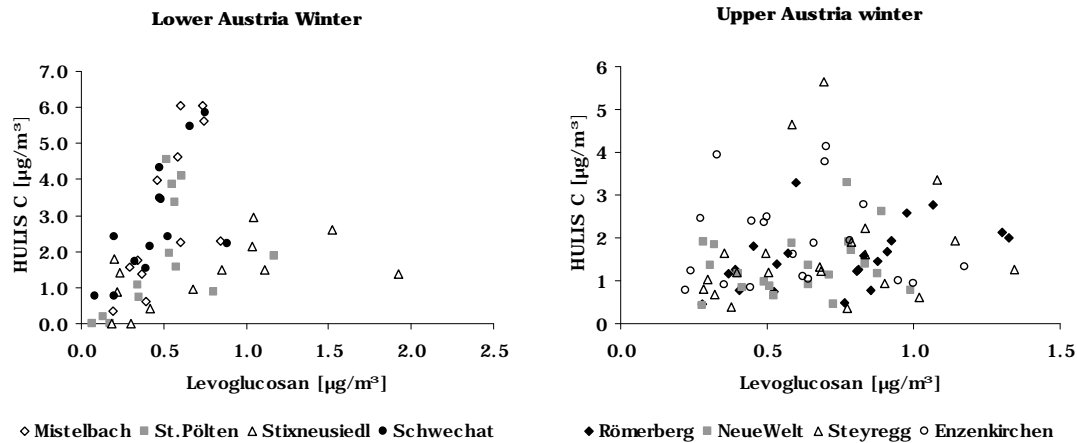


Figure 81: Comparison of HULIS_r carbon and levoglucosan in Lower Austria (left) and Upper Austria (right)

Weak, though still significant, positive correlation in Upper Austria appeared only at the urban traffic impacted site RÖME ($r=0.466$), whereas HULIS carbon levels at the site NEWE in the industrial zone of the city, and the urban fringe site and the rural background site seem not to be connected to a biomass burning source.

Significant positive correlations in summer appeared at two urban sites (RÖME, $r=0.977$; GRAS, $r=0.832$) and two background sites Bockberg (BOCK, $r=0.894$; ANTH, $r=0.965$) with ratios at the lower end of the summer scale 8.1-14.5. A connection of biomass smoke and ambient HULIS carbon levels at HULIS carbon and levoglucosan ratios of 10 ± 5 % therefore might be typical for regions that are impacted by open biomass burning, most likely via the regional or long-range transport of air masses. Since only a low number of data pairs in summer ($n=4-8$) were available, the non-correlation of HULIS carbon and levoglucosan at other sites does not exclude them from these considerations.

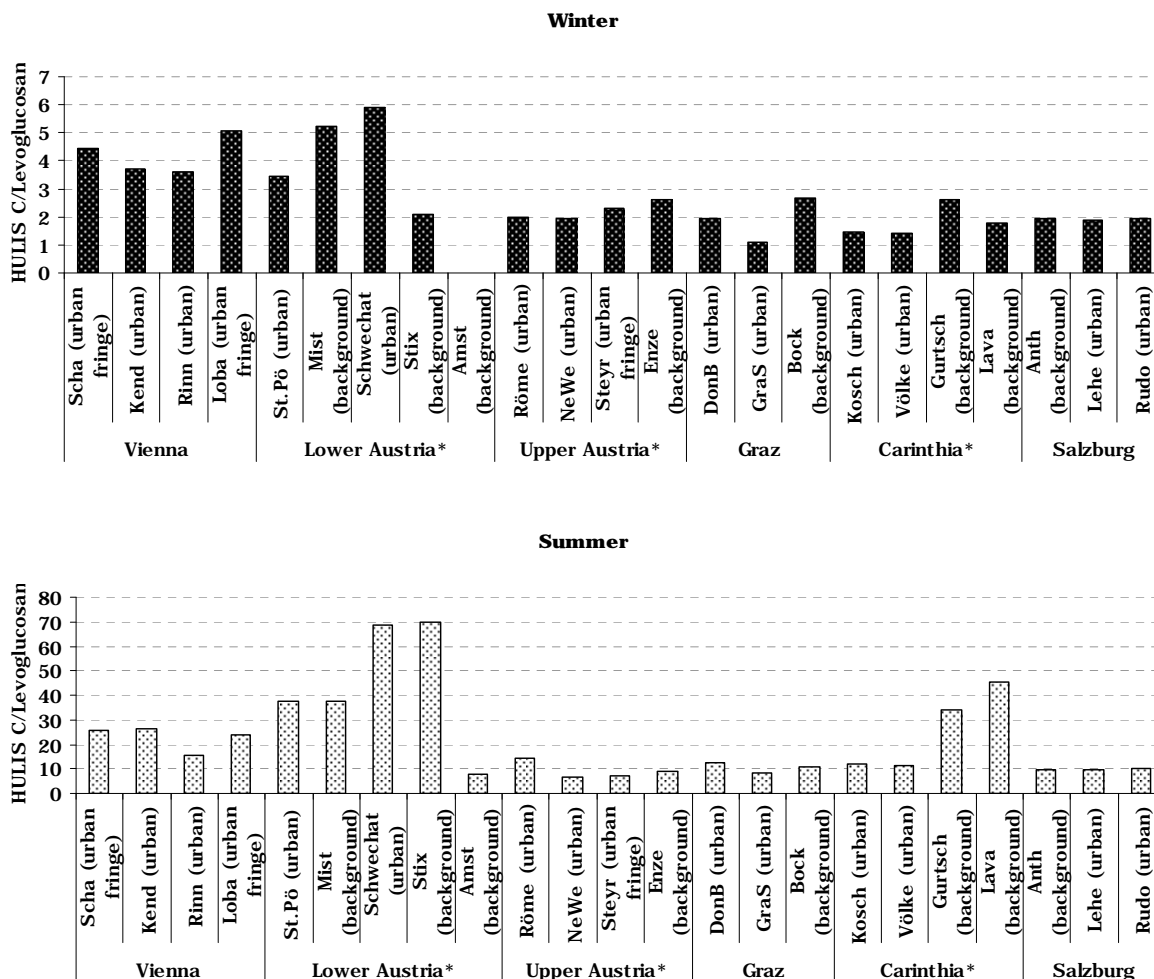


Figure 82: Comparison of HULIS_T C/levoglucosan ratios in Austria. Vienna, Graz and Salzburg: winter (January, February, December 2004) and summer (June – August 2004). *winter: Carinthia: December 04 to February 05; Upper Austria: December 05 to February 06, Lower Austria: January and February 05. Summer: Carinthia and Upper Austria: July 05; Lower Austria: June 05.

8.3 Discussion

Comparing the 23 Austrian sites averaged HULIS_T concentrations appeared in a range of 0.46 -1.61 $\mu\text{g C}/\text{m}^3$, the former occurring at a rural background site in Salzburg (ANTH) and the latter at an urban site in Lower Austria (SCHW). The abundance of atmospheric HULIS_T did not show a trend to occur preferred at sites with specific characteristics. Regarding the respective regions HULIS levels at background sites were slightly higher or similar than the respective urban sites (Vienna, Upper Austria), markedly lower (Salzburg) or higher (Carinthia). In Lower Austria HULIS_T levels at two background sites (STIX, AMST) were markedly lower and similar (MIST) to the urban sites, respectively. The majority of the 23 sampling sites showed maximum HULIS_T concentrations in fall or winter with a winter enrichment factor in the range of 2-4. Only four sites did show almost no seasonality. Two background sites in Carinthia and the urban site in the capital of Lower Austria (STPÖ) showed no or very weak seasonality at a rather high HULIS_T

level of $1.4 \pm 0.3 \mu\text{g C/m}^3$, pointing to constant and rather effective source emissions, such as industrial activities, related to the atmospheric occurrence of HULIS_T.

Average contributions (annual average in Vienna, Graz and Salzburg, six month average for Carinthia and Lower Austria, nine month average for Upper Austria) of HULIS_T carbon at the 23 sites varied between 9 and 44 %. Average contributions of HULIS_T to PM10 appeared in a range of 0.5-16.2%. A proxy factor for the conversion of HULIS_T related carbon to organic matter of 1.9 was applied (Kiss et al., 2002; Krivácsy et al., 2002; Salma et al., 2007 and 2010; Lin et al., 2010a).

The impact of wood smoke and its relation to HULIS_T was assessed by comparison of HULIS_T and levoglucosan levels. Ratios of HULIS_T carbon and levoglucosan were calculated from studies reported in literature at six background sites in Europe (Feczko et al., 2007) and a major biomass burning event in Brazil (Mayol-Bracero et al., 2002) and were in excellent agreement with results from the present study. HULIS carbon and levoglucosan ratios at a major biomass burning event in Styria ranged from 2.08-2.78. The winter average, calculated from two and three month averages, respectively, of HULIS_T carbon and levoglucosan ratios occurred in a rather narrow range of 1.1- 5.9. The average ratio, weighed according the Austrian fuel wood consumption, in samples from wood stove emission was 0.33 in a range of 0.11-0.68. Open burning of leaves on the contrary leads to ratios of HULIS carbon and levoglucosan of 9.32 (Schmidl et al., 2008b). Seasonal averaged HULIS carbon and levoglucosan ratios in Vienna, Graz and Salzburg maximise in summer with values 4-7 times higher than in winter. Intermediate values occurred during transition month lying closer to winter values. Wintry HULIS_T C/levoglucosan ratios furthermore revealed a trend for higher values in Eastern Austrian regions (3.4 -5.9, with the exception of the site STIX) and lower in western and southern Austria (1.1-2.7) and a tendency to be lower at urban sites. Summer ratios showed generally the same trend and were higher at all sites and showed higher dispersion of HULIS_T carbon and levoglucosan ratios in the range of 6.4-69.6.

Significant correlation of HULIS_T and levoglucosan was observed for most, but not all, sites in winter. We observed significant and good correlation for the sites in Vienna ($r \sim 0.74-0.93$) and Salzburg ($r \sim 0.70-0.88$). Lacking correlation of HULIS_T and levoglucosan levels at the background and urban fringe sites in Upper Austria and Carinthia indicate other sources than wood smoke.

Significant positive correlations in summer appeared at two urban sites (RÖME, $r=0.977$; GRAS, $r=0.832$) and two background sites (BOCK, $r=0.894$; ANTH, $r=0.965$) with ratios of HULIS_T/ levoglucosan at the lower end of the summer scale (8.1-14.5). A connection of biomass smoke and ambient HULIS_T carbon levels at HULIS_T carbon and levoglucosan ratios of 10 ± 5 therefore might be typical for regions that are impacted by open biomass burning or agricultural fires in summer, most likely via the regional or long-range transport of air masses. Since only a low number of data pairs in summer ($n=4-8$) were

available, the non-correlation of HULIS_T carbon and levoglucosan at other sites does not exclude them from these considerations.

The general trend for higher HULIS_T to levoglucosan ratios in the well ventilated Eastern part of Austria might make the ratio suitable to distinguish between local or regional/supraregional origin of HULIS_T.

9 Thermal Characterisation of HULIS_{AS} and HULIS_{WS} isolated from Upper Austrian PM10

Thermal methods have a long tradition in aerosol science (Puxbaum, 1979; Ellis and Novakov, 1982) and have been used widely to investigate thermal stability, volatilization and oxidation properties of the bulk carbonaceous species as well as black carbon (Jankowski et al., 2008; Gelencsér, 2004). Where there are few studies on the thermal characteristics of bulk WSOC (Yu et al. 2002, 2004) and water-insoluble fractions of airborne PM10 (Gelencsér et al., 2000a; Mayol-Bracero et al., 2002; Hoffer et al., 2006a) there are even fewer studies that report on subfractions of WSOC (Duarte et al., 2008; Cheng et al., 2012). To the best of our knowledge the present work is the first that investigates isolated alkaline and water soluble fractions of HULIS with a thermal method. In the present work water and alkaline soluble fractions of HULIS isolates were investigated with a thermal-optical transmission method with linear temperature programme to shed light on thermal stability, volatilization and oxidation properties. Resulting thermograms are qualitatively investigated on similarities and differences between “summer” and “winter” HULIS, aqueous and alkaline extracted HULIS isolates and HULIS from rural and urban sites.

9.1 Sampling Sites and chemical Analysis

Two sites in Upper Austria were chosen for thermal characterisation of the alkaline and water soluble fractions of HULIS: the rural background site Enzenkirchen (ENZE, 13° 40' 16.1" E, 48° 23' 30.2" N, 525 m a.s.l.) and the urban traffic impacted site Römerberg (RÖME, 14° 16' 58.0" E, 48° 18' 10.0" N, 262 m a.s.l.) in the capital of Upper Austria (Figure 31). Beside the traffic emissions, Linz is also influenced by an industrialized area near the city centre (Umweltbundesamt, 2009). Sampling and weighing was conducted by the local authority and took place daily in July 2005 and January 2006 on both sites (for detailed description of sampling and sampling sites see sections 4 and 5.1). Sampling and analysis were part of the AQUELLA/AQUELLIS project. HULIS isolation, quantification and their recording of the thermograms were conducted in the scope of the present work. Analysis of other species and parameters were conducted by the AQUELLA-team and taken from the AQUELLA data base. Results of HULIS analysis are parts of the publications from Schmidl et al. (2008a and 2008b), Wonaschütz et al. (2009) and the AQUELLA/AQUELLIS project reports (Bauer et al., 2006, 2007a, 2007b, 2008a, 2008b and 2008c; Puxbaum et al., 2006, Schmidl et al., 2008c and Jankowski et al., 2009a and 2009b).

9 Thermal Characterisation of HULISAS and HULISWS isolated from Upper Austrian PM10

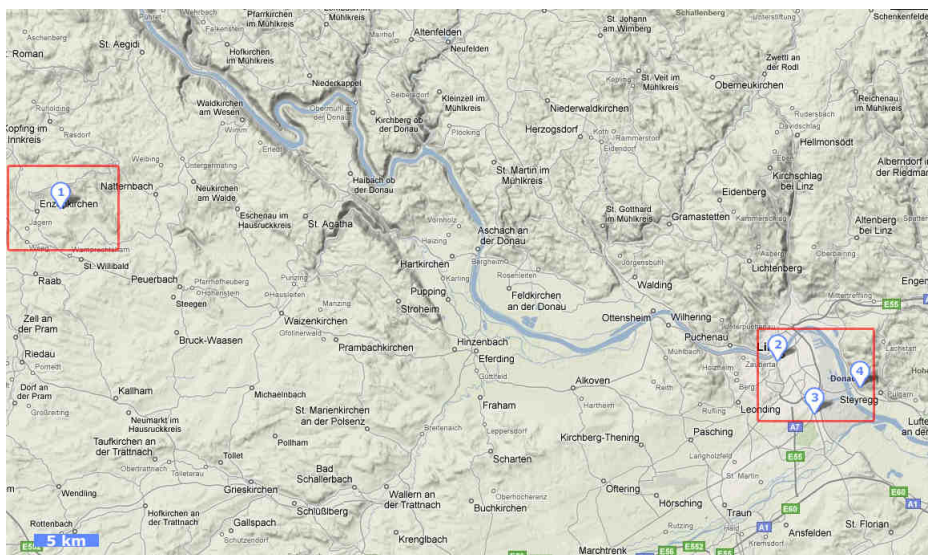


Figure 83: Sampling sites Oberösterreich. 1: Enzenkirchen (background site), 2: Römerberg (urban traffic impacted site); based on Google maps, supplemented with marks for sampling sites/regions.

Aliquots of PM10 filters from each filter in July and January, respectively, were pooled and subjected to water and subsequent alkaline extraction. Extraction and isolation procedure are described in detail in section 6.1. Since the thermal investigations requires higher amounts of HULIS than their quantification the, second isolation step was conducted off-line on a SAX cartridge, instead of introducing the samples in the flow-injection system. HULIS isolates (eluates after the SAX-step in a matrix of diluted ammonium hydroxide) were dropped on quartz fibre filters with a diameter of 12mm and dried in an exsiccator over silica gel at room temperature for about 2 hours. Resulting carbon loads on the filter punches were in the range of 5-10 $\mu\text{g C/cm}^2$.

After drying filters showed slight colouration from bright yellow to light brown. A sample punch of the quartz fibre filter (10 or 12mm diameter) was placed in a horizontal furnace FROK 200/50/1000 (AHT Austria) at room temperature in oxygen and then heated in O_2 (4.8) to 800°C at a rate of 20°C/min. A manganese oxide catalyst heated to 700°C converts the carbonaceous gases to CO_2 , which is continuously measured using an NDIR analyzer (Maihak UNOR 6N). During the heating procedure the transmittance of a laser beam through the filter punch is recorded. The change of the transmittance in general gives information about charring phenomena of the organic carbon leading to increased blackness of the filter. For details see Bauer et al. (2006) and references therein. Due to the slight colouration of the filter the change of the laser signal was very weak and though not evaluable in case of the HULIS isolates.

9.2 Results

9.2.1 The Colour of HULIS and thermal Characteristics of Humic Acid Standards

Figure 84 depicts the isolated HULIS in diluted ammonium hydroxide showing colours of extracts from almost colourless (aqueous extracted HULIS, July) to a strong gold-brown (alkaline extracted HULIS, January). The extraction procedure was as well applied on wood chips (beech). HULIS isolated from alkaline extracts, gained from filter aliquots before extracted with ultrapure water, showed more intense and more brownish colouration, respectively, for HULIS from urban and rural winter PM10.

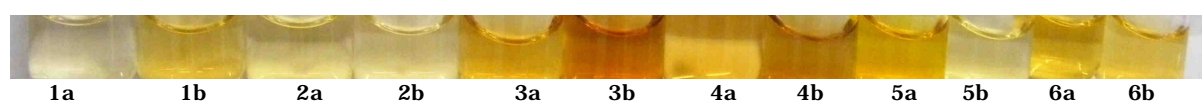


Figure 84: Colours of pure HULIS extracted from PM10 (1-4), wood chips (5) and potting soil (6). 1: urban summer; 2: rural summer; 3: urban winter, 4: rural winter, 5: wood chips, 6: potting soil. A: HULIS isolated from water extracts; b: HULIS isolated from alkaline extracts (note that alkaline extraction was conducted on before water-extracted filter samples).

The colours of HULIS isolates appear in the same range of yellow to brown colouring as reported for fulvic and humic acids (Stevenson et al., 1994). The filter areas from winter and summer samples, subjected to the extraction and preparative isolation of HULIS, were very similar, though the general less intense colouration of HULIS isolated in summer mainly reflects the 3- 5 times lower concentrations. Alkaline extracted HULIS from urban samples (winter and summer) and for wintry rural HULIS isolates appeared in a stronger colouration than their water extracted counterparts. Isolates from the rural site in summer and wood chips and potting soil showed rather same coloration for both HULIS fractions and, in case of extracts from wood chips, stronger coloration for HULIS_{WS}.

Recorded thermograms of solid humic acid revealed two quite well resolved peaks with peak maxima at 295°C and 475°C, respectively, where ~20 % of the carbon evolves at the lower temperature peak. This behaviour is as well observed for its alkaline soluble fraction, extracted in 0.1M sodium hydroxide coherent with the definition of humic acid to be completely soluble at high pH (Stevenson et al., 1994). The aqueous extracted humic acid fraction, which represents the standard utilised for the quantification of HULIS applied in the present work, showed maximum signal strength at ~300 °C and smaller, shoulders at ~ 350 and 450 °C, respectively (Figure 85). The lower temperature peak represents a subfraction of humic acid with higher water solubility and lower molecular weight according the definition and fractionation protocols for aquatic and terrestrial humic substances (Stevenson et al., 1994). Andreae et al. (2006) recorded a similar thermogram for solid humic acid with two rather well resolved peaks at around 400°C

and 600°C. The authors did not provide details on experimental conditions such as heating rate and the combustion atmosphere, though most likely different experimental conditions are the reason for the peaks evolving at higher temperatures.

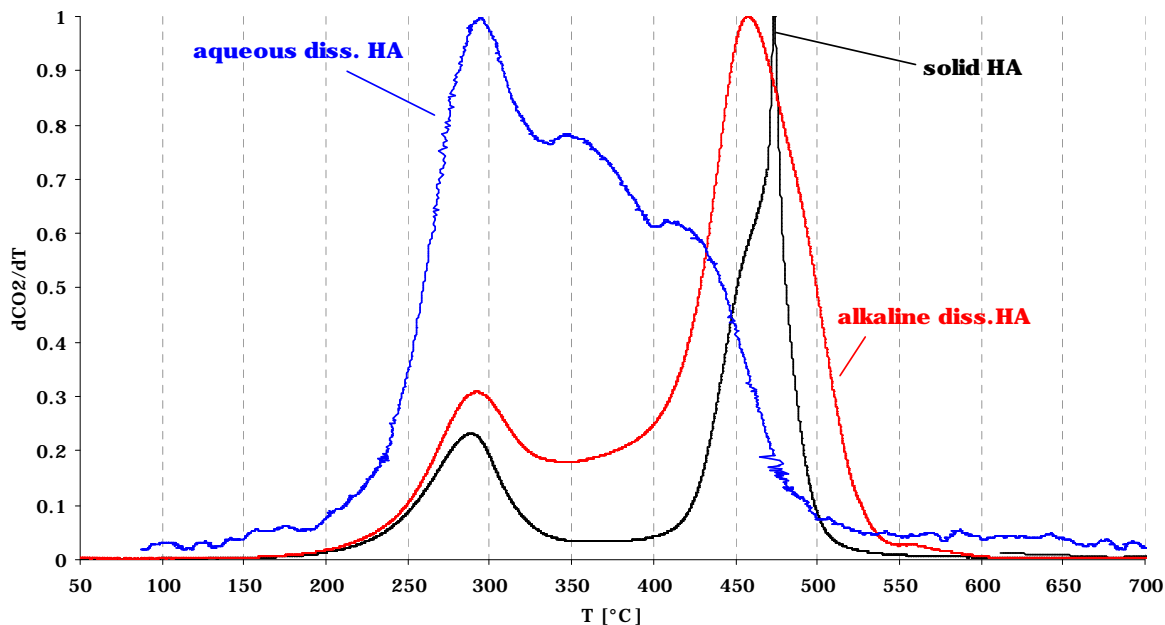


Figure 85: Thermograms of solid humic acid (HA), alkaline dissolved humic acid and humic acid dissolved in ultra-pure water

9.2.2 General Characteristics of Thermograms of HULIS

Thermal methods are widely used to characterise ambient carbonaceous bulk particulate matter and to differ between organic and elemental carbon (e.g. Bauer et al., 2006; Jankowski et al., 2008) and to quantify these two fractions. Volatile and semi-volatile compounds are oxidised at temperatures below 250°C whereas non-volatile carbonaceous compounds decompose or combust in the range of 250-400°C (Bauer et al., 2006). Signals in a temperature range of 400-500°C and above are attributed to the combustion of soot and the decarboxylation of calcium carbonates, respectively (e.g. Jankowski et al., 2008; Bauer et al., 2007a). Thermograms of HULIS_{AS} and HULIS_{WS} extracted from urban and rural PM10 in July and January as well as isolates gained through application of the HULIS isolation protocol on wood chips and potting soil, showed carbon signals in the range of 100-650°C. Peak maxima occurred in the range of 300-350°C (Figure 87, Figure 88). As shown in section 7.3.2, the water-soluble fraction of humic acid showed very similar thermal characteristics as HULIS isolated from ambient PM10, concerning their major peak maximising slightly below 300°C. An obvious difference of HULIS thermogram compared to those of water-soluble humic acid standard is the wider temperature range of evolving carbon dioxide (Figure 86). The signals in the high volatility region between 100 and 200°C (Figure 87 and Figure 88) are not observed

in the water soluble humic acid standard. Possible reasons for carbon dioxide signals in this range might be partly due to interactions between sample and matrix or sample matrix residues such as methanol (boiling point 65°C) and ammonium carbonate (decomposition above 58°C), the latter stemming from absorption of ambient carbon dioxide to ammonium hydroxide (Limbeck et al., 2005). Single interfering high-volatile compounds present in ambient aerosol are rather unlikely to cause these signals since the method is highly selective and interference tests did not reveal co-eluting analytes. Last but not least, these high volatile carbonaceous compounds might be part of thermal decomposition products of HULIS, since even single compounds can decompose stepwise, resulting in multiple discrete peaks (Grosjean et al., 1994) especially when interacting with inorganic salts (Yu et al., 2004; Jankowski et al., 2008).

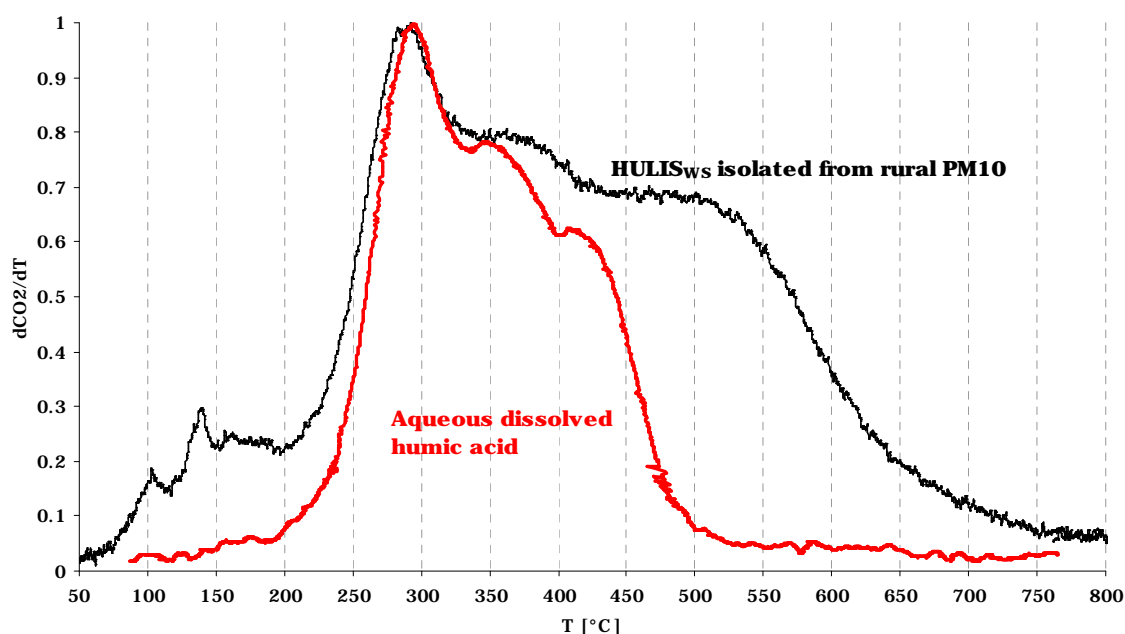


Figure 86: Thermogram of water-soluble humic acid and water-soluble HULIS

The most pronounced peaks in the high volatile region of HULIS_{WS} occurred at slightly above 120°C for urban and rural summer HULIS isolates whereas wintry HULIS_{WS} and HULIS_{AS} high volatile peaks occurred in a range of 130-140°C (Figure 87 and Figure 88). However, since the low-volatile organic carbon fraction accounts for at most only 10% of the carbon in HULIS isolates, the thermograms prove the high selectivity of the applied method on one hand and the refractory nature of the HULIS fractions on the other. The observed signals of HULIS isolates at higher temperatures compared to water-soluble humic acid, is an effect that is related to the absence of catalysing ions such as potassium (Hoffer et al., 2006a; Mayol-Bracero et al., 2002).

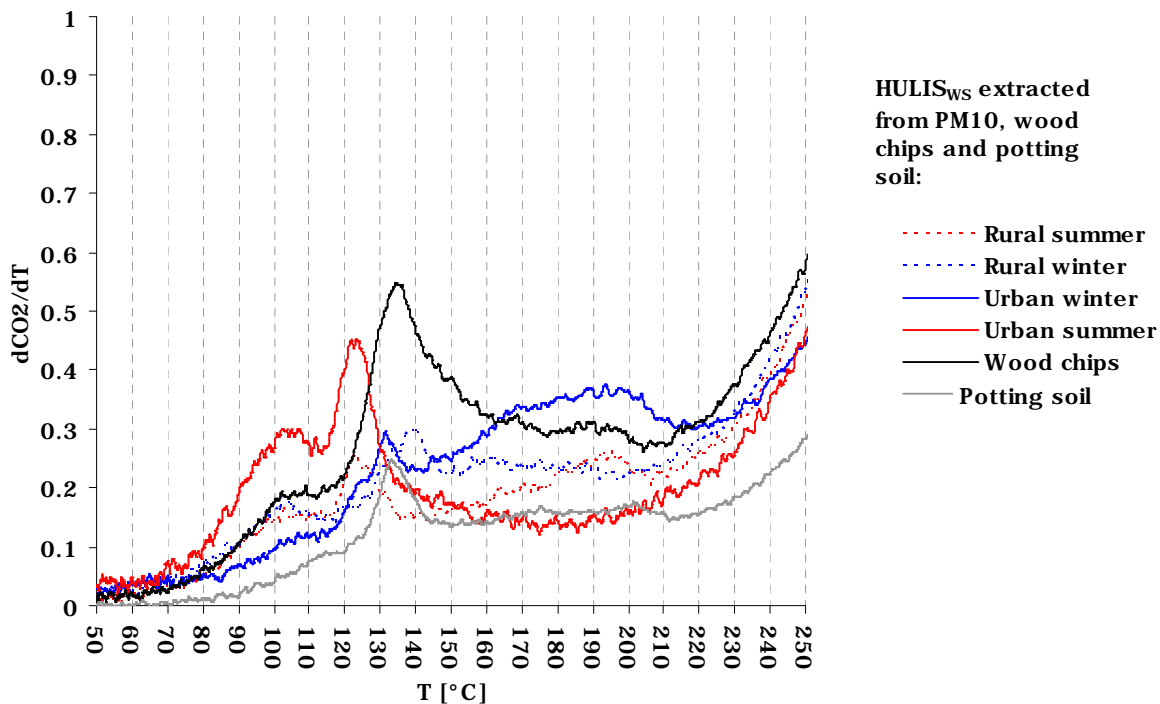


Figure 87: High volatile region of thermograms of HULIS_{WS}

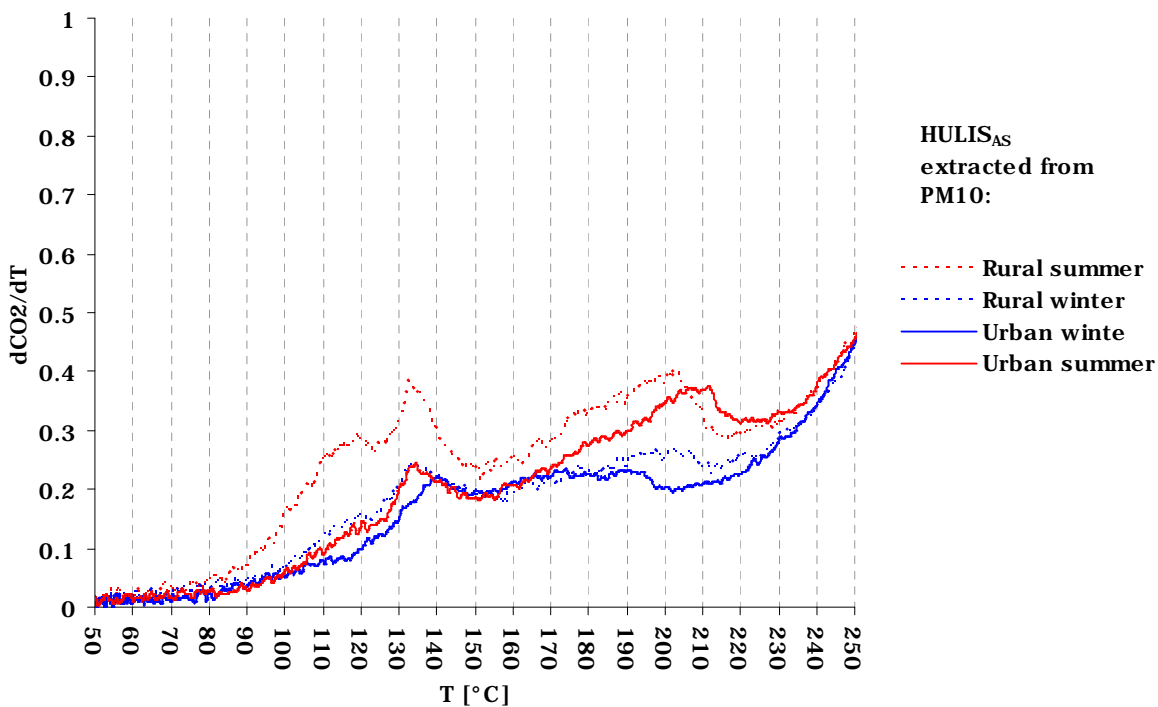


Figure 88: High volatile region of thermograms of HULIS_{AS}

9.2.3 Comparison of thermal Characteristics of HULIS_{WS} and HULIS_{AS}

Normalised thermograms of HULIS isolates from urban summer aerosol (Figure 89) revealed a more or less distinct peak evolving just below 300°C, appearing more distinct for the water extracted HULIS fraction compared to the alkaline extracted HULIS fraction. Winter HULIS revealed a shift of peak maxima for both fractions to higher temperatures and even less resolved peak features pointing to higher thermal stability. HULIS_{WS} and HULIS_{AS} showed rather similar thermal behaviour for both summer and winter samples, though a more pronounced shoulder between 350°C and 450°C in summer and more pronounced peaks at 300°C and 500°C in winter.

Thermograms of isolated HULIS from urban airborne PM10

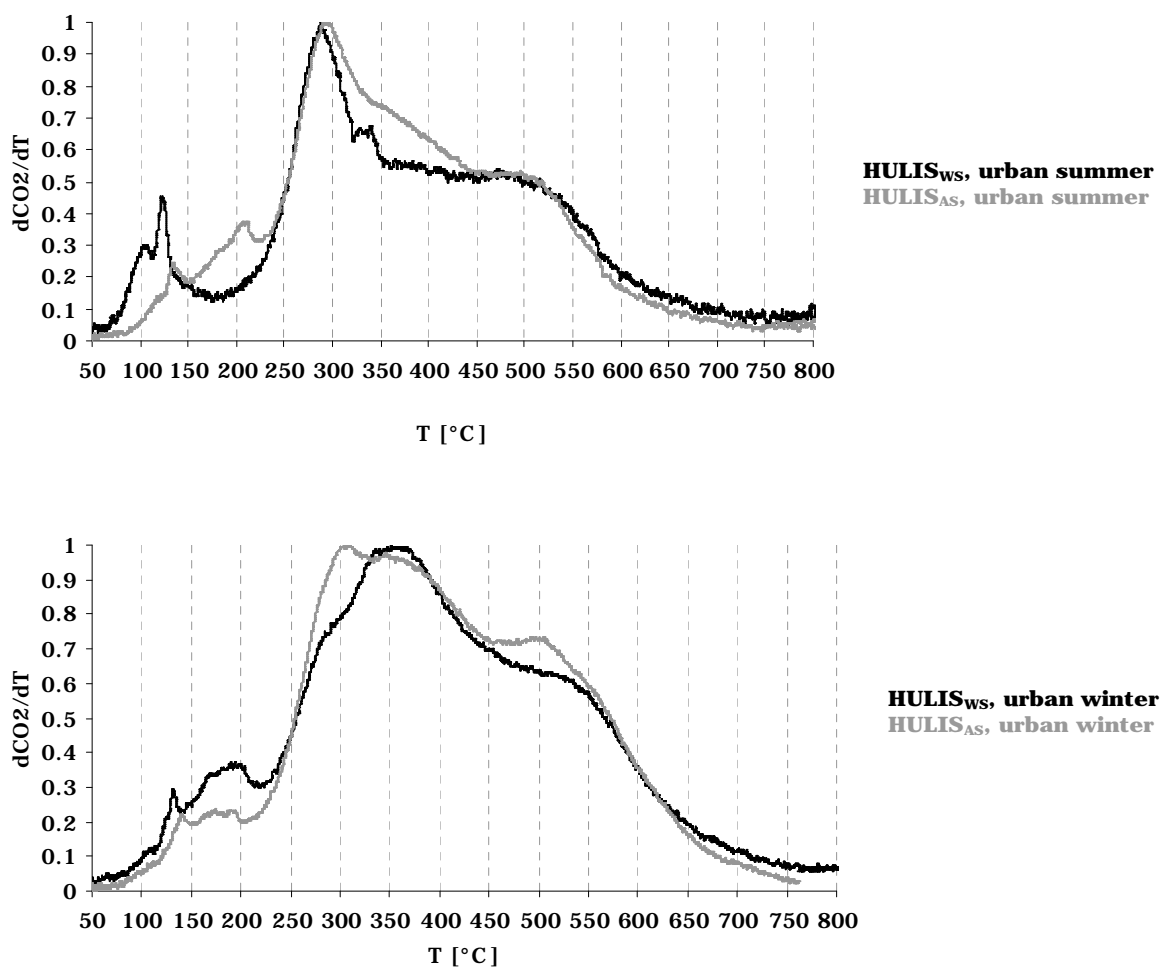


Figure 89: Thermograms of HULIS isolated from urban PM10 (Römerberg, Upper Austria, winter: January 2006; Summer July 2005).

Rural HULIS isolates (Figure 90) as well showed peak maxima at ~300°C similar for both HULIS fractions.

Thermograms of isolated HULIS from rural airborne PM10

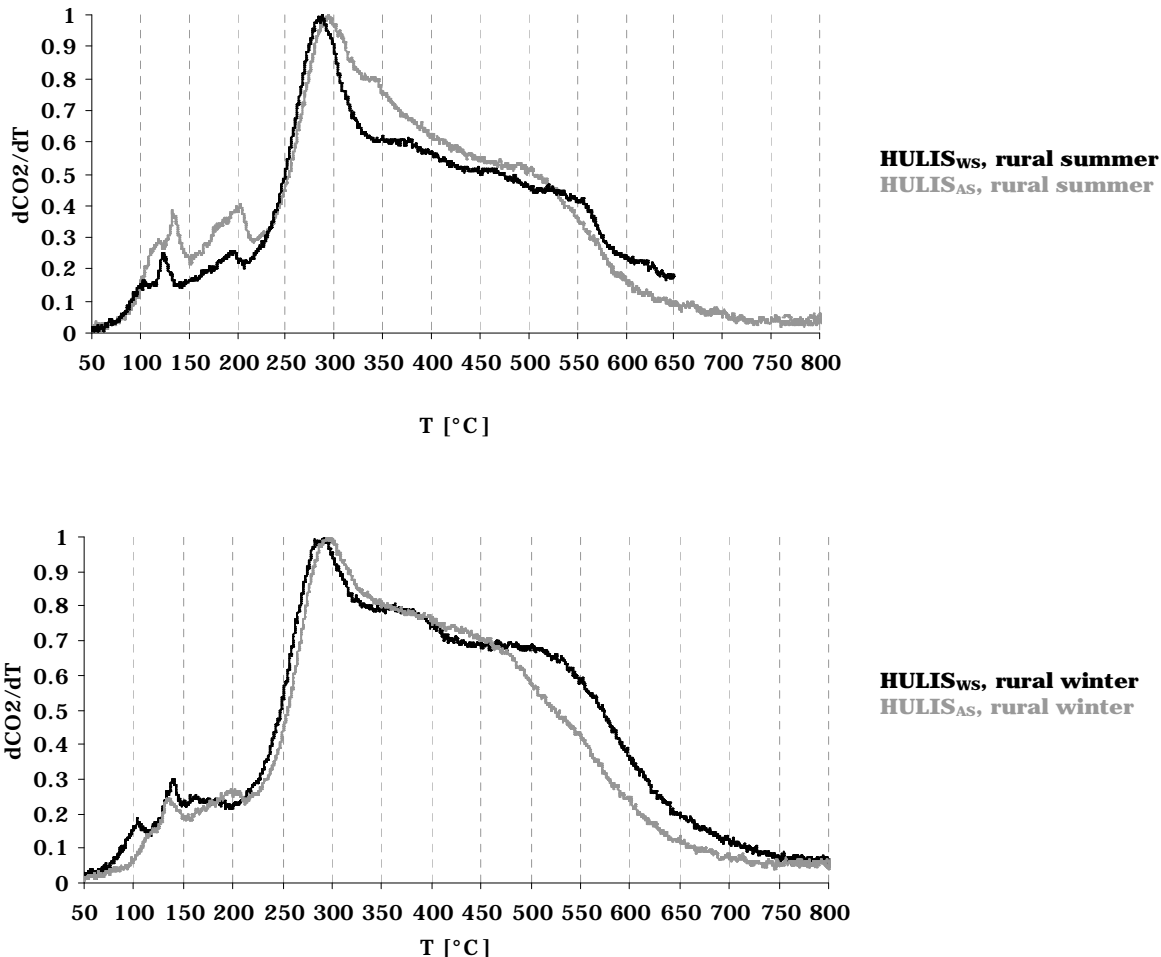


Figure 90: Thermogram of HULIS isolated from water and aqueous alkaline extracts from rural PM10 (Enzenkirchen, Upper Austria, winter: January 2006; summer: July 2005).

9.2.4 Spatial and seasonal Variations of thermal Characteristics of HULIS Isolates

Monthly averages of HULIS_T and PM10 as well as correlation coefficients with other selected aerosol species are summarised in Table 24. Calculated shares of HULIS that were primarily emitted are based on considerations discussed in detail in section 7.3.8.1.

Table 24: Summary of HULIS_T abundance, comparison with selected other aerosol species and estimated primary shares of HULIS emissions to measured HULIS_T; bold numbers denote significant correlation of HULIS_T and the respective analyte on a 95% level of likelihood

| | | July (n=4) | | January (n=10) | |
|---|---|--------------|--------------|----------------|--------------|
| | | RÖME | ENZE | RÖME | ENZE |
| | PM10 [$\mu\text{g}/\text{m}^3$] | 39.4 | 18.5 | 65.2 | 38.6 |
| | HULIS _T [$\mu\text{g}/\text{m}^3$] | 0.52 | 0.33 | 1.58 | 2.63 |
| Correlation coefficient between HULIS _T and selected species | EC | 0.994 | 0.995 | 0.558 | 0.857 |
| | Si | 0.799 | 0.974 | 0.352 | 0.790 |
| | NH ₄ ⁺ | 0.066 | 0.921 | 0.815 | 0.834 |
| | K ⁺ | 0.978 | 0.986 | 0.400 | 0.350 |
| | NO ₃ ⁻ | 0.984 | -0.420 | 0.714 | 0.521 |
| | SO ₄ ²⁻ | 0.977 | 0.935 | 0.803 | 0.793 |
| | Oxalate | 0.999 | 0.994 | 0.639 | 0.817 |
| | Cellulose | 0.875 | -0.193 | -0.085 | -0.134 |
| | Levoglucosan | 0.997 | -0.726 | 0.677 | 0.378 |
| | Fe | 0.991 | 0.973 | 0.511 | 0.689 |
| | Pb | 0.941 | 0.955 | 0.357* | 0.729 |
| | As | 0.877 | 0.691 | 0.291 | 0.825 |
| | Sb | 0.598 | 0.705 | 0.652 | 0.822 |
| | SO ₂ | ND | 0.970 | ND | 0.717 |
| | Ozone | ND | 0.997 | ND | 0.396 |
| Estimated primary HULIS contributions to HULIS _T | HULIS _{prim, WSE+DVE} [%] | 27 | 11 | 20 | 7 |
| | HULIS _{prim, WSE} [%] | 2 | 4 | 16 | 6 |
| | HULIS _{prim, DVE} [%] | 25 | 7 | 4 | 1 |
| | HULIS C/levoglucosan | 14.5 | 9.1 | 2.1 | 5.3 |

*Pb is correlated significantly as well at the urban site RÖME, if restraining the sample from January 1st from calculations. Most likely New Years activities such as fire works are responsible for a Pb higher than 150 ng/m³ whereas on all other days in January concentrations were found below 50 ng/m³ (Jankowski et al., 2009b and AQUELLA data base).

Superimposition of thermograms for isolated HULIS (Figure 91) reveals remarkable resemblance between urban and rural “summer” HULIS resulting in almost perfectly congruent curve progressions even more surprising concerning that about 60 km distance lay between the urban, traffic impacted sampling site in Linz (Römerberg) and the background site Enzenkirchen. Strong positive correlations of HULIS_T (Table 24) at both

sites with primary species EC, lead and iron suggest an influence of industrial related emissions such as coal burning and activities from steel production on the ambient occurrence of HULIS (Jankowski et al. 2009b; Limbeck et al., 2009; Spangl et al., 2006). At both sites a strong link to secondary species oxalate and sulfate indicate that secondary formation mechanisms are operative as well. Biomass burning seems as well influencing urban HULIS_T levels (strong significant correlations with levoglucosan and potassium). Correlation with potassium is as well found at the rural site but seem to be rather soil than biomass burning related (correlation with silicium, none with levoglucosan). Overall HULIS_T seems to be connected to fossil fuel combustion processes (e.g. industrial coal combustion) at both sites, with additional biomass burning contributions at the urban site and a source linked to agricultural activities at the rural site (correlation with ammonium, potassium and silicium; (Spangl et al., 2006, Bauer et al., 2006)). Since HULIS isolated from potting soil revealed a broader “hump” and showed no distinct peak at ~300°C, as observed for airborne summerly HULIS, the correlation with silicium and potassium at the rural sight indicates soil derived particles to play a role as seed particles for secondary formation of HULIS (Limbeck et al., 2003) rather than direct release of terrestrial humic acid to the atmosphere. However, the refractory characteristic of HULIS seems to be quite independent from different source types and suggest atmospheric conditions such as the presence of atmospheric oxidants to be the determinant factor.

Direct comparison of isolated “summer” HULIS from rural and urban airborne PM10

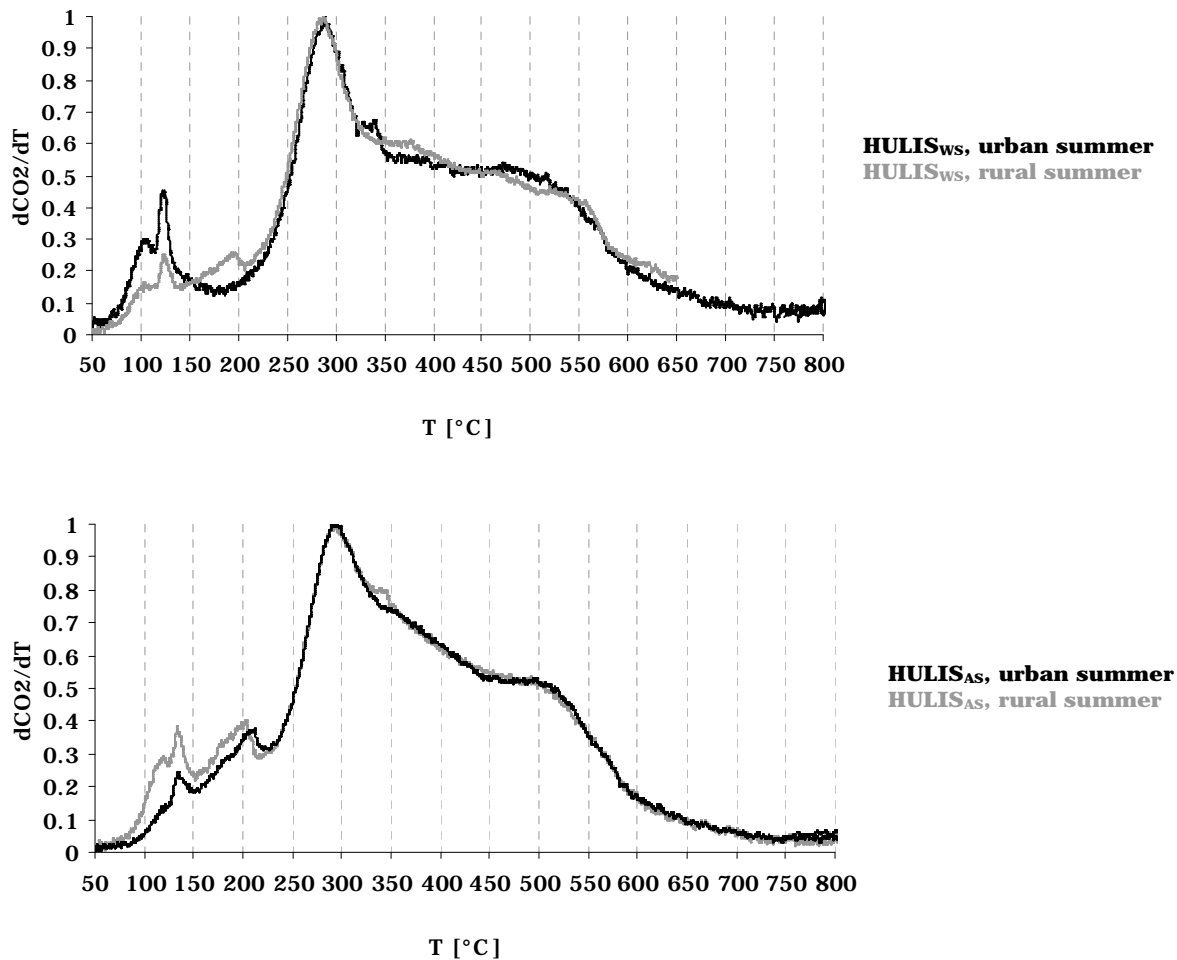


Figure 91: Thermograms of HULIS isolated from water and aqueous alkaline extracts from rural PM10 (Enzenkirchen, Upper Austria, winter: January 2006; summer: July 2005).

Direct comparison of isolated “winter” HULIS from rural and urban airborne PM10

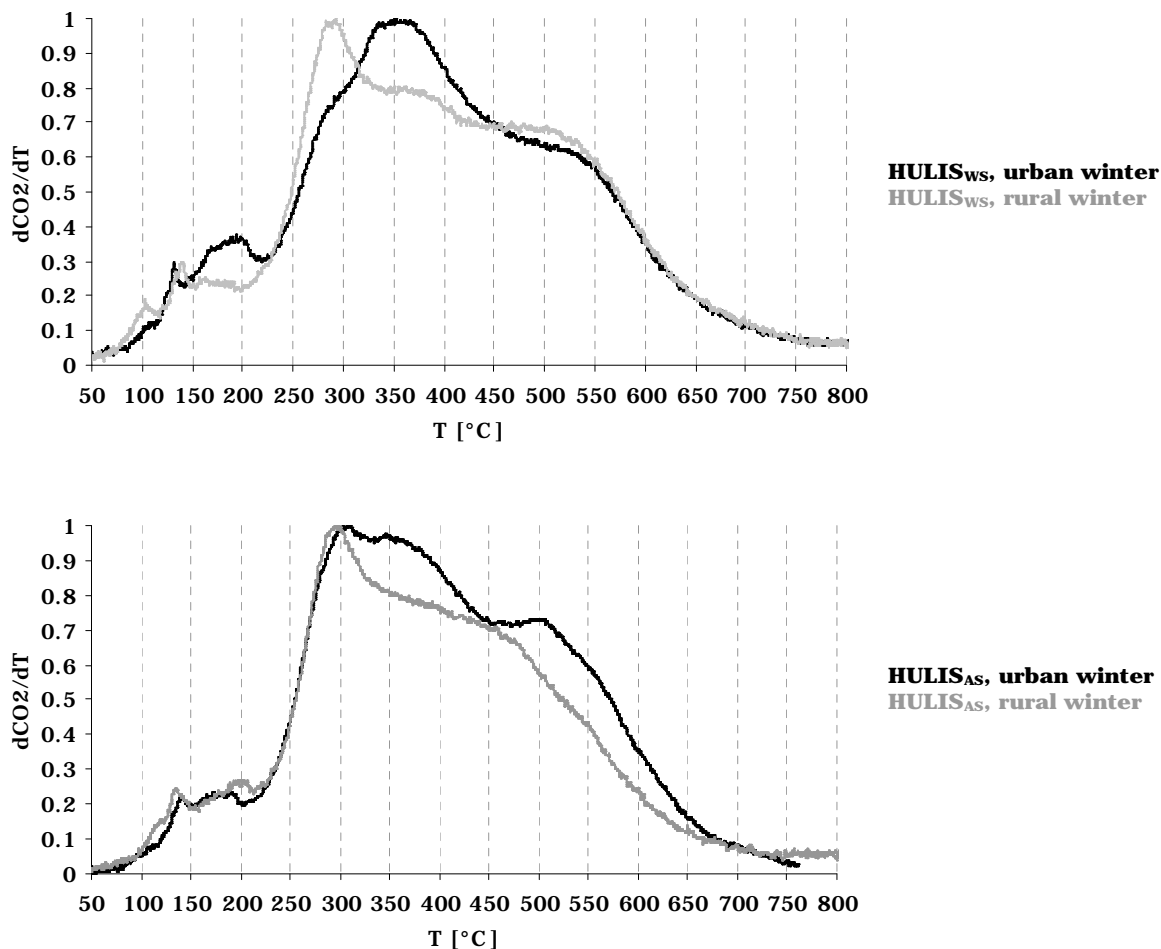


Figure 92: Thermograms of HULIS isolated from water and aqueous alkaline extracts from urban (Römerberg) and rural (Enzenkirchen) PM10 (Upper Austria, winter: January 2006; summer: July 2005).

Thermal characteristics of wintry HULIS_{WS} and HULIS_{AS} reveals less spatial uniformity than in summer (Figure 92), although the species correlated to HULIS in winter are mainly those that were as well observed in summer. A reason for the shift of the peak maximum at the urban site might be the higher source strength of wood combustion (correlation of HULIS with levoglucosan; higher HULIS_{prim, WSE} shares, see Table 24).

Direct comparison of isolated “summer” and “winter” HULIS from rural airborne PM10

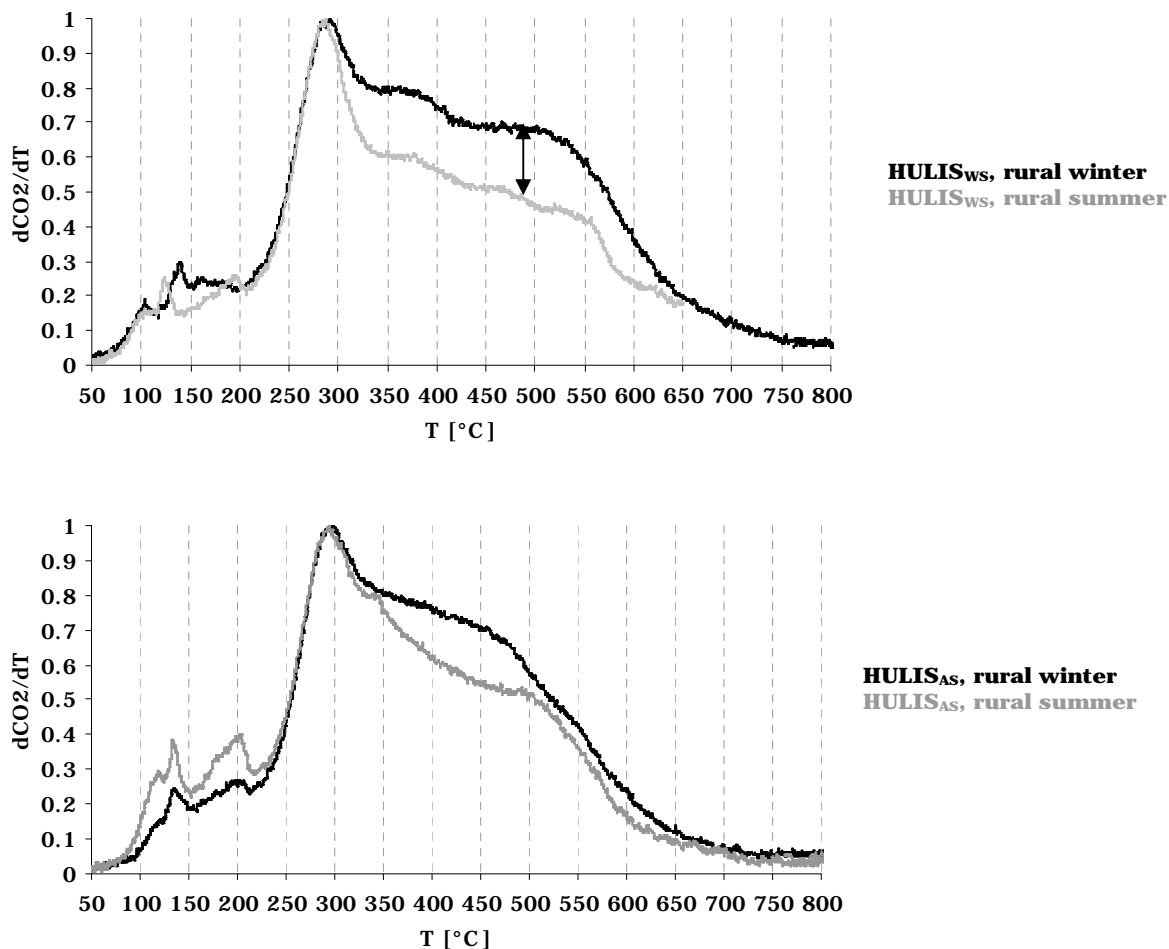


Figure 93: Thermograms of HULIS isolated from water and aqueous alkaline extracts from rural (Enzenkirchen) PM10 (Upper Austria, winter: January 2006; summer: July 2005).

In contrast to urban sites, both HULIS fractions at the rural sites showed identical peak maxima in summer and winter HULIS isolates, though wintry HULIS show higher shares of refractory components (Figure 95). Potentially this is caused by the presence of more aromatic, less polar compounds, emitted in larger amounts during winter. Due to correlation with lead in summer and winter and additional correlation with arsenic in winter, higher emissions stemming from coal combustion might cause larger fractions of higher refractory HULIS.

Direct comparison of isolated “summer” and “winter” HULIS from urban airborne PM10

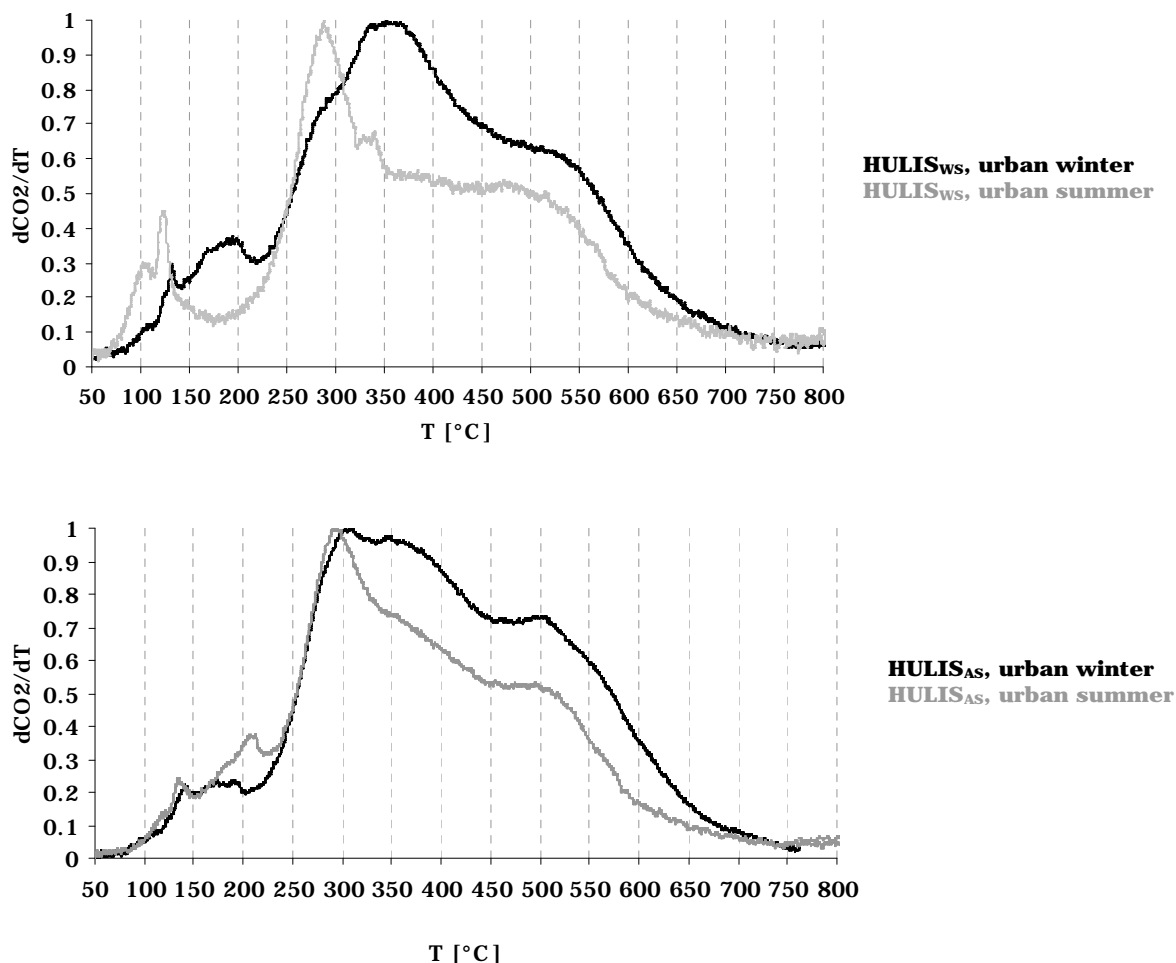


Figure 94: Thermograms of HULIS isolated from water and aqueous alkaline extracts from urban (Römerberg) PM10 (Upper Austria, winter: January 2006; summer: July 2005).

HULIS_{WS} at the urban site show rather different peak shapes in winter compared to summer thermograms (Figure 94). Were HULIS_{AS} in winter and summer shows parallel curve devolution, though with higher shares of more refractory HULIS carbon, the dominating carbon peak for HULIS_{WS} is shifted to higher temperatures in winter at the urban site. Thermograms of isolates, gained after the isolation protocol for atmospheric HULIS (see section 6.1), from wood chips and potting soil are depicted in Figure 95. Both extracts show broader peak maxima at ~300°C and 350°C, respectively, compared to HULIS extracted from ambient PM10. HULIS_{WS} isolated from potting soil additional reveal two peak shoulders at 475 and 625 °C in the thermogram. Due to the isolation procedure, the thermogram of isolates from potting soil might reflect the thermal characteristics of fulvic acids. Unfortunately, due to technical problems at the time of analysis, thermograms of alkaline-soluble HULIS isolates from wood smoke and potting soil are not available. However the broader main peak in wintry urban HULIS would be

coherent with the general features of HULIS_{WS, wood chips} and thus with higher primary contributions from wood combustion to atmospheric HULIS_T levels in winter (Table 24).

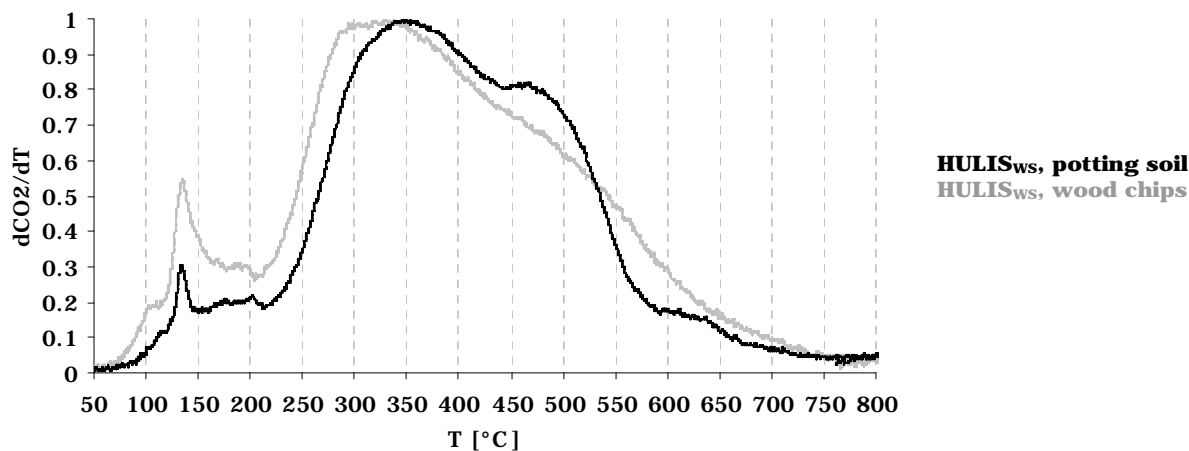


Figure 95: Thermograms of HULIS isolated from wood chips and potting soil.

9.3 Discussion

Water and alkaline extracted fractions of HULIS (HULIS_{AS} and HULIS_{WS}) were isolated from PM10 at a regional background site (ENZE) and an urban traffic impacted site (RÖME) in Upper Austria and thermograms were recorded to gain insight in differences and similarities between these two fractions as well as on spatial and seasonal variations of thermal characteristics. All thermograms showed peak maxima from slightly below 300°C up to 350°C and very refractory behaviour. Complete combustion of carbon species occurred at temperatures above 700°C. HULIS_{AS} and HULIS_{WS} showed rather similar devolution of evolving carbon. Summerly HULIS_{AS} at both sites revealed a slight shoulder between 350 and 450 °C compared to those of HULIS_{WS}. Wintry HULIS_{AS} and HULIS_{WS} at the rural site were almost superimposable whereas the alkaline soluble fraction of HULIS at the urban site in winter revealed slightly stronger signals at 300°C and a higher amount of carbonaceous species at 550°C.

HULIS_T (in the present work defined as sum of HULIS_{WS} and HULIS_{AS}) seems to be strongly connected to secondary formation (strong significant correlation with sulfate and oxalate) and combustion related sources (EC) at both sites in summer as well as in winter. Significant positive correlation of HULIS_T and lead indicates fossil fuel combustion, especially coal combustion (Jankowski et al. 2009n; Limbeck et al., 2009; Spangl et al., 2006), to be important for the atmospheric abundance of HULIS in summer and winter at both sites. Levoglucosan correlated with HULIS_T at the urban site in July and January whereas no such connection occurred at the rural sites. HULIS carbon to levoglucosan factors of 14.5 and 2.1 in July and January, furthermore indicate a change of sources for HULIS_T and levoglucosan. Possibly regional or long-range transported air masses influenced by open fires in summer and wood stove combustion for space heating

purposes in winter play a role in that change. Furthermore agricultural activities (correlation with Si, Ammonium and potassium; Spangl et al., 2006) seem to contribute to HULIS at the rural site. Despite the not uniformly involved sources at the urban and rural site the thermograms of both HULIS fractions were almost identical. Comparison of rural and urban extracts in winter revealed a more distinct peak at $\sim 300^{\circ}\text{C}$ for both HULIS fractions at the rural site and lower shares of more refractory material compared to HULIS isolated from PM10 at the urban site.

Water extracted isolates of HULIS gained from wood chips and potting soil showed broader peaks of evolving carbonaceous species than ambient HULIS isolates and appeared to be more similar to urban wintry than to summerly or rural HULIS isolates. These finding confirms the opinion (Sambuova et al., 2005b; Baduel et al., 2010; Havers et al., 1998) that direct introduction of HULIS via wood combustion in summer and resuspended soil in general is of minor importance concerning potential HULIS sources. The correlation of HULIS_T with silicium and potassium at the rural site might therefore indicate soil derived particles to play a role as seed material for the formation of HULIS rather than direct release of terrestrial humic acids in the atmosphere.

Summarising the differences of thermal characteristics between HULIS_{AS} and HULIS_{WS} are rather small. Comparison of summer and winter samples showed higher shares of more refractive material in winter at the rural and urban site. Wintry urban HULIS showed a considerable shift to higher refractive material with peak maxima shifted from ~ 300 to 350°C evidencing a change of composition compared to summerly and rural wintry isolates. These regional differences have not been observed for summerly HULIS isolates. Both HULIS fractions from urban and rural sites showed almost perfectly congruent thermograms which supports the findings in chapter 7.3.4, where HULIS levels were found in a narrow range during summer and showed larger spreads during the cold season. These results indicate a stronger influence of different rather local sources during the cold time of the year. Better ventilation conditions in summer and constantly emitting sources, such as traffic related emissions and industrial coal combustion, as well as ubiquitous formation of HULIS from gaseous biogenic precursors, might lead to more uniform HULIS levels. However, regarding the perfectly congruent summerly HULIS thermograms-in case of secondary formation-the type of precursor seems to have minor influence on the thermal characteristics of HULIS.

10 Summary and Conclusions

Annual averaged HULIS_T levels occurred in comparable heights in the **three Austrian cities Vienna, Graz and Salzburg** and ranged from 0.46 µg C/m³ to 1.24 µg C/m³. Regarding the ten sampling sites in the three regions, HULIS_T did not reveal a distinct general trend to be more present at urban or background sites. Highest HULIS_T levels occurred at the suburban sites in Vienna, a traffic impacted site in Graz and an urban residential site in Salzburg. The seasonal devolution of atmospheric HULIS_T levels qualitatively was the same in the three cities, with minima in summer and maxima during winter. HULIS_T concentrations in winter were 2.0 to 2.8 times higher than in summer. The concentrations levels occurred in a narrower range in summer and had a bigger spread in the cold season, what points to a higher impact of local emissions on atmospheric HULIS_T levels in fall and winter. Annual averaged contributions of HULIS_T to PM10 and OC occurred in a range of 3.8- 8.9 % and 10.1- 28.9 %, respectively. Higher relative shares appeared at the background sites. Urban sites showed generally very stagnant relative HULIS_T concentrations throughout the year in Vienna and Graz. Seasonal averaged contributions of HULIS C to OC at the five background and suburban sites and the urban sites were 25±5% and 14±3%, respectively. The **water extractable HULIS fractions** (HULIS_{WS}) contributed to HULIS_T in a range of 55% ±5% in the majority of the sample pools at the ten sampling sites. Results from combining observations of HULIS_{AS} and HULIS_{WS} levels with meteorological conditions from periods with well understood origin and chemical composition of PM10, results from the AQUELLA projects (Bauer et al., 2006, 2007a und 2007b), might point to a linkage of the relative abundance of HULIS_{WS} and HULIS_{AS} and the age of HULIS, since HULIS_{WS} shares to the total fraction of HULIS of about 30% and below were observed at a heavily biomass burning episode in Styria. Meteorological observations and source composition (Bauer et al., 2006 and 2007a) would as well support spatial and temporal variations of HULIS_T composition in Vienna. The **application of a dilution tracer, elemental carbon emitted by diesel engined cars (EC_D)**, at two urban traffic impacted sites revealed that unfavourable meteorological conditions in the cold season are of minor importance for the elevated HULIS_T levels in winter, accounting only with 7 and 12 % to the HULIS_T winter enrichment at the traffic impacted sites in Vienna and Graz, respectively. Thus additional sources and/ or higher formation rates are actually responsible for the observed winter enrichment. **HULIS_T quantification in source emissions samples** from wood, lignite and anthracite combustion, diesel vehicular emissions and cooking, conducted in the scope of the AQUELLA/AQUELLIS projects (Jankowski et al., 2009a; Puxbaum et al., 2006, Schmidl et al., 2008a, 2008b and 2008c), revealed contributions to PM10 in the range of 1-7%, 4-5%, 0.9-1.3% and up to 0.7%, respectively. The

amount in diesel vehicular exhaust is quite surprising since the occurrence of atmospheric HULIS was closely connected to biomass burning and the formation from various gaseous precursors (Graber and Rusich, 2006). These results indicate that combustion of fossil fuels, especially mobile sources and coal combustion (Bauer et al., 2006 and 2007a) can not be ignored in considerations on the potential sources of HULIS. Processing ratios of HULIS_T carbon and unique or main tracers in source emission samples on ambient tracer levels, revealed that on annual average, up to 25% of HULIS_T carbon could be of **primary origin emitted by diesel vehicles and wood stoves**. Primary emissions from diesel vehicles, cooking activities and wood stoves can contribute up to 46% of the measured ambient HULIS_T level in a sample pool from April at the urban residential site in Graz (GRAS). The findings from investigating source emission samples are confirmed in observations from correlations of HULIS_T (as sum of HULIS_{AS} and HULIS_{WS}) and other aerosol species in Vienna and the region of Graz. Averaged correlation coefficients from species that correlated significantly at all sites in Graz and Vienna, revealed that in both cities, beside biomass combustion, secondary formation plays an important role in winter regarding the atmospheric abundance of HULIS_T. Potential precursors might stem from fossil as well as from biomass combustion (Bauer et al., 2006 and 2007a). Strong significant correlation with lead, a primary emitted pollutant connected to coal combustion (Pacyna, 1987; Limbeck et al., 2009; Puxbaum et al., 2004), was observed at the sites in Vienna and Graz. Lead showed even better correlation with HULIS_T than levoglucosan at the Styrian sites (Table 25). At the urban sites additionally local sources such as diesel vehicle emissions and cooking activities can contribute to atmospheric HULIS_T levels. At all sites where ozone data was available, significant negative correlation, more pronounced at the urban site compared to background sites, points to effective degradation of HULIS_T being at work in winter.

Table 25: Regional averaged correlation coefficients for HULIS_T in wintry PM10 (averages from species which are correlated significantly on a 95% confidence level at each site in the respective region)

| Species correlated significantly at all sites in Vienna | Regional averaged correlation coefficients (winter) | Species correlated significantly at all sites in Styria | Regional averaged correlation coefficients (winter) |
|---|---|---|---|
| Levoglucosan | 0.838 | NH ₄ ⁺ | 0.888 |
| NO ₃ ⁻ | 0.821 | Oxalate | 0.886 |
| K ⁺ | 0.814 | NO ₃ ⁻ | 0.874 |
| EC | 0.798 | Pb | 0.871 |
| NH ₄ ⁺ | 0.793 | SO ₄ ²⁻ | 0.866 |
| Oxalate | 0.787 | K ⁺ | 0.761 |
| SO ₄ ²⁻ | 0.777 | Levoglucosan | 0.637 |
| Pb* | 0.758 | Ozone | -0.626 |
| Benzo(ghi)perylene | 0.726 | | |
| Benzo(de)anthracen-7-on | 0.619 | | |
| Ozone* | -0.694 | | |

*Ozone data was available for the urban fringe site LOBA (Vienna) and BOCK (rural background) and GRAS (urban residential); Pb data was available for three sites in Vienna (SCHAF, RINN, KEND) and two in Graz (BOCK and DONB)

Correlation patterns occurring in summer in the region of Graz suggest forest or open agricultural fires as a “background” source and local impact of diesel engined vehicles to contribute to atmospheric HULIS_T. Primary emissions and secondary formation are both possible. Biogenic secondary contributions could not be investigated in the present work due to the lack of an appropriate tracer, but of course can not be excluded as potential source of HULIS_T.

Comparing the **23 Austrian sites** averaged HULIS_T concentrations appeared in a range of 0.46 -1.61 $\mu\text{g C/m}^3$, the former occurring at a rural background site in Salzburg (ANTH) and the latter at an urban site in Lower Austria (SCHW). The abundance of atmospheric HULIS_T did not show a trend to occur preferred at sites with specific characteristics. Regarding the respective regions HULIS_T levels at background sites were slightly higher or similar than the respective urban sites (Vienna, Upper Austria), markedly lower (Salzburg) or higher (Carinthia). In Lower Austria HULIS_T levels at two background sites (STIX, AMST) were markedly lower and similar (MIST) to the urban sites, respectively. **The majority of the 23 sampling sites showed maximum HULIS_T concentrations in fall or winter with a winter enrichment factor in the range of 2-4. Only four sites did show almost no seasonality.** Two background sites in Carinthia and the urban site in the capital of Lower Austria (STPÖ) showed no or very weak seasonality at a rather high HULIS_T level of $1.4 \pm 0.3 \mu\text{g C/m}^3$, pointing to constantly and rather effective source emissions, such as industrial activities, related to the atmospheric occurrence of HULIS_T. Average contributions (annual average in Vienna, Graz and Salzburg, six month average for Carinthia and Lower Austria, nine month average for Upper Austria) of HULIS_T carbon to OC at the 23 sites varied between 9 and 44 %. Average contributions of HULIS_T to PM10 appeared in a range of 0.5-16.2%. A proxy factor for the conversion of HULIS related carbon to organic matter of 1.9 was applied (Kiss et al., 2002; Krivácsy et al., 2002; Salma et al., 2007 and 2010; Lin et al., 2010a). **The impact of wood smoke** and the relation to HULIS_T was assessed by comparison of HULIS_T and levoglucosan levels (Caseiro et al., 2009). Ratios of HULIS_T carbon and levoglucosan were calculated from studies reported in literature at six background sites in Europe (Feczko et al., 2007) and a major biomass burning event in Brazil (Mayol-Bracero et al., 2002) and were in excellent agreement with results from the present study. HULIS carbon and levoglucosan ratios at a major biomass burning event in Styria (Wonschütz et al., 2009) ranged from 2.08-2.78. The winter average, calculated from two and three month averages, respectively, of HULIS_T carbon and levoglucosan ratios occurred in a rather narrow range of 1.1- 5.9. The average ratio, weighed according the Austrian fuel wood consumption, in samples from wood stove emission was 0.33 in a range of 0.11-0.68 (Schmidl et al., 2008a). Open burning of leaves on the contrary leads to ratios of HULIS_T carbon and levoglucosan of 9.32 (Schmidl et al., 2008b). Seasonal averaged HULIS_T carbon and levoglucosan ratios in Vienna, Graz and

Salzburg maximise in summer with values 4-7 times higher than in winter. Intermediate values occurred during transition month lying closer to winter values. Wintry HULIS_T C/levoglucosan ratios furthermore revealed a trend for higher values in Eastern Austrian regions (3.4 -5.9) and lower in western and southern Austria (1.1-2.7) and a tendency to be lower at urban sites. Summer ratios showed generally the same trend and were higher at all sites and showed higher dispersion of HULIS_T carbon and levoglucosan ratios in the range of 6.4-69.6. **Significant correlation of HULIS_T and levoglucosan was observed for most, but not all, sites in winter.** We observed significant and good correlation for the sites in Vienna ($r=0.74-0.93$) and Salzburg ($r=0.70-0.88$). Lacking correlation of HULIS_T and levoglucosan levels at the background and urban fringe sites in Upper Austria and Carinthia indicate other sources than wood combustion. Significant positive correlations in summer appeared at two urban sites (RÖME, $r=0.977$; GRAS, $r=0.832$) and two background sites (BOCK, $r=0.894$; ANTH, $r=0.965$) with HULIS_T carbon and levoglucosan ratios at the lower end of the summer scale (8.1-14.5). A connection of biomass smoke and ambient HULIS_T levels at HULIS_T carbon and levoglucosan ratios of 10 ± 5 therefore might be typical for regions that are impacted by open biomass burning or agricultural fires in summer, most likely via the regional or long-range transport of air masses. Since only a low number of data pairs in summer ($n=4-8$) were available, the non-correlation of HULIS_T and levoglucosan at other sites does not exclude them from these considerations. The general trend for higher HULIS_T to levoglucosan ratios in the well ventilated Eastern part of Austria might make the ratio suitable to distinguish between a local or regional/supraregional origin of HULIS_T.

Water and alkaline extractable fractions of HULIS (HULIS_{WS} and HULIS_{AS}) were isolated from PM₁₀ in Upper Austria and thermally characterised with a thermal-optical transmission method with linear temperature program. Recorded thermograms shed light on differences and similarities between these two fractions as well as on spatial and seasonal variations of thermal characteristics. All thermograms showed peak maxima from slightly below 300°C up to 350°C and very refractory behaviour. Complete combustion of carbon species occurred at temperatures above 700°C. HULIS_{AS} and HULIS_{WS} showed rather similar devolution of evolving carbonaceous species. Summerly HULIS_{AS} at both sites revealed a slight shoulder between 350 and 450 °C compared to those of HULIS_{WS}. Wintry HULIS_{AS} and HULIS_{WS} at the rural site were almost superimposable whereas the alkaline soluble fraction of HULIS at the urban site in winter revealed slightly stronger signals at 300°C and a higher amount of carbonaceous species at 550°C. HULIS_T (in the present work defined as sum of HULIS_{WS} and HULIS_{AS}) seems to be strongly connected to secondary formation (strong significant correlation with sulfate and oxalate) and combustion related sources (EC) at both sites in summer as well as in winter. Significant positive correlation of HULIS_T and lead indicates fossil fuel combustion,

especially coal combustion (Pacyna, 1987), to be important for the atmospheric abundance of HULIS_T in summer and winter at both sites. Levoglucosan correlated with HULIS_T at the urban site in July and January whereas no such connection occurred at the rural sites. HULIS_T carbon to levoglucosan factors of 14.5 and 2.1 in July and January, furthermore indicate a change of sources for HULIS_T and levoglucosan. Possibly regional or long-range transported air masses influenced by open fires in summer and wood combustion for space heating purposes in winter play a role in this change of sources. Despite the not uniformly involved sources at the urban and rural site, thermograms of both HULIS fractions were almost identical. Comparison of rural and urban extracts in winter revealed a more distinct peak at ~300°C for both HULIS fractions at the rural site and lower shares of more refractory material compared to HULIS isolated from PM10 at the urban site. Water extracted isolates of HULIS gained from wood chips and potting soil showed broader peaks of evolving carbonaceous species than ambient HULIS isolates and appeared to be more similar to urban wintry than to summerly or rural HULIS isolates. These finding confirms that direct introduction of HULIS_T into the atmosphere via wood combustion in summer and resuspended soil in general is of minor importance. Summarising, the **differences of thermal characteristics between HULIS_{AS} and HULIS_{WS} are rather small**. Comparison of summer and winter samples showed higher shares of more refractive material in winter at the rural and urban site. Wintry urban HULIS showed a considerable shift to higher refractive material with peak maxima shifted from ~300 to 350°C evidencing a change of composition compared to summerly and rural wintry isolates. These regional differences have not been observed for summerly HULIS isolates. Both HULIS fractions from urban and rural sites showed almost perfectly congruent thermograms what supports the findings in chapter 7.3.4, where HULIS levels were found in a narrow range during summer and showed larger spreads during the cold season. Both results indicate a stronger influence of different rather local sources during the cold time of the year. Better ventilation conditions in summer and constantly emitting sources, such as traffic related emissions and industrial coal combustion, as well as ubiquitous formation of HULIS from gaseous biogenic precursors, might lead to more uniform HULIS levels. However, regarding the perfectly congruent urban and rural HULIS thermograms in summer-in case of secondary formation-the type of precursor seems to have minor influence on the characteristics of HULIS.

References

- Adelhelm, C., Niessner, R., Pöschl, U., Letzel, T.: Analysis of large oxygenated and nitrated polycyclic aromatic hydrocarbons formed under simulated diesel engine exhaust conditions (by compound fingerprints with SPE/LC-API-MS); *Anal. Bioanal. Chem.* 391, 2599-2608, 2008.
- Andreae, M. O. and Gelencsér, A.: Black carbon or brown carbon? The nature of light-absorbing carbonaceous aerosols, *Atmos. Chem. Phys.*, 6, 3131–3148, 2006.
- Allard, B., Boren, H. and Grimvall, A. (Eds.): *Humic Substances in the aquatic terrestrial environment*. Springer-Verlag, Berlin, 1991.
- Altieri, K. E., Seitzinger, S. P., Carlton, A. G. et al.: Oligomers formed through in-cloud methylglyoxal reactions: Chemical composition, properties, and mechanisms investigated by ultrahigh resolution FT-ICR mass spectrometry, *Atmos. Environ.*, 42, 1476–1490, 2008.
- Arakaki, T., Saito, K., Okada, K., Nakajima, H. and Hitomi, Y.: Contribution of fulvic acid to the photochemical formation of Fe(II) in acidic Suwannee River fulvic acid solutions, *Chemosphere*, 78(8), 2010.
- ARBÖ, 2004, http://www.ots.at/presseaussendung/OTS_20040916_OT0159/arboe-weg-mit-der-strafsteuer-fuer-pkw-ohne-partikelfilter; last access: 5 July 2013.
- Arey, J., Winer, A. M., Atkinson, R., Aschmann, S.M., Long, W.D. and Morrison, C.L.: The emission of (Z)-3-hexen-1-ol, (Z)-3-hexenylacetate and other oxygenated hydrocarbons from agriculture plant species, *Atmospheric Environment*, 25, 1063–1075, 1991.
- Asfinag, 2005. VCÖ Investigation 2005. 25 Roads with most traffic in Austria (original title: Die 25 Straßen mit dem meisten Verkehr in Österreich). Report 2005-139 of 29.06.2005.
- Badger, C. L., George, I., Griffiths, P. T., Braban, C. F., Cox, R. A. and Abbatt, J. P. D.: Phase transitions and hygroscopic growth of aerosol particles containing humic acid and mixtures of humic acid and ammonium sulphate, *Atmos. Chem. Phys.*, 6, 755-768, doi:10.5194/acp-6-755-2006, 2006.

- Baduel, C., Voisin, D. and Jaffrezo, J. L.: Comparison of analytical methods for Humic Like Substances (HULIS) measurements in atmospheric particles, *Atmos. Chem. Phys.*, **9**, 5949–5962, 2009.
- Baduel, C., Voisin, D., and Jaffrezo, J.-L.: Seasonal variations of concentrations and optical properties of water soluble HULIS collected in urban environments, *Atmos. Chem. Phys.*, **10**, 4085-4095, doi:10.5194/acp-10-4085-2010, 2010.
- Baduel, C., Monge, M. E., Voisin, D., Jaffrezo, J. L., George, Ch., El Haddad, I., Marchand, N. and D'Anna, B.: Oxidation of Atmospheric Humic Like Substances by Ozone: A Kinetic and Structural Analysis Approach, *Environmental Science & Technology*, **45**(12), 5238-5244, 2011.
- Baltensperger, U., Kalberer, M., Dommen, J., Paulsen, D., Alfarra, M. R., Coe, H., Fisseha, R., Gascho, A., Gysel, M. and Nyeki, S.: Secondary organic aerosols from anthropogenic and biogenic precursors, *Faraday Discussions*, **130** (Atmospheric Chemistry), 265-278, 2005.
- Bauer, H., Kasper-Giebl, A., Zibuschka, F., Kraus, G. F., Hitzemberger, R. and Puxbaum, H.: Determination of the carbon content of airborne fungal spores, *Journal of Analytical Chemistry*, **74**, 91-95, 2002a.
- Bauer, H., Kasper-Giebl, A., Löflund, M., Giebl, H., Hitzemberger, R., Zibuschka, F. and Puxbaum, H.: The contribution of bacteria and fungal spores to the organic carbon content of cloud water, precipitation and aerosols, *Journal of Atmospheric Research*, **64**, 109-119, 2002b.
- Bauer, H., Giebl, H., Hitzemberger, R., Kasper-Giebl, A., Reischl, G., Zibuschka, F. and Puxbaum, H.: Airborne bacteria as cloud condensation nuclei, *Journal of Geophysical Research*, **108**, (D21), 4658, doi:10.1029/2003JD003545, 2003.
- Bauer, H. Marr, I., Kasper-Giebl, A., Limbeck, A., Caseiro, A., Handler, M., Jankowski, N., Klatzer, B., Kotianova, P., Pouresmaeil, P., Schmidl, C., Sageder, M., Puxbaum, H. and the AQUELLA Team: Aquella Vienna – Determination of Sources contributing to the Particulate Matter Burden in Vienna, Austria (Original Title: Aquella Wien – Bestimmung von Immisionsbeiträgen in Feinstaubproben), Final Report UA/AQWien, Vienna University of Technology, Institute of Chemical Technologies and Analytics, Vienna, Austria, 174 pages, 2006.

Bauer, H., Marr, I., Kasper-Giebl, A., Limbeck, A., Caseiro, A., Handler, M., Jankowski, N., Klatzer, B., Kotianova, P., Pouresmaeil, P., Schmidl, C., Sageder, M., Puxbaum, H. and the AQUELLA Team: Aquella Styria – Determination of Sources contributing to the Particulate Matter Burden in Styria, Austria (Original Title: Aquella Steiermark – Bestimmung von Immisionsbeiträgen in Feinstaubproben), Final Report UA/AQGraz 2007, Vienna University of Technology, Institute of Chemical Technologies and Analytics, Vienna, Austria , 163 pages, 2007a.

Bauer, H., Marr, I., Kasper-Giebl, A., Limbeck, A., Caseiro, A., Handler, M., Jankowski, N., Klatzer, B., Kotianova, P., Pouresmaeil, P., Schmidl, Ch., Sageder, M., Puxbaum, H. and the AQUELLA Team: AQUELLA Salzburg- Determination of Sources contributing to the Particulate Matter Burden in Salzburg, Austria (Original Title: Aquella Salzburg – Bestimmung von Immisionsbeiträgen in Feinstaubproben), Final Report UA/AQUELLA Salzburg, Vienna University of Technology, Institute of Chemical Technologies and Analytics, Vienna, 150 pages, 2007b.

Bauer, H., Marr, I., Kasper-Giebl, A., Limbeck, A., Caseiro, A., Handler, M., Jankowski, N., Klatzer, B., Kotianova, P., Pouresmaeil, P., Schmidl, Ch., Sageder, M., Puxbaum, H. and the AQUELLA Team: AQUELLA Carinthia- Determination of Sources contributing to the Particulate Matter Burden in Salzburg, Austria (Original Title: Aquella Kärnten – Bestimmung von Immisionsbeiträgen in Feinstaubproben), Final Report UA/AQKärnten/Klagenfurt, Vienna University of Technology, Institute of Chemical Technologies and Analytics, Vienna, 161 pages, 2008a.

Bauer, H., Marr, I., Kasper-Giebl, A., Limbeck, A., Caseiro, A., Handler, M., Jankowski, N., Klatzer, B., Kotianova, P., Pouresmaeil, P., Schmidl, Ch., Sageder, M., Puxbaum, H., and the AUQUELLA Team: AQUELLA Lower Austria- Determination of Sources contributing to the Particulate Matter Burden in Lower Austria (Original Title: Aquella Niederösterreich– Bestimmung von Immisionsbeiträgen in Feinstaubproben), Final Report Bericht UA/AQNiederösterreich 2008, Vienna University of Technology, Institute of Chemical Technologies and Analytics, Vienna, 129 pages, 2008b.

Beine, H., Colussi, A. J., Amoroso, A., Esposito, G., Montagnoli, M. and Hoffmann, M. R.: HONO emissions from snow surfaces, *Environ. Res. Lett.*, 3, 045005, 2008.

Beine, H., Anastasio, C., Esposito, G., Patten, K., Wilkening, E., Domine, F., Voisin, D., Barret, M., Houdier, S. and Hall, S.: Soluble, light-absorbing species in snow at Barrow, Alaska, *J. Geophys. Res.*, 116, 2011.

- Bernstein, J. A., Alexis, N., Barnes, C., Bernstein, I. L., Nel, A., Peden, D., Diaz-Sanchez, D., Tarlo, S. M. and Williams, P. B.: Health effects of air pollution, *J Allergy Clin Immunol.*, 114 (5), 1116-23, 2004
- Blando, J. D. and Turpin, B. J.: Secondary organic aerosol formation in cloud and fog droplets: a literature evaluation of plausibility, *Atmospheric Environment*, 34, 1623–1632, 2000.
- Blazsó, M., Janitsek, S., Gelencsér, A., Artaxo, P., Graham, B. and Andreae, M.: Study of tropical organic aerosol by thermally assisted alkylation-gas chromatography mass spectrometry, *Journal of Analytical Applications, Pyrolysis*, 68-69, 351-369, 2003.
- Bond, T. C., Streets, D.G., Yarber, K. F., Nelson, S. M., Woo, J. H. and Klimont, Z.: A technology-based global inventory of black and organic carbon emissions from combustion, *Journal of Geophysical Research*, 109 (D14), D14203/1-D14203/43, 2004.
- Brigante M., D'Anna, B., Conchon, P. and George, Ch.: Multiphase Chemistry of Ozone on Fulvic Acids Solutions, *Environ. Sci. Technol.*, 42 (24), 9165-9170, 2008.
- Cachier, H., Bremond, M. P. and Buat-Ménard, P.: Determination of atmospheric soot carbon with a simple thermal method, *Tellus*, 41B, 379-390, 1989.
- Calace, N., Petronio, B. M., Cini, R., Stortini, A. M., Pampaloni, B. and Udisti, R.: Humic marine matter and insoluble materials in Antarctic snow, *Int. J. Environ. Anal. Chem.*, 79, 331–348, 2001.
- Cappiello, A., De Simoni, E., Fiorucci, C., Mangani, F., Palma, P., Trufelli, H., Decesari, S., Facchini, M. C. and Fuzzi, S.: Molecular characterization of the water-soluble organic compounds in fogwater by ESIMS/MS, *Environ. Sci. Technol.*, 37, 1229–1240, 2003.
- Carlton, A. G., Turpin, B. J., Altieri, K. E., Reff, A., Seitzinger, S., Lim, H. J. and Ervens, B.: Atmospheric Oxalic Acid and SOA Production from Glyoxal: Results of Aqueous Photooxidation Experiments, *Atmos. Environ.*, 41, 7588–7602, 2007.
- Caseiro, A., Marr, I. L., Claeys, M., Kasper-Giebl, A., Puxbaum, H. and Casimiro, P.: Determination of saccharides in atmospheric aerosol using anion.exchange high-performance liquid chromatography and pulsed-amperometric detection, *Journal of Chromatography*, A. 1171 (1-2), 37-45, 2007.

Caseiro, A., Bauer, H., Schmidl, Ch., Pio, C. A. and Puxbaum, H.: Wood burning impact on PM10 in three Austrian regions, *Atmospheric Environment*, 43, 2186–2195, 2009.

Cass, G. R.: Organic molecular tracers for particulate air pollution sources, *Trends in Analytical Chemistry*, 17, 356-366, 1998.

Cavalli, F., Facchini, M. C., Decesari, S., Mircea, M., Emblico, L., Fuzzi, S., Ceburnis, D., Yoon, Y. J., O'Dowd, C. D., Putaud, J. P. and Dell'Acqua, A.: Advances in characterization of size-resolved organic matter in marine aerosol over the North Atlantic, *J. Geophys. Res.-Atmos.*, 109, D24215, 2004.

Chen, H., Zheng, B., Song, Y and Qin, Y.: Correlation between molecular absorption spectral slope ratios and fluorescence humification indices in characterizing CDOM, *Aquat Sci*, 73, 103–112, doi:10.1007/s00027-010-0164-5, 2011.

Cheng, Y., He, K., Duan, F., Du, Z., Mei Zheng and Yong-liang Ma,: Characterization of carbonaceous aerosol by the stepwise-extraction thermal-optical-transmittance (SE-TOT) method, *Atmospheric Environment*, 59, 551-558, 2012.

Cini, R., Innocenti, N. D., Loglio, G., Oppo, C., Orlandi, G., Stortini, A. M., Tesei, U. and Udisti, R.: Air-sea exchange: Sea salt and organic micro components in Antarctic snow, *Int. J. Environ. Anal. Chem.*, 63, 15–27, 1996.

Cini, R., Innocenti, N. D., Loglio, G., Stortini, A. M., and Tesei, U.: Spectrofluorometric Evidence Of The Transport Of Marine Organic-Matter In Antarctic Snow Via Air-Sea Interaction, *Int. J. Environ. Anal. Chem.*, 55, 285–295, 1994.

Claeys, M., Vermeylen, R., Yasmeeen, F., Gómez-González, Y., Chi, X., Maenhaut, W., Mészáros, T. and Salma, I.: Chemical characterisation of humic-like substances from urban, rural and tropical biomass burning environments using liquid chromatography with UV/vis photodiode array detection and electrospray ionisation mass spectrometry, *Environmental Chemistry*, 9 (3), 273-284, 2012.

Decesari, S., Facchini, M. C., Fuzzi, S., et al.: Characterization of water-soluble organic compounds in atmospheric aerosol: A new approach, *Journal of Geophysical Research*, 105 (D1), 1481-1489, 2000.

Decesari, S., Facchini, M. C., Matta, E., Lettini, F., Mircea, M., Fuzzi, S., Tagliavini, E. and Putaud, J.P.: Chemical features and seasonal variation of fine aerosol water-soluble

organic compounds in the Po Valley, Italy, *Journal of Atmospheric Environment*, 35, 3691-3699, 2001.

Decesari, S., Facchini, M. C., Matta, E., Mircea, M., Fuzzi, S., Chughtai, A. R. and Smith, D. M.: Water soluble organic compounds formed by oxidation of soot, *Atmospheric Environment*, Volume 36 (11) Elsevier – Apr 1, 2002.

De Laurentiis, E., Maurino, V. and Brigante, M.: Could triplet-sensitised transformation of phenolic compounds represent a source of fulvic-like substances in natural waters?, *Chemosphere*, 90 (2), 881, 2013a.

De Laurentiis, E., Sur, B., Pazzi, M., Maurino, V., Minero, C., Mailhot, G., Brigante, M. and Vione, D.: Phenol transformation and dimerisation, photosensitised by the triplet state of 1-nitronaphthalene: A possible pathway to humic-like substances (HULIS) in atmospheric waters, *Atmospheric Environment*, Volume 70 Elsevier, 2013b.

Dereppe, J.-M., Moreaux, C. and Debyser, Y.: Investigation of marine and terrestrial humic substances by ¹H and ¹³C nuclear magnetic resonance and infrared spectroscopy, *Org. Geochem.*, 2, 117-124, 1980.

Dinar, E., Mentel, T. F. and Rudich, Y.: The density of humic acids and humic like substances (HULIS) from fresh and aged wood burning and pollution aerosol particles, *Atmos. Chem. Phys.*, 6, 5213-5224, doi:10.5194/acp-6-5213-2006, 2006a.

Dinar, E., Taraniuk, I., Graber, E. R., Katsman, S., Moise, T., Anttila, T., Mentel, T. F. and Rudich, Y.: Cloud Condensation Nuclei properties of model and atmospheric HULIS, *Atmos. Chem. Phys.*, 6, 2465-2482, doi:10.5194/acp-6-2465-2006, 2006b.

Dinar, E., Taraniuk, I., Graber, E., Anttila, T., Mentel, T. and Rudich, Y.: Hygroscopic growth of atmospheric and model humic-like substances, *J. Geophys. Res.*, 112, D05211, doi:10.1029/2006JD007442, 2007.

Dragunov, C. C., Zhelokhovtseva, H. H. and Strelkova, E. I.: A comparative study of soil and peat humic acids. *Pochvovedenie*, 1, 409–420, 1948.

Duarte, R. M. B. O. and Duarte, A. C.: Application of Non-Ionic Solid Sorbents (XAD Resins) for the Isolation and Fractionation of Water-Soluble Organic Compounds from Atmospheric Aerosols, *Journal of Atmospheric Chemistry*, 51, 79–93, 2005a.

Duarte, R. M. B. O., Pio, C. A. and Duarte, A. C.: Spectroscopic study of the water-soluble organic matter isolated from atmospheric aerosols collected under different atmospheric conditions, *Analytica Chimica Acta*, 530, 7–14, 2005b.

Duarte, R. M. B. O. and Duarte, A. C.: Thermogravimetric characteristics of water-soluble organic matter from atmospheric aerosols collected in a rural–coastal area, *Atmospheric Environment*, 42, 6670–6678, 2008.

Emmenegger, Ch., Reinhardt, A., Hueglin, Ch., Zenobi, R. and Kalberer, M.: Evaporative Light Scattering: A Novel Detection Method for the Quantitative Analysis of Humic-like Substances in Aerosols, *Environmental Science & Technology*, 41 (7), 2473-2478, 2007.

El Haddad, I., Marchand, N., Dron, J., Temime-Roussel, B., Quivet, E., Wortham, H., Jaffrezo, J. L., Baduel, Ch., Voisin, D., Besombes, J. L. and Gille G.: Comprehensive primary particulate organic characterization of vehicular exhaust emissions in France, *Atmospheric Environment*, Volume 43, Issue 39, 6190–6198, 2009.

El Haddad, I., Marchand, N., Temime-Roussel, B., Wortham, H., Piot, C., Besombes, J. L., Baduel, Ch., Voisin, D., Armengaud, A. and Jaffrezo, J. L.: Insights into the secondary fraction of the organic aerosol in a Mediterranean urban area: Marseille, *Atmospheric Chemistry and Physics*, 11 (5), 2059-2079, 2011.

Ellis, E. C. and Novakov, T.: Application of thermal-analysis to the characterization of organic aerosol particles, *Science of the Total Environment*, 23, 227-238, 1982.

Facchini, M. C., Fuzzi, S., Zappoli, S., Andracchio, A., Gelencser, A., Kiss, G., Krivacsy, Z., Meszaros, E., Hansson, H. C., Alsberg, T. and Zebuhr, Y.: Partitioning of the organic aerosol component between fog droplets and interstitial air, *Journal of Geophysical Research*, [Atmospheres], 104, (D21), D2126821-D2126832, 1999.

Fan, X., Song, J. and Peng, P.: Comparison of isolation and quantification methods to measure humic-like substances (HULIS) in atmospheric particles, *Atmospheric Environment*, 60, 366-374, 2012.

Feczko, T., Puxbaum, H., Kasper-Giebl, A., Handler, M., Limbeck, A., Gelencse ´r, A., Pio C., Preunkert, S. and Legrand, M.: Determination of water and alkaline extractable atmospheric humic-like substances with the TU Vienna HULIS analyzer in samples from six background sites in Europe, *J. Geophys. Res.*, 112 (D23), 23S10/1-D23S10/9, 2007.

Feng, J. S. and Moller, D.: Characterization of water-soluble macromolecular substances in cloud water, *J. Atmos. Chem.*, **48**, 217–233, 2004.

FGW, 2011, <https://www.gaswaerme.at/fw/services/prinfo/prinfo/details?uid=3185>; last access: 11 February 2011.

Finlayson-Pitts, B. J. and Pitts, J. N. Jr.: Tropospheric air pollution: ozone, airborne toxics, polycyclic aromatic hydrocarbons, and particles, *Science (New York, N.Y.)*, **276** (5315), 1045-1052, 1997.

Finlayson-Pitts, B. J. and Pitts, J. N. (Eds.): *Chemistry of the Upper and Lower Atmosphere*, Academic Press, San Diego, 2000.

Fisseha, R., Dommen, J., Gaeggeler, K., Weingartner, E., Samburova, V., Kalberer, M. and Baltensperger, U.: Online gas and aerosol measurement of water soluble carboxylic acids in Zurich, *J. Geophys. Res.*, **111**, D12316, 2006.

Fooker, U., Liebezeit, G., *Huminsäuren in Oberflächensedimenten der Nordsee-Indikatoren für terrestrischen Eintrag?*, PhD thesis, Fachbereich Chemie, Carl von Ossietzky Universität von Oldenburg, 175 pp., 1999.

France, J. L., King, M. D., Frey, M. M., Erbland, J., Picard, G., Preunkert, S., MacArthur, A. and Savarino, J.: Snow optical properties at Dome C (Concordia), Antarctica; implications for snow emissions and snow chemistry of reactive nitrogen, *Atmos. Chem. Phys.*, **11**, 9787-9801, doi:10.5194/acp-11-9787-2011, 2011.

France, J. L., Reay, H. J., King, M. D., Voisin, D., Jacobi, H. W., Domine, F., Beine, H. J., Anastasio, C., MacArthur, A. and Lee-Taylor, J.: Hydroxyl radical and NO_x production rates, black carbon concentrations and light-absorbing impurities in snow from field measurements of light penetration and nadir reflectivity of on-shore and off-shore coastal Alaskan snow, *J. Geophys. Res.*, doi:10.1029/2011JD016639, 2012.

Fuchs, W.: *Huminsäuren*, *Kolloid. Z.* **52**, 248-252, 1930.

Fuzzi, S., Decesari, S., Facchini, M. C., et al.: A simplified model of the water-soluble organic component of atmospheric aerosols, *Geophysical Research Letters*, **28** (21), 4079-4082, 2001.

Gao, S., Keywood, M., Ng, N. L., Surratt, J., Varutbangkul, V., Bahreini, R., Flagan, R. C. and Seinfeld, J. H.: Low-molecularweight and oligomeric components in secondary organic aerosol from the ozonolysis of cycloalkenes and alpha-pinene, *J. Phys. Chem. A*, **108**, 10147–10164, 2004a.

Gao, S., Ng, N. L., Keywood, M., Varutbangkul, V., Bahreini, R., Nenes, A., He, J. W., Yoo, K. Y., Beauchamp, J. L., Hodyss, R. P., Flagan, R. C. and Seinfeld, J. H.: Particle phase acidity and oligomer formation in secondary organic aerosol, *Environ. Sci. Technol.*, **38**, 6582–6589, 2004b.

Gelencsér, A., Hoffer, A., Molnár, A., Krivácsy, Z., Kiss, G. and Mészáros, E.: Thermal behaviour of carbonaceous aerosol from a continental background site, *Journal of Atmospheric Environment*, **34**, 823-831, 2000a.

Gelencsér, A., Sallai, M., Krivácsy, Z., Kiss, G. and Mészáros, E.; Voltammetric evidence for the presence of humic-like substances in fog water, *Journal of Atmospheric Research*, **54**, 157-165, 2000b.

Gelencsér, A., Mészáros, T., Blazsó, M., Kiss, G., Krivácsy, Z., Molnár, A. and Mészáros, E.: Structural characterisation of organic matter in fine tropospheric aerosol by pyrolysis-gas chromatography-mass spectrometry, *Journal of Atmospheric Chemistry*, **37**, 173-183, 2000c.

Gelencsér, A., Hoffer, A., Krivácsy, Z., Kiss, G., Molnár, A. and Mészáros, E.: On the possible origin of humic matter in fine continental aerosol, *Journal of Geophysical Research*, **107** (D21), doi:10.1029/2001JD001299, 2002.

Gelencsér, A., Hoffer, A., Kiss, G., Tombacz, E., Kurdi, R., Bencze, L., 2003. In-situ Formation of Light-Absorbing Organic Matter in Cloud Water. *Journal of Atmospheric Chemistry* **45** (1), 25-33.

Gelencsér, A. (Ed.): *Carbonaceous Aerosol*, Atmospheric and Oceanographic Sciences Library, Vol 30, Mysak, L.A. and Hamilton, K. (Eds.), Springer, Dordrecht 2004.

Gomez-Gonzalez, Y., Surratt, J. D., Cuyckens, F., Szmigielski, R., Vermeylen, R., Jaoui, M., Lewandowski, M., John H. Offenberg, Kleindienst, T. E., Edney, E. O., Blockhuys, F., Van Alsenoy, Ch., Maenhaut, W. and Claeys, M.: Characterization of organosulfates from the photooxidation of isoprene and unsaturated fatty acids in ambient aerosol using liquid

chromatography/(-) electrospray ionization mass spectrometry, *J. Mass Spectrom*, **43**, 371–382, 2008.

Google Maps: <https://maps.google.com/>, Kartendaten (c) 2013 Geobasis-DE/BKG ((c)2009), last access: 27 August 2009.

Góra, R. and Hutta, M.: Reversed-phase liquid chromatographic characterization and analysis of air particulates humic (-like) substances in presence of pollens, *Journal of Chromatography A*, **1084**, 39–45, 2005.

Graber, E. R. and Rudich, Y.: Atmospheric HULIS: How humic-like are they? A comprehensive and critical review, *Atmos. Chem. Phys.*, **6**, 729-753, doi:10.5194/acp-6-729-2006, 2006.

Griffin, R. J., Cocker III, D. R., Flagan, R. C. and Seinfeld, J. H.: Organic aerosol formation from the oxidation of biogenic hydrocarbons, *Journal of Geophysical Research*, **104**, 3555-3567, 1999.

Grosjean, D., Williams II, E. L., Grosjean, E. and Novakov, T.: Evolved Gas Analysis of Secondary Organic Aerosols, *Aerosol Science and Technology*, **21**, 306-324, 1994.

Gross, D. S., Galli, M. E., Kalberer, M., Prevot, A. S. H., Dommen, J., Alfarra, M. R., Duplissy, J., Gaeggeler, K., Gascho, A., Metzger, A. and Baltensperger, U.: Real-time measurement of oligomeric species in secondary organic aerosol with the aerosol time-of-flight mass spectrometer, *Anal. Chem.*, **78**, 2130–2137, doi:10.1021/ac060138l, 2006.

Guenther, A., Hewitt, C. N., Erickson, D., Fall, R., Geron, C., Graedel, T., Harley, P., Klinger, L., Lerdau, M., McKay, W. A., Pierce, T., Scholes, B., Steinbrecher, R., Tallamraju, R., Taylor, J. and Zimmerman, P. A.: Global-Model of Natural Volatile Organic-Compound Emissions, *J. Geophys. Res. Atmos.*, **100** (D5), 8873–8892, 1995.

Handler, M.: Entwicklung einer Analysenmethode zur Bestimmung von Huminstoffen in atmosphärischen Aerosolen mittels Festphasenextraktion, gekoppelt mit Kohlenstoff-, Fluoreszenz- und UV-Detektion, M.S. thesis, Institut für Chemische Technologien und Analytik, Technische Universität Wien, Austria, 66 pp., 2003.

Handler, M., Puls, C., Zbiral, J., Marr, I., Puxbaum, H. and Limbeck, A.: Size and composition of particulate emissions from motor vehicles in the Kaisermühlen-Tunnel, Vienna, *Atmospheric Environment*, **42** (9), 2173-2186, 2008.

- Hatcher, P. G. and Orem, W. H.: Structural interrelationships among humic substances in marine and estuarine sediments as delineated by CP/MAS ¹³C-NMR. GEOC, Abstracts of papers. National meeting of the Am. Chem.Soc.: paper 39, 1985.
- Havers, N., Burba, P., Lambert, J. and Klockow, D.: Spectroscopic characterization of humic-like substances in airborne particulate matter, *Journal of Atmospheric Chemistry*, 29 (1), 45-54, 1998.
- Haworth, R. D.: The chemical nature of humic acids, *Soil Sci*, 111, 71-79, 1971.
- Hede, T., Li, X., Leck, C., Tu, Y. and Ågren, H.: Model HULIS compounds in nanoaerosol clusters – investigations of surface tension and aggregate formation using molecular dynamics simulations, *Atmos. Chem. Phys.*, 11, 6549-6557, doi:10.5194/acp-11-6549-2011, 2011.
- Hitzenberger, R., Berner, A., Giebl, H., Kromp, R., Larson, S. M., Rouc, A., Koch, A., Marischka, S., and Puxbaum, H.: Contribution of carbonaceous material to cloud condensation nuclei concentrations in European background (Mt. Sonnblick) and urban (Vienna) aerosols., *Atmos. Environ.*, 33, 2647-2659, 1999.
- Hoffer, A., Kiss, G., Blazso, M. and Gelencser, A.: Chemical characterization of humic-like substances (HULIS) formed from a lignin-type precursor in model cloud water, *Geophysical Research Letters*, 31 (6), L06115/1-L06115/4, 2004.
- Hoffer, A., Gelencsér, A., Blazsó, M., Guyon, P., Artaxo, P. and Andreae, M. O.: Diel and seasonal variations in the chemical composition of biomass burning aerosol, *Atmos. Chem. Phys.*, 6, 3505-3515, 2006a.
- Hoffer, A., Gelencsér, A., Guyon, P., Kiss, G., Schmid, O., Frank, G. P., Artaxo, P. and Andreae, M. O.: Optical properties of humic-like substances (HULIS) in biomass-burning aerosols, *Atmos. Chem. Phys.*, 6, 3563-3570, 2006b.
- Holmes, B. J. and Petrucci, G. A.: Oligomerization of levoglucosan by Fenton chemistry in proxies of biomass burning aerosols, *J. Atmos. Chem.*, 58, 151–166, 2007.
- Hopkins, R. J., Tivanski, A. V., Marten, B. D. and Gilles, M. K.: Chemical bonding and structure of black carbon reference materials and individual carbonaceous atmospheric aerosols, *Journal of Aerosol Science*, 38 (6), 573-591, 2007.

Houghton, J. T., Ding, Y., Griggs, D. J., Noguer, M., Van der Linden, P. J., Dai, X., Maskell, K. and Johnson, C. A.: *Climate Change 2001: The Scientific Basis (Contribution of Working Group I to the Third Assessment Report of the Intergovernmental Panel on Climate Change)*, Cambridge University Press, Cambridge, 2001.

Hung, H. M., Katrib, Y. and Martin, S. T.: Products and mechanisms of the reaction of oleic acid with ozone and nitrate radical, *J. Phys. Chem. A*, 109, 4517–4530, 2005.

Iinuma, Y., Boge, O., Gnauk, T. and Herrmann, H.: Aerosol-chamber study of the α -pinene/O₃ reaction: influence of particle acidity on aerosol yields and products, *Journal of Atmospheric Environment*, 38, 761-773, 2004.

Iinuma, Y., Müller, C., Berndt, T., Böge, O., Claeys, M. and Herrmann, H.: Evidence for the Existence of Organosulfates from α -Pinene Ozonolysis in Ambient Secondary Organic Aerosol, *Environ. Sci. Technol.*, 41 (19), 6678–6683, 2007.

IPPC Working Group: *Climate Change 2001, The Scientific Basis*. Cambridge, University Press, 83 pages, 2001.

Jang, M. and Kamens, R.: Atmospheric secondary aerosol formation by heterogeneous reaction of aldehydes in the presence of a sulfuric acid aerosol catalyst, *Environmental Science and Technology*, 35, 4758-4766, 2001.

Jang, M., Czoschke, N., Lee, S. and Kamens, R. M., Heterogeneous atmospheric aerosol formation by acid catalysed particle-phase reactions, *Science*, 298, 814-817, 2002.

Jang, M., Carroll, B., Chandramouli, B. and Kamens, R. M.: Particle Growth by Acid-catalyzed Heterogeneous Reactions of Organic Carbonyls on Pre-existing Aerosols, *Environ. Sci. Technol.*, 37, 3827-3837, 2003.

Jankowski, N., Schmidl, C., Marr, I.L., Bauer, H. and Puxbaum, H.: Comparison of methods for the quantification of carbonate carbon in atmospheric PM₁₀ aerosol samples, *Atmospheric Environment*, 42 (34), 8055-8064, 2008.

Jankowski, N., Bauer, H., and Puxbaum, H.: Project Report: Aquellis M – PM₁₀ Aerosol Emissions of mobile Sources. Source Profiles of Vehicle Emissions: Profiles of Exhaust, Brake and Tire Abrasion Products for Application in the CMB Model (original title: Endbericht zum Projekt “Auellis M” PM₁₀ Aerosol Emissionen aus mobilen Quellen. Quellenprofile von Kraftfahrzeugs-Emissionen: Abgas, Brems- und Reifenabrieb für die

Anwendung im PM10 Aerosolmassenbilanzmodell (CMB), Project No. D16421050500, 58 pages, 2009a.

Jankowski, N., Sageder, M., Bauer, H., Marr, I., Kasper-Giebl, A., Limbeck, A., Caseiro, A., Handler, M., Klatzer, B., Kotianova, P., Pouresmaeil, P., Schmidl, C., Ramirez-Santa-Cruz, C., Dattler, A., Andrade-Sanches, L., and Puxbaum, H.: Project Report: Aquella Linz-Upper Austria – Determination of Sources contributing to the Particulate Matter Burden in Upper Austria (original title: Aquella Linz – Oberösterreich – Aerosolquellenanalyse für Linz – Oberösterreich), 184 pages, 2009b.

Kalberer, M., Paulsen, D., Sax, M., Steinbacher, M., Dommen, J., Prevot, A. S. H., Fisseha, R., Weingartner, E., Frankevich, V., Zenobi, R. and Baltensperger, U.: Identification of Polymers as Major Components of Atmospheric Organic Aerosols, *Science*, 303, 1659–1662, 2004.

Kalberer, M., Sax, M. and Samburova, V.: Molecular size evolution of oligomers in organic aerosols collected in urban atmospheres and generated in a smog chamber, *Environ. Sci. Technol.*, 40, 5917–5922, 2006.

Katrib, Y., Martin, S. T., Hung, H. M., Rudich, Y., Zhang, H. Z., Slowik, J. G., Davidovits, P., Jayne, J. T. and Worsnop, D. R.: Products and mechanisms of ozone reactions with oleic acid for aerosol particles having core-shell morphologies, *J. Phys. Chem. A*, 108, 6686–6695, 2004.

Kiss, G., Varga, B., Galambos, I. and Ganszky, I.: Characterization of water-soluble organic matter isolated from atmospheric fine aerosol, *Journal of Geophysical Research*, 107 (D21), 8339, doi:10.1029/2001JD000603, 2002.

Kiss, G., Tombácz, E., Varga, B., Alsberg, T. and Persson, L.: Estimation of the average molecular weight of humic-like substances isolated from fine atmospheric aerosol, *Journal of Atmospheric Environment*, 37, 3783–3794, 2003.

Kiss, G., Tombacz, E. and Hansson, H. C.: Surface tension effects of humic-like substances in the aqueous extract of tropospheric fine aerosol, *J. Atmos. Chem.*, 50, 279–294, 2005.

Kleindienst, T.E., Lewandowski, M., Offenberg J.H., Edney, E. O., Jaoui, M., Zheng, M., Ding, X. and Edgerton, E. S.: Contribution of Primary and Secondary Sources to Organic

Aerosol and PM_{2.5} at SEARCH Network Sites, *Journal of the Air & Waste Management Association*, 60: 11, 1388-1399, doi: 10.3155/1047-3289.60.11.1388, 2010.

Kolb, C. E.: Atmospheric chemistry: Iodine's air of importance, *Nature*, 417, 597-598, doi: 10.1038/417597a, 2002.

Konovalov, I. B., Beekmann, M., D'Anna, B. and George, C.: Significant light induced ozone loss on biomass burning aerosol: evidence from chemistry-transport modeling based on new laboratory studies, *Geophys. Res. Lett.*, doi: 10.1029/2012GL052432, 2012.

Kotianová, P., Puxbaum, H., Bauer, H., Caseiro, A., Marr, I. L. and Ck, G.: Temporal patterns of nalkanes at traffic exposed and suburban sites in Vienna, *Atmospheric Environment*, 42, 2993-3005, 2008.

Krivácsy, Z., Kiss, G., Varga, B., Galambos, I., Sárvári, Zs., Gelencsér, A., Molnár, A., Fuzzi, S., Facchini, M.C., Zappoli, S., Andracchio, A., Alsberg, T., Hansson, H. C. and Persson, L.: Study of humic-like substances in fog and interstitial aerosol by size-exclusion chromatography and capillary electrophoresis, *Journal of Atmospheric Environment*, 34, 4273-4281, 2000.

Krivacsy, Z., Gelencser, A., Kiss, G., Meszaros, E., Molnar, A., Hoffer, A., Meszaros, T., Sarvari, Z., Temesi, D., Varga, B., Baltensperger, U., Nyeki, S. and Weingartner, E.: Study on the chemical character of water soluble organic compounds in fine atmospheric aerosol at the Jungfraujoch, *J. Atmos. Chem.*, 39, 235–259, 2001a.

Krivacsy, Z., Kiss, G., Ceburnis, D., Jennings, G., Maenhaut, W., Salma, I. and Shooter, D.: Study of water-soluble atmospheric humic matter in urban and marine environments, *Journal of Atmospheric Research*, 87 (1), 1-12, 2008.

Kunit, M. and Puxbaum, H.: Enzymatic determination of the cellulose content of atmospheric aerosols, *Journal of Atmospheric Environment*, 30, 1233-1236, 1996.

Legrand, M., Preunkert, S., Schock, M., Cerqueira, M., Kasper-Giebl, A., Afonso, J., Pio, C., Gelencsér, A. and Dombrowski-Etchevers, I.: Major 20th century changes of carbonaceous aerosol components (EC, WinOC, DOC, HULIS, carboxylic acids, and cellulose) derived from Alpine ice cores, *Journal of Geophysical Research*, VOL. 112, D23S11, doi: 10.1029/2006JD008080, 2007a.

- Legrand, M. and Puxbaum, H.: Summary of the CARBOSOL project: Present and retrospective state of organic versus inorganic aerosol over Europe, *Journal of Geophysical Research*, VOL. 112, D23S01, doi:10.1029/2006JD008271, 2007b.
- Liggio, J. and Li, S. M.: Organosulfate formation during the uptake of pinonaldehyde on acidic sulfate aerosols. *Environment Canada, Can, Geophysical Research Letters*, 33 (13), L13808/1-L13808/4, 2006.
- Likens, G. E., Edgerton, E. S. and Galloway, J. N.: The composition and deposition of organic carbon in precipitation, *Chemical and Physical Meteorology*, 35B(1), 16-24, 1983.
- Limbeck, A., Puxbaum, H., Otter, L. and Scholes, M. C.: Semivolatile behaviour of dicarboxylic acids and other polar organic species at a rural background site (Nylsvley, RSA), *Atmospheric Environment*, 35 (10), 1853-1862, 2001.
- Limbeck, A., Kulmala, M. and Puxbaum, H.: Secondary organic aerosol formation in the atmosphere via heterogeneous reaction of gaseous isoprene on acidic particles, *Geophysical Research Letters*, 30 (19), doi:10.1029/2003GL017738, 2003.
- Limbeck, A., Rendl, J., Heimbürger, G., Kranabetter, A. and Puxbaum, H.: Seasonal variation of palladium, elemental carbon and aerosol mass concentrations in airborne particulate matter, *Atmospheric Environment*, 38, 1979–1987, 2004.
- Limbeck, A., Handler, M., Neuberger, B., Klatzer, B. and Puxbaum, H.: Carbon-Specific Analysis of Humic-like Substances in Atmospheric Aerosol and Precipitation Samples, *Journal of Analytical Chemistry*, 77 (22), 7288-7293, 2005.
- Limbeck, A., Handler, M., Puls, Ch., Zbiral, J., Bauer, H. and Puxbaum, H.: Impact of mineral components and selected trace metals on ambient PM10 Concentrations, *Atmospheric Environment*, 43, 530–538, 2009.
- Lin, P., Huang, X.-F., He, L.-Y. and Yu, J. Z.: Abundance and size distribution of HULIS in ambient aerosols at a rural site in South China, *Journal of Aerosol Science*, 41(1), 74-87, 2010a.
- Lin, P., Engling, G. and Yu, J. Z.: Humic-like substances in fresh emissions of rice straw burning and in ambient aerosols in the Pearl River Delta Region, China, *Atmospheric Chemistry and Physics*, 10 (14), 6487-6500, 2010b.

Lin, P. and Yu, J. Z.: Generation of Reactive Oxygen Species Mediated by Humic-like Substances in Atmospheric Aerosols, *Environmental Science & Technology*, 45 (24), 10362-10368, 2011.

Lin, P, Yu, J. Z., Engling, G. and Kalberer, M.: Organosulfates in humic-like substance fraction isolated from aerosols at seven locations in East Asia: a study by ultra-high-resolution mass spectrometry, *Environ. Sci. Technol.*, 46 (24), 13118-13127, 2012a.

Lin, P., Rincon, A. G., Kalberer, M. and Yu, J. Z.: Elemental composition of HULIS in the Pearl River Delta Region, China: results inferred from positive and negative electrospray high resolution mass spectrometric data, *Environ. Sci. Technol.*, 46 (14), 7454-7462, 2012b.

Löflund, M., Kasper-Giebl, A., Tschewenka, W., Schmid, M., Giebl, H., Hitzemberger, R., Reischl G. and Puxbaum, H.: The performance of a gas and aerosol monitoring system (GAMS) for the determination of acidic water soluble organic and inorganic gases and ammonia as well as related particles from the atmosphere, *Atmospheric Environment*, 35, 2861-2869, 2001.

Lohmann, U. and Feichter, J.: Global indirect aerosol effects: A review, *Atmospheric Chemistry and Physics*, 5 (3), 715-737, 2005.

Lukacs, H., Gelencser, A., Hammer, S., Puxbaum, H., Pio, C., Legrand, M., Kasper-Giebl, A., Handler, M., Limbeck, A. and Simpson, D.: Seasonal trends and possible sources of brown carbon based on 2-year aerosol measurements at six sites in Europe, *Journal of Geophysical Research [Atmospheres]*, 112 (D23), D23S18/1-D23S18/9, 2007.

Mancinelli, V., Decesari, St., Emblico, L., Tozzi, R., Mangani, F., Fuzzi, S. and Facchini, M. C.: Extractable iron and organic matter in the suspended insoluble material of fog droplets, *Water, Air, and Soil Pollution*, Volume 174, Issue 1-4, 303-320, 2006.

Mancinelli, V., Rinaldi, M., Finessi, E., Emblico, L., Mircea, M., Fuzzi, S., Facchini, M. C. and Decesari, St.: An anion-exchange high-performance liquid chromatography method coupled to total organic carbon determination for the analysis of water-soluble organic aerosols, *Journal of Chromatography A*, 1149, 385-389, 2007.

Martin, F., González-Vila, F. J., Del Rio, J. C. and Verdejo, T.: Pyrolysis derivatization of humic substances 1. Pyrolysis of fulvic acids in the presence of tetramethylammonium hydroxide, *Journal of Analytical Applications Pyrol.* 28, 71-80, 1994.

Müller, J. F.: Geographical-Distribution and Seasonal-Variation of Surface Emissions and Deposition Velocities of Atmospheric Trace Gases, *J. Geophys. Res.-Atmos.*, **97**, 3787–3804, 1992.

Mayol-Bracero, O. L., Guyon, P., Graham, B., Roberts, G., Andreae, M. O., Decesari, S., Facchini, M. C., Fuzzi, S. and Artaxo, P.: 1. Water-soluble organic compounds in biomass burning aerosols over Amazonia; 2. Apportionment of the chemical composition and importance of the polyacidic fraction, *Journal of Geophysical Research [Atmospheres]*, **107** (D20), LBA59/1-LBA59/15, 2002.

Mladenov, N., Alados-Arboledas, L., Olmo, F.J., Lyamani, H., Delgado, A., Molina, A., I, Reche, I.: Applications of optical spectroscopy and stable isotope analyses to organic aerosol source discrimination in an urban area, *Atmospheric Environment*, **45** (11), 1960–1969, 2011.

Mukai, H. and Ambe, Y.: Characterization of a humic acid-like brown substance in airborne particulate matter and tentative identification of its origin, *Journal of Atmospheric Environment*, **20** (5), 813-819, 1986.

Neuberger, B.: Saisonalität des Auftretens von luftgetragenen Huminstoff artigen Substanzen (HULIS) im Raum Wien und Umgebung, M.S. thesis, Institut für Chemische Technologien und Analytik, Technische Universität Wien, Austria, 75 pp., 2005.

Ng, N. L., Canagaratna, M. R., Zhang, Q., Jimenez, J. L., Tian, J., Ulbrich, I. M., Kroll, J. H., Docherty, K. S., Chhabra, P. S., Bahreini, R., Murphy, S. M., Seinfeld, J. H., Hildebrandt, L., Donahue, N. M., DeCarlo, P. F., Lanz, V. A., Prévôt, A. S. H., Dinar, E., Rudich, Y. and Worsnop, D. R.: Organic aerosol components observed in Northern Hemispheric datasets from Aerosol Mass Spectrometry, *Atmos. Chem. Phys.*, **10**, 4625-4641, 2010.

Okochi, H., Sato, E., Matsubayashi, Y. and Igawa, M.: Effect of atmospheric humic-like substances on the enhanced dissolution of volatile organic compounds into dew water, *Atmospheric Research*, **87**, 213-223, 2008.

Pacyna, J.: Lead, Mercury, Cadmium and Arsenic in the Environment, Hutchinson, T.C., Meema, K.M., (Eds.), Chapter 7- Lead and Mercury from High Temperature Processes in Power Generation and Industry, Wiley, Lilestrom, 1987.

- Pandis, S. N., Paulson, S. E., Seinfeld, J. H. and Flagan, R. C.: Aerosol formation in the photooxidation of isoprene and β -pinene, *Journal of Atmospheric Environment*, 25A, 997-1008, 1991.
- Pavlovic, J. and Hopke, P. K.: Chemical nature and molecular weight distribution of the water-soluble fine and ultrafine PM fractions collected in a rural environment, *Atmospheric Environment*, 59, 264-271, 2012.
- Piccot, S. D., Watson, J. J. and Jones, J. W.: A global inventory of volatile organic compound emissions from anthropogenic sources, *J. Geophys. Res.*, 97, 9897–9912, 1992.
- Pöschl, U.: Atmospheric aerosols: Composition, transformation, climate and health effects, *Angewandte Chemie, International Edition*, 44 (46), 7520-7540, 2005.
- Polidori, A., Turpin, B. J., Davidson, C. I., Rodenburg, L. A. and Maimone, F.: Organic PM 2.5 Fractionation by Polarity, FTIR Spectroscopy, and OM/OC Ratio for the Pittsburgh Aerosol, *Aerosol Science and Technology*, 233-246, 2008.
- PRTR registry, Umweltbundesamt, 2013; http://www5.umweltbundesamt.at/PRTR-web/state.do?stateId=SUCHE_KARTE&txid=4e2325bd980fb604cf95ed61475e02c463853560, last access: 5 July 2013.
- Puxbaum, H.: Thermo Gas-Analyser for the Characterization of Carbonaceous and Sulphurous Compounds in Atmospheric Particles, *Fresenius Zeitschrift für Analytische Chemie*, 298, 250-259, 1979.
- Puxbaum, H., Rendl, J., Allabashi, R., Otter, L. and Scholes, M.C.: Mass balance of atmospheric aerosol in a South-African subtropical savanna (Nylsvley, May 1997), *Journal of Geophysical Research*, 105, 20697-20706, 2000.
- Puxbaum, H. and Tenze-Kunit, M.: Size distribution and seasonal variation of atmospheric cellulose, *Journal of Atmospheric Environment*, 37, 3693-3699, 2003.
- Puxbaum, H., Bauer, H., Schmidl, C. and Abe, Y.: AQUELLIS IGL-PM10 emissions from industry, craft and agriculture. (Original title: AQUELLIS IGL-PM10 Aerosol-emissionen aus Industrie, Gewerbe und Landwirtschaft), Final report CTA/UPA/06/01 Wien 2007, Vienna University of Technology, Institute of Chemical Technologies and Analytics, Vienna, Austria, 74 pages, 2006.

Puxbaum, H., Gomiscek, B., Kalina, M., Bauer, H., Salam, A., Stopper, S., Preining, O. and Hauck, H.: A dual site study of PM₁₀ and pm 2.5 aerosol chemistry in the larger region of Vienna, *Atmospheric Environment*, **38**, 3949–3958, 2004.

Puxbaum, H., Caseiro, A., Sánchez-Ochoa, A., Kasper-Giebl, A., Claeys, M., Gelencsér, A., Legrand, M., Preunkert, S. and Pio, C.: Levoglucosan levels at background sites in Europe for assessing the impact of biomass combustion on the European aerosol background, *Journal of Geophysical Research*, **112** (D23), D23S05/1-D23S05/11, 2007.

Reemtsma, T. and These, A.: On-line Coupling of Size Exclusion Chromatography with Electrospray Ionization-Tandem Mass Spectrometry for the Analysis of Aquatic Fulvic and Humic Acids, *Anal. Chem.*, **75**, 1500-1507, 2003.

Reinhardt, A., Emmenegger, Ch., Gerrits, B., Panse, Ch., Dommen, J., Baltensperger, U., Zenobi, R. and Kalberer, M.: Ultrahigh Mass Resolution and Accurate Mass Measurements as a Tool to Characterize Oligomers in Secondary Organic Aerosols, *Anal. Chem.*, **79**, 4074-4082, 2007.

Rogge, W. F., Hildemann, L. M., Mazurek, M. A., Cass, G. R. and SImoneit, B. R. T.: Sources of Fine Organic Aerosol. 1. Charbroilers and Meat Cooking Operations, *Environ. Sci. Technol.*, **25**, 1112-1125, 1991.

Rogge, W. F., Mazurek, M. A., Hildemann, L. M., Cass, G. R. and Simoneit, B. R. T.: Quantification of urban organic aerosols at a molecular level: identification, abundance and seasonal variation, *Journal of Atmospheric Environment*, **27A**, 1309-1330, 1993a.

Rogge, W. F., Hildemann, L. M., Mazurek, M. A., Cass, G. R., Simoneit, B. R. T.: Sources of fine organic aerosol, 4. Particulate abrasion products from leaf surfaces of plants, *Journal of Environmental Science and Technology*, **27**, 2700-2711, 1993b.

Romero, F. and Oehme, M.: Organosulfates - A New Component of Humic-Like Substances in Atmospheric Aerosols, *Journal of Atmospheric Chemistry*, **52** (3), 283-294, 2005.

Salma, I., Ocskay, R., Chi, X. and Maenhaut, W.: Sampling artefacts, concentration and chemical composition of fine water-soluble organic carbon and humic-like substances in a continental urban atmospheric environment, *Atmospheric Environment*, **41** (19), 4106-4118, 2007.

Salma, I., Ocskay, R. and Láng G. G.: Properties of atmospheric humic-like substances – water system, *Atmos. Chem. Phys.*, **8**, 2243–2254, 2008a.

Salma, I. and Lang, G. G.: How many carboxyl groups does an average molecule of humic-like substances contain?, *Atmos. Chem. Phys.*, **8**, 5997–6002, 2008b.

Salma, I., Mészáros, T., Maenhaut, W., Vass, E. and Majer, Z.: Chirality and the origin of atmospheric humic-like substances, *Atmos. Chem. Phys.*, **10**, 1315–1327, 2010.

Salma, I., Meszaros, T. and Maenhaut, W.: Mass size distribution of carbon in atmospheric humic-like substances and water soluble organic carbon for an urban environment, *Journal of Aerosol Science*, **56**, 53–60, 2013.

Samburova, V., Zenobi, R. and Kalberer, M.: Characterization of high molecular weight compounds in urban atmospheric particles, *Journal of Atmospheric Chemistry and Physics*, **5** (8), 2163–2170, 2005b.

Samburova, V., Szidat, S., Hueglin, C., Fisseha, R., Baltensperger, U., Zenobi, R. and Kalberer, M.: Seasonal variation of high-molecular-weight compounds in the water-soluble fraction of organic urban aerosols, *Journal of Geophysical Research [Atmospheres]*, **110** (D23), D23210/1–D23210/9, 2005a.

Samburova, V., Didenko, T., Kunenkov, E., Emmenegger, Ch., Zenobi, R. and Kalberer, M.: Functional group analysis of high-molecular weight compounds in the water-soluble fraction of organic aerosols, *Journal of Atmospheric Environment*, **41** (22), 4703–4710, 2007.

Sax, M., Zenobi, R., Baltensperger, U. and Kalberer, M.: Time resolved infrared spectroscopic analysis of aerosol formed by photo-oxidation of 1,3,5-trimethylbenzene and α -pinene, *Aerosol Science and Technology*, **39**, 822–830, 2005.

Saxena, P. and Hildemann, L. M.: Water-soluble organics in atmospheric particles: A critical review of the literature and application of thermodynamics to identify candidate compounds, *Journal of Atmospheric Chemistry*, **24**, 57–109, 1996.

Scheuch, 2013;

http://www.scheuch.com/de/naturbelassen_abgasentstaubung_elektrofilter, last access: 28 April 2013.

- Shinozuka, T., Shibata, M. and Yamaguchi, T.: Molecular Weight Characterization of Humic Substances by MALDI-TOF-MS, *J. Mass Spectrom. Soc. Jpn.*, Vol. 52, No. 1, 2004.
- Schmid, H., Laskus, L., Abraham, H. J., Baltensperger, U., Lavanchy, V., Bjjzak, M., Burba, P., Chachier, H., Crow, D., Chow, J., Gnauk, T., Even, A., ten Brink, H. M., Giesen, K. P., Hitzemberger, R., Hueglin, C., Maenhaut, W., Pio, C., Carvalho, A., Putaud, J. P., Sauntry, D. T. and Puxbaum, H.: Results of the “carbon conference” international aerosol carbon round robin test stage I., *Atmospheric Environment*, 35 (12), 2111-2121., 2001.
- Schmid, H., Pucher, E., Ellinger, R., Biebl, P. and Puxbaum, H.: Decadal reductions of traffic emissions on a transit route in Austria – results of the Tauerntunnel experiment 1997, *Atmospheric Environment*, 35, 3585-3593, 2001.
- Schmidl, Ch., Peng, G., Bauer, H., Puxbaum, H. and the AQUELLA Team: AUQELLIS FB- Aerosol sources: Combustion of solid fuels (Original Title: AQUELLIS FB- Aerosolquellen-Verbrennung fester Brennstoffe) Final Report, Vienna, 2006, Vienna University of Technology, Institute of Chemical Technologies and Analytics, Vienna, Austria , 118 pages, 2008c
- Schmidl, Ch., Marr, I. L., Caseiro, A., Kotianova, P., Berner, A., Bauer, H., Kasper-Giebl, A. and Puxbaum, H.: Chemical characterization of fine particle emissions from wood stove combustion of common woods growing in mid-European Alpine regions, *Journal of Atmospheric Environment*, 42 (1), 126-141, 2008a.
- Schmidl, Ch., Bauer, H., Dattler, A., Hitzemberger, R., Marr, I. L. and Puxbaum, H.: Chemical characterisation of particle emissions from burning leaves, *Atmospheric Environment*, 42, 9070-9079, 2008b.
- Schnitzer, M.: Humic substances: Chemistry and reactions, *Soil Org. Matter*, 8, 67-71, 1978.
- Schulten, H.-R. and Leinweber, P.: Characterization of humic and soil particles by analyticalpyrolysis and computer modelling, *J. Anal. Appl. Pyrol*, 38, 1-53, 1996.
- Seinfeld, J. H. and Pandis, S. N.: *Atmospheric Chemistry and Physics*, Wiley, New York, 1998.

Simoneit, B. R. T.: Organic matter in eolian dusts over the Atlantic Ocean, *Mar. Chem.*, 5, 443-464, 1977.

Simoneit, B. R. T.: Eolian particulates from oceanic and rural areas - their lipids, fulvic and humic acids and residual carbon, *Physics and Chemistry of the Earth (1956-1998)*, 12 (Adv. Org. Geochem. 1979), 343-52, 1980.

Simoneit, B. R. T., Schauer, J. J., Nolte, C. G., Oros, D. R., Elias, V. O., Fraser, M. P., Rogge, W. F. and Cass G. R.: Levoglucosan, a tracer for cellulose in biomass burning and atmospheric particles, *Journal of Atmospheric Environment*, 33, 173-182, 1999.

Slanar, H., Schandl H. and Kührtreiber, F.: *Österreichischer Unterstufen-Atlas*. Ed.Hölzel Ges.m.b.H, Wien, 1985.

Song, J., He, L., Peng, P., Zhao, J. and Shexia Ma, S.: Chemical and Isotopic Composition of Humic-Like Substances (HULIS) in Ambient Aerosols in Guangzhou, South China, *Aerosol Science and Technology*, 46,533-546, 2012.

Spangl, W., Nagl, C., Schneider, J., Kaiser, A.: Source Analysis of PM10 Burdens in Austria- Long-range transport and Regional contributions (Original title: Herkunftsanalyse der PM10- Belastung in Österreich-Ferntransport und regionale Beiträge), *Environment Agency Austria, Vienna, Report REP-0034*,112 pp., 2006.

Srimuruganandam, B. and Shiva Nagendra, S. M.: Source characterization of PM10 and PM2.5 mass using a chemical mass balance model at urban roadside, *Science of the Total Environment*, 433, 8–19, 2012.

Stevenson, F.J. (Ed.): 1994. *Humus Chemistry*. Wiley, New York, 1994.

Stone, E. A., Hedman, C. J., Sheesley, R. J., Shafer, M. M. and Schauer, J. J.: Investigating the chemical nature of humic-like substances (HULIS) in North American atmospheric aerosols by liquid chromatography tandem mass Spectrometry, *Atmospheric Environment*, 43, 4205–4213, 2009.

Subbalakshmi, Y., Patti, A .F., Lee, G. S. H., Hooper, M. A.: Structural characterisation of macromolecular organic material in air particulate matter using Py-GC-MS and solid state ¹³C-NMR, *Journal of Environ. Monit.*, 2, 561-565, 2000.

Surratt, J. D., Kroll, J. H., Kleindienst, T. E., Edney, E. O., Claeys, M., Sorooshian, A., Ng, N. L., Offenberg, J. H., Lewandowski, M., Jaoui, M., Flagan, R. C. and Seinfeld, J. H.: Evidence for Organosulfates in Secondary Organic Aerosol, *Environ. Sci. Technol.*, **41** (2), 517-527, 2007.

Surratt, J. D., Gomez-Gonzalez, Y., Chan, A. W. H., Vermeulen, R., Shahgholi, M., Kleindienst, T. E., Edney, E. O., Offenberg, J. H., Lewandowski, M., Jaoui, M., Maenhaut, W., Claeys, M., Flagan, R. C. and Seinfeld, J. H.: Organosulfate Formation in Biogenic Secondary Organic Aerosol, *J. Phys. Chem. A*, **112** (36), 8345-8378, 2008.

Szidat, S., Jenk, T. M., Gaggeler, H. W., Synal, H. A., Fisseha, R., Baltensperger, U., Kalberer, M., Samburova, V., Wacker, L., Saurer, M., Schwikowski, M. and Hajdas, I.: Source apportionment of aerosols by ¹⁴C measurements in different carbonaceous particle fractions. *Radiocarbon* **46** (1), 475-484, 2004.

Taraniuk, I., Graber, E. R., Kostinski, A. and Rudich, Y.: Surfactant properties of atmospheric and model humic-like substances (HULIS), *Geophys. Res. Lett.*, **34**, L16807, doi:10.1029/2007GL029576, 2007.

Taraniuk, I., Rudich, Y. and Graber E.R.: Hydration-influenced sorption of organic compounds by model and atmospheric humic-like substances (HULIS). *Environ Sci Technol.*, **43** (6):1811-7, 2009.

Tolocka M.P. et al.: Formation of oligomers in secondary organic aerosol, *Environ Sci Technol.*, **38**, 1428–1434, 2004.

Umweltbundesamt, 2009,

http://umweltbundesamt.at/umweltsituation/luft/luftguete_aktuell/tgl_bericht, last access: 1 July 2009.

Utry, N., Ajtai, T., Filep, A., Pintér, M. D., Hoffer, A., Bozokia, Z. and Szabó, G.: Mass specific optical absorption coefficient of HULIS aerosol measured by a four-wavelength photoacoustic spectrometer at NIR, VIS and UV wavelengths, *Atmospheric Environment*, **69**, 321–324, 2013.

Vandenbroucke, M., Pelet, R., Debyser, Y.: Geochemistry of humic substances in marine sediments. In: Aiken, G.R., McKnight, D.M., Wershaw, R.L., MacCarthy, P., (eds). *Humic Substances in Soil, Sediment and Water*. Wiley & Sons Inc., New York: 249-273, 1985.

Varga, B., Kiss, G., Ganszky, I., Gelencsér, A. and Krivácsy, Z.: Isolation of water soluble organic matter from atmospheric aerosol, *Talanta*, 55, 561-572, 2001.

Voisin, D., Jaffrezo, J.-L., Houdier, St., Barret, M., Cozic, J., King, M. D., France, J. L., Reay, H. J., Grannas, A., Kos, G., Ariya, P. A., Beine, H. J. and Domine, F.: Carbonaceous species and humic like substances (HULIS) in Arctic snowpack during OASIS field campaign in Barrow, *J. Geophys. Res.*, 117, D00R19, 2012.

Walgraeve, C., Demeesere, K., Dewulf, J., Zimmermann, R., Van Langenhove, H.: Review-Oxygenated polycyclic aromatic hydrocarbons in atmospheric particulate matter: Molecular characterization and occurrence, *Atmospheric Environment*, 44, 1831-1846, 2010.

Wonaschütz, A., Hitzenberger, R., Bauer, H., Pournesmaeil, P., Klatzer, B., Caseiro, A. and Puxbaum, H.: Application of the Integrating Sphere Method to Separate the Contributions of Brown and Black Carbon in Atmospheric Aerosols, *Environ. Sci. Technol.*, 43 (4), 1141 – 1146, doi:10.1021/es8008503, 2009.

Yu, J. Z., Xu, J. and Yang, H.: Charring Characteristics of Atmospheric Organic Particulate Matter in Thermal Analysis, *Environ. Sci. Technol.*, 36, 754-761, 2002.

Yu, J. Z., Yang, H., Zhang, H. Y., Lau, A. K. H.: Size distributions of water-soluble organic carbon in ambient aerosols and its size-resolved thermal characteristics, *Journal of Atmospheric Environment*, 38 (7), 1061-1071, 2004.

Zahardis, J., Geddes, S. and Petrucci, G. A.: The ozonolysis of primary aliphatic amines in fine particles, *Atmos. Chem. Phys.*, 8, 1181–1194, 2008.

Zappoli, S., Andracchio, A., Fuzzi, S., Facchini, M. C., Gelencser, A., Kiss, G., Krivacsy, Z., Molnar, A., Meszaros, E., Hansson, H. C., Rosman, K. and Zebuhr, Y.: Inorganic, organic and macromolecular components of fine aerosol in different areas of Europe in relation to their water solubility, *Journal of Atmospheric Environment*, 33 (17), 2733-2743, 1999.

Zelenay, V., Huthwelker, T., Krepelova, A., Rudich, Y. and Ammann, M.: Humidity driven nanoscale chemical separation in complex organic matter, *Environmental Chemistry*, 8 (4), 450-460, 2011.

Ziese, M., Wex, H., Nilsson, E., Salma, I., Ocskay, R., Hennig, T., Massling, A. and Stratmann, F.: Hygroscopic growth and activation of HULIS particles: experimental data

and a new iterative parameterization scheme for complex aerosol particles, *Atmos. Chem. Phys.*, **8**, 1855-1866, 2008.

List of Tables

| | |
|---|-----|
| Table 1: Atmospheric abundance of HULIS (based on Krivácsy et al., 2008; updated and extended)..... | 33 |
| Table 2: Analytical methods for the characterization of HULIS, polycarboxylic acids, oligomers, organosulfates and macromolecular compounds in organic aerosol (based on Kalberer et al., 2006; updated and extended by extraction/isolation techniques)..... | 34 |
| Table 3: Overview of PM10 sampling sites investigated in the present work (compiled from information from Umweltbundesamt, 2009) | 52 |
| Table 4: Sampling periods and number of analysed pools (note that sampling was conducted daily, pools denote the temporal resolution) | 54 |
| Table 5: Analytical characteristics..... | 67 |
| Table 6: Summary of recently reported interference studies, part I..... | 75 |
| Table 7: HULIS concentrations ($\mu\text{g C/m}^3$) Vienna, Graz and Salzburg 2004; winter: December-February; spring: March-May; summer: June-August; fall: September-November | 79 |
| Table 8: Contributions of HULIS _T to PM10 and HULIS _T carbon to OC in Vienna, Graz and Salzburg, 2004; Winter: December-February; Spring: March-May; Summer: June-August; Fall: September to November | 84 |
| Table 9: Correlations between HULIS _T (defined as sum of HULIS _{WS} und HULIS _{AS} ; y, $\mu\text{g C/m}^3$) and HULIS _{WS} (x, $\mu\text{g C/m}^3$) | 89 |
| Table 10: Meteorological characteristics and PM10 burden at high relative HULIS _{AS} periods in Vienna; ND...no data; surface wind directions, inversion situation, dominating PM10 sources are from Bauer et al. (2007a) | 91 |
| Table 11: Meteorological characteristics and PM10 burden at high relative HULIS _{AS} periods in Graz; ND...no data; surface wind directions, inversion situation, dominating PM10 sources are from Bauer et al. (2007a) | 93 |
| Table 12: Ambient concentrations of elemental carbon, levoglucosan and HULIS _T at two traffic impacted sites in Vienna and Graz, 2004 | 99 |
| Table 13: Assignment of measured winter increase of HULIS _T concentration to higher source emissions/ formation rates and meteorological influences..... | 99 |
| Table 14: Assignment of measured winter increase of EC levels to higher source emissions and meteorological influences; Meteorological changes calculated from EC _D winter/summer ratio | 100 |
| Table 15: Contribution of HULIS carbon to PM10 from source emissions, part 1..... | 105 |
| Table 16: Contribution of HULIS carbon to PM10 from source emissions, part 2..... | 106 |
| Table 17: HULIS-Tracer source ratios (HTSR), bold numbers were applied for estimations on primary HULIS emissions | 109 |
| Table 18: Species selected for correlation analyses with HULIS _T | 117 |

| | |
|---|-----|
| Table 19: Correlation coefficient among HULIS _T and major aerosol constituents/tracer components in PM10 (Dec-Feb)* | 119 |
| Table 20: Correlation coefficient of HULIS _T and major aerosol constituents/tracer components in PM10 at three sites in Styria (Jun-Aug)* | 125 |
| Table 21: Regional averaged correlation coefficients for HULIS _T in wintry PM10 (averages from species which are correlated significantly on a 95% confidence level at each site in the respective region) | 128 |
| Table 22: Seasonal averages of HULIS _T C and contributions to OC and PM10 at the 23 Austrian sampling sites | 135 |
| Table 23: Summary of HULIS _T carbon and levoglucosan ratios in fine particulate matter and source emissions, calculated and compiled from recent literature ^a , the AQUELLA and AQUELLIS project reports and related publications and the present work ^b | 137 |
| Table 24: Summary of HULIS _T abundance, comparison with selected other aerosol species and estimated primary shares of HULIS emissions to measured HULIS _T ; bold numbers denote significant correlation of HULIS _T and the respective analyte on a 95% level of likelihood..... | 154 |
| Table 25: Regional averaged correlation coefficients for HULIS _T in wintry PM10 (averages from species which are correlated significantly on a 95% confidence level at each site in the respective region) | 163 |

List of Figures

| | |
|--|----|
| Figure 1: Aerosols — the big picture (from Kolb, 2002) | 1 |
| Figure 2: Scientific publications containing the keyword “HULIS” (from SciFinder®) | 4 |
| Figure 3: Suggested structure for aquatic humic acid after Schulten and Leinweber, 1996. | 6 |
| Figure 4: Terms reported in literature, naming fractions of organic aerosol, related to HULIS. | 7 |
| Figure 5: Sampling sites in Austria selected for the present work (based on Google Maps; supplemented with marks for sampling sites)..... | 35 |
| Figure 6: Prevalent climate types in Austria (based on Slanar et al., 1985; complemented with marks for sampling sites). | 36 |
| Figure 7: Sampling sites in Vienna. 1: Schafbergbad; 2: Kandlerstraße; 3: Rinnböckstraße; 4: Lobau..... | 38 |
| Figure 8: Sampling sites Schafbergbad (left) and Kandlerstraße (right) (taken from Umweltbundesamt, 2009). | 38 |
| Figure 9: Sampling site Rinnböckstraße (left) and Lobau (right) (taken from Umweltbundesamt, 2009). | 38 |
| Figure 10: Sampling sites Graz. 1: Bockberg (background); 2: Don Bosco (urban); 3: Graz Süd (urban) (based on Google Maps; supplemented with marks for sampling sites). | 39 |
| Figure 11: Background site Bockberg (based on Google Maps; supplemented with marks for sampling sites)..... | 40 |
| Figure 12: Sampling site Bockberg (left) and Graz Süd (right) (taken from Umweltbundesamt, 2009). | 40 |
| Figure 13: Sampling site Don Bosco (taken from Umweltbundesamt, 2009)..... | 40 |
| Figure 14: Sampling sites Salzburg. 1: Anthering (background); 2a: Lehen (urban); 2b: Freisaalweg; 3: Rudolfsplatz (urban) (based on Google Maps; supplemented with marks for sampling sites)..... | 41 |
| Figure 15: Sampling site Lehen Fasangasse (left) and Freisaalweg (right) (taken from Umweltbundesamt, 2009). | 42 |
| Figure 16: Sampling site Rudolfsplatz (taken from Umweltbundesamt, 2009). | 42 |
| Figure 17: Sampling sites Carinthia. 1: Koschatstraße, 2: Völkermarkterstraße, 3: Gurtschitschach, 4: Lavamünd (based on Google Maps; supplemented with marks for sampling sites)..... | 43 |
| Figure 18: Urban sampling sites Klagenfurt. 1: Koschatstraße; 2: Völkermarkterstraße (based on Google Maps; supplemented with marks for sampling sites)..... | 43 |
| Figure 19: Regional surrounding Gurtschitschach (based on Google Maps; supplemented with marks for sampling sites). | 44 |

| | |
|---|----|
| Figure 20: Regional surrounding Lavamünd (based on Google Maps; supplemented with marks for sampling sites). | 44 |
| Figure 21: Urban sampling sites Koschatstraße (left) and Völkermarkterstraße (right) (taken from Umweltbundesamt, 2009). | 45 |
| Figure 22: Rural sampling sites Lavamünd (left) and Gurtschitschach (right) (taken from Umweltbundesamt, 2009). | 45 |
| Figure 23: Sampling sites in Lower Austria. 1: Amstetten; 2: St.Pölten; 3: Mistelbach; 4: Schwechat; 5: Stixneusiedl (based on Google Maps; supplemented with marks for sampling sites). | 46 |
| Figure 24: Regional surrounding of Amstetten (based on Google Maps; supplemented with marks for sampling sites). | 46 |
| Figure 25: Regional surrounding of St.Pölten (based on Google Maps; supplemented with marks for sampling sites). | 47 |
| Figure 26: Regional surrounding of Mistelbach (based on Google Maps; supplemented with marks for sampling sites). | 47 |
| Figure 27: Regional surrounding of Schwechat (based on Google Maps; supplemented with marks for sampling sites). | 48 |
| Figure 28: Regional surrounding of Stixneusiedl (based on Google Maps; supplemented with marks for sampling sites). | 48 |
| Figure 29: Sampling sites Schwechat (left) and Stixneusiedl (right) (taken from Umweltbundesamt, 2009). | 49 |
| Figure 30: Sampling sites St.Pölten (left), Mistelbach (middle) and Amstetten (right) (taken from Umweltbundesamt, 2009). | 49 |
| Figure 31: Sampling sites Oberösterreich. 1: Enzenkirchen. 2, 3, 4: urban sampling sites in Linz (Figure 32) (based on Google Maps; supplemented with marks for sampling sites). | 50 |
| Figure 32: Sampling sites Linz. 1: Römerberg; 2: Neue Welt; 3: Steyregg (based on Google Maps; supplemented with marks for sampling sites). | 50 |
| Figure 33: Sampling site Römerbergtunnel (left) and Steyregg (right) (taken from Umweltbundesamt, 2009). | 51 |
| Figure 34: Sampling sites Neue Welt (left) and Enzenkirchen (right) (taken from Umweltbundesamt, 2009). | 51 |
| Figure 35: Background site Enzenkirchen (based on Google Maps; supplemented with marks for sampling sites). | 51 |
| Figure 36: Chemical structure of the SPE (C18-EC, left) and the anion exchange sorbent (SAX, right) applied in the first and second isolation step, respectively (taken from http://biotage.com/product-page). | 56 |
| Figure 37: Flow injection manifold, developed by Limbeck et al. (2005); 2. Valve position A: fill/inject; Valve position B: load (after Neuberger, 2005). | 57 |

| | |
|--|-----|
| Figure 38: Scheme of extraction, isolation and quantification of HULIS; 1: Solid phase extraction; 2: Online separation with an ion-exchange micro column integrated in a flow injection system; 3: Carbon specific detection with dissolved organic carbon analyser... | 65 |
| Figure 39: Thermograms of solid and aqueous and alkaline dissolved humic acid..... | 69 |
| Figure 40: Thermograms from HULIS _{AS} isolated from urban PM10 in winter and aqueous dissolved humic acid standard..... | 69 |
| Figure 42: Annual averages of HULIS _T concentrations, Vienna, Graz and Salzburg, 2004. Bars: minimum and maximum monthly averages; Stars: median concentrations; dotted line: regional median. | 79 |
| Figure 43: Regional median HULIS levels in Vienna and the regions of Graz and Salzburg. | 80 |
| Figure 44: Seasonal averaged HULIS carbon concentrations, Vienna 2004..... | 81 |
| Figure 45: Seasonal averaged HULIS carbon concentrations, Graz 2004..... | 81 |
| Figure 46: Seasonal averaged HULIS carbon concentrations, Salzburg 2004. | 81 |
| Figure 47: Regional spread (as relative standard deviations (RSD)) of seasonal HULIS levels in Vienna, Graz and Salzburg. | 82 |
| Figure 48: Meter above sea level of the sampling sites in Vienna, Graz and Salzburg | 83 |
| Figure 49: HULIS _T C contribution to OC, annual averages, Vienna, Graz and Salzburg, 2004. Bars: minimum and maximum monthly averages; Stars: median concentrations. | 85 |
| Figure 50: HULIS _T C contribution to OC, seasonal averages, Vienna 2004..... | 86 |
| Figure 51: HULIS _T C contribution to OC, seasonal averages, Graz, 2004..... | 86 |
| Figure 52: HULIS _T C contribution to OC, seasonal averages, Salzburg 2004. | 86 |
| Figure 53: Correlation between HULIS _{WS} and HULIS _T , Vienna. | 90 |
| Figure 54 : Correlation between HULIS _{WS} and HULIS _T , Graz. | 90 |
| Figure 55: Correlation between HULIS _{WS} and HULIS _T , Salzburg. | 90 |
| Figure 56: Calculated elemental carbon stemming from diesel vehicles (EC _D), monthly averages, urban traffic impacted sites, Vienna, Graz and Salzburg, 2004..... | 97 |
| Figure 57: Fuel types used for domestic heating, 2004; numbers....absolute number of households using the respective heating type | 98 |
| Figure 58: Influence of meteorological conditions on winter enrichment of HULIS _T at the urban traffic impacted sites in Vienna and Graz. | 100 |
| Figure 59: Non-exhaustive map of anthracite- (black spots) and lignite-fired (brown spots) power plants (from www.wikienergy.de ; ©2013 GeoBasis DE/BG and Google ©2009) (left) and percentage of energy produced by coal power plants in selected European countries (source: International Energy Agency (IEA): Energy Statistics Division 08/2011, © OECD/IEA; British Petroleum (BP): Statistical Review of World Energy 2011) (right)..... | 104 |
| Figure 60: Open fires detected by MODIS fire monitoring satellites, July 2005 (from: http://firemaps.geog.umd.edu)..... | 108 |

| | |
|--|-----|
| Figure 61: Wood demand for energetic use, Austria 2005 and 2008 (from http://lebensministerium.at)..... | 110 |
| Figure 62: Calculated contributions of primarily emitted HULIS _T ; HULIS _{rest} is the difference of HULIS _{measured} and the sum of HULIS _{prim, WSE+DVE} | 111 |
| Figure 63: Annual averaged contributions of calculated primary HULIS from wood stove emissions (HULIS _{prim,WSE}) and Diesel vehicle emissions (HULIS _{prim,DVE}) to measured total HULIS; Vienna, Graz and Salzburg 2004..... | 112 |
| Figure 64: Contributions of primarily emitted HULIS by wood stoves and diesel vehicles (calculated) to HULIS _T (measured) in Vienna, Graz and Salzburg 2004; solid squares: urban sites; open squares: urban fringe or rural sites. | 113 |
| Figure 65: Seasonality of contributions from HULIS primary (calculated) to total HULIS (measured) from wood stove emissions (left column) and diesel vehicle emissions (right column), Vienna, Graz and Salzburg 2004. | 114 |
| Figure 66: Absolute levels of calculated HULIS _{prim, WSE} and HULIS _{prim,DVE} ; HULIS rest: HULIS _{measured} - HULIS _{prim, WSE+DVE} ; Vienna 2004. | 115 |
| Figure 67: Seasonal averages of calculated HULIS _{prim, WSE} and HULIS _{prim, DVE} ; HULIS rest: HULIS _{measured} - HULIS _{prim, WSE+DVE} and semi-quantitative estimated apportionment of HULIS _{rest} based on findings from the present work. | 116 |
| Figure 68: Correlation of HULIS _T carbon and levoglucosan (left) and lead (right) in Styria (December-February). | 121 |
| Figure 69: Atmospheric levels of ozone and HULIS _T (top), HULIS _{AS} (middle) and HULIS _{WS} (bottom) in winter samples at urban (solid squares) and open circles and triangles; red lines denote actual correlation function; grey line was added to guide the eye. | 122 |
| Figure 70: Correlation of HULIS _T carbon and aerosol species from the AQUELLA database (winter); red: significant linear correlation on a 95% confidence level. | 123 |
| Figure 71: Correlation of HULIS _T carbon and aerosol species from the AQUELLA database (winter); red: significant linear correlation on a 95% confidence level. | 124 |
| Figure 72: (Quasi-) annual average HULIS _T carbon levels in Austrian PM10; Vienna, Graz and Salzburg 12 month average; *Carinthia: November& December 2004, January-March & July 2005; Lower Austria: January-June 2005 (AMST April-June 2005); Upper Austria: April, May, June, October-December 2005, January-March 2006); bars indicate analytical uncertainty. | 130 |
| Figure 73: Seasonal cycles for HULIS _T (as sum of water and alkaline extractable HULIS) at the AQUELLA sites | 131 |
| Figure 74: Seasonality of HULIS _T at 23 sites in Austria. Broken lines...rural or suburban sites; solid lines...urban sites..... | 132 |
| Figure 75: (Quasi-) annual average of HULIS _T carbon shares to OC in Austrian PM10; Vienna, Graz and Salzburg 12 month average; *Carinthia: November& December 2004, January-March & July 2005; Lower Austria: January-June 2005 (AMST April-June 2005); | |

| | |
|--|-----|
| Upper Austria: April, May, June, October-December 2005, January-March 2006); bars indicate analytical uncertainty of HULIS carbon quantification. | 133 |
| Figure 76: (Quasi-) annual average of HULIS _T contributions to PM ₁₀ ; Vienna, Graz and Salzburg 12 month average; *Carinthia: November& December 2004, January-March & July 2005; Lower Austria: January-June 2005 (AMST April-June 2005); Upper Austria: April, May, June, October-December 2005, January-March 2006); bars indicate analytical uncertainty of HULIS carbon quantification. | 134 |
| Figure 77: HULIS _T C/Levoglucosan ratios Vienna, Graz and Salzburg, 2004. | 139 |
| Figure 78: Monthly averaged HULIS carbon to levoglucosan ratios (a.u.), Carinthia. ... | 140 |
| Figure 79: Monthly averaged HULIS carbon to levoglucosan ratios (a.u.), Lower Austria, 2005..... | 140 |
| Figure 80: Monthly averaged HULIS _T carbon to levoglucosan ratios (a.u.), Upper Austria, 2005..... | 140 |
| Figure 81: Comparison of HULIS _T carbon and levoglucosan in Lower Austria (left) and Upper Austria (right)..... | 142 |
| Figure 82: Comparison of HULIS _T C/levoglucosan ratios in Austria. Vienna, Graz and Salzburg: winter (January, February, December 2004)) and summer (June – August 2004). *winter: Carinthia: December 04 to February 05; Upper Austria: December 05 to February 06, Lower Austria: January and February 05. Summer: Carinthia and Upper Austria: July 05; Lower Austria: June 05. | 143 |
| Figure 83: Sampling sites Oberösterreich. 1: Enzenkirchen (background site), 2: Römerberg (urban traffic impacted site); based on Google maps, supplemented with marks for sampling sites/regions. | 147 |
| Figure 84: Colours of pure HULIS extracted from PM ₁₀ (1-4), wood chips (5) and potting soil (6). 1: urban summer; 2: rural summer; 3: urban winter, 4: rural winter, 5: wood chips, 6: potting soil. A: HULIS isolated from water extracts; b: HULIS isolated from alkaline extracts (note that alkaline extraction was conducted on before water-extracted filter samples)..... | 148 |
| Figure 85: Thermograms of solid humic acid (HA), alkaline dissolved humic acid and humic acid dissolved in ultra-pure water..... | 149 |
| Figure 86: Thermogram of water-soluble humic acid and water-soluble HULIS | 150 |
| Figure 87: High volatile region of thermograms of HULIS _{WS} | 151 |
| Figure 88: High volatile region of thermograms of HULIS _{AS} | 151 |
| Figure 89: Thermograms of HULIS isolated from urban PM ₁₀ (Römerberg, Upper Austria, winter: January 2006; Summer July 2005). | 152 |
| Figure 90: Thermogram of HULIS isolated from water and aqueous alkaline extracts from rural PM ₁₀ (Enzenkirchen, Upper Austria, winter: January 2006; summer: July 2005).153 | |

| | |
|---|-----|
| Figure 91: Thermograms of HULIS isolated from water and aqueous alkaline extracts from rural PM10 (Enzenkirchen, Upper Austria, winter: January 2006; summer: July 2005). | 156 |
| Figure 92: Thermograms of HULIS isolated from water and aqueous alkaline extracts from urban (Römerberg) and rural (Enzenkirchen) PM10 (Upper Austria, winter: January 2006; summer: July 2005). | 157 |
| Figure 93: Thermograms of HULIS isolated from water and aqueous alkaline extracts from rural (Enzenkirchen) PM10 (Upper Austria, winter: January 2006; summer: July 2005). | 158 |
| Figure 94: Thermograms of HULIS isolated from water and aqueous alkaline extracts from urban (Römerberg) PM10 (Upper Austria, winter: January 2006; summer: July 2005). | 159 |
| Figure 95: Thermograms of HULIS isolated from wood chips and potting soil. | 160 |
| Figure 96: Weather situation in Europe on January 1 ^{s+} and November 30 th 2004; (yellow bars denote fog events) from www.Wetterzentrale.de | 201 |
| Figure 97: Weather situation in Europe on November 29 th 2004; (yellow bars denote fog events) from www.Wetterzentrale.de | 202 |
| Figure 98: Seasonality of HULIS _T contributions to OC at sampling sites in Carinthia (top), Lower Austria (middle) and Upper Austria (bottom). | 203 |

List of Equations

| | |
|--|-----|
| $EC_D = EC - EC_W$ (Equation 1)..... | 96 |
| $EC_W = PM10_W * 0.15$ (Equation 2)..... | 96 |
| $PM10_W = levoglucosan * 10.7$ (Equation 3)..... | 96 |
| $EC_D = EC - 1.6 \times levoglucosan$ (Equation 4)..... | 96 |
| $C_{HULIS, primary} = HTSR \times C_{Tracer, ambient}$ (Equation 5)..... | 109 |

Appendix

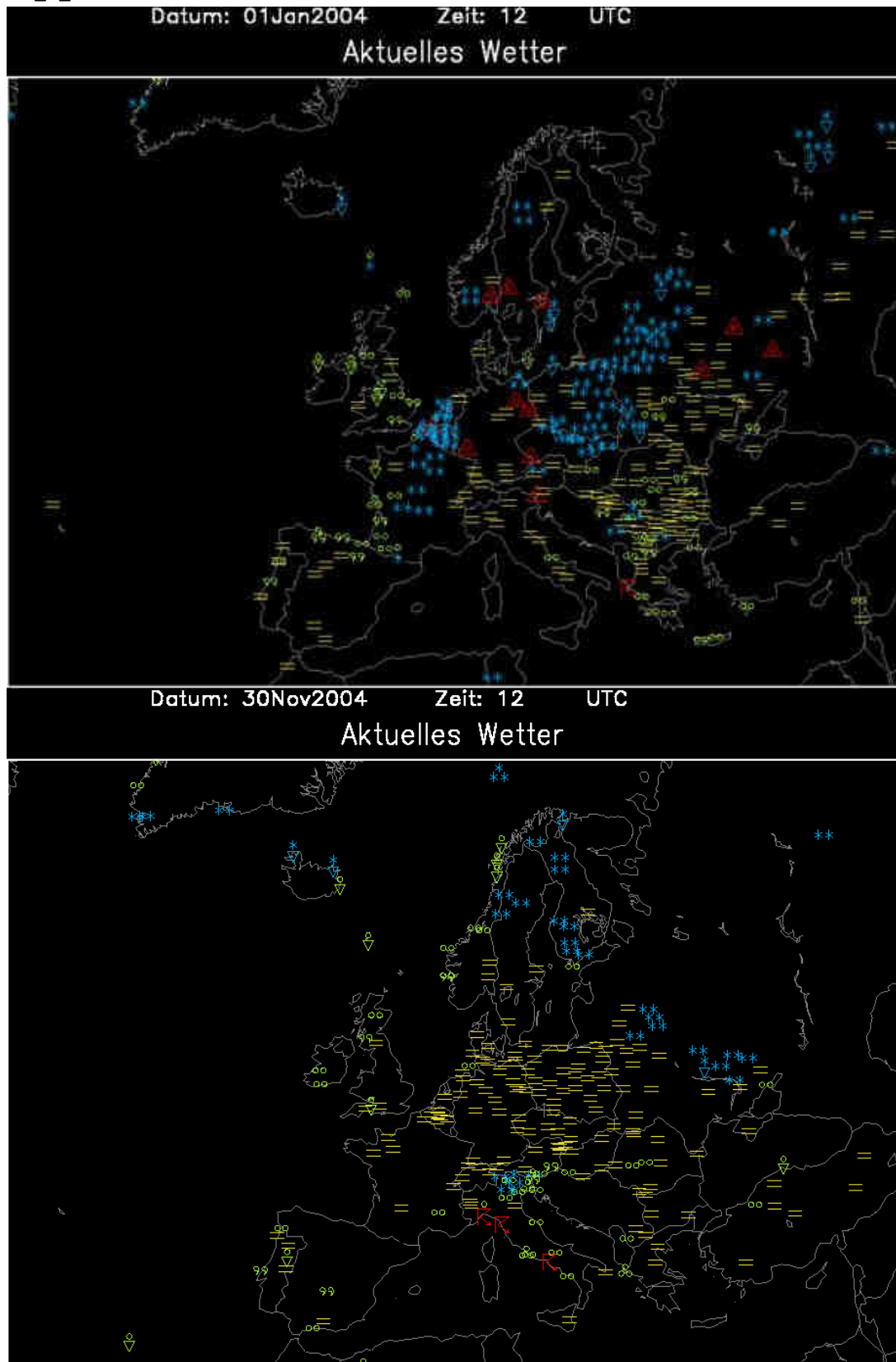


Figure 96: Weather situation in Europe on January 1st and November 30th 2004; (yellow bars denote fog events) from www.Wetterzentrale.de

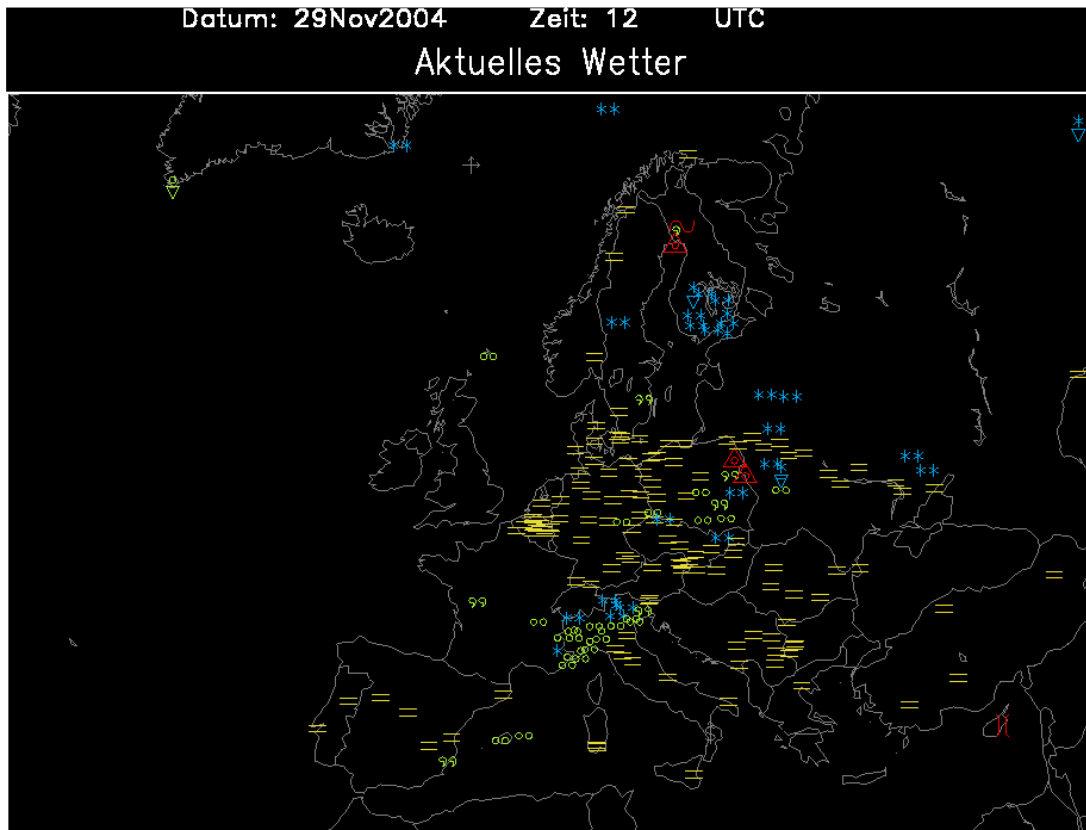


Figure 97: Weather situation in Europe on November 29th 2004; (yellow bars denote fog events) from www.Wetterzentrale.de

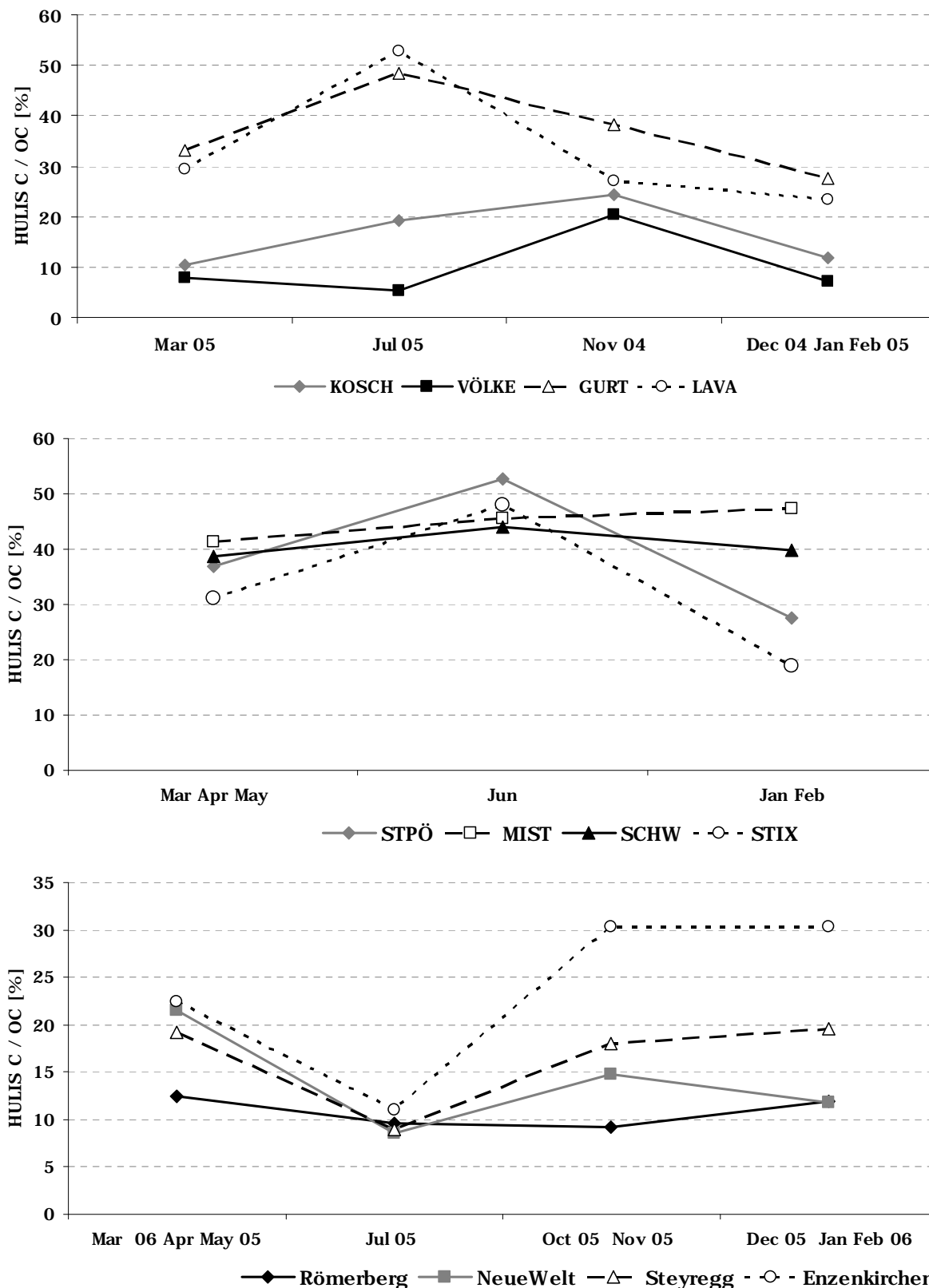


Figure 98: Seasonality of HULIS_T contributions to OC at sampling sites in Carinthia (top), Lower Austria (middle) and Upper Austria (bottom).